1-1-1984

Characterization of interactions between blood and SilasticÃ‚Â®/hydrogel composites by scanning electron microscopy and Fourier transform infrared spectroscopy

Michael John Cyr
Iowa State University

Characterization of interactions between blood and Silastic®/hydrogel composites by scanning electron microscopy and Fourier transform infrared spectroscopy

by

Michael John Cyr

A Thesis Submitted to the
Graduate Faculty in Partial Fulfillment of the
Requirements for the Degree of
MASTER OF SCIENCE

Major: Biomedical Engineering

Iowa State University
Ames, Iowa

1984

TABLE OF CONTENTS

LIST OF TABLES

LIST OF FIGURES

DEDICATION

To

Ellen and Lisa

INTRODUCTION

The search for nonthrombogenic biomaterials for cardiovascular use has been extensive. It will continue since all biomaterials studied to date are in some degree thrombogenic. Some materials, such as Dacron, show good results in large diameter applications, but the need for an off-the-shelf type implant with an inner diameter of 6 mm or less still exists. This work describes aspects of compatibility for hydrogel coatings applied to a widely used implant material, silicone rubber. Silicone rubber is used frequently as a catheter material, and is a material of interest for potential tubular prosthesis applications.

Proteins in the blood are rapidly deposited onto a biomaterial as a layer approximately 100 to 300 Å thick. It is generally accepted that it is the nature of this protein layer that determines the thrombogenic character of that biomaterial. Biomaterials research has resulted in finding of a number of surface parameters that influence the protein reaction with that surface. These parameters include texture (micro and macro), wettability, critical surface tension, ionic charge, immunologic response, structural strength, flexibility, and chemical stability. Adsorption of proteins may also be determined by the plasma components themselves. In general, it is not a single parameter that determines the suitability of a material, but a complex interrelation among many parameters, including the plasma components.

This investigation characterizes the acute cellular and molecular response of blood to surfaces that vary in texture, wettability, and critical surface tension. Silicone rubber substrates ranging in

concentration of diatomacious silica filler were tested by using an ex vivo shunt system in mongrel dogs to study composites of the silicone rubber substrates and hydrogel. Five formulations of HEMA (hydroxyethyl methacrylate) and NVP (N-vinyl-pyrrolidone) were radiation grafted onto tubular silicone rubber substrates. Total protein deposited was measured with Fourier transform infrared spectroscopy, and surface morphology was analyzed using scanning electron microscopy.

LITERATURE REVIEW

Blood-Surface Interactions

General

When a material is placed in contact with blood, many events occur as a result. The sequence of events appears to be the following:

1. Adsorption of plasma proteins,
2. Adhesion of platelets and leukocytes,
3. Activation of adhered platelets leading to the release reaction,
4. Recruitment of nearby platelets by the released products such as adenosine diphosphate (ADP) and thromboxane A_2,
5. Aggregation of recruited platelets upon the layer of adhered platelets with eventual formation of a mural thrombus (Lindsay et al., 1980).

Some components of blood

There are three major types of plasma proteins - albumin, globulin, and fibrinogen (Bloom and Fawcett, 1975, p. 153). Albumin is the most abundant and the smallest of the plasma proteins. It plays an important function in the transport of metabolic products throughout the body. Globulins have a wide range of sizes as well as functions. They are divided into several fractions of which gamma globulins have the greatest interest. This fraction includes the immune globulins or antibodies that provide the immunological defenses against bacteria, toxins, and foreign material. Fibrinogen is a large protein that has the major function of defense for the body against serious blood loss. Soluble fibrinogen is polymerized to insoluble fibrin by thrombin, an enzyme that is activated as

a result of a complex cascade of reactions leading to a clot. Globulin and fibrinogen are glycoproteins, whereas albumin is not (Lee and Kim, 1974b). A glycoprotein is a protein that has branches of oligosaccharide chains.

In addition to the plasma proteins, blood contains many types of formed blood elements of which the platelet is important in thrombus formation. Platelets are multifunctional cells in terms of their intercellular reactions and their contributions to different biological processes (Gordon and Milner, 1976). The formation of platelets is a process called thrombopoiesis (Bloom and Fawcett, 1975, p. 221). Platelets are formed as a result of fragments of megakaryocyte cytoplasm being pinched off (Gordon and Milner, 1976). They have a functional life of about ten days, with about 2/3 of the total number circulating and 1/3 sequestered in the spleen (Robbins et al., 1981). On the basis of light microscope observations, platelets have been divided into two histological regions. A thick central dark staining region containing small granules is called the granulomere or chromomere. The thin peripherial zone is called the hyalomere (Bloom and Fawcett, 1975, p. 140). With the development of electron microscopy, the anatomic features of platelets have been divided into three functional zones. These zones were suggested on the assumption that the structure and function of platelets are similar to that of other types of cells (Caen et al., 1977, p. 10).

The peripheral zone consists of the plasma membrane and associated structures covering the external surface of the platelet and the open channel system. It is in this zone where the reactions of adhesion and aggregation occur. This zone is also involved in the reception and transfer of events that trigger the release reactions.

The sol-gel zone consists of several filamentous systems in the internal part of the platelet. This zone involves the cellular skeleton to maintain the shape of the platelet and the contractile system which participates in the release reactions and aggregation processes.

The organelle zone consists of mitochondria and granules. This zone serves in metabolic functions and the storage of products released during the release reactions. Glycogen is also found in this zone. The granules are divided between the α-granules which contain cationic proteins, fibrinogen, and other proteins and the dense granules which contain ADP, adenosine triphosphate (ATP), 5-hydroxytryptamine (serotonin), and Ca^{++}.

The primary function of platelets is to form a plug or patch on small defects in the endothelial lining of blood vessels so as to limit the amount of hemorrhage, and later to initiate the repair of the defect.

Adsorption of plasma proteins

The adsorption of plasma proteins onto a surface of a material happens very quickly, possibly within 3 seconds (Bruck, 1977). The amount of protein adsorbed is small, in the range of Ø.2 to 2 $\mu g/cm^2$ (Horbett and Hoffman, 1975; Watkins and Robertson, 1977). It is generally recognized that the composition of the protein layer has a major influence on subsequent interactions with formed blood elements, especially platelets (Bruck, 1977; Kim et al., 1974; Brash et al., 1974). How the protein layer does influence the interactions with platelets might be explained by a few models. Brash et al. (1974) suggest a mechanism where the adsorbed protein layer has reached an equilibrium with the plasma liquid phase with possible exchange occurring. They propose that the proteins being desorbed

are altered to some degree so that the clotting cascade is initiated. This leads to activation of thrombin which is a potent stimulator of the release reactions. These reactions then lead to platelet adhesion and aggregation (Gordon and Milner, 1976). Bagnall (1977) and Hoffman (1974) describe how the protein is altered. In general, the protein configuration can be altered by following the 'like dissolves like' rule of thumb (Morrison and Boyd, 1973, p. 31). A protein in its native form in an aqueous enviroment will be globular (Curtis, 1975, p. 74). The globular shape is due to the tertiary structure of the protein, and loss of this stucture is known as denaturation. To maintain this shape, the 'surface' of the protein will have ionic- , hydrogen- , and polar-bonding-capable side groups of the amino acids making up the backbone of the protein oriented outward. These groups will interact or 'dissolve' into the polar and ionic aqueous environment. The inner 'core' of the protein will then be shielded from the aqueous environment by the 'surface', allowing the hydrophobic side groups to interact or "dissolve" into each other. This helps to hold the shape of the protein, and the shape is further stabilized by crosslink bonds. Anything that disrupts the 'like dissolves like' rule will alter the shape of the protein so that the effects imposed by the change are minimized. Thus, when a protein adsorbs onto a hydrophobic material, the protein will react by 'opening up' or denaturing so its hydrophobic core can 'dissolve' into the surface of the material. Once a protein is denatured, it will not spontaneously reform its shape, even if the disrupting force is removed. This does depend on the extent of the denaturation, however. A hydrophilic material would be expected not to denature a protein adsorbed onto the surface since the hydrophilic outer surface of a protein should 'dissolve'

easily into the hydrophilic surface of the implant material being tested. It would also be expected that a hydrophilic surface will desorb proteins easily whereas proteins denatured on a hydrophobic surface will not be so easily given up. This has been found to be generally true as reported by Hoffman (1974).

Adhesion of platelets

Another model describing the important influence of the protein layer on subsequent interaction with platelets is presented by Kim et al. (1974) and Lee and Kim (1974b). This model or mechanism describes a reaction between glycosyl transferases (enzymes) on the platelet membrane with glycoproteins adsorbed onto the surface of a foreign material. The reaction between the enzyme and the glycoprotein results in the formation of a glycosidic linkages or complexes. The stability of these complexes determines the strength and duration of the adhesion. A similar model is proposed by Roseman (1970) for the phenomena of platelet aggregation.

It would be expected that a surface with mostly albumin character, either through pre-coating or selective adsorption, would be more thromboresistant than a surface with mostly glycoprotein character. This has been shown by many investigators who have suggested that the nonglycoprotein character of the albumin is responsible for this action (Nyilas et al., 1975; Kim et al., 1974; Lyman et al., 1974; Vroman et al., 1977; Barber et al., 1979).

Activation and the release reactions

Once a platelet has become adhered to a surface, activation of the platelet occurs. The activation stage of a platelet is a complex series of biochemical reactions which result in the release reactions. The processes involved are not fully understood, but some mechanisms have been found (Gordon and Milner, 1976).

The reaction is initiated by a release-inducing agent which binds to a specific recognition site on the cell membrane. Stimuli which are capable of this include: (1) adhesion to surfaces such as collagen fibrils, and possibly glycoproteins, (2) platelet-platelet contact, (3) immune reactions at the platelet membrane surface, (4) ADP, (5) adrenalin, (6) thrombin and other proteolytic enzymes such as trypsin and papain, and (7) divalent cation ionophores. These stimuli are capable of causing local changes in the ionic distribution of Ca^{++} at the membrane surface as a result of binding to the recognition site. This change in ionic distribution stimulates the formation of cyclic guanosine 3',5'-monophosphate (cGMP), and inhibits the formation of cyclic adenosine 3',5'-monophosphate (cAMP), thus altering the cyclic AMP/GMP ratio. The resulting decrease in cAMP activates the contractile protein system which causes intracellular changes leading to formation of pseudopods and fusion of storage granules (α- and/or dense) with the surface connected tubular system (open channel system). The granule contents are then rapidly extruded through the channel system to the cell surface. The energy requirements for these processes are considerable. Platelets metabolize glycogen and extracellular glucose to generate energy in the form of ATP by glycolysis, the Krebs cycle, and oxidative phosphorylation. During activation,

platelets respond by increasing the activity of both the glycolytic pathway and the Krebs cycle, possibly so that these energy requirements can be met (Macintyre, 1976).

Activation of the platelet results in Release Reaction I, where the contents of the dense granules are released locally. Any aggregation that would occur at this stage would be reversible. This is followed by Release Reaction II, where the contents of the α-granules are released. Aggregation at this stage is irreversible. This is followed by Consolidation, or forming a firm platelet plug by contraction. This contraction is mediated by the contractile protein, actomyosin (thrombosthenin) (Robbins et al., 1981).

It has been demonstrated that ADP causes almost immediate platelet aggregation, and the concentration needed is very small, being on the order of 100 nanograms per ml of plasma. The mechanism by which ADP induces aggregation seems to require the presence of a certain type of protein or proteins on the surface of the platelet, and divalent cations such as Ca^{++}. Considerable evidence suggests that fibrinogen, or some closely related subtance, is the protein that participates in this mechanism. It is believed that the action of thrombin converts the fibrinogen on the surface of the platelets to fibrin, which then binds the platelets together (fibrinogen is converted to a fibrin monomer and then to a fibrin polymer in the presence of Factor XIII, fibrin stabilizing factor) (Medway et al., 1969, p. 252). Using the present techniques of electron microscopy, it would be difficult to detect the polymerized fibrin in the monomer state. However, a method using ferritin-conjugated anti- fibrin/fibrinogen antibodies demonstrated the occurrence of fibrin or fibrinogen within

platelet aggregates (Shirasawa et al., 1972). These findings indicated that fibrinogen released from within the platelets contributed to the structural bonds between platelets in the aggregate. Also, a dense layer of fibrin has been shown to be present on the outer surfaces of platelet aggregates formed in response to thrombin (Cooper et al., 1976).

Once a plug is stable, factors are released from the platelets which are chemotactic to neutrophils, which are themselves chemotactic, and macrophages are attracted so cleanup of the fibrin and debris can occur. Thus, the process of thrombosis induces the processes of inflammation and repair (Thomson, 1984).

Characterization of Adsorbed Proteins

General

It is generally accepted that the proteins adsorbed onto the surface of a material have a major influence on its thrombogenesis. Watkins and Robertson (1977) have outlined three areas that must be considered when studying the adsorption process. These areas are: 1) the types and amounts of proteins adsorbed by the surface; 2) the kinetics of the adsorption process; and 3) the extent of fluid flow, as well as the presence of cellular elements such as red blood cells, on the adsorption process.

Many methods of quantifying the nature of the adsorbed proteins have been devised for in vitro, in vivo, and ex vivo conditions. One of the simplest techniques involves the depletion of a protein from solution after addition of a material with a high specific surface area (Puszkin et al.,

1975). A second method involves the elution of the adsorbed proteins, followed by electrophoresis (Lyman et al., 1974). A third method uses radiolabeling techniques for a protein of interest, and correlates its activity in response to a surface by use of a gamma counter (Weathersby et al., 1977). A fourth method involves spectroscopic examination of the adsorbed protein layer. This can be accomplished with total internal reflection devices designed for infrared, ultraviolet, and visible (from fluoresence) electromagnetic radiation (National Institutes of Health, 1979, p. 48).

Each of these methods has been employed for the study of protein adsorption. However, the information obtainable from spectroscopic techniques puts this method far ahead of the others. For example, the protein depletion technique lacks sensitivity for materials with inherently low specific surface areas, making it incapable of testing a large number of materials that fall into this catagory. The chemical techniques have been useful for the study of equilibrium adsorption, but not for kinetic or competitive adsorption behavior (Watkins and Robertson, 1977). Also, radiolabeling has been shown to alter the natural behavior of a protein and thus its response to the surface of a material (Grant et al., 1977). For example, adsorption of the radiolabel itself may dominate the adsorption process to some materials and thus introduce an artifact. Also, the label itself, as well as the method used to attach the label, can alter the structure of the protein significantly. The altered protein structure can then have an effect on the adsorption characteristics by introducing other artifacts.

Brash and Lyman (1969) recognized the limitations of the protein depletion and the elution techniques. They realized that when dealing with biological systems, subtle changes such as denaturation of proteins (possibly those in the clotting cascade) at the surface of a material may have a significant role in the thrombogenesis of that material. With these methods, changes like this could not be observed. They suggested that infrared internal reflection spectroscopy may be a technique that provides a direct and sensitive examination of the surface-adsorbate complex. Using this system, they were able to measure the quantity of protein adsorbed as a function of solution concentration for various polymer substrates. Lee and Kim (1974a) were able to study adsorption isotherms and kinetics of single protein solutions using this technique, also. However, Brash and Lyman (1969) concluded from their experiments that proteins could not be distinguished from one another because the absorption bands of all proteins and peptides are identical. Thus, competitive studies of mixtures of proteins or whole blood could not be made. Also, adsorbed water has absorption bands in the same regions as protein which leads to masking of information. Because of this, both research groups had to dry the samples in air before taking a spectrum.

These problems were inherent in the instrument used, and with the development of Fourier Transform Infrared Spectroscopy, in conjunction with attenuated total reflectance devices, it became possible to study the protein adsorbate-polymer substrate complex in detail.

Infrared spectroscopy

There are many types of spectroscopic techniques available for the study of molecules of which infrared spectroscopy is one of the most important. Infrared spectroscopy covers the electromagnetic radiation range from about 13,300 cm^{-1} to 10 cm^{-1}. This region is subdivided into several ranges of which the fundamental infrared region (5000 cm^{-1} to 400 cm^{-1}) is the most useful (Kendall, 1966, p. 3).

To understand how infrared radiation can be used to generate a spectrum first requires having an understanding of the nature of the molecules to be examined. The energy of a molecule can be expressed by the equation:

E(mol) = E(trans) + E(rot) + E(vib) + E(el) where,

E(mol) = energy of the molecule

E(trans) = translational energy

E(rot) = rotational energy

E(vib) = vibrational energy

E(el) = electronic energy

E(trans) has no effect on molecular spectra so it can be disregarded. E(rot) is primarily observed in molecules that are able to rotate freely in the vapor state. In solid or liquid conditions, molecular rotation is hindered so that molecular rotation absorption bands are not seen. E(el) deals with three kinds of electrons in molecules: 1) those that belong to only one atom; 2) those which are shared by two adjacent atoms; and 3)

those shared by more than two atoms. This energy variable is only important when electrons are excited to energy levels that contribute to rotational or vibrational transitions. Infrared radiation is weak in terms of the energy required for these transitions, so the transitions normally do not occur. Thus, the above equation becomes (Kendall, 1966, p. 10):

$$E(mol) = E(vib)$$

An infrared spectrum is obtained by forming a plot of the intensity of radiation leaving the sample compared to the intensity of the radiation going into the sample versus the energy of the radiation (usually measured in units of wavenumbers, cm^{-1}). Classical electrodynamics specifies that in order for a molecule to absorb radiation energy, it must possess a vibrational or rotational frequency that is the same as that of the electromagnetic radiation, and a change in the magnitude and/or direction of the dipole moment must occur (Meloan, 1963, p. 67). Spectra measuring the quantity of a particular sample (or subsample) are normally plotted as absorbance versus wavenumber. This is done because the absorbance is proportional to the concentration of the sample and the pathlength through which the radiation travels (Beer-Lambert law) (Adams et al., 1979, p. 497).

The reason that the fundamental infrared region is the most useful is because the frequencies of the oscillations (vibrational or rotational) of atoms in any molecule not at absolute temperature are in the infrared region (oscillations on the order of 10^{14} to 10^{13} Hz, correspond to the region of 3000 cm^{-1} to 300 cm^{-1}) (Kendall, 1966, p. 6).

Fourier transform infrared spectroscopy

The generation of an infrared (IR) spectrum can be accomplished either of two ways. The traditional method involves a dispersion instrument which contains a monochromator or dispersing element. In this instrument, polychromatic radiation is separated into 'units' of almost monochromatic radiation. This dispersed radiation is passed through the sample to the detector. The detector produces a signal that is proportional to the intensity of the radiation striking it. Thus, this system is basically a series of radiometric measurements. A nonconventional approach is the Fourier Transform spectrometer (FTS). In this system, no dispersion is needed. Instead, a Fourier transform operation is performed on the entire polychromatic signal to generate the intensity-frequency information. It should be noted that, although these two systems differ greatly in the method used to generate a spectrum, the end results are identical (Low, 1970).

The FTS offers an advantage over the conventional dispersion instrument in terms of the signal to noise ratio (S/N). This is based on the amount of signal that can be processed and the time required to do so. For example, the dispersion instrument requires energy wasting filters or slits, whereas the FTS system does not, and is therefore capable of more radiation throughput. Also, suppose that, in order to obtain good S/N, 1 second of 'observation' time was needed for one 'resolution' element, of which 2000 elements are needed. The dispersion instrument would require 2000 seconds or 33 minutes to form the spectrum, while the FTS system would only need 1 second for the same S/N ratio. Thus, in the same amount of time it takes for the dispersion instrument to make the spectrum with a S/N

ratio of X, the FTS system could produce a spectrum with an increase in S/N of about 45X (based on $\sqrt{N}$, where N equals the number of scans; Low, 1970).

FTS systems today have a dedicated digital computer which makes it possible to perform the Fourier transform accurately and economically. Since the data are digitized, mathematical operations can be performed with the data simply through use of appropriate software. Thus, the problems that Brash and Lyman (1969) expressed can be addressed and overcome. For example, adsorbed water can be spectrally subtracted out to reveal the information that was masked by its absorption bands. Also, since a better S/N ratio is obtainable in a satisfactory amount of time, characteristic absorption bands of a protein could be found so it would be possible to distinguish different proteins from each other. Conformational information could be assembled, and changes could be followed. By using carefully controlled experimental techniques, all of this information could be collected in real-time. This has been done by Gendreau et al. (1981).

Internal reflection spectroscopy

When studying the spectroscopic characteristics of a molecule, problems sometimes arise. This is particularly apparent with solids. Forming a thin enough sample for transmission of the electromagnetic radiation is sometimes not possible. This problem is overcome, however, by a procedure known as internal reflection spectroscopy. This procedure is based on the principle of total internal reflection. When total internal reflection occurs, the electromagnetic radiation does not stay in the optically dense medium, but actually penetrates into the less dense optical medium at the interface of the two mediums for some depth of penetration,

dp. For example, when infrared radiation is passed through a prism in such a way that total internal relection occurs at a point where the prism is interfaced with another material (e.g. silicone rubber), the reflected beam is no longer the same as the incident beam. The radiation at the reflection point will penetrate into the silicone rubber some distance, dp. If absorbance of some wavelength of the incident beam by the silicone rubber can occur, it will, thus altering the composition of the reflected beam. The depth of peneration is about one wavelength, which indicates that only a very thin layer of a sample at the interface can be analyzed; the thickness of this layer increases with increasing wavelength (Alpert et al., 1970, p. 339). For an internal reflection system, the depth of penetration is defined as the distance into a sample where the evanescent field amplitude decays to e^{-1} of its magnitude at the prism-sample interface (Mattson et al., 1975). If the prism is made of germanium (n=4, where n is the refractive index) and is in contact with water (n=1.33) and the angle of incidence is 45°, dp is 0.064 λ_o, where λ_o is the <u>in vacuo</u> wavelength (Mattson et al., 1975). Eighty-four percent of a peak intensity observed in this example is from absorbing molecules within one dp of the interface, and 95 % of a peak intensity is due to molecules within two dp. Thus, for a peak at 1650 cm^{-1}, 95 % of the band intensity comes from a 7750 Å thin region at the germanium-water interface (Mattson et al., 1975). It is assumed that perfect contact exists at the interface which, however, with most solid materials is a problem. Therefore, working from the basis that several poor contacts will give a path length equivalent to one good contact, many internal reflection devices now are

multiple-reflection designs (attenuated total reflection or ATR) (Alpert et al., 1970, p. 339).

Protein-surface studies using IR/ATR spectroscopy

Infrared spectrometrists have relied on the positions and intensities of certain absorption bands in the infrared (IR) spectrum to help in interpreting the secondary structure of proteins (Mattson et al., 1975). Alpert et al. (1970, p. 281) provide a brief listing of these absorption bands. These bands are signified by the name Amide, and are followed by a Roman numeral to indicate the areas of the band in the IR spectrum.

Amide I: The amide I band appears to be primarily a C=O stretching vibration. For secondary amides (includes proteins), it is in the 1680 cm^{-1} - 1630 cm^{-1} range.

Amide II: The amide II band is found for both primary and secondary amides in the region from 1600 cm^{-1} to 1500 cm^{-1}. This band is apparently due to the vibration of several structural units such as -NH and CN. Study of N-methylacetamide has suggested that the band is 60% -NH bending and 40% CN stretch. The conformation of polypeptides (proteins) determines the position of this band. Koenig and Tabb (1980) indicate that the amide II vibration for proteins is mostly -NH bending.

Amide III, IV, and V: The amide III band is a vibration near 1290 cm^{-1} for secondary amides. The amide IV band appears between 630 cm^{-1} and 600 cm^{-1} for secondary amides. The amide V band occurs for hydrogen-bonded secondary amides near 720 cm^{-1}. The band is usually broad and of medium intensity.

Mattson et al. (1975) demonstrated the potential usefulness of IR/ATR techniques in studying a protein in its natural enviroment (aqueous) as it is adsorbed at an interface (germanium). By using a single protein solution of fibrinogen, they showed that the absorption bands that are characteristic of proteins could be resolved. Through the technique of spectral subtraction, they showed that the amide I band at 1640 cm^{-1} could be observed after removal of the water band at 1639 cm^{-1}. A shift was noted in the amide I position in going from a wet to a dried protein film condition, also. This change was not very large, from 1640 cm^{-1} (wet) to 1650 cm^{-1} (dry). From this, they attributed the observed 'splitting' in the amide I band maximum (two maxima, one at 1650 cm^{-1} and another at 1640 cm^{-1}) to possible combinations of strongly adsorbed (1650 cm^{-1}) and more 'native' protein (wet, 1640 cm^{-1}) in the interphase.

The actual use of FTIR/ATR spectroscopy is new in terms of studying the process of protein adsorption. The majority of the work done thus far has been accomplished at the Battelle Columbus Laboratories by Jakobsen and co-workers.

Gendreau and Jakobsen (1978) stated that molecular information on the adsorption process of proteins is almost nonexistent, and any information would be of great value. The study of surface-induced thrombosis led

Jakobsen et al. (1981) to propose five requirements that must be met. These requirements are:

1. The study must be done in a natural environment (i.e., aqueous)
2. The study must be physiological (i.e., in vivo or ex vivo)
3. It must be a flowing system (i.e., dynamic)
4. The technique must record events as they occur (i.e., real-time)
5. The technique must be sensitive enough to detect both major and minor components, and both major and minor changes.

The Battelle group suggests that FTIR/ATR spectroscopy represents the only technique that has a chance of meeting these requirements. Many of their experiments have been aimed at showing that this may be the case.

Gendreau et al. (1982) have shown that the identification of components of a binary protein solution (1:1 albumin - γ-globulin) can be accomplished through spectral subtraction. By taking the spectrum of the 1:1 mixture (after spectral subtraction of water) and spectrally subtracting a reference spectrum (i.e., albumin, also after water subtraction), the resulting spectrum closely matched the reference spectrum of the other component (i.e., γ-globulin, less the water band, also).

They have also demonstrated that kinetic studies can be made by plotting individual IR band intensities verses time. Depending on the IR band used, plots of the total amount of protein adsorbed or the relative amount of a particular protein adsorbed can be obtained. By plotting the intensity of the 1550 cm^{-1} amide II band (common to all proteins) versus time, it can be seen that the protein adsorption initially occurs very rapidly for about 45 seconds, after which it slows down (Gendreau et al.,

1981). The relative kinetics of individual proteins can be obtained by finding the ratio of characteristic peaks, also (Gendreau et al., 1982). For example, the relative kinetics of albumin to fibrinogen over time can be obtained by finding the ratio of the 1300 cm^{-1} band to the 1250 cm^{-1} band. This ratio appears to follow the relative depostion of these two proteins since the 1300 cm^{-1} band is due mainly to albumin, and the 1250 cm^{-1} band is mainly due to fibrinogen. This information was obtained from the study of a binary solution of 1:1 albumin-fibrinogen.

A summary of the protein adsorption behavior of the 1:1 albumin-fibrinogen has been described. For the first 1.5 minutes, the total amount of protein that will be adsorbed has occurred, and albumin appears to be the dominant species. For the next 6 minutes, its concentration in the adsorbate increases. The following 15 minutes shows fibrinogen replacing albumin. At the 19 minute mark, a conformational change in fibrinogen has occurred as indicated by changes in the 1250 cm^{-1} band. From this point on (up to 222 minutes), fibrinogen continues to replace albumin at the surface (Gendreau et al., 1982).

When using an ex vivo shunt as the supply of blood, this system gives much useful information. The initial spectra show that albumin and glycoproteins adsorb within the first few seconds. This is immediately followed by increased adsorption of fibrinogen and other proteins not identified. Albumin then seems to be replaced by other proteins (Gendreau et al., 1981).

From these experiments, the Battelle group seems to have shown that FTIR/ATR can satisfy the five requirements stated previously. They believed, however, the real-time requirement appeared to be a problem,

since the required S/N ratio meant spectral accumulation could only be carried out at 5 second intervals (Gendreau, 1982). With detector and software changes, useful spectra could be collected in Ø.8 seconds so that adsorption kinetics and transient changes could be followed with more confidence (Gendreau, 1982). This meant that it was possible to study the initial adsorption process more closely. With the previous system, it was determined that most of the total protein adsorbed occurred within 45 seconds. With the changes implemented, the newer system showed that this was true, also. However, half of the total protein adsorption occurred within 2Ø seconds. Also, by comparing successive spectra, it was shown that transient features occur within the first 3Ø seconds, some lasting only a few seconds long. It was noted that as spectra are obtained faster, the signal to noise ratio decreases, and thus, the sensitivity decreases (Gendreau, 1982).

Microstructural Details of Thrombogenesis

General

The general functional properties of platelets include adhesion, aggregation, release, procoagulant activity, and clot consolidation. It is through these functions that platelets are involved in the central role of hemostasis and thrombosis, and have minor roles in inflammation and immunological reactions. Morphological change in the platelet is usually associated with these functional expressions (Frojmovic and Milton, 1982).

Circulating platelets

It is generally agreed that 65-90 % of the circulating platelets in healthy donors are smooth, disc-shaped cells. The remaining 10-35 % have been less clearly defined. However, Frojmovic and Milton (1982) have developed a classification system. Using phase-contrast microscopy, the disc-shaped cells are referred to as discocytes (D). Viewed edge-on, these cells are ellipsoid with a clear center. While viewed face-on, they are circular with a dark center. Platelets that are circular with a white center are called spheroechinocytes (SE). Platelets that do not satisfy either of these criteria are called discoechinocytes (DE). Echinocyte is used to refer to DE and SE, collectively. Echinocytes usually have visible pseudopods (Frojmovic and Milton, 1982).

The surfaces of discocytes appear smooth and featureless, but closer examination reveals small protuberances and small openings or apertures. The small protuberances, or elevations, are present in both activated and unactivated platelets. The maximal cross section of the elevations is 0.3 x 0.3 μm^2. These protuberances are thought to be caused by the secretory granules projecting outward from the interior of the platelet. There are approximately 30 apertures in the surface of the discocyte and these are predominantly clustered along the periphery. The apertures are believed to be funnel-shaped, with wide variation in size (0.05-0.2 μm in diameter). The apertures are believed to be entrances into the surface-connected canalicular system. The apertures play a role in increasing the surface area of platelets during shape change, and may be involved in determining the sites of pseudopod formation (Frojmovic and Milton, 1982).

Activation of platelets generally leads to echinocyte formation from discocytes. A platelet shape change is defined as any morphological alteration in the platelet indicated by changes in volume and/or in the topology and surface area of the plasma membrane. The presence of pseudopods and a larger surface area differentiates the echinocytes from the discocytes. Upon stimulation, an equilibrium shift from predominate discocyte form to echinocyte form, and ultimately the spread form (on a solid surface), occurs, depending on the strength and length of stimulation (Lewis et al., 1980; Frojmovic and Milton, 1982). A tentative summary of the sequence of changes in platelet morphology in going from the discocyte to the echinocyte is provided by Frojmovic and Milton (1982). The presence of pseudopods 1-3 μm long, generated at the periphery of the discocyte without loss of discoidicity, is generally recognized as the initial step in platelet shape change. This step may be preceded, however, by a short-lived DE, which has only blunt pseudopods as suggested by interpretation of transmission electron microscopy information. Next, the body of the discocyte becomes more spherical with increased surface roughness (short, blunt pseudopods, 0.5 μm in major cross sectional diameter) and longer pseudopods. Finally, as the platelet body becomes more spherical, there is an increase in the number of long pseudopods and in blunt pseudopod number and size. The rate of shape change is often complete in less than 5 seconds (Frojmovic and Milton, 1982).

Surface-platelet interaction

Pseudopods, generated by platelets free in suspension or in contact with other platelets, are different from those generated in response to a

solid surface. Generally, the pseudopods formed on surfaces are immobile and not retractable unless acted on by a drug such as cytochalasin B. Pseudopods induced by adhesion to solid surfaces occur normally. However, it appears that these pseudopods are precursors to the formation of more morphologically varied pseudopods that lead to spreading of the platelet over the surface. Pseudopods on solid surfaces are able to branch, and with time, the hyalomere spreads radially over the surface to form a spread platelet with diameter of the order of 7 μm (Frojmovic and Milton, 1982).

Allen et al. (1979) cite three ways that the platelet undergoes spreading. The first involves the spreading of the hyalomere radially, either symmetrically or asymmetrically, without pseudopod formation. A second method involves hyalomere spreading radially as a 'web' between adjacent pseudopodia which have extended outward along the surface from 2 to 10 μm. The 'web' connects the pseudopods as it moves outward. The third method involves a thick pseudopod that extends, and then stops. The hyalomere then spreads laterally from the pseudopod. Using ciné films, all of these processes have been seen, sometimes more than one process taking place in different regions on the same platelet.

Pseudopod length can undergo dynamic alterations by spontaneous extension and retraction (Frojmovic and Milton, 1982; Allen et al., 1979). The process of pseudopod extension and retraction is an uncoordinated event. The variability in pseudopod extension velocity ranges from 0.75 to 7.5 μm/min. The maximum retraction velocity has been observed to be -1.9 μm/min. The spreading of the hyalomere is a much slower process than pseudopod extension. The time required to completely spread after contact with a surface is as little as 10-12 minutes, and is

seldom longer than 30 minutes. The initial velocity of hyalomere extension is 0.5 μm/min, but decreases as the platelet approaches the maximal spread state. The leading edge of the extending hyalomere is usually its thickest part, and it sometimes shows ruffling activity (Allen et al., 1979).

The transition from discocyte to echinocyte, as viewed with stereo scanning electron microscopy, shows that pseudopod development, once initiated, can proceed independent of any further surface contact. When viewed in stereo, it is seen that most cells transforming from discocyte to echinocyte are not always in full contact with the foreign surface. The state of partial contact continues as the spreading continues until the final stages of spreading, whereupon the cell shifts towards greater surface contact (Lewis et al., 1980).

Echinocyte surface area

The surface area of a discocyte is 18 μm^2, while the surface area of the main body of a spheroechinocyte (disregarding the pseudopods) is 13 μm^2. This means that 5 μm^2 of external plasma membrane is available to ensheath all of the pseudopods on the surface of the echinocyte. This corresponds to a single pseudopod of mean radius 0.075 μm and length 10 μm. Pseudopods of this length normally have a cylindrical cross section of 0.1-0.2 μm, with an average of 3-6 pseudopods per platelet. Thus, the surface area available from the external membrane is exceeded. Also, using a mean radius of 3.5 μm for spread platelets corresponds to a surface area of 70 μm^2, which is 4 times the area of a discocyte (Frojmovic and Milton, 1982).

Two possible sources for the additional membrane required for the shape change are 1) synthesis by the platelet or 2) externalization of already existing internal membrane. The first possibility is unlikely since platelets don't have enough of the membrane precursors for synthesis, and the rate of synthesis is slow compared to the rate of shape change (less than 5 seconds). Thus, it appears reasonable that the increase in surface area accompanying the transformation of discocyte to echinocyte is by externalization of internal membrane. The internalized membrane exists as surface-connected canalicular system, dense tubular system (which is not usually surface connected), and the membranes that enclose the granules. Studies using hypotonic media have been used to estimate the surface area that is internalized by the surface-connected canalicular system. Graded hypotonic solutions convert discocytes to echinocytes and, finally, to smooth-surfaced cells or spherocytes. Spherocytes are 100 % larger in surface area than discocytes, so the surface connected canalicular system can externalize 18 μm^2 of plasma membrane surface area. Still, sphereocyte surface area (30-40 μm^2) is smaller than spread platelet surface area (70 μm^2). Therefore, more internalized membrane must be externalized. This needed membrane probably comes from the granules that fuse with the plasma membrane during the release reactions. It has been estimated that the increase in total surface area as a result of the release reaction would be between 14 μm^2 and 32 μm^2. For a small membrane-bound vacuole, the surface area exceeds its volume so that incorporation of the vacuole membrane into the plasma membrane would increase the surface area out of proportion to its volume change. Thus, it appears that the induced shape change plays a role in the functions of the platelet. As the platelet transforms from

discocyte to echinocyte, the cytoplasmic organelles are concentrated into a region which facilitates the release of granule contents. The products released are then able to carry out their function such as procoagulation activity and clot consolidation (Frojmovic and Milton, 1982).

Shape change in relation to the release reaction

During the pseudopodial and early stages of spreading, the granulomere forms a dome-shaped hillock that contains many granules of different size. As the hyalomere flows from the hillock during spreading, the hillock gradually flattens out. Not all platelets spread, while others do so completely. Studies utilizing a differential interference contrast microscope to obtain a sequence of photomicrograghs, record dynamic changes in the structure of living platelets. The granules, such as the dense granules, can be seen to fuse to the external surface, and form craters. As release and spreading continue, the granules within the hillock become progressively more visible. The dense granules are seen to be greater than or equal to 0.3 μm in diameter, while smaller, less dense granules are 0.2 μm in diameter or less. The exocytosed contents of the dense granules (a particle visible with SEM) can usually be followed as granules rise out of the granulomere and settle on, or in the vicinity of, the platelet that released them. The degranulation process (release reaction) can occur at any time during the transformation process. There is a tendency of hyalomeres to overlap each other when platelets are crowded in a small area on the surface, suggesting that there is no contact inhibition. However, when a platelet falls on a platelet that has spread, it rarely spreads

itself. This appears to be a consequence of the top platelet being blocked by the spread platelet from making contact with the surface of the material. The top platelets may, however, form pseudopodia that are free, and may partially degranulate even though they have not spread. If a pseudopod can come in contact with the surface, it will induce shape change and spreading of that platelet, even on top of an already spread platelet. In aggregates, it is the bottom layer that shows fully spread hyalomeres, while platelets adhering to spread platelets underneath are only partially degranulated, and the pseudopods that have formed tend to interlock with pseudopods from adjacent platelets, holding the aggregate together (Allen et al., 1979).

Role of platelet zones in shape changes

The shape of the platelet is intimately tied with the sol-gel zone. The sol-gel zone contains several fiber systems in various states of polymerization which provide support for the discocyte shape and provide a contractile system for shape change, pseudopod extension and retraction, internal contraction (where the granules are concentrated in the center of the cell, forming the hillock of the granulomere), and secretion. The elements of the contractile system make up approximately 55 % of the total protein content of the platelet, thus comprising the major components of the platelet. Changes in the sol-gel zone are triggered by stimuli that bind to receptors in the peripheral zone. The peripheral zone accomplishes this by translating the signals received on the external surface into chemical messages that lead to the physical changes required for platelet activation and release (White, 1979).

Thrombogenesis and embolism on biomaterials

The exposure of flowing nonanticoagulated whole blood to a biomaterial results in platelet deposition and activation, thrombus formation, and embolization over a period of 0.5 to 60 minutes of blood contact. Using a catheter system, Wenning and Höpker (1981) showed that the first detectable change soon after contact with blood was a 'hiding' of the topology of the substrate by a morphologically detectable film that probably consists of adsorbed plasma proteins. Platelets are seen to adhere to the surface of a material after 0.5 minute of exposure. These adherent platelets exhibit short protuberances. However, some adhered cells are still in the discocyte form. From 0.5 to about 5 minutes of blood contact, there is an increase in the number of platelets adhered to the surface exhibiting significant shape change (Lelah et al., 1983). However, the largest increase in platelet deposition, coupled with further shape change, occurs between 5 and 10 minutes from initial contact with blood (Lelah et al., 1983; Barber et al., 1978). The thrombi peak in size and number at about the 20 minute mark of blood contact. The thrombi are composed mainly of platelets, with leukocytes seen occasionally. Thrombi usually range in size between 10 and 100 μm in diameter (although this is dependent on many conditions such as flow rate). The shape of the large platelet thrombi indicate that retraction may occur prior to, or in conjunction with, detachment (embolization). These thrombi are surrounded by an area almost completely denuded of platelets (Lelah et al., 1983). Adams et al. (1983) have studied the kinetics of platelet and thrombus formation using epifluorescent microscopy techniques on collagen-coated glass tubes. They have found that initial platelet adhesion appears to be a random

process. However, a study of the kinetics of thrombus formation shows trends that are not random. Most aggregates had elliptical bases with the major axis oriented in the same direction as the flow of blood. Growth of the thrombus, in both major and minor axes, was linear with time; the major axis growing at a faster rate than the minor axis. The base area of the thrombus grew at a rate of 0.074 $\mu m^2/sec^2$. One possible explanation of this type of growth is that conditioning of the platelets for adhesion may be the result of collision with the upstream edge of the aggregate. After this initial contact with the aggregate, the platelet could be further conditioned to adhere by the released products of the platelets in the aggregate. By the time the platelet has flowed to the distal edge of the aggregate, there may have been sufficient conditioning for adherence. However, it is not known how quickly a platelet can become activated under such conditions. Some thrombi lose small clumps of platelets from the surface, making the thrombus surface appear irregular (Barber et al., 1979). After 20 to 60 minutes of blood exposure, most of the large thrombi detach, leaving a lawn of single platelets or small aggregates. At early blood contact times, local variations in the density of the platelet lawn can be seen. During the peak deposition period around 15 minutes, areas covered with only a platelet lawn or small aggregates can be seen adjacent to areas where extensive thrombus formation has occurred (Lelah et al., 1983). Evidence of a dynamic equilibrium of formation and embolization of small thrombi usually occurs from this point onward (Goodman et al., 1984).

It has recently been suggested by Goodman et al. (1984) that highly thrombogenic surfaces induce more shape change and aggregation than less

thrombogenic surfaces. However, there is an apparent contradiction between highly thrombogenic materials, which have a low initial rate of platelet deposition, compared with less thrombogenic materials, which have higher initial depostion rates.

Properties of Materials

Silicone rubber

Silicone rubber (polydimethyl siloxane) is among the best polymers that are least active in thrombogenesis (Merrill and Salzman, 1978). Medical-grade silicone rubber can be divided into heat-vulcanizing types and room-temperature-vulcanizing types (commonly called RTVs) (Braley, 1970). The heat-vulcanizing type of silicone rubber contains a very pure, finely divided silica filler with a particle size of about 30 mμ in diameter. This filler is incorporated into the silicone rubber matrix to give the rubber sufficient strength. Generally, the more filler used, the harder the rubber is.

The RTV silicone rubber is divided into two component RTV (vulcanization requires a catalyst to be mixed into the base) and one component RTV (vulcanization is initiated by absorption of water vapor from the air). The two component RTV rubber contains diatomaceous earth particles for filler, ranging in size from 1 to 30 μm, with an average maximum diameter of 10 μm (R. T. Greer, personal communication, Biomedical Engineering, Iowa State University, 1984). The base is a fluid silicone polymer, mixed with filler and a cross-linking agent. Upon initiation (usually through the catalytic action of the organo-metallic

compound, stannous octoate), the silicone polymer units are cross-linked by the cross-linking agent (usually propyl orthosilicate) forming the silicone rubber with filler dispersed in the matrix (Braley, 1970).

Chawla (1978) has found that filler free silicone rubber has better compatibility with formed elements of blood compared with silicone rubber with filler (such as Silastic). This dichotomy of compatibility is based on the suggestion that the fewer the number of platelets adhering to a foreign surface, the less thrombogenic is that surface. No hypothesis is offered to explain the differences seen between filler free silicone rubber and silicone rubber containing filler.

Hydrogels

Hydrogel materials have been used in a wide variety of biomaterial applications. The reason for this is due to the physical properties of hydrogel materials and their resemblance to living tissue. One of the potential advantages of hydrogels is the low interfacial tension which may be exhibited between a hydrogel surface and an aqueous solution. The low interfacial tension should reduce the process of adsorption and unfolding of proteins from the body fluids (Ratner and Hoffman, 1976)

One of the problems of hydrogels is their inherent low strength. However, this problem can be overcome by radiation grafting techniques. Ratner et al. (1975) have used radiation grafting procedures for covalently bonding HEMA and NVP hydrogels to silicone rubber. When the hydrogel formed is poly(HEMA), the graft is localized on the surface of the silicone rubber as a coating, while the NVP graft is dispersed within the silicone rubber matrix as an impregnation. This accounts for the

differences in wettability of these two surfaces. Those that have poly(HEMA) surface grafts are hydrophilic, and exhibit the protein binding characteristics of hydrophilic surfaces (loosely held), while those that have NVP impregnation grafts resemble the hydrophobic character of the silicone rubber and exhibit the protein binding characteristics of a hydrophobic surface (tightly held).

Surface properties affecting thrombogenesis

Baier (1972) suggests that there are three primary surface characteristics that are important in determining the ultimate thrombogenicity of a biomaterial. These characteristics are surface texture, surface charge, and surface chemistry. Studying the surface chemistry of many biomaterials has lead to the suggestion of a hypothetical zone of blood compatibility. This zone is delineated by critical surface tension values of the surfaces of the materials in the range of 20 to 30 dynes/cm. Many of the materials that show good blood compatibility have critical surface tensions that fall within this range. Also, in support of this zone, independent research using cell culture techniques has shown that minimal cell attachment and cell spreading occurs on surfaces that have critical surface tensions in this range.

Lyman et al. (1968) found that for very short contact times with blood on hydrophobic surfaces (including Silastic®), there was a direct relationship between critical surface tension and the average number of adhered platelets. The average number of platelets adhered generally increases as the critical surface tension of a material increases. However, with increased contact times, these trends seem to be masked

(Dutton et al., 1968). Every surface studied eventually accumulated the same apparent saturated density of platelets, regardless of the original critical surface tension, although different fates during long-term implantations occurred among the materials tested (Baier, 1972).

Since a protein layer developes on a material very quickly after contact with blood, studies have been done to explain the relation between critical surface tension and how it influences the protein molecules that are adsorbed and which may have an effect on the activation of the clotting mechanism and the adhesion of platelets. It has been found that the ratio of native to denatured protein that has been adsorbed onto a high energy surface will be no more than 4:5, while a low energy surface can be up to 1:1, suggesting that the mechanism by which low critical surface tension materials have better blood compatibility is that it allows relatively more adsorption of proteins in less denatured states than high energy surfaces (Baier, 1972).

Another parameter that is important to thrombogenesis is surface roughness. Merrill and Salzman (1978) suggest that the criteria for roughness are different for protein molecules and cells. For example, peak-to-peak and peak-to-valley distance must be measured in terms of molecules (protein) and formed elements (cells). It is suggested that a peak-to-peak or peak-to-valley distance of 1000 Å is rough on the protein level while a distance of 10^2 μm to 10^8 Å is rough on the cellular level. A surface judged to be rough on the cellular level would be very rough on the molecular level. On the protein level, thrombogenesis can be activated if proteins are sheltered from dilution by the flowing blood in the roughness of the surface.

MATERIALS AND METHODS

Materials

Arteriovenous shunt model

An ex vivo model consisting of a femoral arteriovenous (AV) shunt made of, or coated with, a test surface of interest was used in mongrel dogs.

Shunt materials

Surfaces of the shunts tested were: (1) silicone rubber (SR); (2) silicone rubber with 2% filler concentration (2%SR); (3) silicone rubber with 12% filler concentration (12%SR); (4) five composites of 2%SR grafted with one of five hydrogels formulated from 20% HEMA to 20% NVP in a 15% methanol solvent (2%SR/20%H/0%N, 2%SR/15%H/5%N, 2%SR/10%H/10%N, 2%SR/5%H/15%N, 2%SR/0%H/20%N); and (5) five composites of 12%SR grafted with one of the hydrogels, also (12%SR/20%H/0%N, 12%SR/15%H/5%N, 12%SR/10%H/10%N, 12%SR/5%H/15%N, 12%SR/0%H/20%N).

Tubing for the shunts consisted of Silastic® tubing (Lot HH063212, Dow-Corning), 0.078" ID x 0.125" OD. Silastic® 382 elastomer (Lot HH082361, 28.9% filler (gm of filler/cc of filler-free elastomer), Dow-Corning) was used to prepare the silicone rubber with 2 or 12% filler concentration. The five hydrogels were prepared with solutions containing different concentrations of 2-hydroxyethyl methacrylate (HEMA) (Lot B889F9, Alcolac, Inc., Baltimore, MD) and N-vinyl-2-pyrrolidone (NVP) (Lot 236-12, Monomer-Polymer and Dajac Labs, Trevose, PA).

Methods

Shunt preparation

All solvents used were of reagent grade except hexane, which was of spectrophotometric grade. All references to water or distilled water refer to glass distilled water.

The bulk tubing was cut into sections 60 cm long. To remove any contaminants, the sections were flushed with a solution of 50% ethanol/50% water several times, and then rinsed several times with water before drying. One of these sections was used as the SR shunt.

The formation of silicone rubber with 2 or 12% filler concentration first involved filtering the filler out of Silastic® 382 elastomer to form filler-free elastomer. Mixing filler-free elastomer with unfiltered 382 elastomer in controlled proportions produces elastomer that can be vulcanized as a coat on the lumenal surface of a tube to form a surface of silicone rubber with a controlled amount of filler concentration.

The Silastic® 382 elastomer was mixed with hexane in a proportion of about 2-3 cc of elastomer to 10 cc of hexane in a 35 cc disposable syringe. A Metricel® membrane filter (Lot 3603072, Gelman Sciences, Ann Arbor, MI) with 0.2 μm pores was assembled and attached to the tip of the syringe before placing the syringe in an apparatus that applies pressure to the syringe plunger, forcing the elastomer/hexane solution through the filter while retaining the filler. The filtrate (filler-free elastomer and hexane) was heated a few degrees above room temperature on a hot plate to drive off any remaining hexane from the elastomer. Care was taken to prevent contamination of the filler-free elastomer from dirt and dust. To

determine the amount of filler-free elastomer to mix with the unfiltered 382 elastomer, the following equation was used:

$$\text{PERCENT FILLER} = \frac{(28.9)\ (X)}{(X)\ +\ (Y)}$$

where (X) = cc of unfiltered 382 elastomer

(Y) = cc of filler-free elastomer

When (X)+(Y) was held to equal 3.5 cc, 12 cc of hexane mixed with the 3.5 cc of elastomer mixture provided a mixture with desirable viscosity for coating the lumenal surface of the tubes.

Therefore, to coat 6 tubes with silicone rubber containing 2% filler, Ø.24 cc of unfiltered 382 elastomer was mixed with 3.26 cc of filler-free elastomer. This was mixed throughly with 12 cc of hexane added. While continually mixing, one drop of Catalyst M (stannous octoate, Lot HH111Ø94, Dow-Corning) was added. A syringe was attached to one end of a tube section while the other end was dipped into the elastomer solution. The syringe plunger was then withdrawn so as to draw elastomer up into the tube. When the elastomer completely filled the tube, the syringe was removed to allow the elastomer to run out, leaving a coating on the lumenal surface of the tube. Forcing the elastomer out by pushing the plunger back into the syringe was avoided because this action formed bubbles inside the tube. The tube was then hung vertically for 24-36 hrs to allow the elastomer coating to vulcanize and the hexane to evaporate. The tubes were carefully handled so as not to pinch or crimp them, insuring that the surface of the coating would be as smooth as possible. The same procedure was used to fabricate the 12%SR tubes except that 2.Ø cc of unfiltered 382

elastomer was mixed with 1.5 cc of filler-free elastomer. One each, of the 2% and 12% filler concentration tubes, was used as the 2%SR and 12%SR shunt surfaces, respectively. The rest of the tubes were grafted with one of five formulations of hydrogel.

Each of the five 2%- and 12%-SR tubes were filled with one of five nitrogen degassed hydrogel monomer solutions. The five formulations were (v/v):

1. 20% HEMA/ 0% NVP/ 12% methanol/ 68% water
2. 15% HEMA/ 5% NVP/ 12% methanol/ 68% water
3. 10% HEMA/ 10% NVP/ 12% methanol/ 68% water
4. 5% HEMA/ 15% NVP/ 12% methanol/ 68% water
5. 0% HEMA/ 20% NVP/ 12% methanol/ 68% water

Both ends of a filled tube were then securely tied, making sure that no leakage would occur and that no bubbles were introduced. The tubes were then irradiated in a ^{60}Co source providing a dose of 0.25 Mrad. Following irradiation, each tube was opened and flushed several times with a 50% ethanol/ 50% water solution, followed by several rinses with distilled water before being filled with, and stored in, distilled water. Twenty-four hours prior to implantation, the tube to be tested was flushed several times with saline before being filled with, and stored in, saline.

Implantation

Dogs weighing between 18-30 kg (Laboratory Animal Resources, Iowa State University, Ames, IA) were fasted overnight. Anesthesia was obtained by an intravenous injection of sodium pentobarbital (29 mg/kg body weight).

Proper anesthesia was maintained throughout the surgical procedure by injecting 0.5 cc of additional sodium pentobarbital as needed. The anesthetized dog was placed in a supine position with the legs extended to facilitate exposure of the desired location. Nonaseptic surgical technique was used.

Pre-surgical blood samples were drawn for activated coagulation time (ACT), platelet counts, and hematocrit measurement. Vacutainer® evacuated collection tubes containing 7.5 mg disodium edetate, an anticoagulant, were used to collect the blood samples for platelet counts and hematocrit measurement. Vacutainer® evacuated collection tubes containing 12 mg of purified siliceous earth were used to measure the ACT.

All platelet counts and hematocrit measurements were duplicated and recorded as the average. A Spencer "Bright Line®" hemacytometer (AO Instruments, Buffalo, NY) was used for counting platlets. Dilution of blood for the platelet counts was standardized by using 1.98 ml Unopette® reservoirs and 20 µl capillary pipettes (Becton-Dickinson, Rutherford, NJ). Capilets® nonheparinized capillary tubes (American Hospital Supply, Corp., Miami, FL) and an Adams hematocrit centrifuge (Clay-Adams, New York, NY) were used to measure the hematocrit values.

Preceding each implantation, a sample for FTIR (4 cm) and SEM (1-2 cm) was cut from the tube for evaluation of the sample before exposure to blood.

A 10-12 cm incision was made parallel to the femoral artery and vein. Blunt dissection was used to expose the vessels. The muscular branch was exposed, clamped with a small bulldog clamp, and cannulated with a 5 cm section of PE-190 tubing (Clay-Adams Co., Parsippany, NJ). The cannula was

secured with two ligatures. An 18 gauge needle attached to a 35 cc syringe was inserted into the end of the cannula. This assembly was used to flush the blood out of the shunt with saline after the time period of exposure elapsed. All other branches on the artery were ligated. The artery was clamped with a large bulldog clamp proximal to (or just upstream of) the femoral artery-muscular branch junction. Approximately 3-4 cm distal (down stream) to this clamp, one end of the tube to be tested (still filled with saline to avoid an air/blood interface or a possible air embolus) was inserted into the artery, and was secured with two ligatures. The other end of the tube was inserted into the femoral vein (also clamped to prevent backflow into the tube), and was secured with a single ligature to complete the ex vivo shunt.

To expose the tube to blood for a specified period of time, both of the clamps were removed simultaneously (the small clamp on the muscular branch remained in place during the exposure period). Once the time period had elapsed, the artery was reclamped in the same position as before, and the small clamp on the muscular branch was removed. Saline was then injected at about the same flow rate as the blood flow through the shunt during the exposure period. If clots were visible, the flush was gentle to prevent detachment. The time periods of cumulative blood exposure were: 0.25, 0.5, 5, 15, and 75 minutes. During the 0.25 and 0.5 minute time periods, the vein-end of the shunt was put into a graduated cylinder instead of the vein so that a starting flow rate could be determined. For all other time periods, the vein-end of the shunt was cannulated in the

vein. The flow rate during the Ø.25 minute time period was recorded as the starting flow rate.

After flushing, the small clamp was placed back in position. The vein-end was removed (if inserted) and cut for FTIR and SEM samples. The FTIR samples were placed in vials filled with saline, while the SEM samples were placed in vials containing a 2% gluteraldehyde solution for fixation. Once the samples were obtained, the vein-end was recannulated into the vein, and was secured with a ligature. Then the syringe was refilled with saline to begin the next time period.

After all time periods had elapsed and samples were collected, post-surgical blood samples were drawn for ACT, platelet counts, and hematocrit measurement to see if any changes had occurred during the procedure. An ending flow rate was determined as before. The dog was euthanized by injection of Sleepaway (Fort Dodge Laboratories, Fort Dodge, IA).

FTIR analysis

The samples to be used for FTIR were cut longitudinally through both sides of the tube with a No. 11 scalpel blade. Care was taken so as not to collapse the tube while cutting.

Preceding the collection of each spectrum, a 45° germanium crystal (5 mm x 5Ø mm x 1Ø mm, IBM Instruments, Danbury, CT) was cleaned with a micro cleaner solution. Methanol and hexane was used to clean the micro cleaner off. Cleaning was finished when a mirror-like surface was obtained. The germanium crystal was used because of its characteristic optics in the

region of interest and its handling properties. The crystal was then placed in an ATR crystal holder (IBM Instruments, Danbury, CT) which was then placed in an ATR alignment cell (IBM Instruments) which had been previously adjusted for optically passing the infrared beam through the crystal. The alignment cell was securely positioned in a nitrogen purge box inside an IBM IR/98 FTIR Spectrometer (IBM Instruments) so that realignment was not necessary for every sample. A reference spectrum of the crystal was then collected using the parameters found in Appendix A. After collection of the reference spectrum, the longitudinally sectioned samples were cut into 1 cm lengths and placed in the center on each side of the crystal. This provided a total sample surface area in contact with the crystal of about 0.62 cm^2. The samples were held tightly in place by a solid sample holder (IBM Instruments). The crystal/sample assembly was then replaced back in the alignment cell for collection of the sample spectrum using the same parameters used for the reference spectrum. A total of 12 spectra were collected for each shunt, an unexposed to blood spectrum and its reference spectrum, and each of the five samples exposed to blood for each of the time periods and their reference spectra. The following samples were collected in this manner: (1) SR, (2) 2%SR, (3) 12%SR, (4) 2%SR/20%H/0%N, (5) 2%SR/15%H/5%N, (6) 2%SR/5%H/15%N, (7) 12%SR/20%H/0%N, (8) 12%SR/15%H/5%N, and (9) 12%SR/10%H/10%N. After doing these samples in the described manner, it was found that the purge time (in the above manner, the purge time was only from the time the lid was closed on the purge box, after placing the crystal in the alignment cell, to the start of data collection; often less than 30 seconds) was not

long enough to purge the water vapor out of the purge box. Water vapor has absorbance bands in the region of interest. To avoid this problem, the purge time was increased to approximately 23 minutes by using a delay command on the computer before the start of data collection. It was also decided to cut the samples 1.5 cm long and to place two on each side of the crystal for the remaining samples for a surface area of 1.87 cm^2. This increased the effective surface area of the sample three times to the area of the other samples. The four remaining samples collected in this manner were: (1) 2%SR/10%H/10%N, (2) 2%SR/0%H/20%N, (3) 12%SR/5%H/15%N, and (4) 12%SR/0%H/20%N.

After all 156 spectra had been collected, a spectrum of saline and of water vapor were collected. The saline spectrum was collected using a liquid cell (Instrument Services, Iowa State University, Ames, IA) instead of a solid cell. The water vapor spectrum was obtained by collecting a spectrum of a clean crystal after a short purge time, and another after a long purge time.

An absorbance spectrum of a sample is obtained by using the AFN (arithmetic function parameter) set equal to AB (absorbance). The arithmetic function executes the equation, $-\log_{10}(SCA \cdot AFA)/(SCB \cdot AFA)$, on the appropriate data collected. With AFA (filename A for arithmetic function) set equal to the filename given to the sample spectrum, and AFB (filename B for arithmetic function) set equal to the filename given to the reference spectrum of the sample spectrum assigned to AFA, and SCA and SCB (scaling factors) set equal to 1, an absorbance plot or file can be

generated. Absorbance files for all 78 samples were obtained before any spectral subtraction was done.

The procedure followed for spectral subtraction was to take the absorbance spectrum of the sample and subtract the saline absorbance spectrum using the SAM (subtract absorbance manual) command with AFA set equal to the filename of the sample absorbance spectrum and AFB set equal to the filename of the saline absorbance spectrum. The subtraction was carried out while monitoring the 1640 cm^{-1} band. Subtraction was stopped just before any part of the 1640 cm^{-1} band (Amide I) began to go below the spectrum baseline. An absorbance file of the resulting spectrum was then generated. This was done for all 6 samples of each shunt (5 exposed, and 1 unexposed to blood). If the sample spectrum was one of the nine that were collected after inadequate purging, a water vapor subtraction was performed. Using the SAM command again, with AFA set equal to the filename given the absorbance file of the sample spectrum less saline, and AFB set equal to the filename of the absorbance spectrum of water vapor, subtraction of the water vapor was done until the water vapor bands were removed from the spectrum. The resulting spectrum was then used to generate yet another absorbance spectrum of the sample (sample less saline and water vapor). Finally, the last subtraction was to remove the base material of the shunt (unexposed to blood) from the protein and cellular elements on the shunt sample exposed to blood. This was accomplished, again, through the SAM command with AFA set equal to the filename of the absorbance spectrum of the sample exposed to blood (less saline and water vapor, if needed) and AFB set equal to the absorbance spectrum of the sample unexposed to blood (less saline and water vapor, if needed, also).

Subtraction was carried out until the 1256 cm^{-1} band common to silicone rubber found in both AFA and AFB was reduced back to the base line, or a first derivative was generated. This absorbance spectrum was plotted and stored. The plots of all the resulting spectra were obtained with the Y-axis (Absorbance Units) scaled so that all spectra were expanded the same.

SEM analysis

The samples for SEM analysis were also cut longitudinally through both sides of the tube using a No. 11 scalpel blade. Care was taken not to pinch the tube, which might destroy the surface features. The samples were then dehydrated in a series of acetone/water baths (30, 60, 75, 90, 100, 100% v/v), for 15 minutes in each bath, mounted on carbon stubs with 'Dag' Dispersion No. 154 (Achesun Colloids Co., Port Huron, MI), coated with 300 A of gold in a sputter coater, and examined in a JEOL-U3 SEM (Japanese Electron Optics, Tokyo, Japan).

Critical surface tension and contact angle values

Values of critical surface tension and contact angle (an inverse measure of wettability) were supplied by R. T. Greer (personal communication, Biomedical Engineering, Iowa State University, 1984). These values can be found in Appendix C.

RESULTS AND DISCUSSION

Results

Table 1 lists all pre- and post-surgical blood data for each dog used (one shunt per dog). These data show that, in general, most of the dogs were healthy, and no large changes in the data were seen as a result of the surgical procedure or exposure to the shunt. Ending flow rate values for some dogs increased, but this was probably due to the dog becoming 'light' in anesthesia (no additional sodium pentobarbital was injected if the final time period was almost complete). Dogs 4205 and 4214 (shunts 2%SR/0%H/20%N and 12%SR/10%H/10%N) had elevated platelet counts above the normal range which may have had an effect on the analysis of the shunts implanted.

All shunts remained patent for the entire 75 minutes of exposure to the blood. However, the 12%SR/10%H/10%N, the 12%SR/5%H/15%N, and the 12%SR/0%H/20%N shunts showed visible signs of reduced flow during the closing minutes of the procedure. These shunts had increased resistance to flushing with saline, and clots visible on the 12%SR/5%H/15%N and the 12%SR/0%H/20%N shunts were removed by the flushing procedure.

Table 2 lists the percent of area covered by thrombus on the samples exposed to blood for 15 minutes (calculated as the ratio of the projected area of the clot on the surface to the total surface area as measured on the samples prepared for SEM using a stereo dissecting microscope).

Figures 1a through 1m show histograms of the number of platelets adhered on the surfaces after each period of exposure. Platelets were counted in an area corresponding to 50 μm x 50 μm on 1000x SEM pictures. Trends of platelet build-up or platelet build-up and subsequent decrease are seen.

Table I. Pre- and post-surgical blood data

Dog Number	Shunt Surface	Flow Rate (cc/min) Pre-	Flow Rate (cc/min) Post-	ACT (seconds) Pre-	ACT (seconds) Post-	Platelet Count (no./µl) Pre-	Platelet Count (no./µl) Post-	Hematocrit (%) Pre-	Hematocrit (%) Post-
4174	SR	180	240	101	140	190,000	246,000	45	40
4145	2%SR	80	160	112	136	324,000	309,000	45	45
4143	12%SR	80	160	91	105	332,000	300,000	47	48
4102	2%SR/20%H/0%N	100	240	130	116	392,000	393,000	46	47
4063	2%SR/15%H/5%N	144	192	101	101	350,000	320,000	49	45
4219	2%SR/10%H/10%N	128	240	107	95	410,000	332,000	41	38
4181	2%SR/5%H/15%N	152	168	117	109	391,000	391,000	46	47
4205	2%SR/0%H/20%N	160	205	117	91	541,000	495,000	43	33
3587	12%SR/20%H/0%N	128	240	99	109	322,000	264,000	49	44
4126	12%SR/15%H/5%N	168	152	95	98	264,000	286,000	49	48
4214	12%SR/10%H/10%N	152	220	129	128	501,000	473,000	44	45
4157	12%SR/5%H/15%N	128	184	106	98	243,000	201,000	47	38
4242	12%SR/0%H/20%N	160	300	108	100	231,000	231,000	40	41

Figures 2a, 2b, and 2c show histograms of the number of platelets adhered after 15 minutes of exposure. Figures 2d, 2e, and 2f show the associated critical surface tension of the surfaces in histogram form.

Table 2. Percent of area covered with thrombus after 15 minutes of exposure to blood

Shunt surface	% Thrombus covered
SR	< 1
2%SR	< 1
12%SR	< 1
2%SR/20%H/0%N	< 1
2%SR/15%H/5%N	< 1
2%SR/10%H/10%N	< 1
2%SR/5%H/15%N	< 1
2%SR/0%H/20%N	7
12%SR/20%H/0%N	< 1
12%SR/15%H/5%N	< 1
12%SR/10%H/10%N	< 1
12%SR/5%H/15%N	90
12%SR/0%H/20%N	3

SEM analysis of shunt surfaces

Unexposed Figures 3 through 15 show the surfaces of all the shunts tested before being exposed to whole flowing blood. The SR surface (Figure 3) shows the roughness of the tubes as they are received, after cleaning. Close examination reveals a regular pattern of 'ridges' which are probably due to the manufacturing process. The 2%SR surface (Figure 4) shows a surface that is smoother, due to the coating, except for the roughness caused by the diatomaceous earth filler that was incorporated into the silicone rubber matrix of the coating. The filler appears to be evenly mixed throughout the coating, but it is not known if the filler is

Figure 1. Histograms of platelet count after each time period of exposure to blood. Asterisk (*) indicates cases where no count was made because there was a red clot (Figure 1K) or the clot was flushed (Figure 1M)

Formulation	Figure
SR	A
2%SR	B
12%SR	C
2%SR/20%H/0%N	D
2%SR/15%H/5%N	E
2%SR/10%H/10%N	F
2%SR/5%H/15%N	G
2%SR/0%H/20%N	H
12%SR/20%H/0%N	I
12%SR/15%H/5%N	J
12%SR/10%H/10%N	K
12%SR/5%H/15%N	L
12%SR/0%H/20%N	M

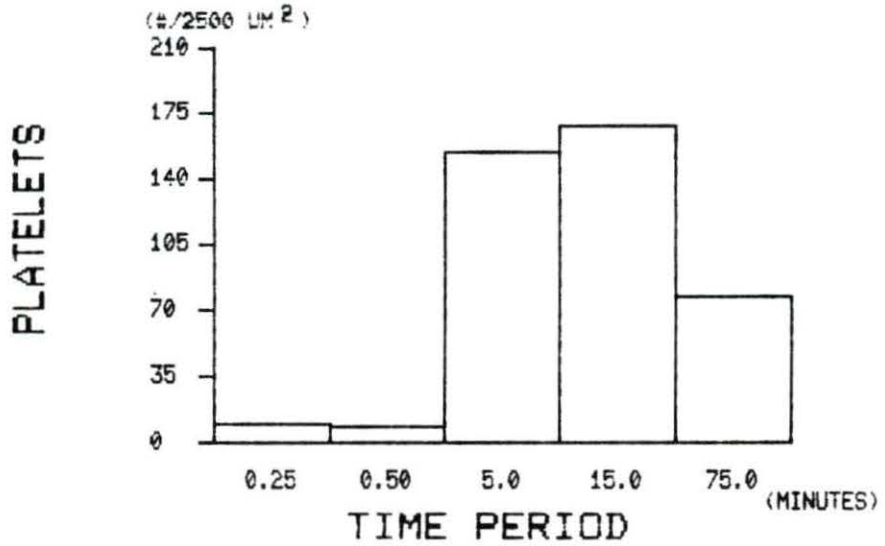
(#/2500 UM 2)
210
175
140
105
70
35
0
PLATELETS
0.25
0.50
5.0
15.0
75.0
(MINUTES)
TIME PERIOD

A

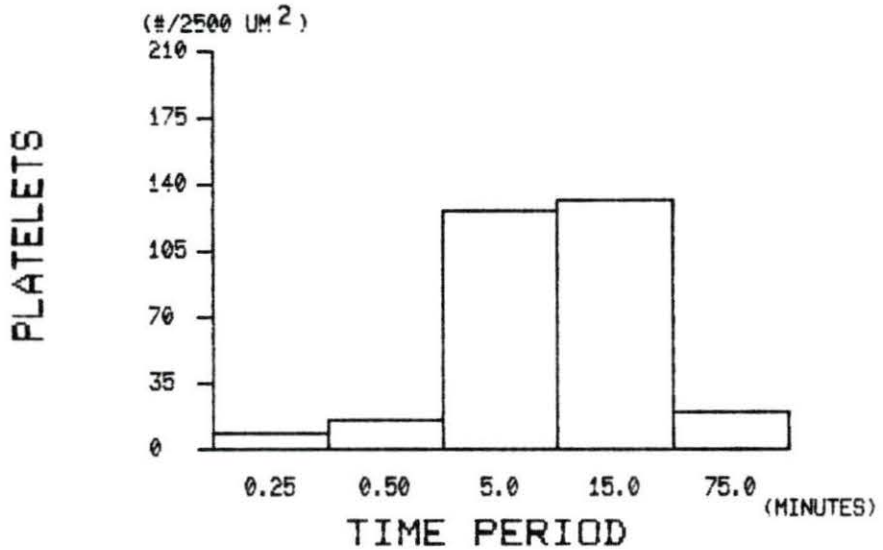
(#/2500 UM 2)
210
175
140
105
70
35
0
PLATELETS
0.25
0.50
5.0
15.0
75.0
(MINUTES)
TIME PERIOD

B

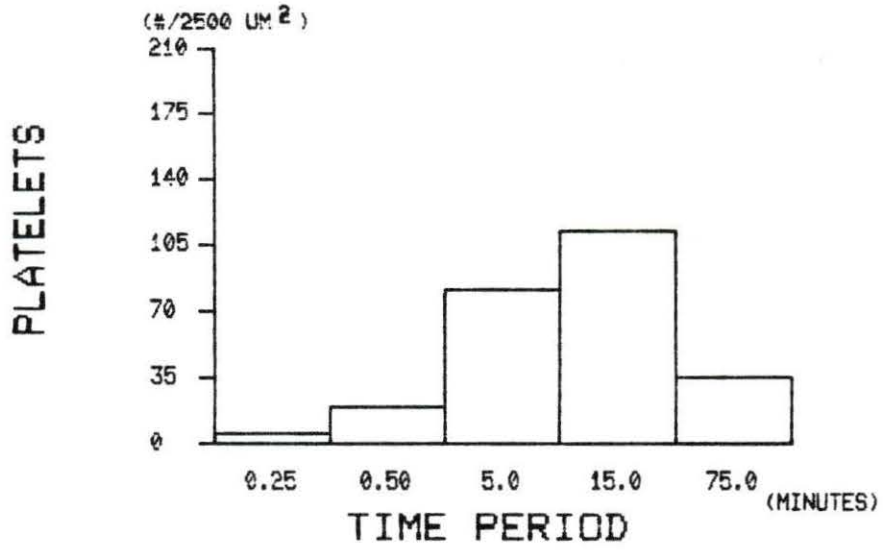

C

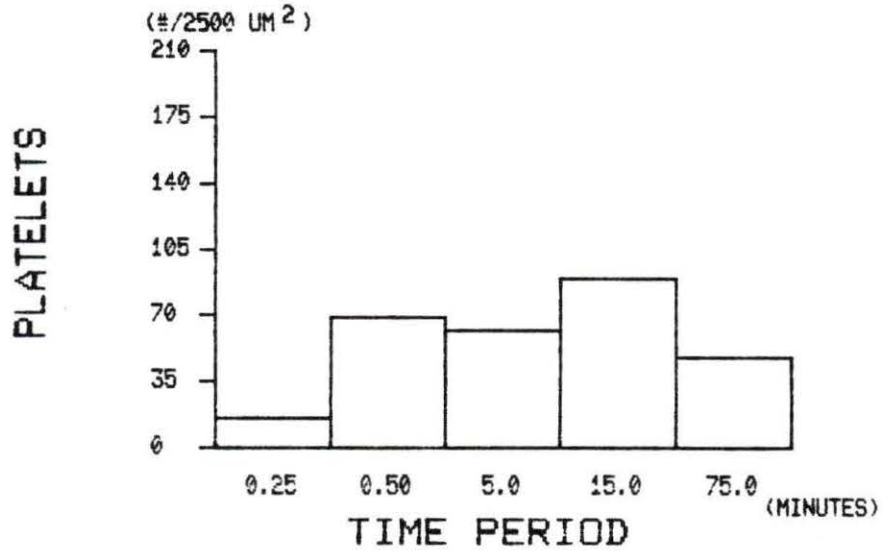

D

Figure 1. (continued)

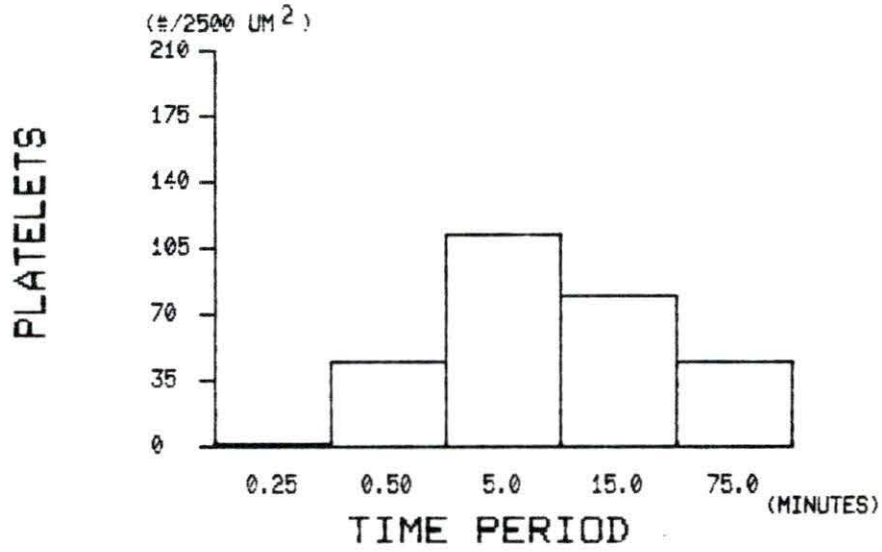

E

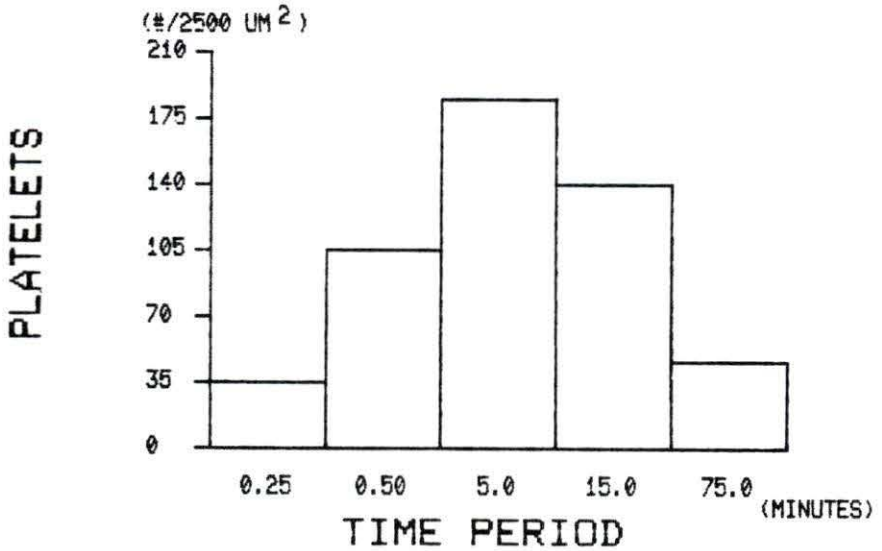

F

Figure 1. (continued)

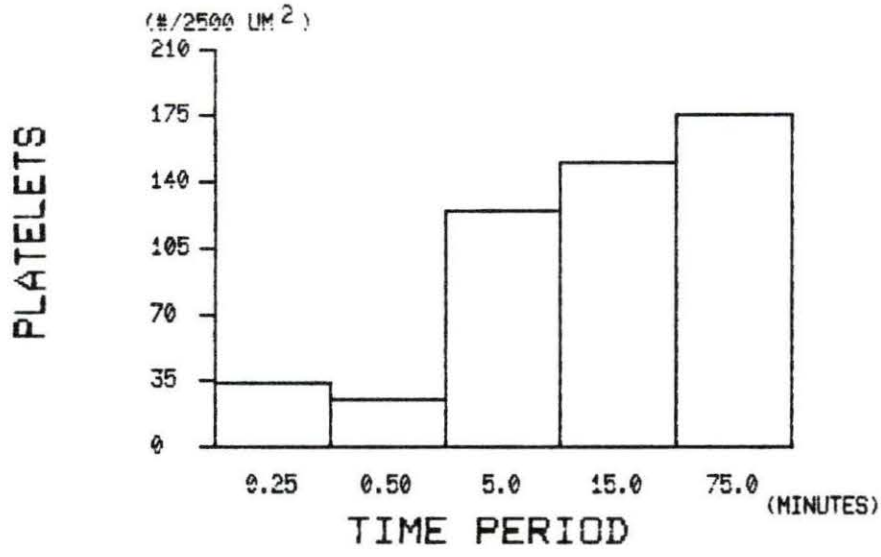

G

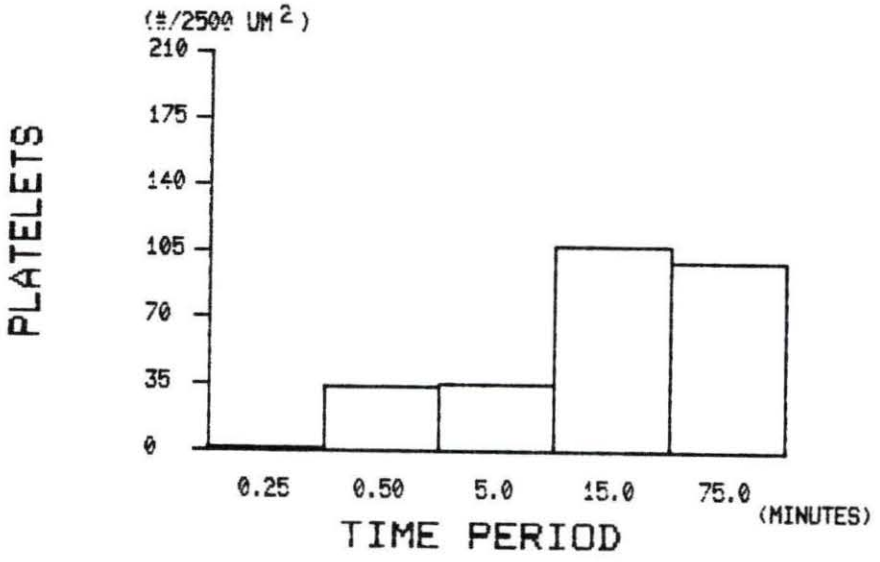

H

Figure 1. (continued)

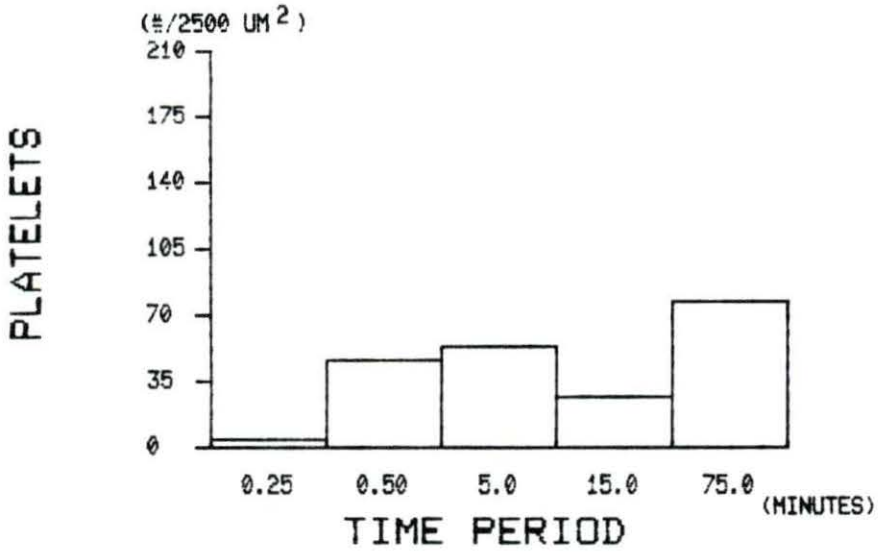

I

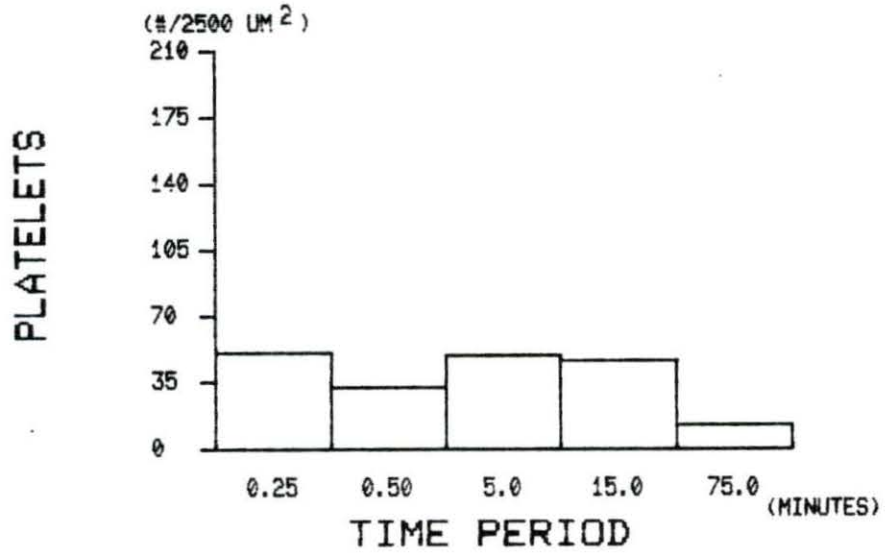

J

Figure 1. (continued)

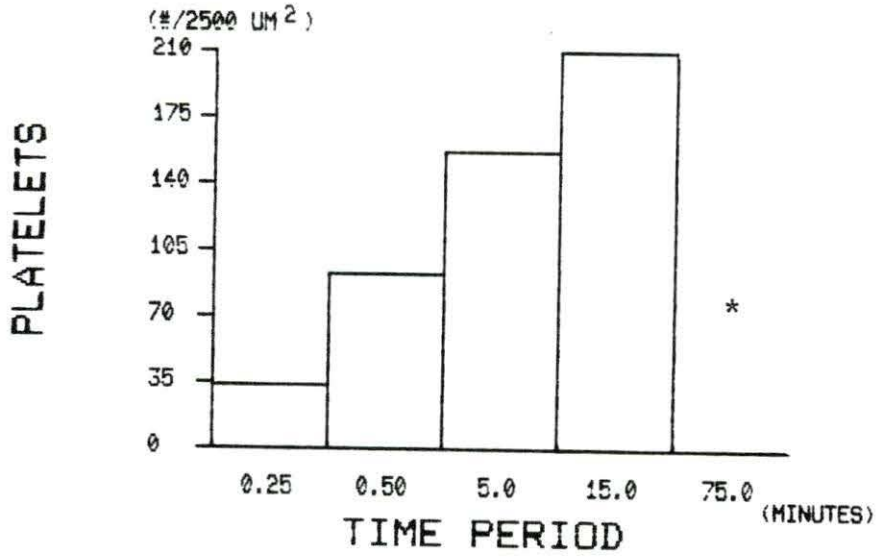

K

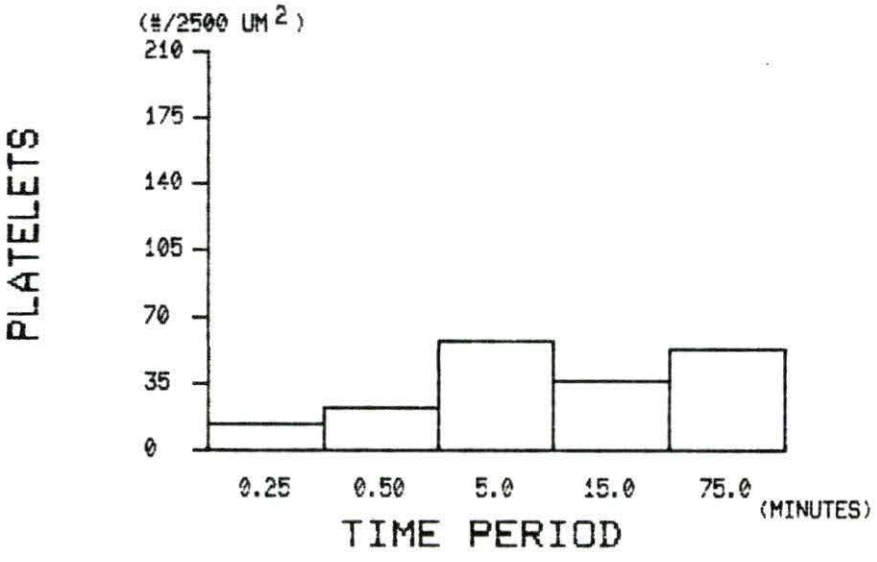

L

Figure 1. (continued)

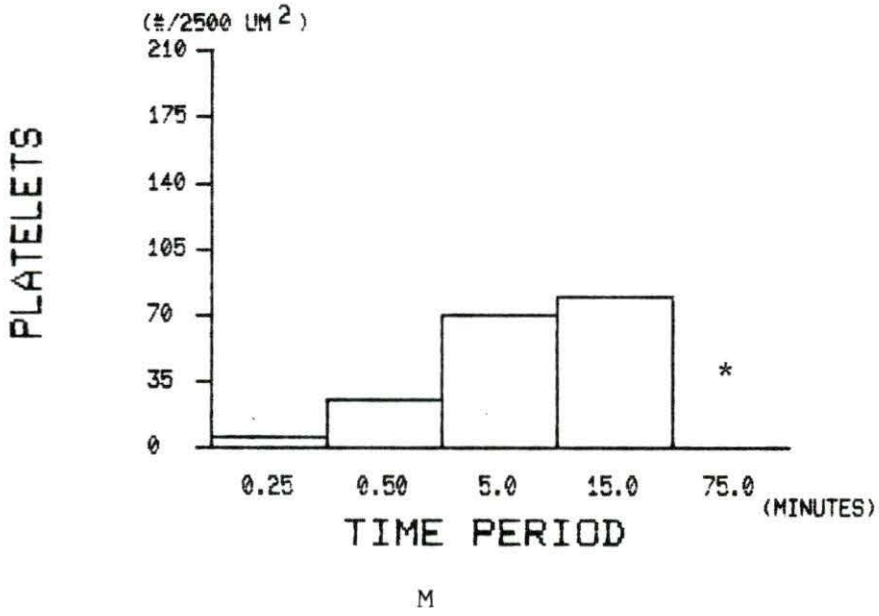

Figure 1. (continued)

Figure 2. Histograms of platelet count after 15 minutes of exposure to blood and critical surface tension for each shunt formulation

Formulation	Figure (Platelet count)	Figure (Critical surface tension)
SR	A	B
2%SR	A	B
12%SR	A	B
2%SR/20%H/0%N	C	D
2%SR/15%H/5%N	C	D
2%SR/10%H/10%N	C	D
2%SR/5%H/15%N	C	D
2%SR/0%H/20%N	C	D
12%SR/20%H/0%N	E	F
12%SR/15%H/5%N	E	F
12%SR/10%H/10%N	E	F
12%SR/5%H/15%N	E	F
12%SR/0%H/20%N	E	F

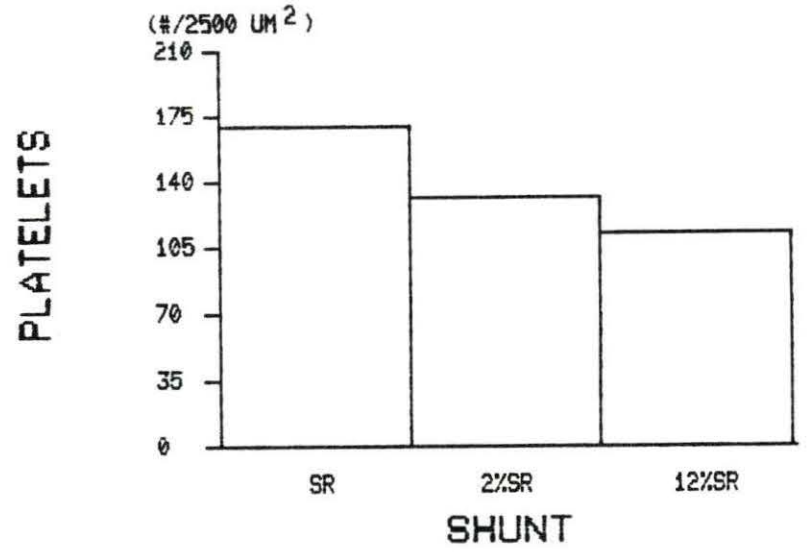
PLATELETS
(#/2500 UM 2)
210
175
140
105
70
35
0
SR
2%SR
12%SR
SHUNT

A

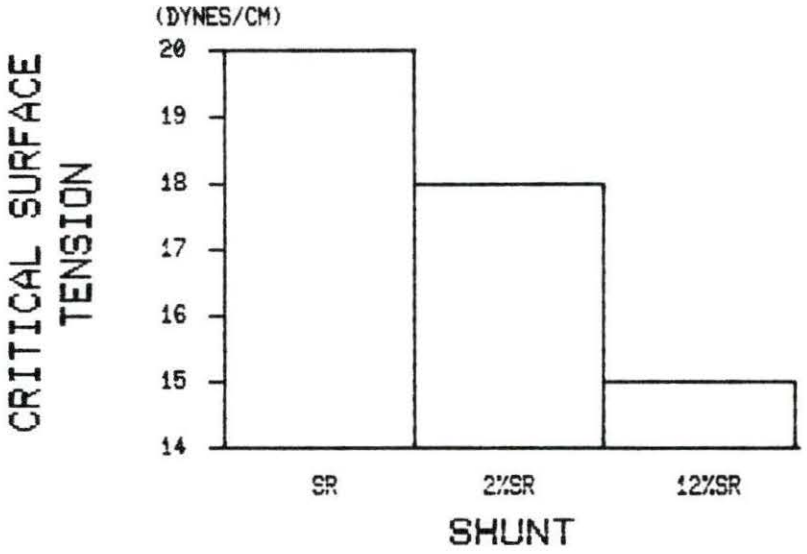
CRITICAL SURFACE TENSION
(DYNES/CM)
20
19
18
17
16
15
14
SR
2%SR
12%SR
SHUNT

B

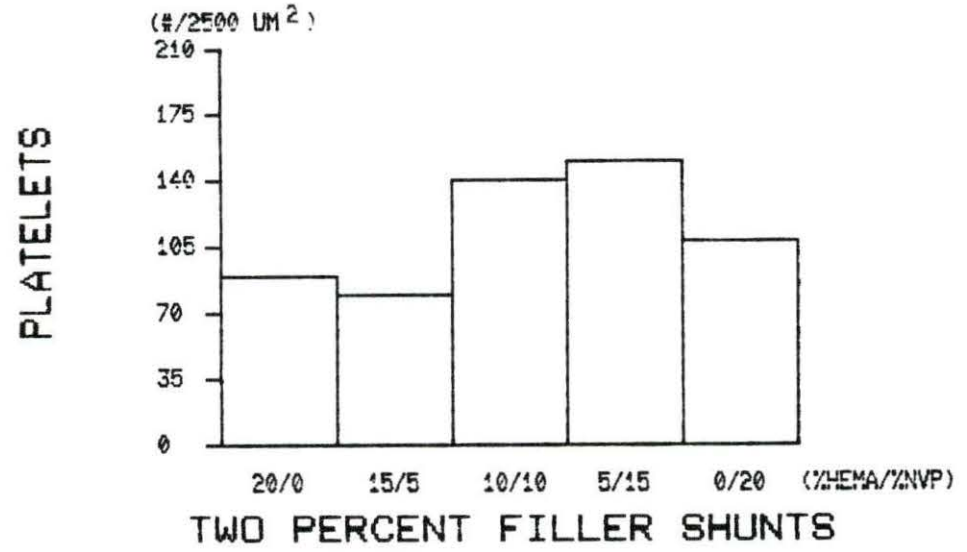

C

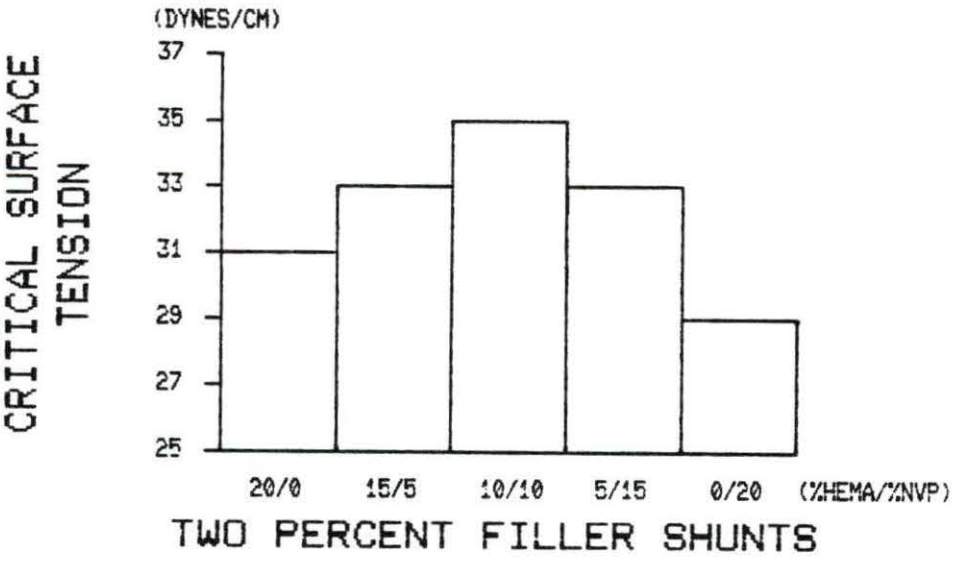

D

Figure 2. (continued)

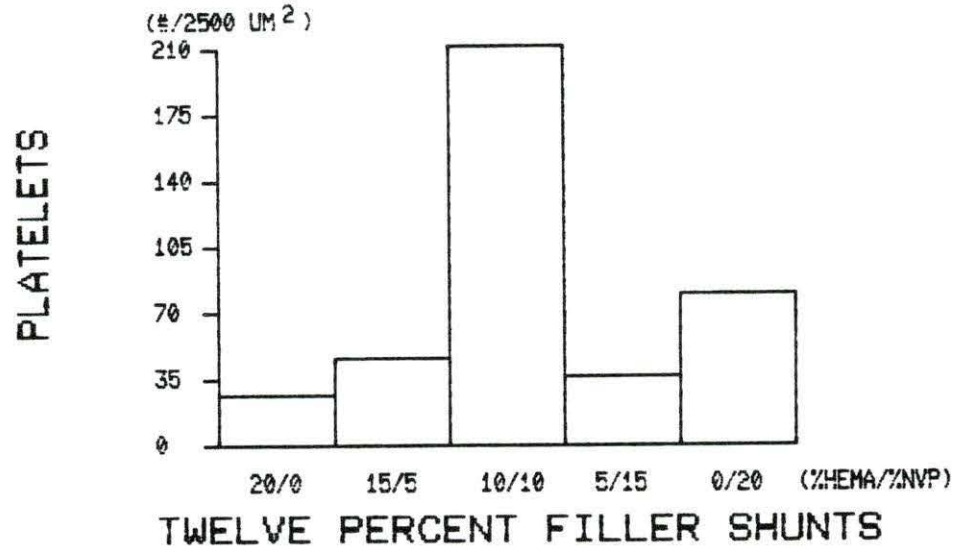

E

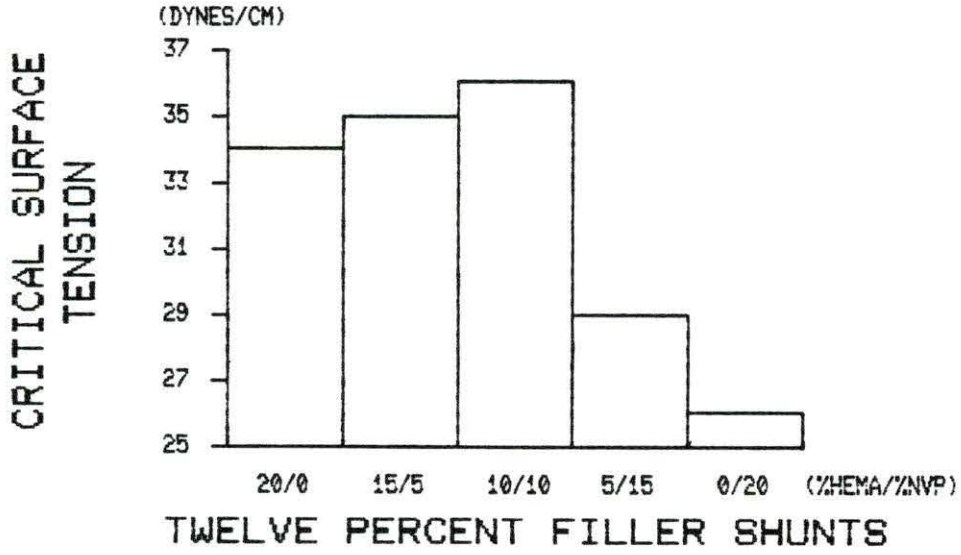

F

Figure 2. (continued)

Figure 3. SEM micrograph of SR shunt before exposure to blood. (scale bar = 10 μm)

Figure 4. SEM micrograph of 2%SR shunt before exposure to blood. (scale bar = 10 μm)

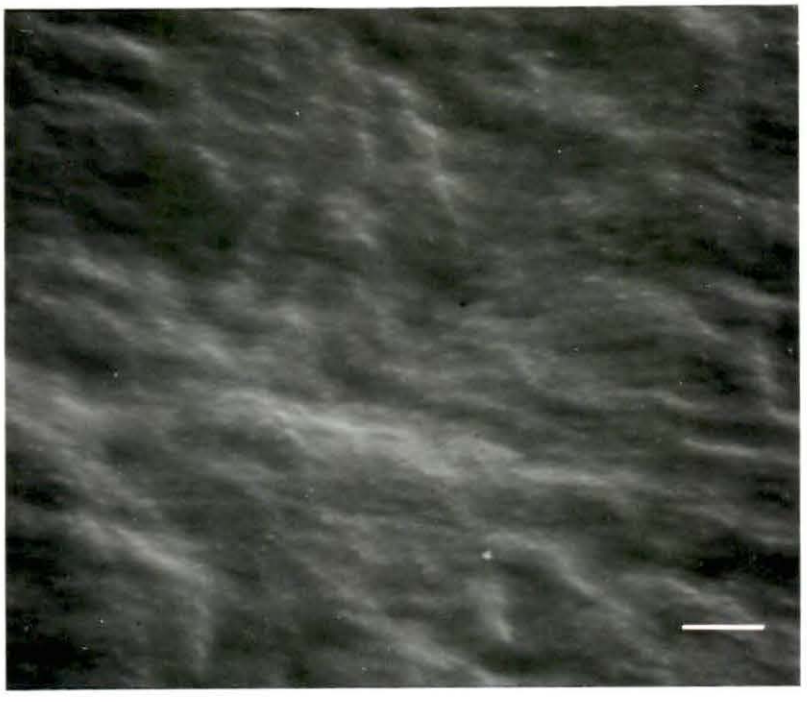

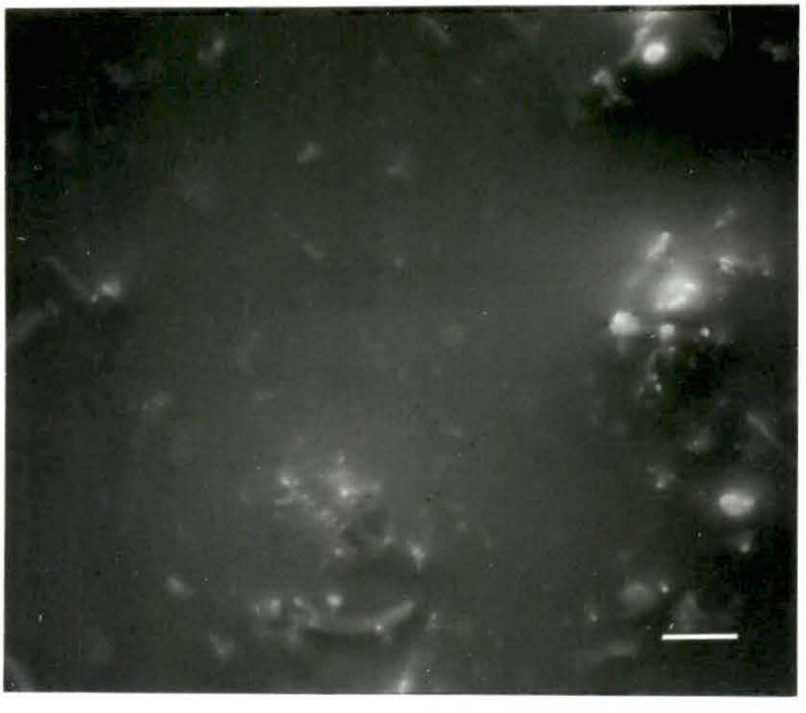

Figure 5. SEM micrograph of 12%SR shunt before exposure to blood. (scale bar = 10 μm)

Figure 6. SEM micrograph of 2%SR/20%H/0%N shunt before exposure to blood. (scale bar = 10 μm)

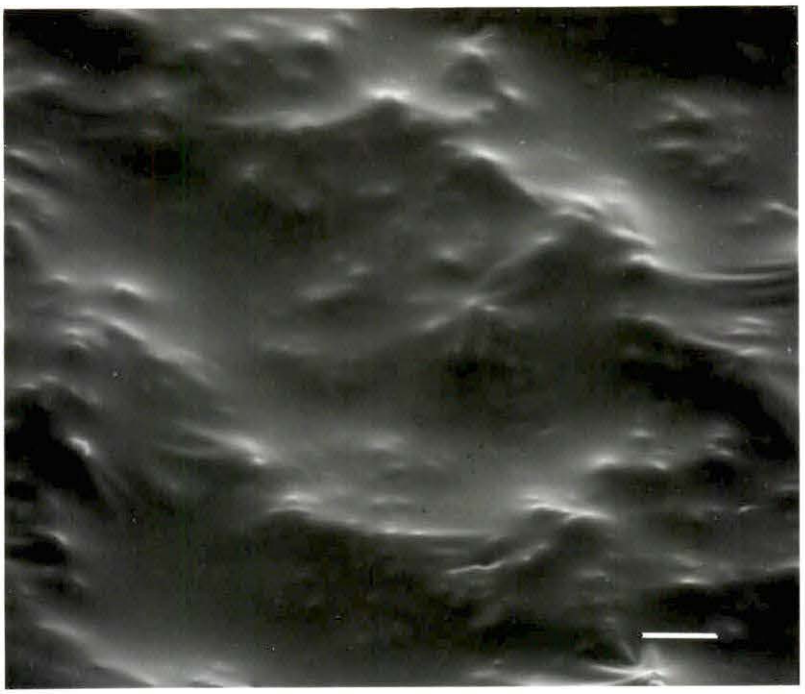

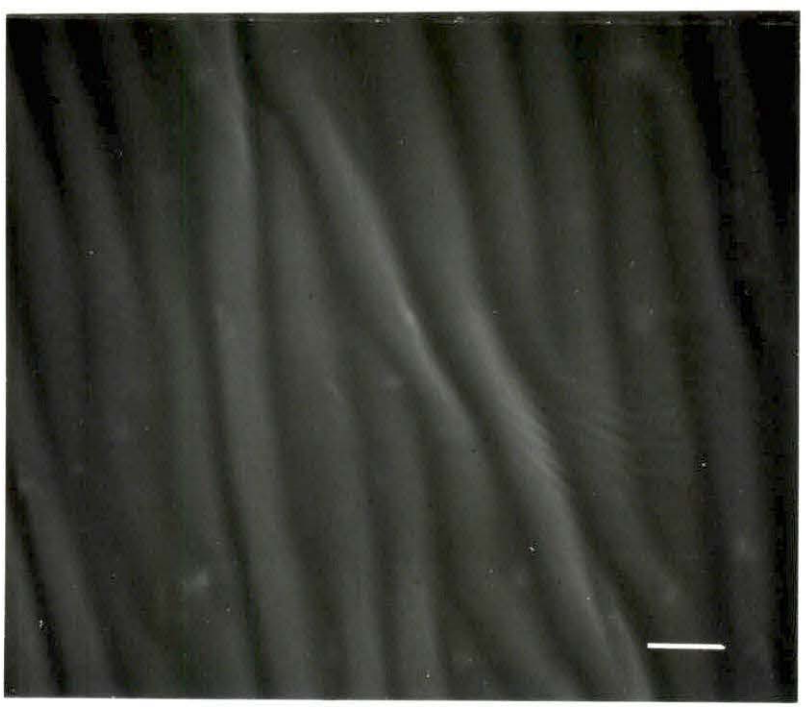

Figure 7. SEM micrograph of 2%SR/15%H/5%N shunt before exposure to blood. (scale bar = 10 μm)

Figure 8. SEM micrograph of 2%SR/10%H/10%N shunt before exposure to blood. (scale bar = 10 μm)

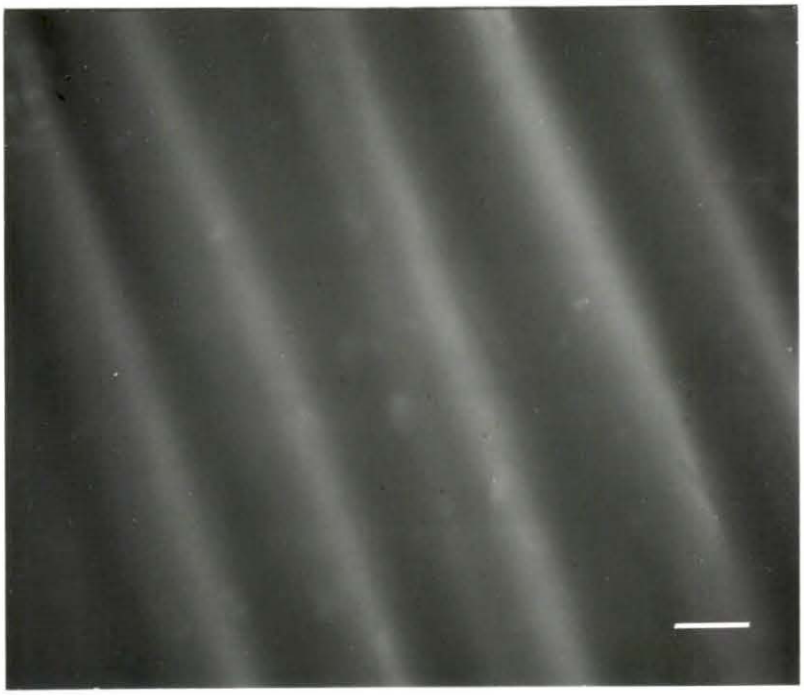

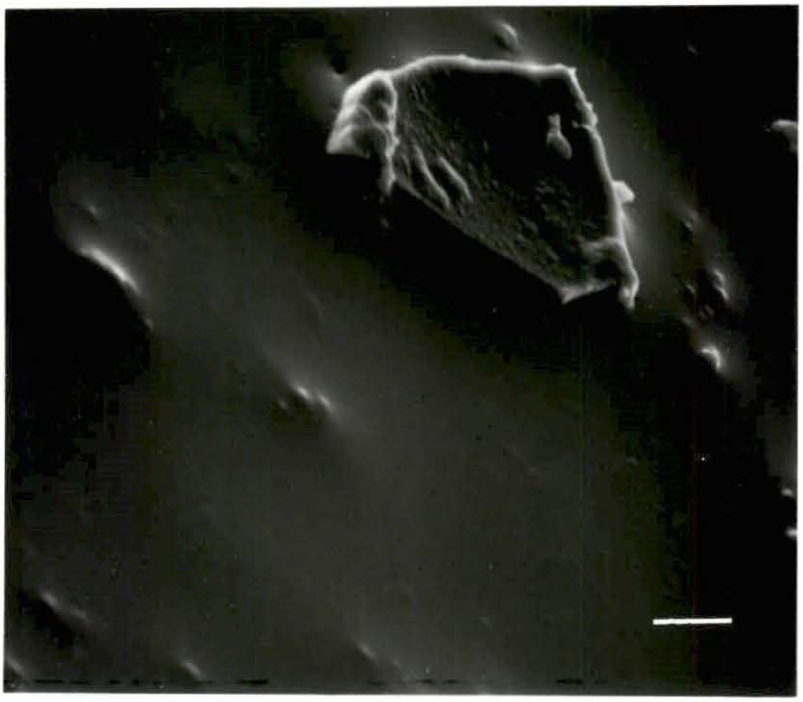

Figure 9. SEM micrograph of 2%SR/5%H/15%N shunt before exposure to blood. (scale bar = 10 μm)

Figure 10. SEM micrograph of 2%SR/0%H/20%N shunt before exposure to blood. (scale bar = 10 μm)

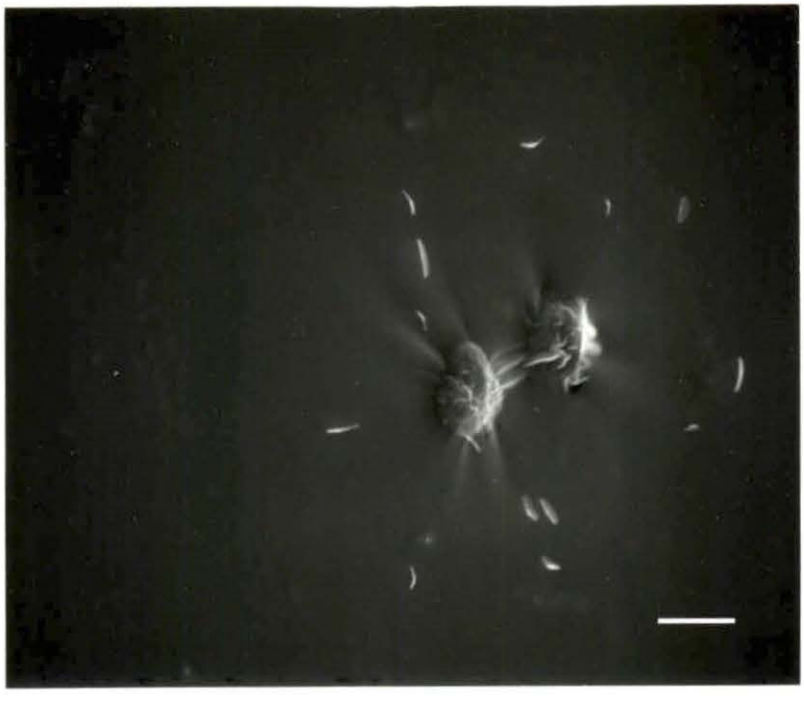

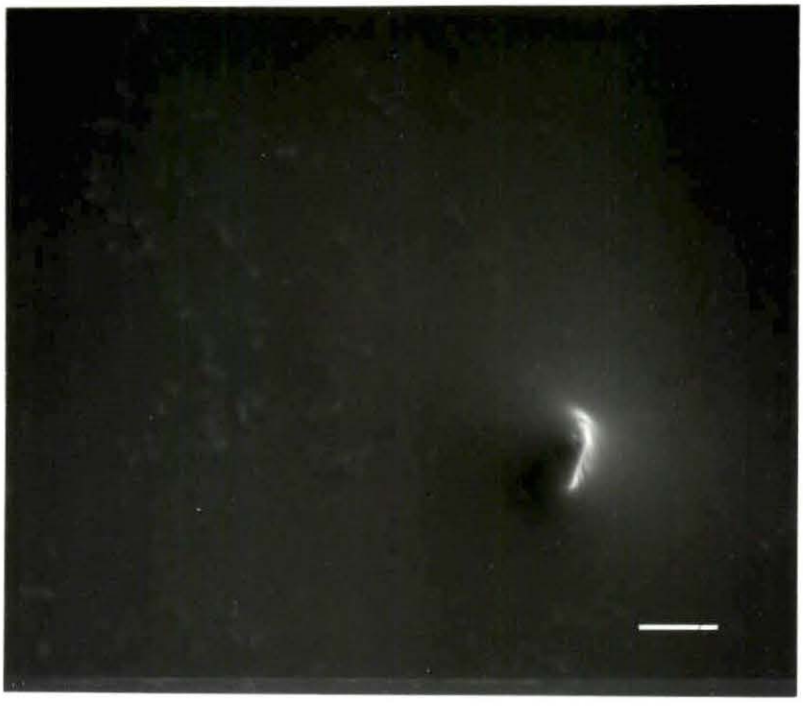

Figure 11. SEM micrograph of 12%SR/20%H/0%N shunt before exposure to blood. (scale bar = 10 μm)

Figure 12. SEM micrograph of 12%SR/15%H/5%N shunt before exposure to blood. (scale bar = 10 μm)

Figure 13. SEM micrograph of 12%SR/10%H/10%N shunt before exposure to blood. (scale bar = 10 μm)

Figure 14. SEM micrograph of 12%SR/5%H/15%N shunt before exposure to blood. (scale bar = 10 μm)

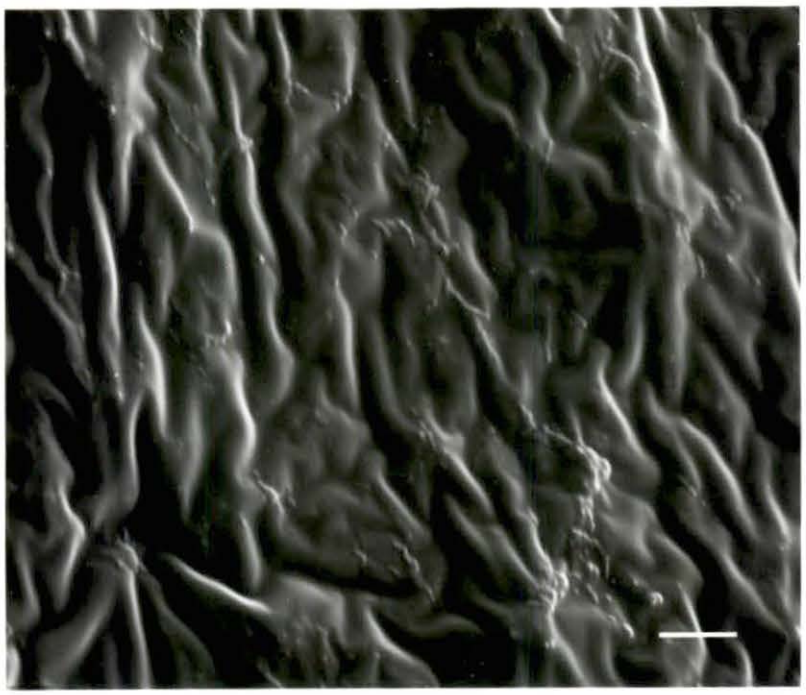

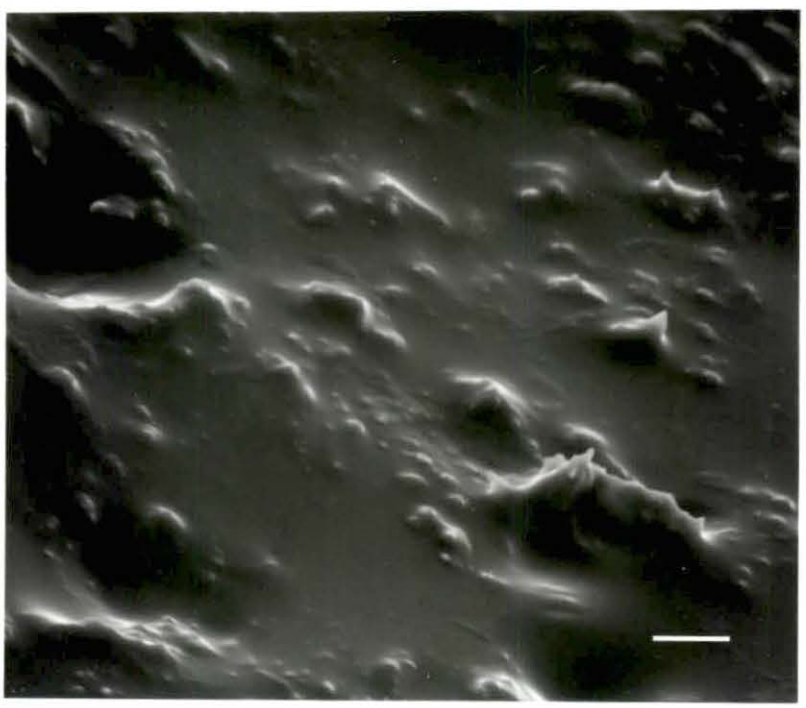

completely covered by silicone rubber. Figure 5 shows the 12%SR surface, which is similiar to the 2%SR surface except for the noticeable increase in filler concentration distributed in the coating as indicated by an increase in surface roughness. Figures 6 through 15 show the shunts which were grafted with a hydrogel. In general, the shunts grafted with a high percentage of HEMA diplayed a smooth surface while those grafted with a high percentage of NVP showed roughness similiar to that seen on the 2%SR and 12%SR shunts caused by the filler. There is a gradient-effect of smoothness on the shunts from very smooth shunts which were grafted with 20% HEMA to very rough shunts grafted with 20% NVP. Figure 16 shows the cross section of the 12%SR shunt. This cross section is typical of the shunts with coatings and grafts of hydrogel. The coating was approximately 150 μm in thickness. However, the actual thickness of the coating probably varied throughout the length of the tube due to gravity effects during the vulcanizing process. The hydrogel graft thickness was negligible by comparison.

15 seconds exposure Figure 17 shows the SR surface after exposure to blood for 15 seconds. A loss of the surface texture seen in the unexposed SR surface is apparent. There is a small number of platelets in both the discocyte and echinocyte form adhered to the surface, also. Residual contaminants are seen on the surface, occasionally. The 2%SR surface (Figure 18) also shows a loss of surface roughness. Platelets seen only in the discocyte form are adhered to the surface. Figure 19 shows the 12%SR surface with a loss of surface roughness, also. Platelets in discocyte form only are seen adhered to the surface. The 2%SR/20%H/0%N surface (Figure 20) is still very smooth. Platelets are seen adhered in the

Figure 15. SEM micrograph of 12%SR/0%H/20%N shunt before exposure to blood. (scale bar = 10 μm)

Figure 16. SEM micrograph of 12%SR shunt showing a cross sectional veiw. Note coating thickness of the 12% filler silicone rubber. (scale bar = 250 μm)

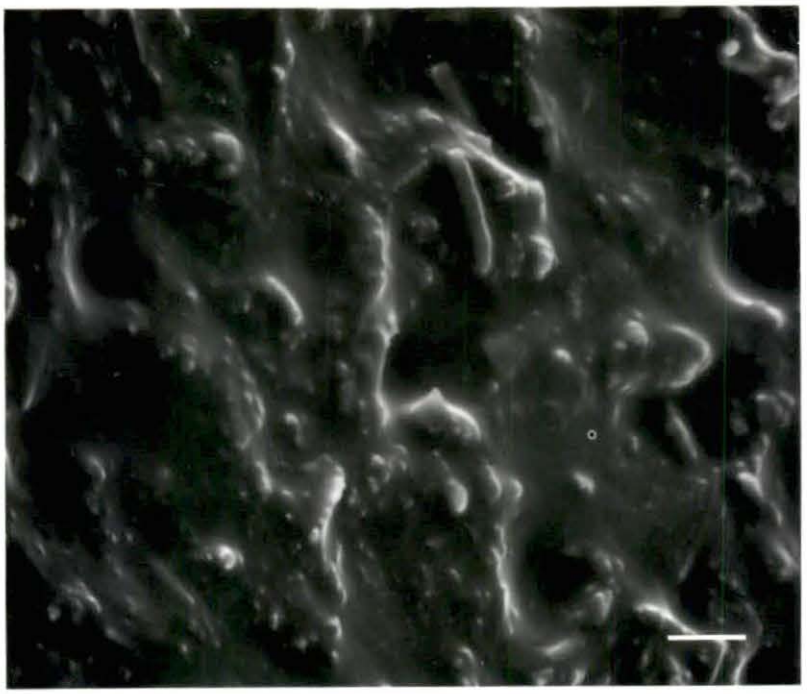

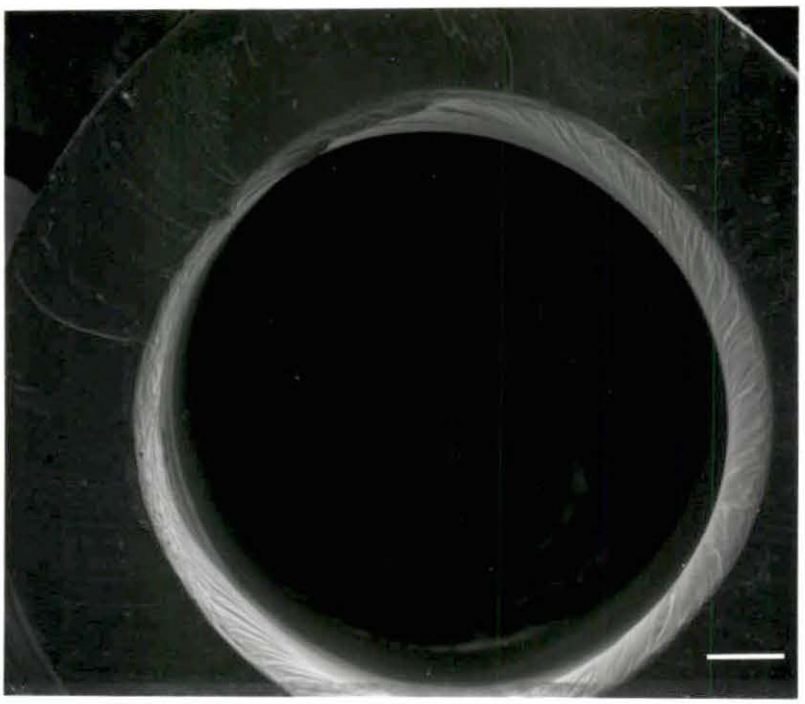

Figure 17. SEM micrograph of SR shunt surface after 0.25 minute exposure to blood. (scale bar = 10 μm)

Figure 18. SEM micrograph of 2%SR shunt surface after 0.25 minute exposure to blood. (scale bar = 10 μm)

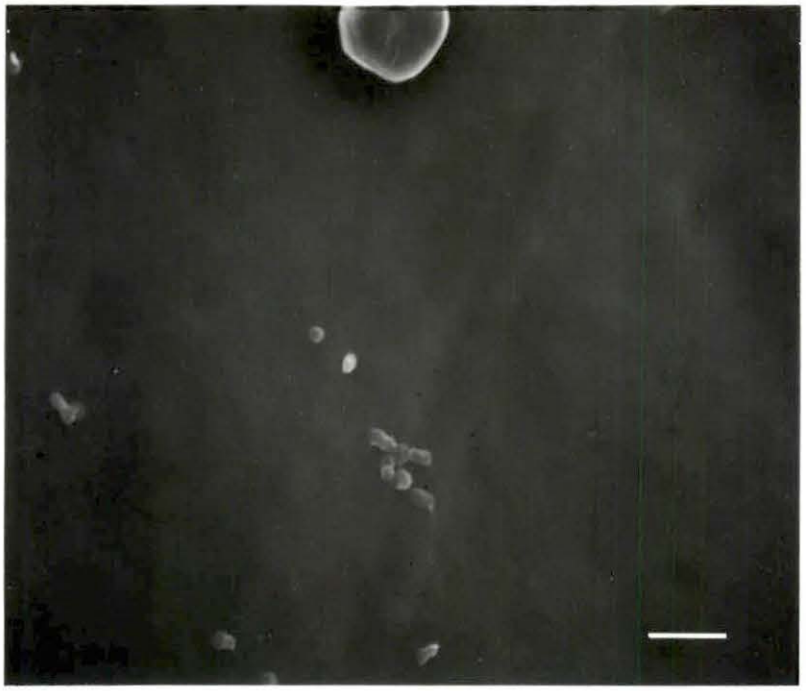

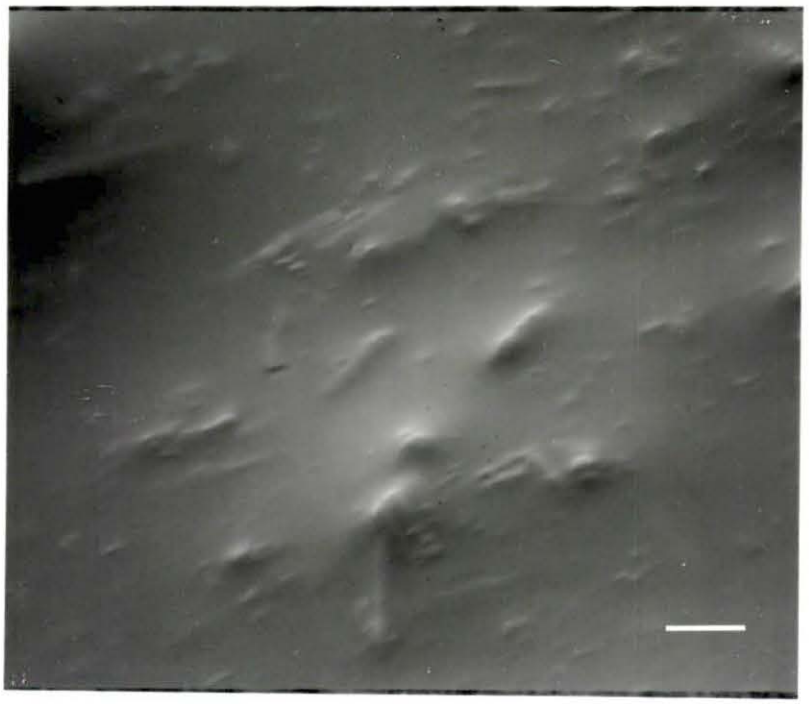

Figure 19. SEM micrograph of 12%SR shunt surface after Ø.25 minute exposure to blood. (scale bar = 1Ø μm)

Figure 2Ø. SEM micrograph of 2%SR/2Ø%H/Ø%N shunt surface after Ø.25 minute exposure to blood. (scale bar = 1Ø μm)

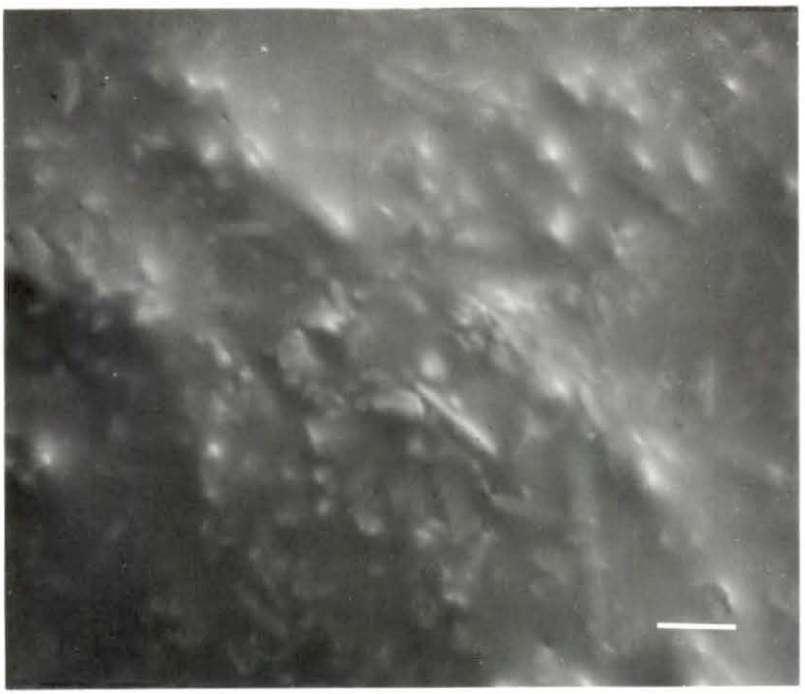

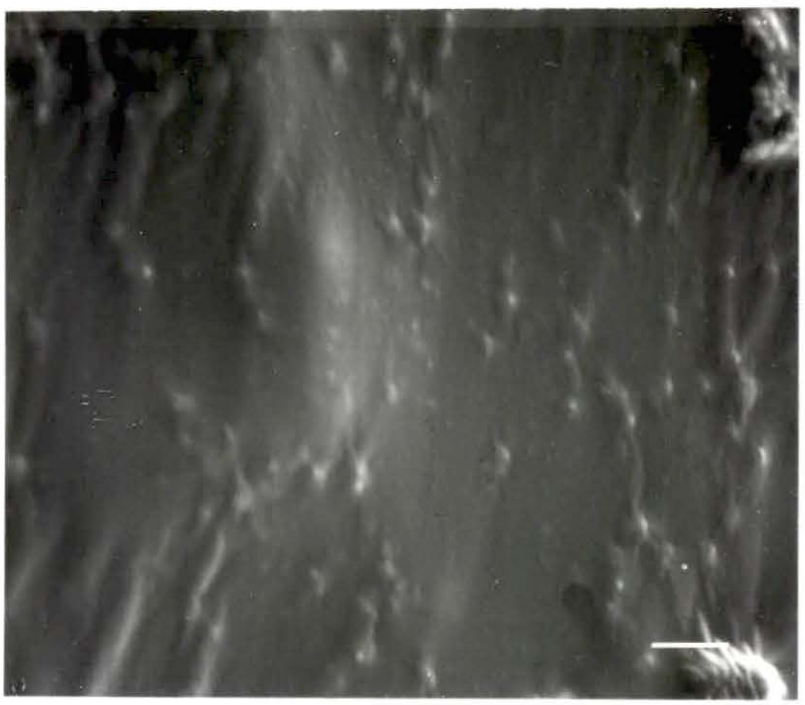

discocyte form only, with a slight 'puckering-effect' seen under some. Figure 21 shows the surface of the 2%SR/15%H/5%N shunt, which also looks very smooth. A few scattered platelets in discocyte form are adhered to the surface. The 2%SR/10%H/10%N surface (Figure 22) shows many platelets adhered in discocyte form. Some platelets are clustered together, displaying the puckering-effect. The area between the platelets has a smooth texture. Figure 23 shows the 2%SR/5%H/15%N surface which is similiar to the 2%SR/10%H/10%N surface (Figure 22). The platelets are adhered in discocyte form showing some clustering and displaying the puckering-effect. The area between platelets is smooth, also. Figure 24 shows the 2%SR/0%H/20%N surface with platelets adhered in discocyte form, also. Filler-induced roughness is slight in comparison to the surface unexposed to blood. A few scattered platelets in discocyte form are seen adhered to the 12%SR/20%H/0%N surface (Figure 25). Some filler-induced roughness is seen, although less prominent than that seen on the unexposed surface. The 12%SR/15%H/5%N surface (Figure 26) shows platelets adhered in discocyte form, also, with some forming clusters and exhibiting the puckering-effect. Platelets adhered in both discocyte and echinocyte form are seen on the 12%SR/10%H/10%N surface (Figure 27). Puckering is seen between platelets that have pseudopods extending towards each other. Figure 28 shows the 12%SR/5%H/15%N surface platelets adhered in discocyte form. There is only a small number of platelets adhered, and slight puckering is seen in some places. Little roughness is seen on the surface that is caused by the underlying filler. The 12%SR/0%H/20%N surface (Figure 29) shows a few scattered platelets in discocyte form, sometimes in clusters with slight puckering, adhered to the surface. The texture of the

Figure 21. SEM micrograph of 2%SR/15%H/5%N shunt surface after 0.25 minute exposure to blood. (scale bar = 10 μm)

Figure 22. SEM micrograph of 2%SR/10%H/10%N shunt surface after 0.25 minute exposure to blood. (scale bar = 10 μm)

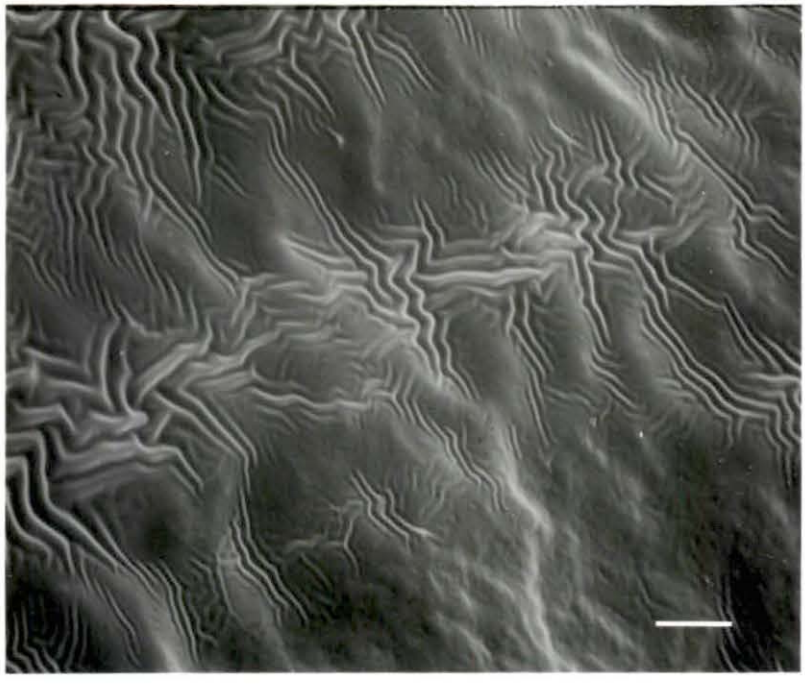

Figure 23. SEM micrograph of 2%SR/5%H/15%N shunt surface after 0.25 minute exposure to blood. (scale bar = 10 μm)

Figure 24. SEM micrograph of 2%SR/0%H/20%N shunt surface after 0.25 minute exposure to blood. (scale bar = 10 μm)

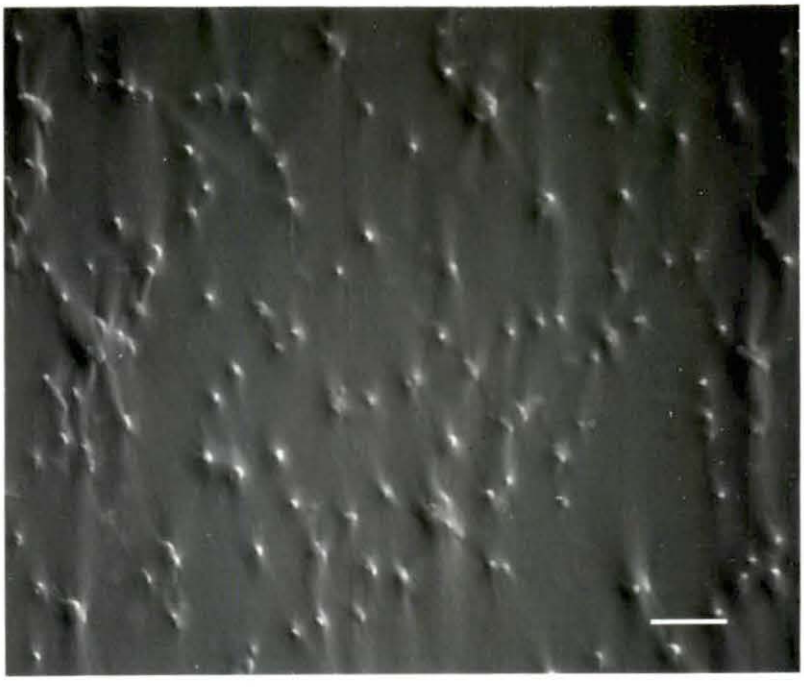

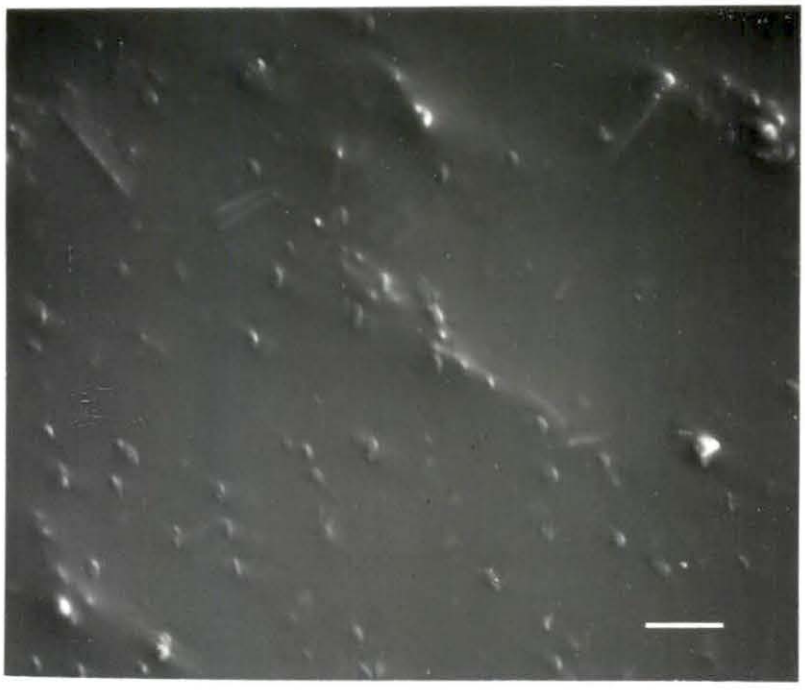

Figure 25. SEM micrograph of 12%SR/20%H/0%N shunt surface after 0.25 minute exposure to blood. (scale bar = 10 μm)

Figure 26. SEM micrograph of 12%SR/15%H/5%N shunt surface after 0.25 minute exposure to blood. (scale bar = 10 μm)

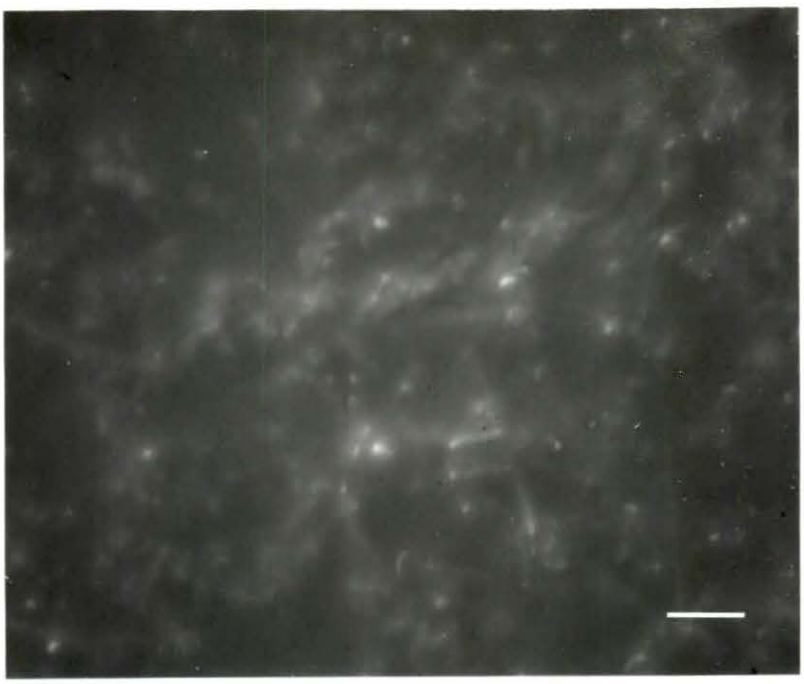

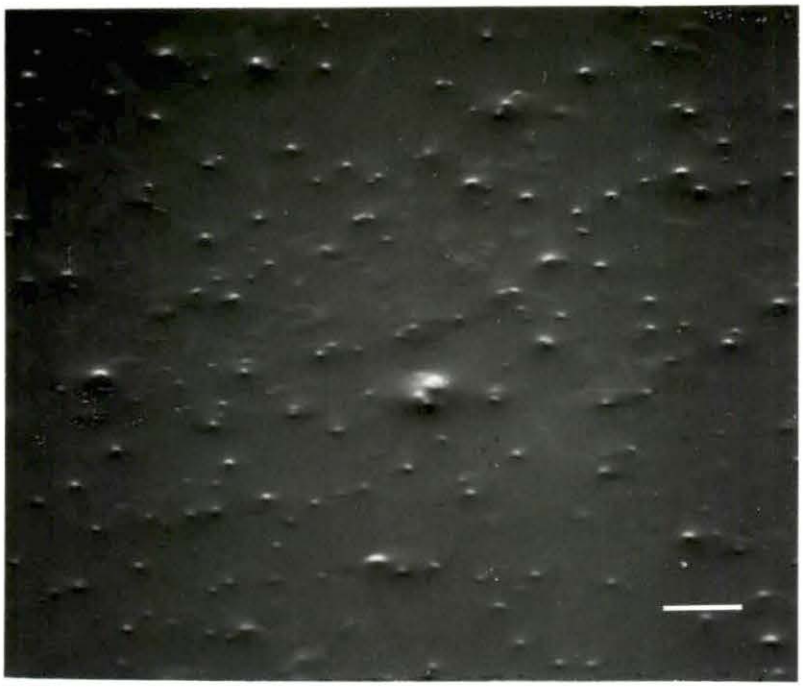

Figure 27. SEM micrograph of 12%SR/10%H/10%N shunt surface after 0.25 minute exposure to blood. (scale bar = 10 μm)

Figure 28. SEM micrograph of 12%SR/5%H/15%N shunt surface after 0.25 minute exposure to blood. (scale bar = 10 μm)

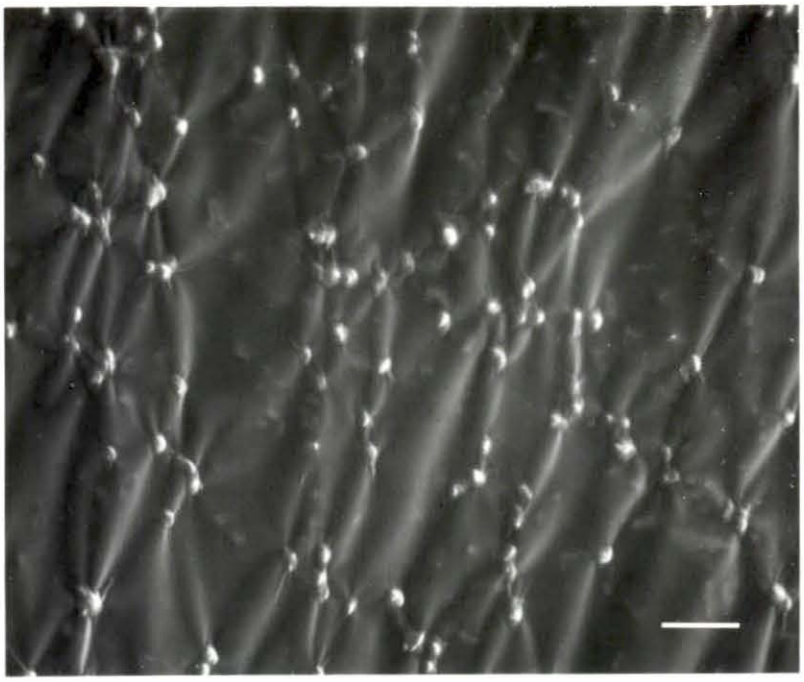

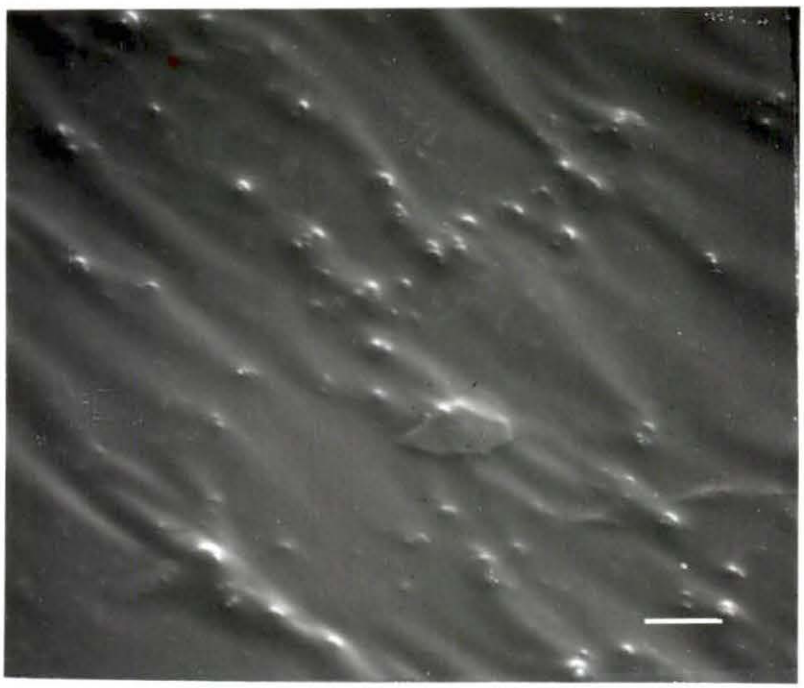

surface is rough in comparison to the 12%SR/5%H/15%N surface (Figure 28).

30 seconds exposure Figure 30 shows the SR surface after an additional 15 seconds of exposure to blood. Platelets are seen in mostly an echinocyte form with some discocytes seen. The 'ridges' on the surface as seen on the unexposed surface are only slightly apparent. Figure 31 shows (in higher magnification) that some of the platelets adhered may have undergone the release reactions, or were about to start. There has been an increase in the number of platelets adhered with the increase in exposure time of blood. The 2%SR surface (Figure 32) shows more platelets adhered with the additional exposure time, also. The platelets appear largely in the discocyte form, with some flattened out over the surface, possibly undergoing the release reaction. Figure 33 shows an increase in the number of platelets adhering to the 12%SR surface, too. Platelets are seen mostly in the discocyte form with no puckering seen. Figure 34 shows the surface of the 2%SR/20%H/0%N shunt. Again, an increase in the number of platelets adhered as discocytes is seen. Puckering is seen under some of the platelets. The surface between platelets is smooth, with no filler-induced roughness seen. The 2%SR/15%H/5%N surface (Figure 35) shows an increase in the number of platelets adhered, predominantly in the echinocyte form (compared to Figure 21). Puckering under the platelets is extensive, as well as puckering under the pseudopods that extend towards each other. Figure 36 shows an increase in the number of platelets adhered in the discocyte form to the 2%SR/10%H/10%N surface compared to Figure 22. Puckering is not seen except under platelets that have formed small clusters. The surface between platelets is smooth. Only a slight increase in the number of platelets adhered to the surface of the 2%SR/5%H/15%N

Figure 29. SEM micrograph of 12%SR/0%H/20%N shunt surface after 0.25 minute exposure to blood. (scale bar = 10 μm)

Figure 30. SEM micrograph of SR shunt surface after 0.50 minute exposure to blood. (scale bar = 10 μm)

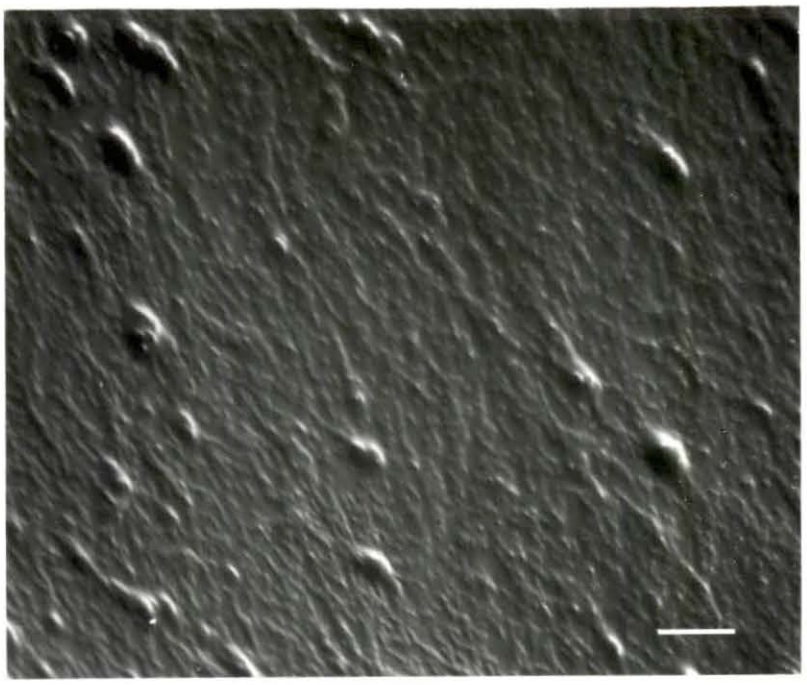

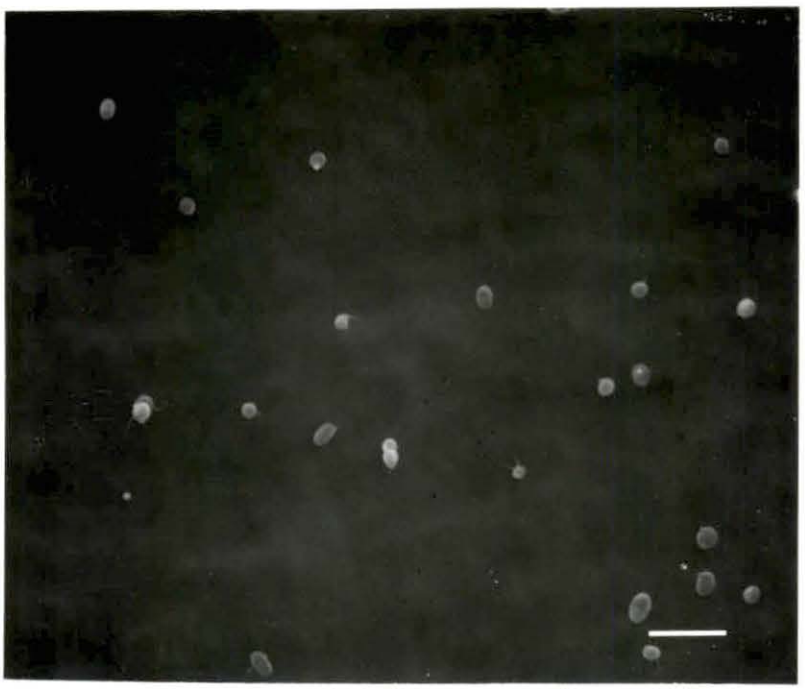

Figure 31. High magnification micrograph of SR shunt surface after 0.50 minute exposure to blood. Note pits and blebs on surface of platelets (arrow). (scale bar = 4 μm)

Figure 32. SEM micrograph of 2%SR shunt surface after 0.50 minute exposure to blood. (scale bar = 10 μm)

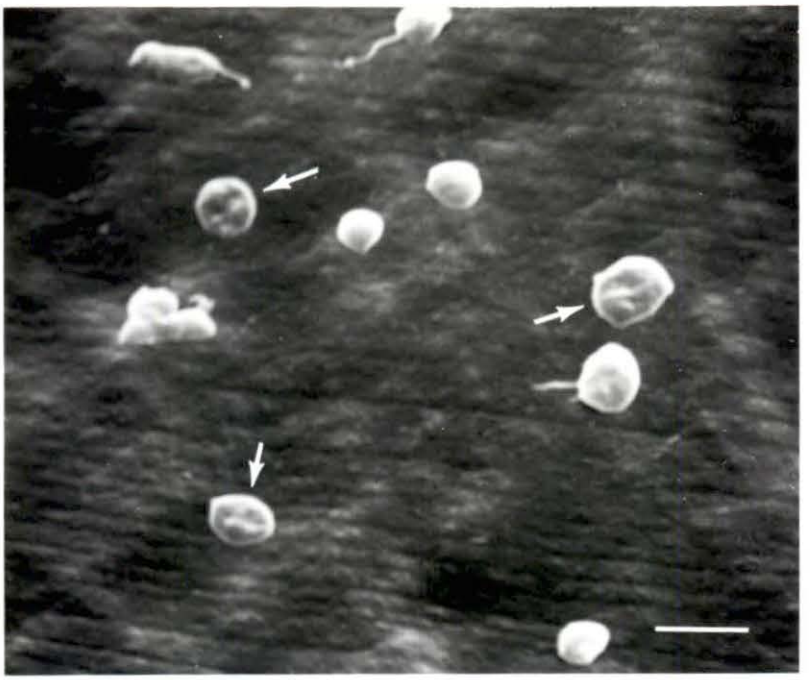

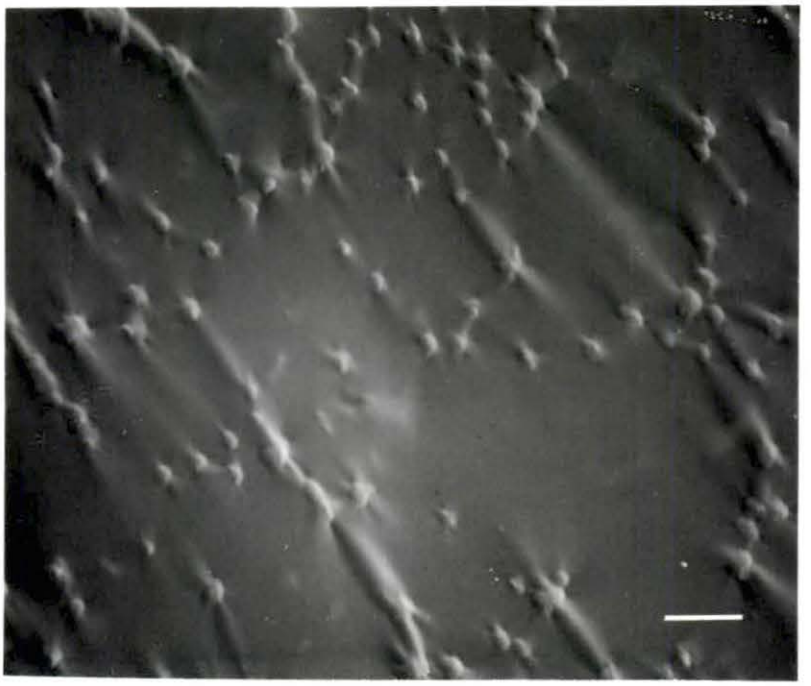

Figure 33. SEM micrograph of 12%SR shunt surface after 0.50 minute exposure to blood. (scale bar = 10 μm)

Figure 34. SEM micrograph of 2%SR/20%H/0%N shunt surface after 0.50 minute exposure to blood. (scale bar = 10 μm)

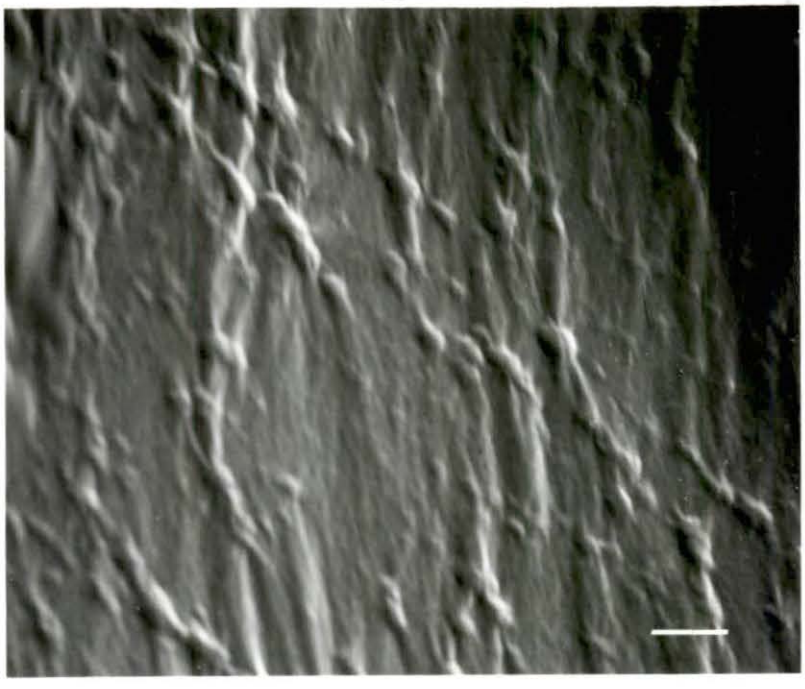

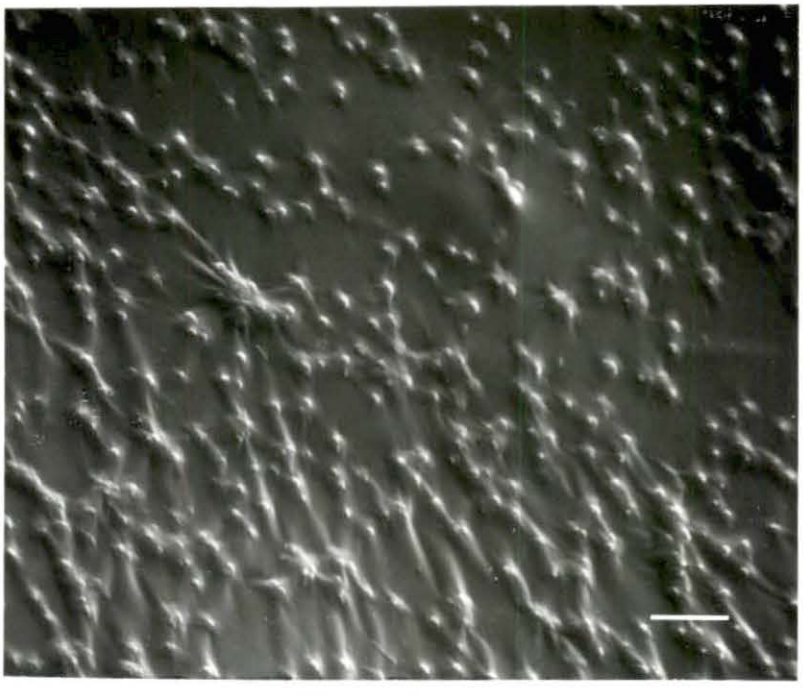

Figure 35. SEM micrograph of 2%SR/15%H/5%N shunt surface after 0.50 minute exposure to blood. (scale bar = 10 μm)

Figure 36. SEM micrograph of 2%SR/10%H/10%N shunt surface after 0.50 minute exposure to blood. (scale bar = 10 μm)

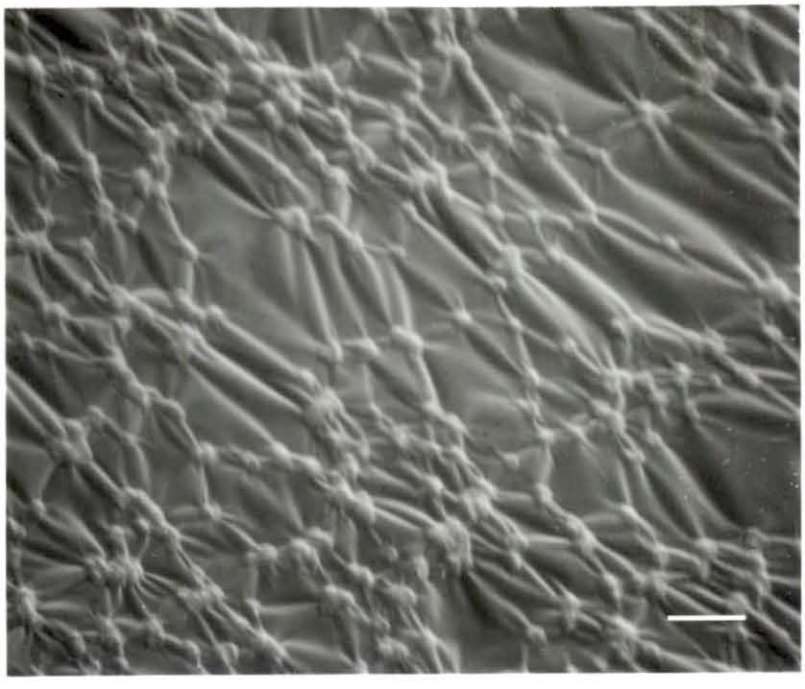

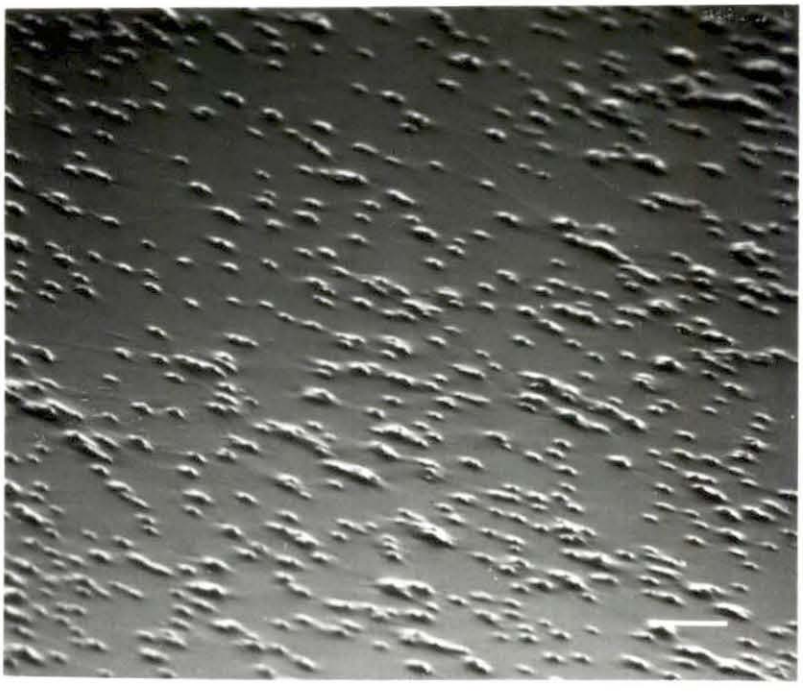

shunt is seen in Figure 37 compared to Figure 23. The platelets are mostly in the discocyte form. Surface roughness caused by filler is slight. Figure 38 shows only a slight increase in the number of platelets adhered to the 2%SR/0%H/20%N surface compared to Figure 24. The platelets are mostly in the discocyte form. There is no puckering seen except in areas where there are clusters of platelets. Some surface roughness is apparent due to the underlying filler. Figure 39 shows an increase in the number of adhered platelets on the 12%SR/20%H/0%N surface compared to Figure 25. The platelets are mostly in the discocyte form with some puckering seen. No filler-induced surface roughness is seen. There is also an increase in the number of platelets adhered to the 12%SR/15%H/5%N surface (Figure 40) compared to Figure 26. Platelets are mostly in the discocyte form with some puckering underneath. The area between platelets is smooth. The 12%SR/10%H/10%N surface (Figure 41) also shows an increase in the number of platelets adhered compared to Figure 27. Most of the platelets are in echinocyte form with pseudopods extended towards platelets that are adhered nearby. Puckering is evident under most of the platelets. The surface of the 12%SR/5%H/15%N shunt (Figure 42) displays only a slight increase in the number of platelets adhered compared to Figure 28. The platelets are mostly in the discocyte form with some puckering seen. Evidence of surface roughness caused by the underlying filler is seen, also. Figure 43 also shows only a slight increase in the number of platelets adhered to the 12%SR/0%H/20%N surface compared to Figure 29. The platelets are in discocyte form for the most part, with slight puckering seen under some platelets. There is some surface roughness seen that is caused by the filler, but it is not as extensive.

Figure 37. SEM micrograph of 2%SR/5%H/15%N shunt surface after 0.50 minute exposure to blood. (scale bar = 10 μm)

Figure 38. SEM micrograph of 2%SR/0%H/20%N shunt surface after 0.50 minute exposure to blood. (scale bar = 10 μm)

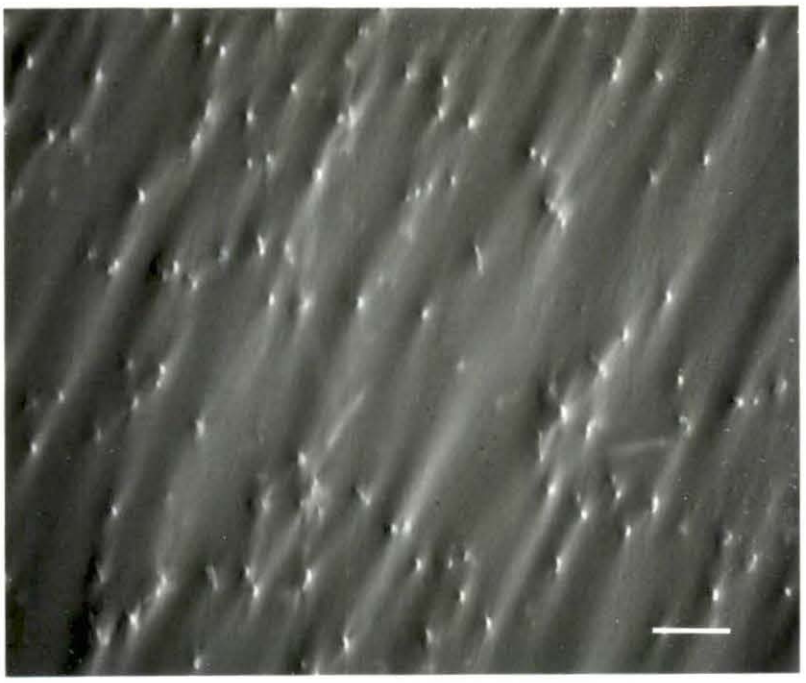

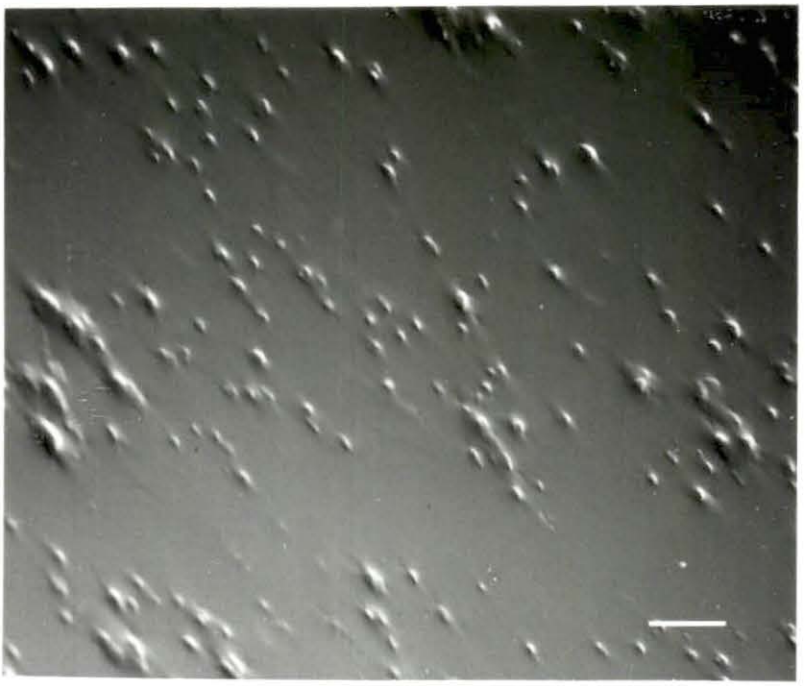

Figure 39. SEM micrograph of 12%SR/20%H/0%N shunt surface after 0.50 minute exposure to blood. (scale bar = 10 μm)

Figure 40. SEM micrograph of 12%SR/15%H/5%N shunt surface after 0.50 minute exposure to blood. (scale bar = 10 μm)

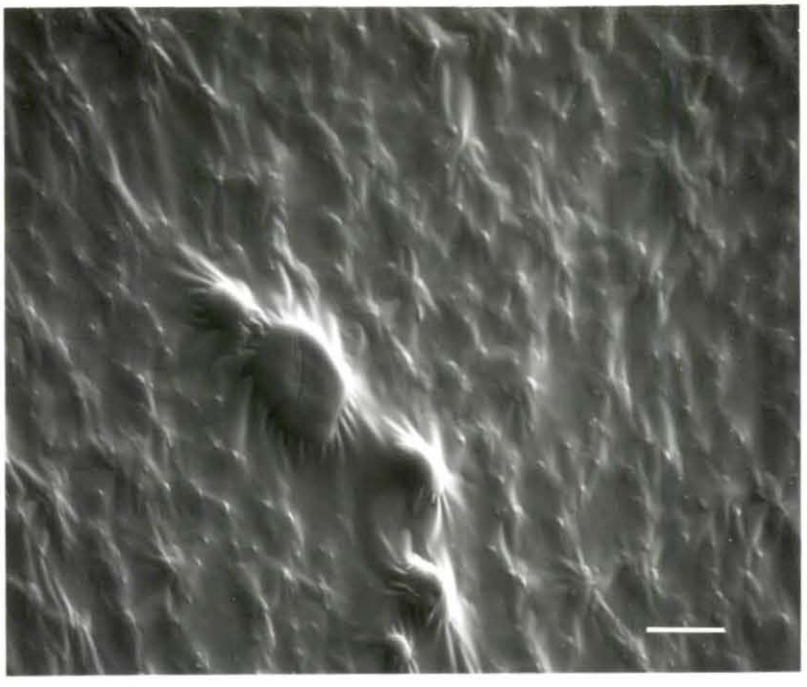

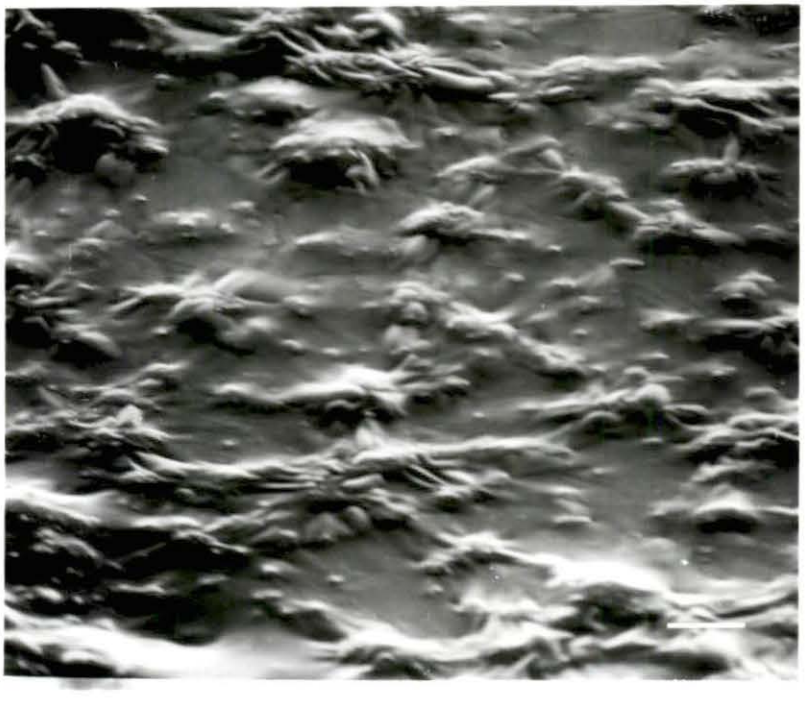

Figure 41. SEM micrograph of 12%SR/10%H/10%N shunt surface after 0.50 minute exposure to blood. (scale bar = 10 μm)

Figure 42. SEM micrograph of 12%SR/5%H/15%N shunt surface after 0.50 minute exposure to blood. (scale bar = 10 μm)

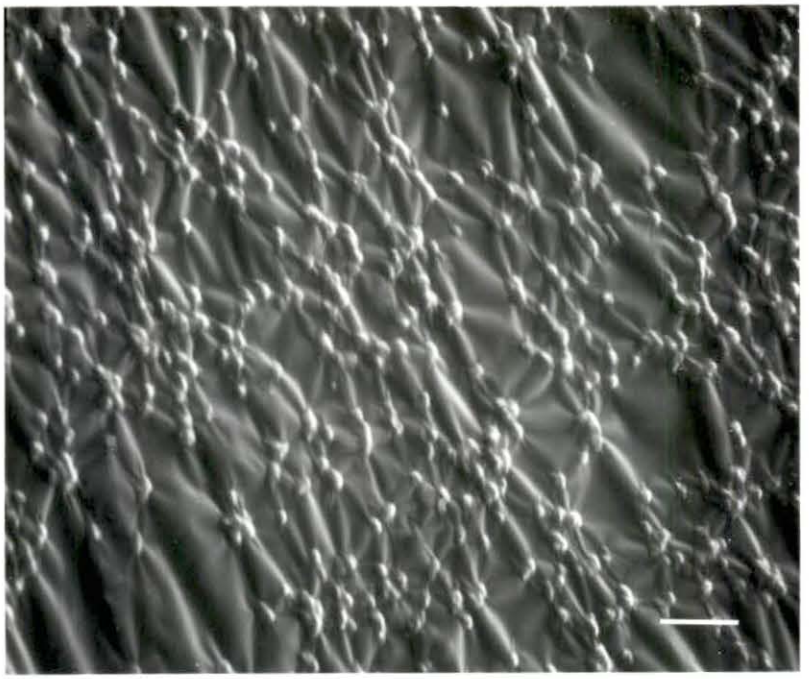

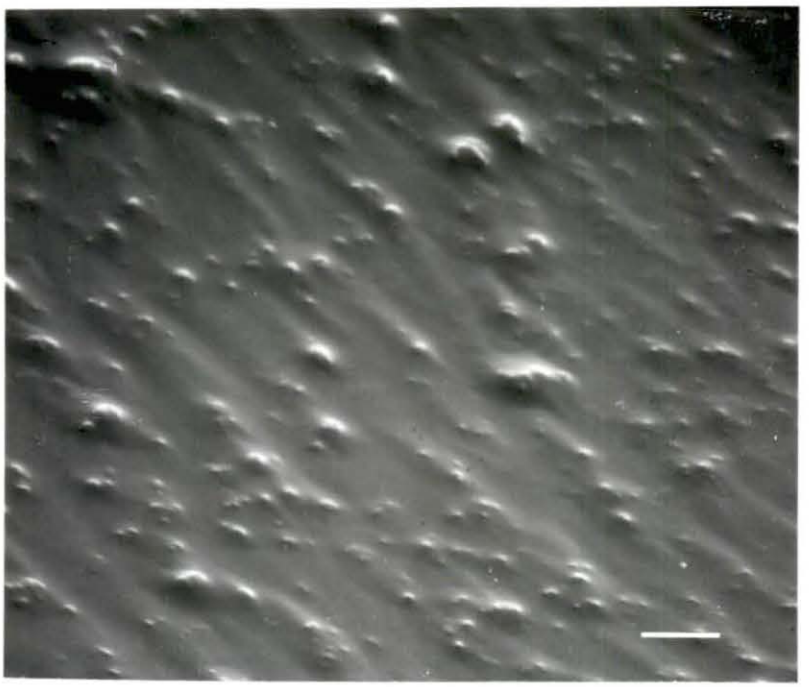

5 minutes exposure Figure 44 shows that after 5 minutes of exposure to blood the SR surface shows aggregation of platelets. The area where aggregation has occurred is adjacent to an area where platelets are in an echinocyte form. These platelets are mostly in an isolated state, forming a platelet lawn. Figure 45 shows that the 2%SR surface has an increase in the number of platelets distributed in the surface compared to Figure 32, and puckering is seen. At higher magnification, Figure 46 shows that platelets still in discocyte form may be adhered to platelets adhered to the surface which are in a possible early stage of spreading. Some of the underlying platelets show pseudopod formation. The 12%SR surface (Figure 47) looks very similiar to the 2%SR surface, with an increase in the number of platelets in discocyte form adhered in a somewhat spread state compared to Figure 33. There is some surface roughness seen caused by the underlying filler. Figure 48 shows that the 2%SR/20%H/0%N surface has more platelets adhered than seen in the 30 second exposure (Figure 34). The platelets are in discocyte form, and puckering is seen. The 2%SR/15%H/5%N surface (Figure 49) shows an increase in the number of platelets adhered compared to Figure 35. The platelets are mostly echinocytes in a slightly advanced stage of spreading. There appears to be platelets (discocytes) adhered to the spread platelets in some areas. There is extensive puckering seen under the platelets. The 2%SR/10%H/10%N surface (Figure 50) shows an increase in the number of platelets adhered (in discocyte form) compared to Figure 36, also. There is a slight amount of puckering under some of the platelets. Some of the platelets are clustered in groups of 3 or more which exhibit more puckering than seen for individual platelets. A possible site of thrombus formation is seen. Notice that the area around

Figure 43. SEM micrograph of 12%SR/0%H/20%N shunt surface after 0.50 minute exposure to blood. (scale bar = 10 μm)

Figure 44. SEM micrograph of SR shunt surface after 5 minutes of exposure to blood. (scale bar = 10 μm)

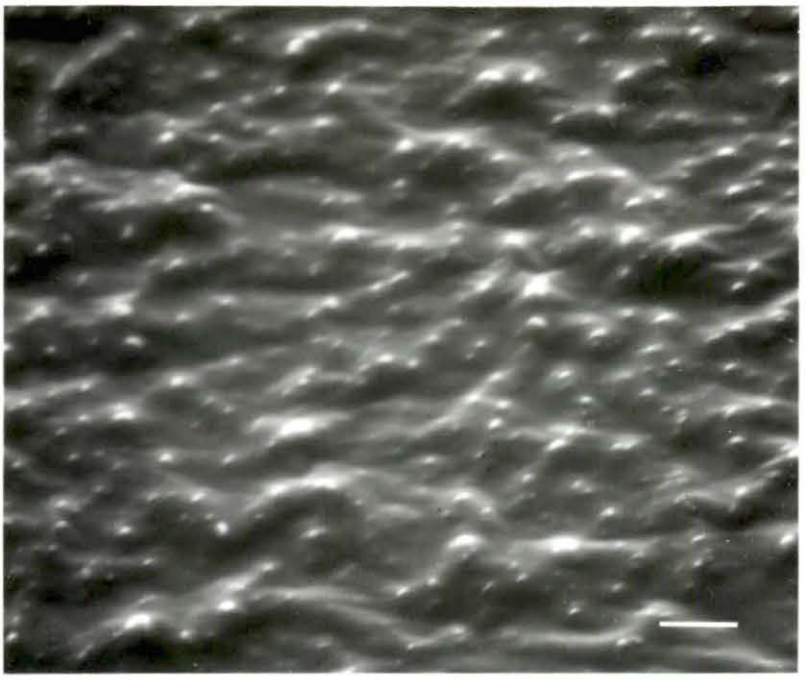

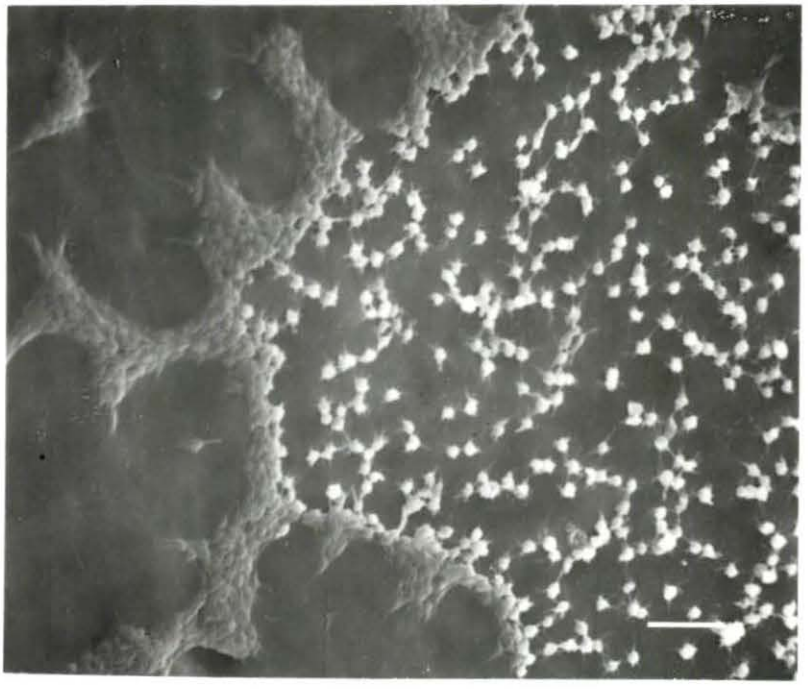

Figure 45. SEM micrograph of 2%SR shunt surface after 5 minutes of exposure to blood. (scale bar = 10 μm)

Figure 46. High magnification micrograph of 2%SR shunt surface after 5 minutes of blood exposure. Note adherance of discocytes on top of platelets in an early stage of spreading.
(scale bar = 5 μm)

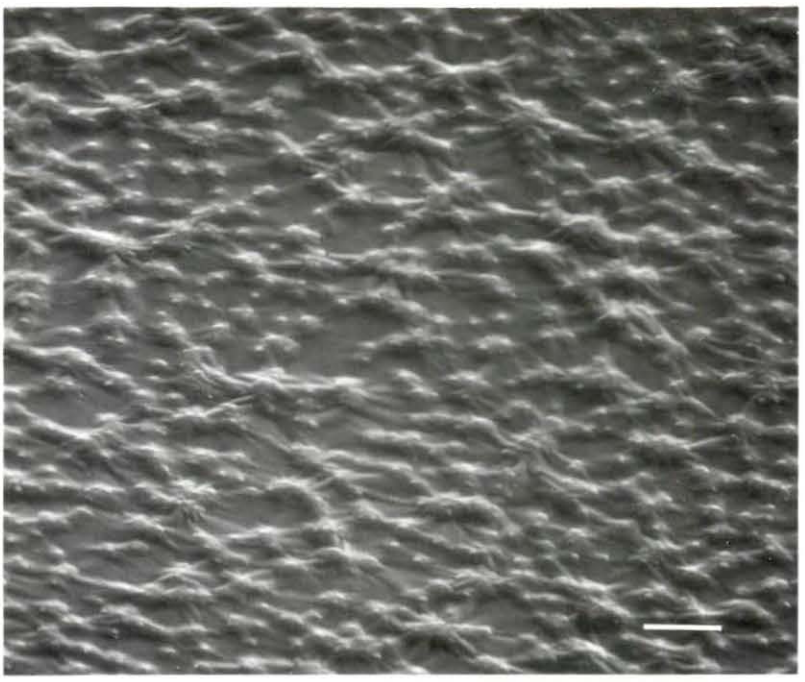

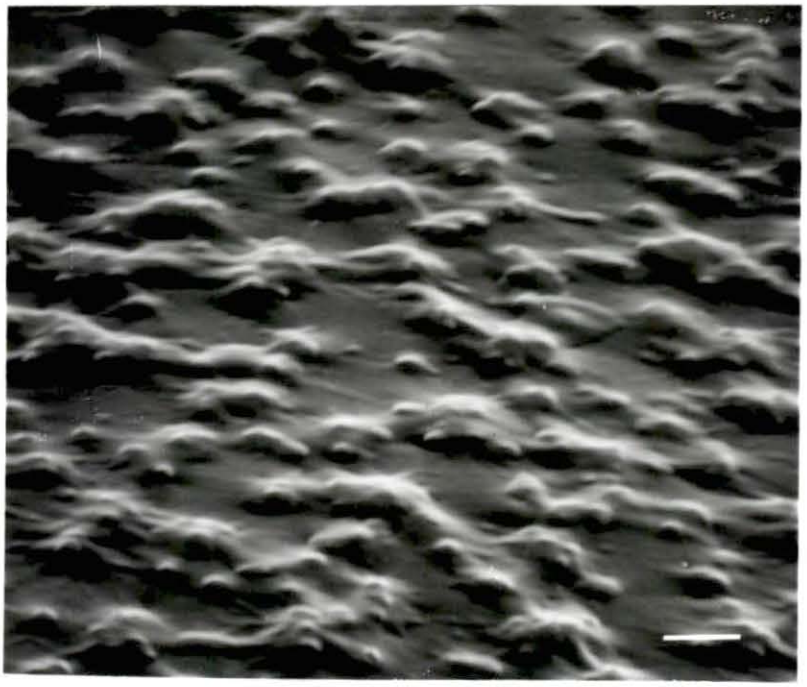

Figure 47. SEM micrograph of 12%SR shunt surface after 5 minutes of exposure to blood. (scale bar = 10 μm)

Figure 48. SEM micrograph of 2%SR/20%H/0%N shunt surface after 5 minutes of exposure to blood. (scale bar = 10 μm)

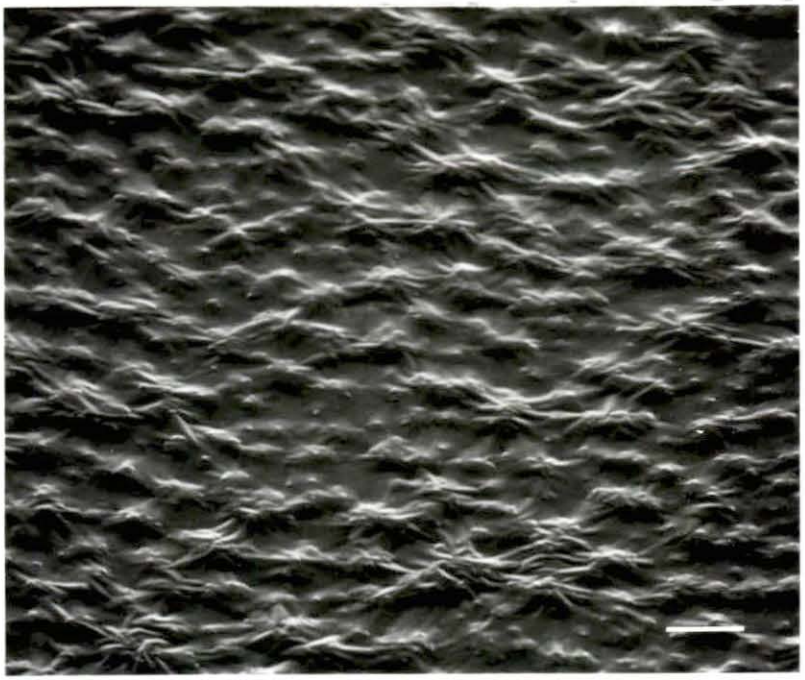

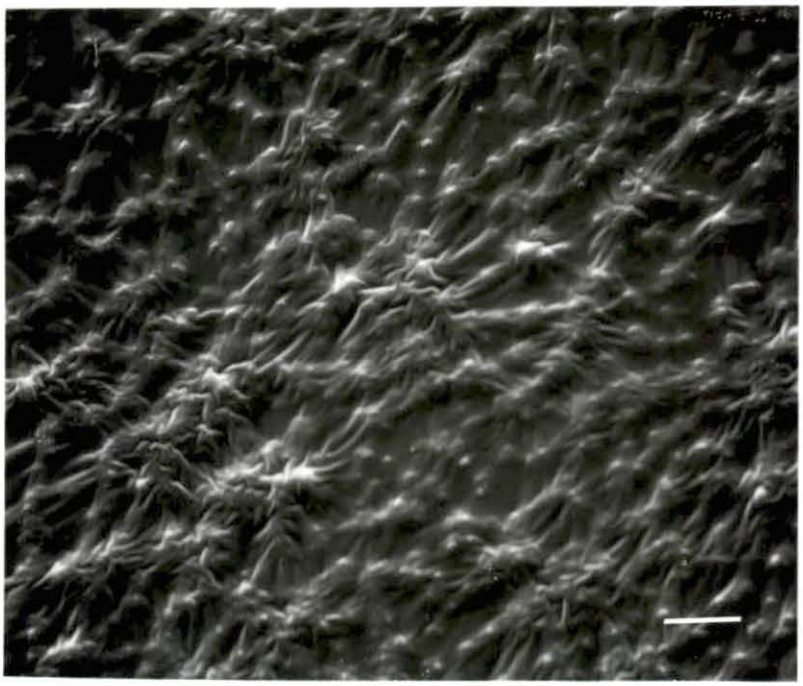

Figure 49. SEM micrograph of 2%SR/15%H/5%N shunt surface after 5 minutes of exposure to blood. (scale bar = 1Ø μm)

Figure 5Ø. SEM micrograph of 2%SR/1Ø%H/1Ø%N shunt surface after 5 minutes of exposure to blood. Note area that appears to be an aggregation of platelets forming a possible thrombus, and that the area around the aggregate is clean of platelets. (scale bar = 1Ø μm)

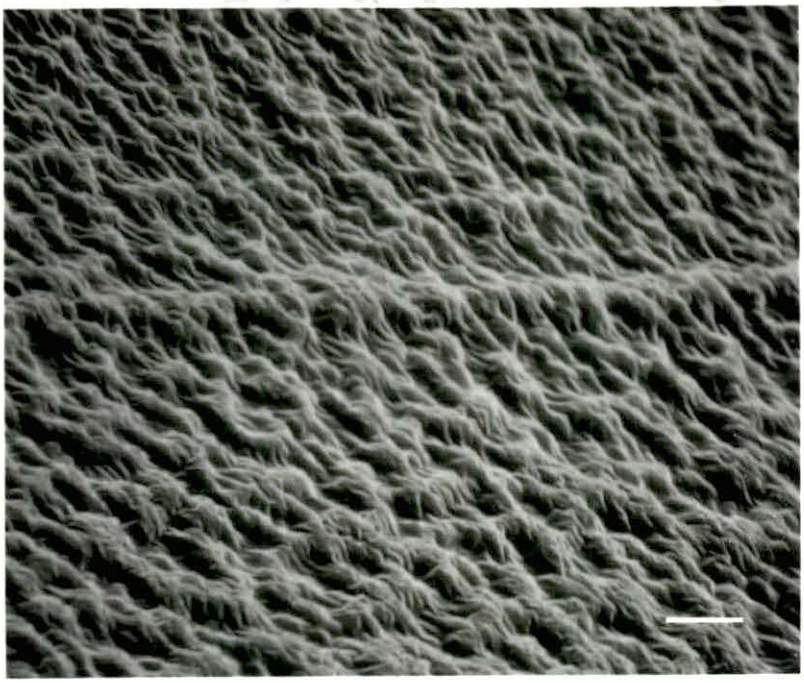

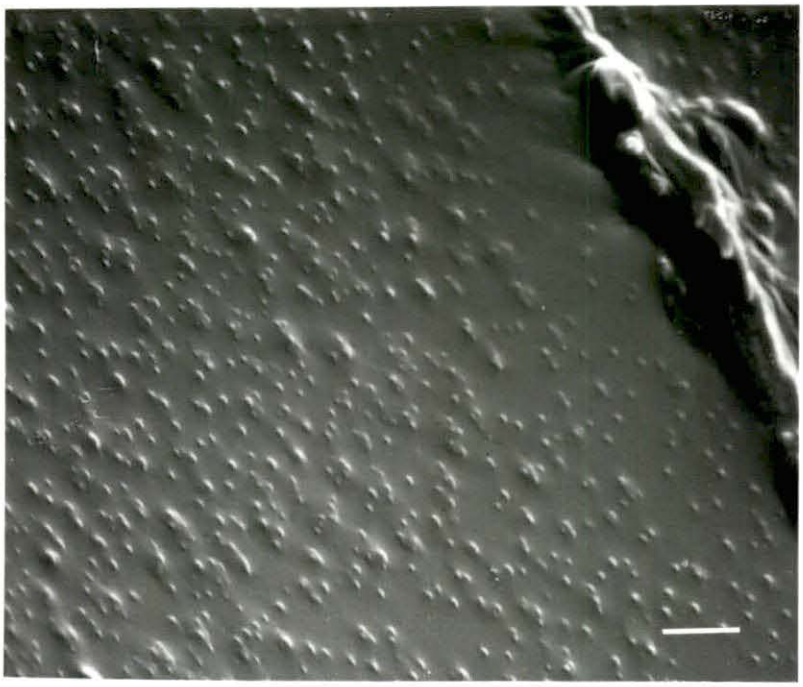

this site is free of platelets. Figure 51 shows the 2%SR/5%H/15%N surface. There is an increase in the number of platelets adhered when compared to the previous time period of exposure. The platelets are mostly in the discocyte form, with clusters of 3 or more seen in some areas. The clusters exhibit a more pronounced puckering effect than seen for individual platelets. The 2%SR/0%H/20%N surface (Figure 52) shows only a slight increase in the number of platelets adhered compared to Figure 38. The platelets are mostly in the discocyte form with some clustering. Slight puckering is seen under some of the platelets. Platelets adhered to the 12%SR/20%H/0%N surface (Figure 53) show similiarities to the 2%SR/20%H/0%N surface (Figure 48). Puckering is seen with possible platelets, in discocyte form, adhered on top of platelets that are in some stage of speading. There is some evidence of surface roughness induced by the filler seen. Figure 54 shows that an increase in the number of platelets adhered to the 12%SR/15%H/5%N surface occurred over that of the previous time period, also. There is puckering seen under some of the platelets. No surface roughness is evident. The 12%SR/10%H/10%N surface (Figure 55) shows an increase in the number of platelets adhered compared to Figure 41, also. The platelets form an extensive lawn of discocytes, and a mild puckering-effect is seen. No clustering or filler induced surface roughness is seen. Figure 56 shows the 12%SR/5%H/15%N surface had only a small increase in the number of platelets adhered compared to Figure 42. Figure 57 shows at higher magnification that platelets adhering to the surface/protein layer are in some stage of spreading, with platelets in discocyte form adhering on top. Some of these platelets show signs of the release reaction. The area between the platelets is smooth. The

Figure 51. SEM micrograph of 2%SR/5%H/15%N shunt surface after 5 minutes of exposure to blood. (scale bar = 10 μm)

Figure 52. SEM micrograph of 2%SR/0%H/20%N shunt surface after 5 minutes of exposure to blood. (scale bar = 10 μm)

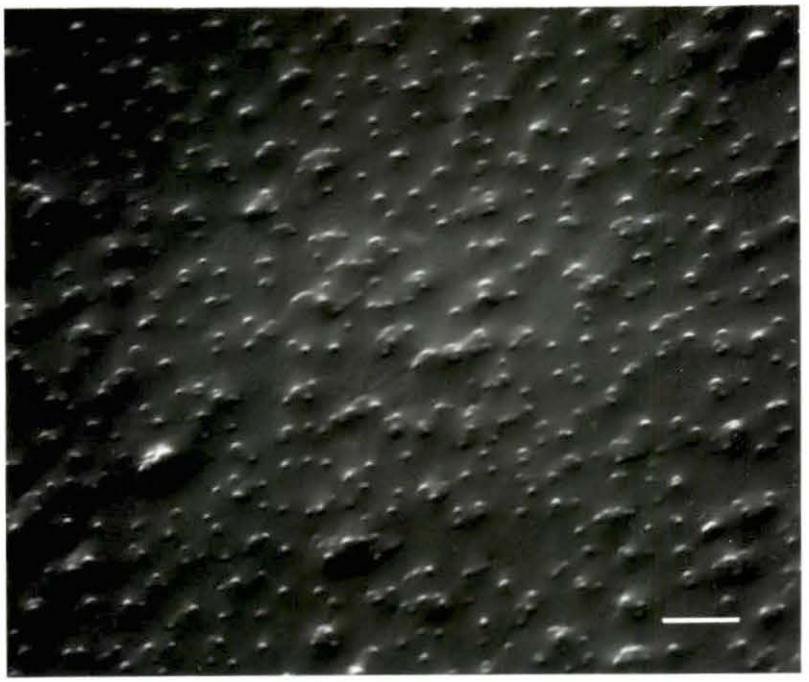

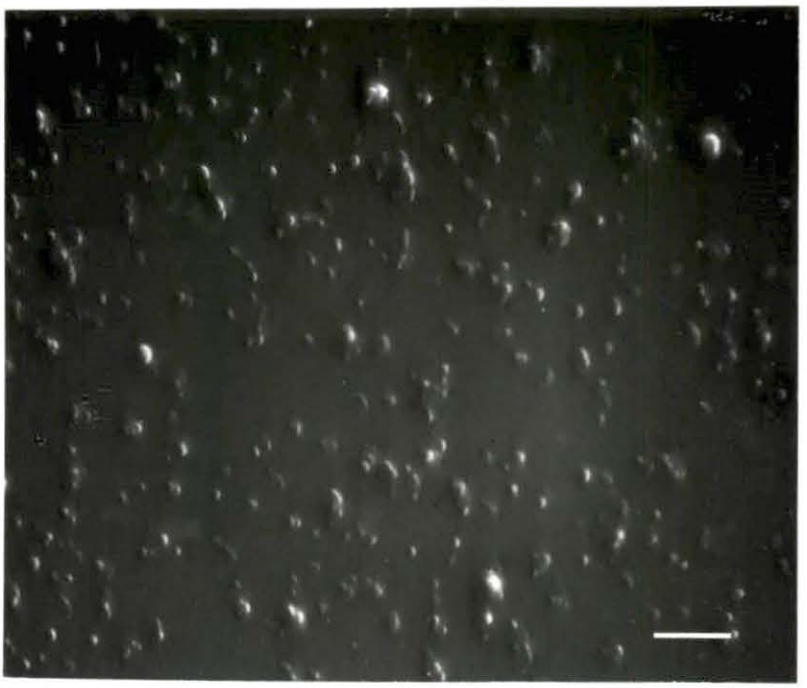

Figure 53. SEM micrograph of 12%SR/20%H/0%N shunt surface after 5 minutes of exposure to blood. (scale bar = 10 μm)

Figure 54. SEM micrograph of 12%SR/15%H/5%N shunt surface after 5 minutes of exposure to blood. (scale bar = 10 μm)

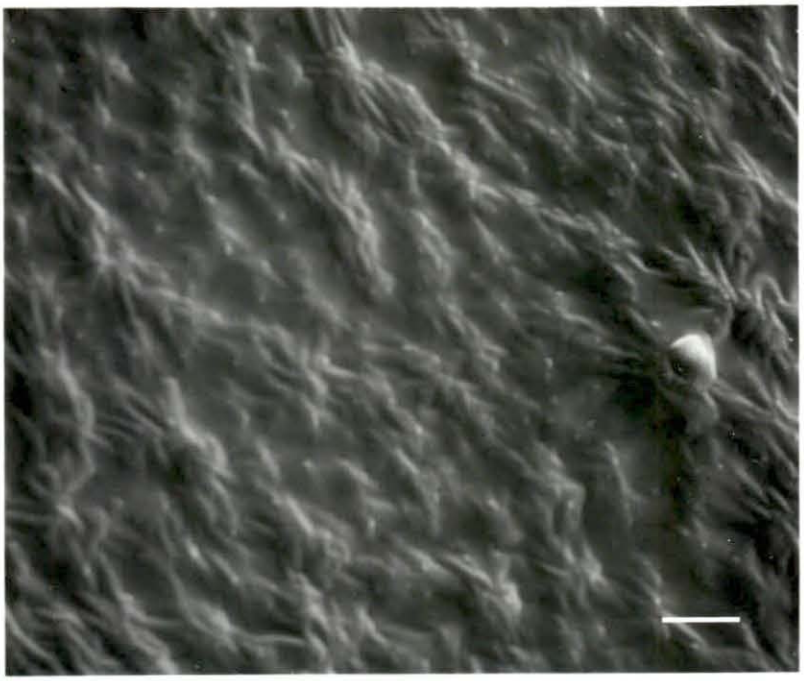

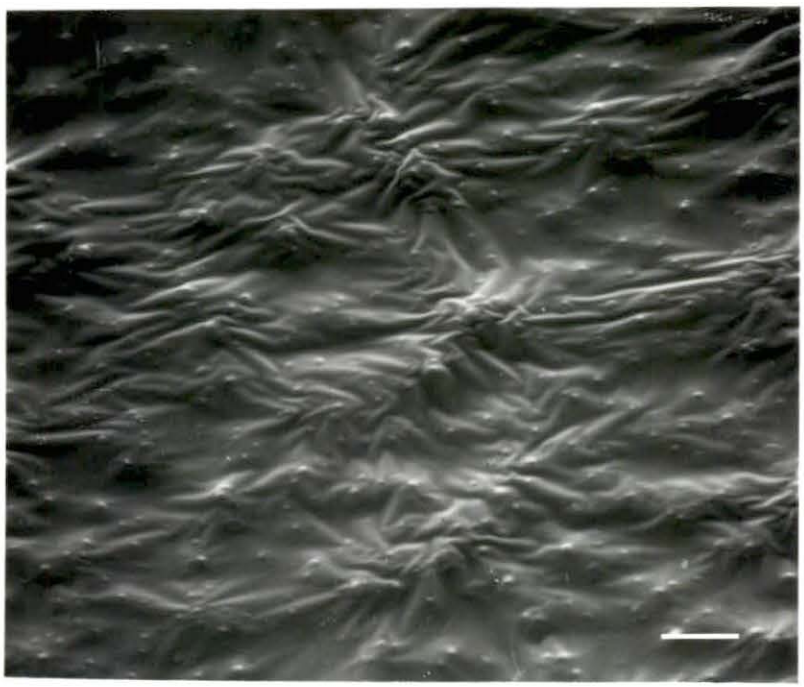

Figure 55. SEM micrograph of 12%SR/10%H/10%N shunt surface after 5 minutes of exposure to blood. (scale bar = 10 μm)

Figure 56. SEM micrograph of 12%SR/5%H/15%N shunt surface after 5 minutes of exposure to blood. (scale bar = 10 μm)

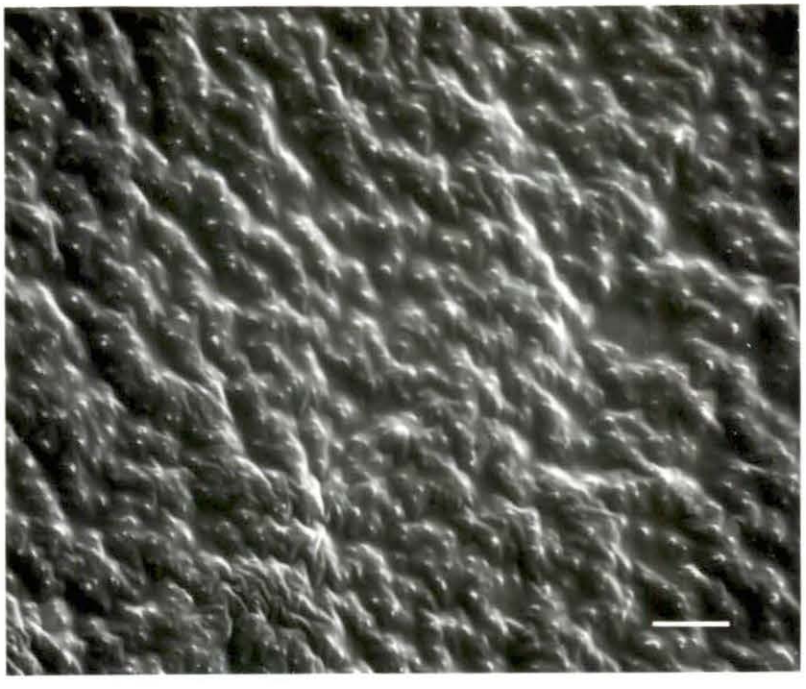

12%SR/0%H/20%N surface (Figure 58) has more extensive platelet aggregates than seen on other samples. Smooth areas between aggregates are smaller in size than those seen on the 12%SR/5%H/15%N surface (Figure 56). Platelets in Figures 56 and 58 show platelets in aggregates without the formation of pseudopods, suggesting that the platelets are predominantly in the discocyte form. These platelet aggregates appear to be smooth, possibly covered by a proteinaceous layer.

15 minutes exposure Figure 59 shows an intensive platelet lawn on the SR surface after a total of 15 minutes of exposure to flowing blood. The platelets are echinocytes in various stages of spreading. No thrombus is seen on this surface. Figure 60 shows at higher magnification that the platelets have possibly been undergoing the release reaction as shown by the pits and small blebs on the surfaces of the spreading platelets. The 2%SR surface (Figure 61) shows no increase in the number of platelets adhered compared to the previous time period. However, there are areas of extensive aggregation seen instead. Lower magnification (Figure 62) shows that thrombus formations occurred by this time. The thrombus is surrounded by an area devoid of platelets and the protein film appears to be under tension with portions being drawn up into the clot. Platelets further from the clot are in discocyte form, sometimes in clusters with more puckering seen than for individual platelets. Figure 63 shows that the number of platelets adhered to the surface of the 12%SR surface did not increase with the increase in time of blood exposure. Puckering increased in areas where aggregates were forming. The pulling up effect is seen, and shows that the protein layer may have been torn near the base of the thrombus. Platelets surrounding this area are in discocyte form with moderate puckering

Figure 57. High magnification micrograph of 12%SR/5%H/15%N shunt surface after 5 minutes of exposure to blood. Note that discocytes are adhered to the top of spread platelets (arrow). (scale bar = 4 μm)

Figure 58. SEM micrograph of 12%SR/0%H/20%N shunt surface after 5 minutes of exposure to blood. (scale bar = 10 μm)

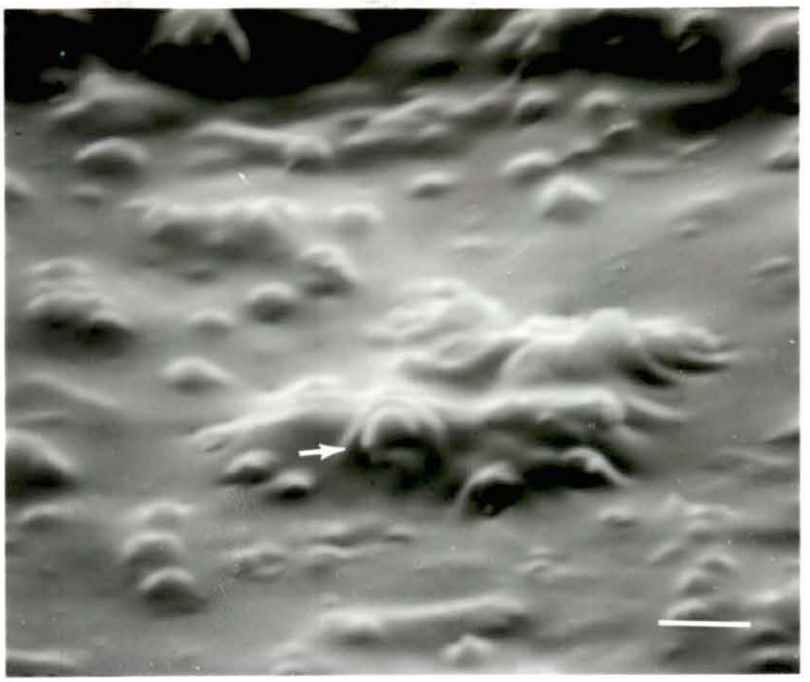

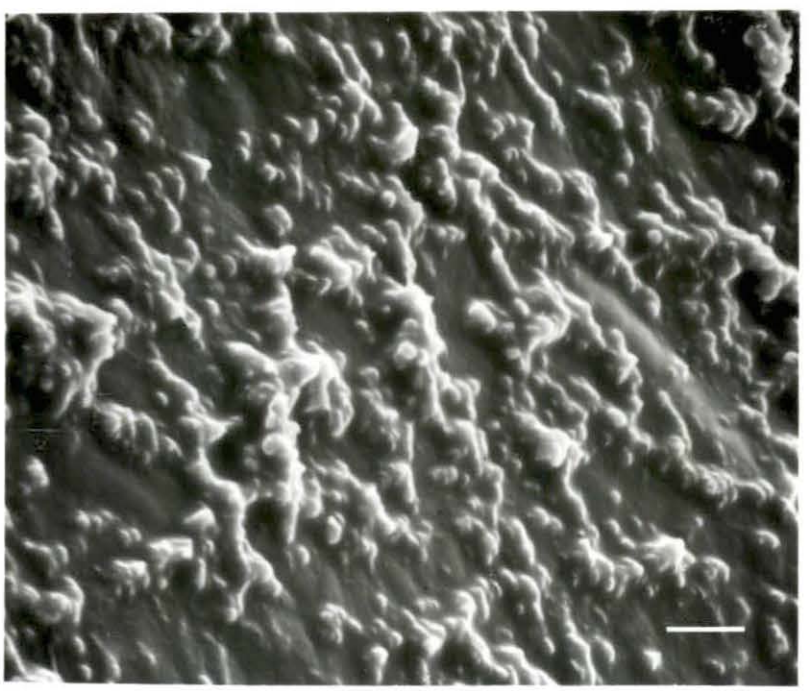

Figure 59. SEM micrograph of SR shunt surface after 15 minutes of exposure to blood. (scale bar = 10 μm)

Figure 60. High magnification micrograph of SR shunt surface after 15 minutes of exposure to blood. Note surface pits and blebs on the platelets, indicating that the release reactions may have been occurring. (scale bar = 5 μm)

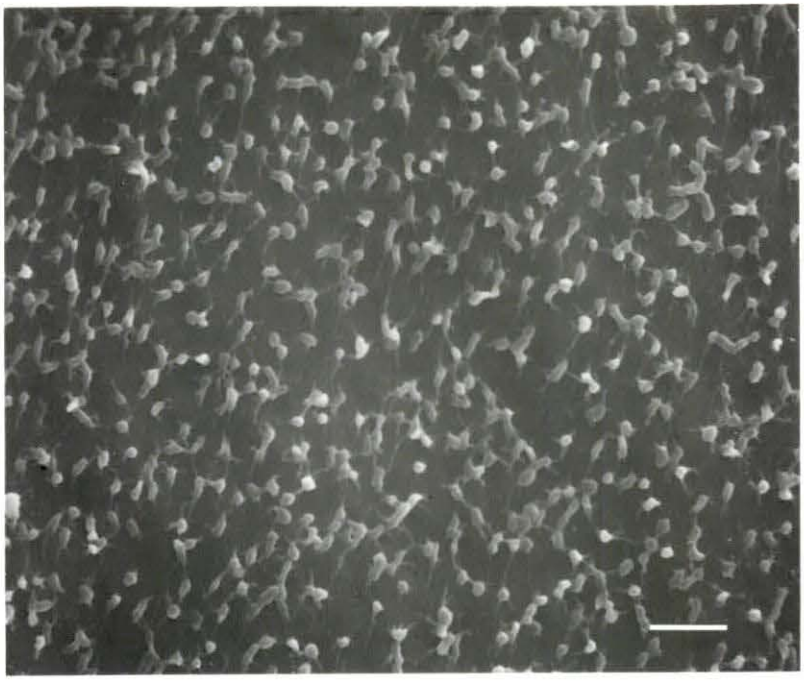

Figure 61. SEM micrograph of 2%SR shunt surface after 15 minutes of exposure to blood. (scale bar = 10 μm)

Figure 62. Low magnification micrograph of 2%SR shunt surface after 15 minutes of blood exposure showing a thrombus formation. Note clean area around base of thrombus which appears to be under tension. (scale bar = 100 μm)

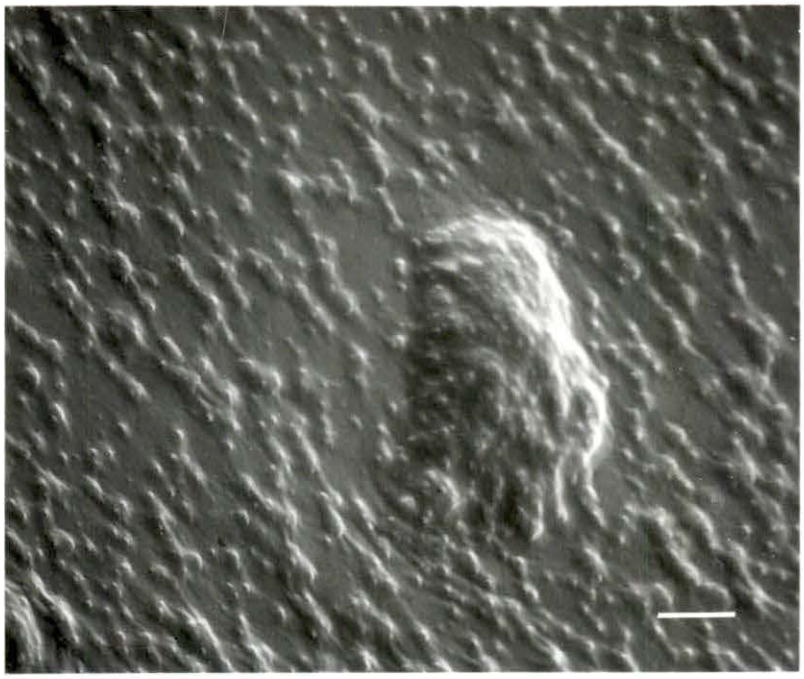

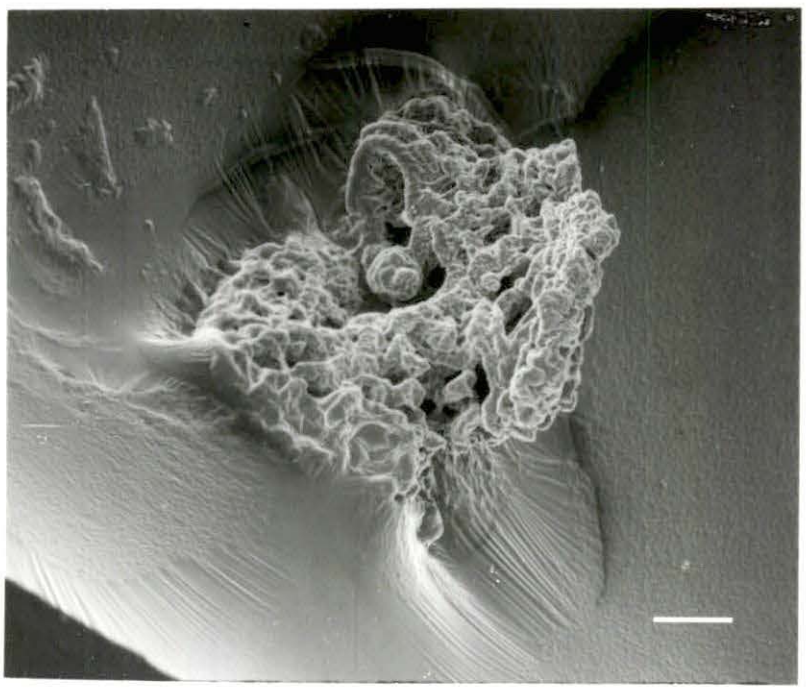

displayed. Figure 64 shows that a thrombus also formed on this surface which has the pulling up effect. At the base of this thrombus (Figure 65), there are platelets in various stages of spreading with surface blebs. The thrombus appears to be elliptical in shape at the base, with the longer dimension almost at a right angle to the direction of flow that went through the shunt. A slight increase in the number of platelets in the spread state is seen on the 2%SR/20%H/0%N (Figure 66) surface compared to Figure 48. Platelets in the discocyte form appear to be adhered to spread platelets, which are adhered to the surface of the shunt, in some places. Large aggregates are on the surface, although no pulling up effect is seen. Figure 67 shows a thrombus that formed on the surface, with a rough texture and the pulling up effect. The base of the thrombus appears to be elliptical, also, but the major axis is parallel with the direction of flow. Figure 68 shows at higher magnification (refer to Figure 66) that platelets within the aggregate have an increased amount of puckering. Some of these platelets have small blebs that possibly could be the dense granules compacting into, and forming, a hillock prior to release. The 2%SR/15%H/5%N surface (Figure 69) shows a loss of adhering platelets compared to Figure 49. The platelets that are adhered are in both the discocyte and echinocyte form. A thrombus on the surface (Figure 70) shows only slight evidence of the pulling up effect. The thrombus is rounder in shape than most thrombi seen, but the texture is still rough. Figure 71 shows a slight decrease in the number of platelets, mostly discocytes, adhered to the 2%SR/10%H/10%N surface compared to Figure 50. Some of the discocytes appear to be adhered to the top of platelets which are in the spread state. Figure 72 shows a thrombus that formed on the surface, and

Figure 63. SEM micrograph of 12%SR shunt surface after 15 minutes of exposure to blood. (scale bar = 10 μm)

Figure 64. Low magnification micrograph of 12%SR shunt surface after 15 minutes of blood exposure showing a thrombus formation. Note elliptical shape of the thrombus base. (scale bar = 100 μm)

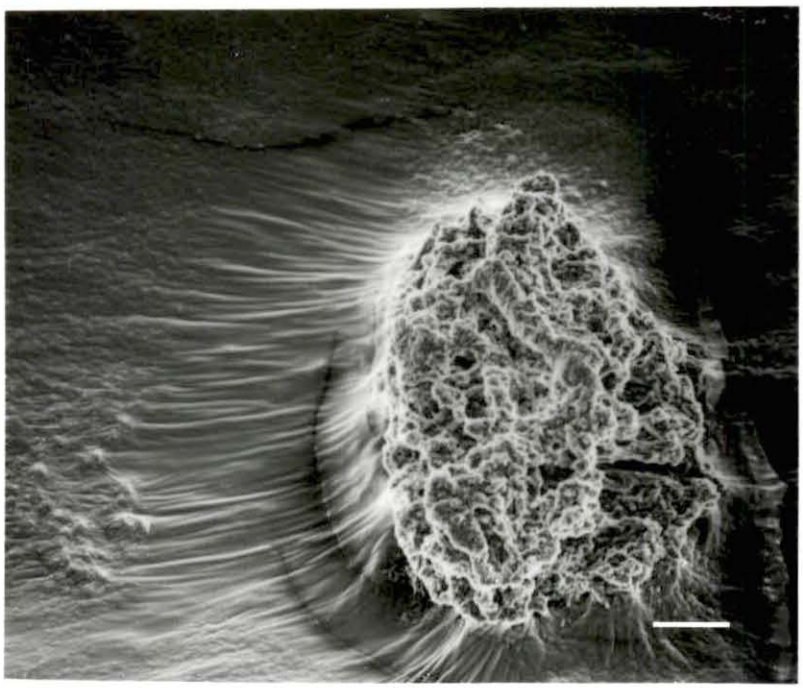

Figure 65. High magnification micrograph of base of thrombus formation seen in Figure 64 showing platelets in various stages of spreading. Some platelets have surface blebs. (scale bar = 10 μm)

Figure 66. SEM micrograph of 2%SR/20%H/0%N shunt surface after 15 minutes of exposure to blood. (scale bar = 10 μm)

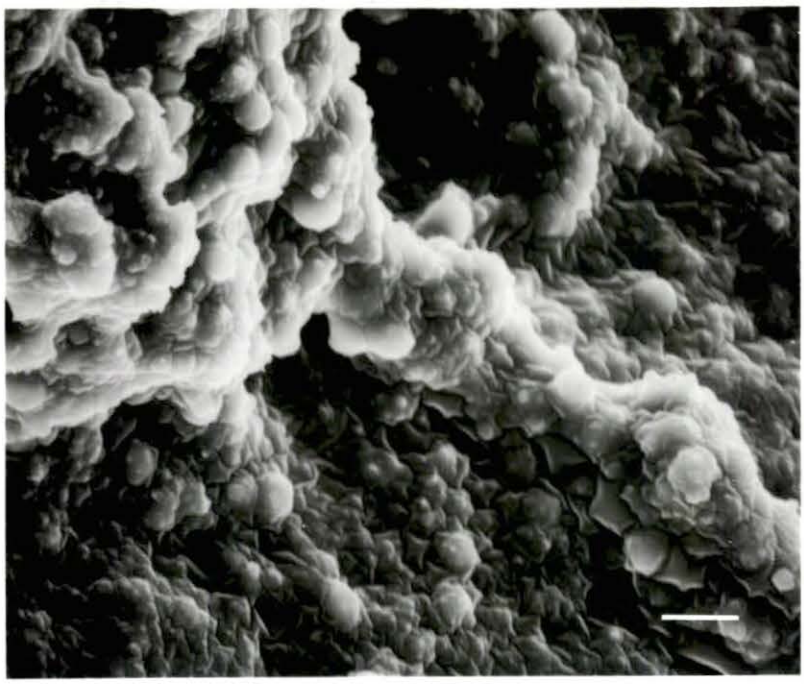

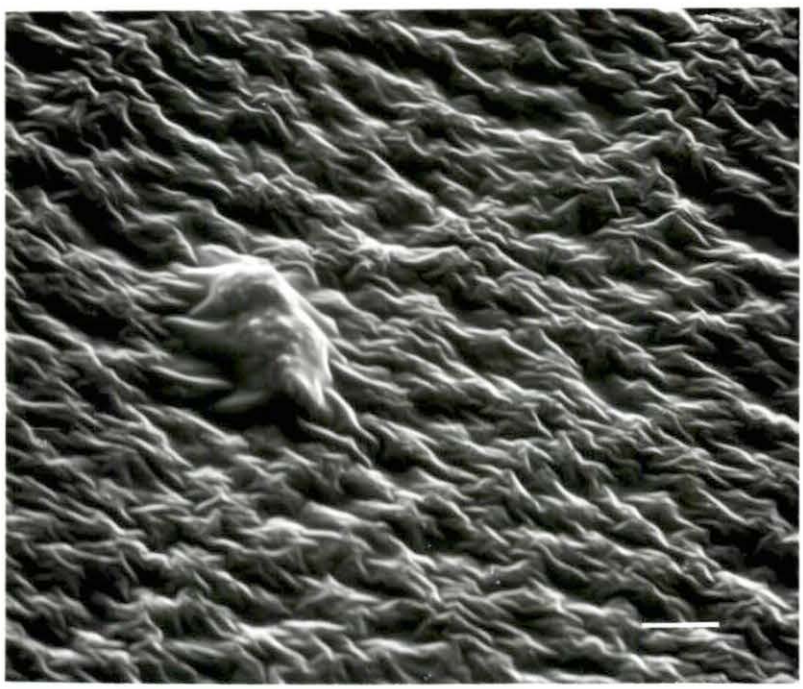

Figure 67. Low magnification micrograph of 2%SR/20%H/0%N shunt surface after 15 minutes of blood exposure showing a thrombus formation. (scale bar = 100 μm)

Figure 68. High magnification micrograph of 2%SR/20%H/0%N shunt surface exposed to blood for 15 minutes. Note puckering and projections on the surface of platelets which are spreading. (scale bar = 10 μm)

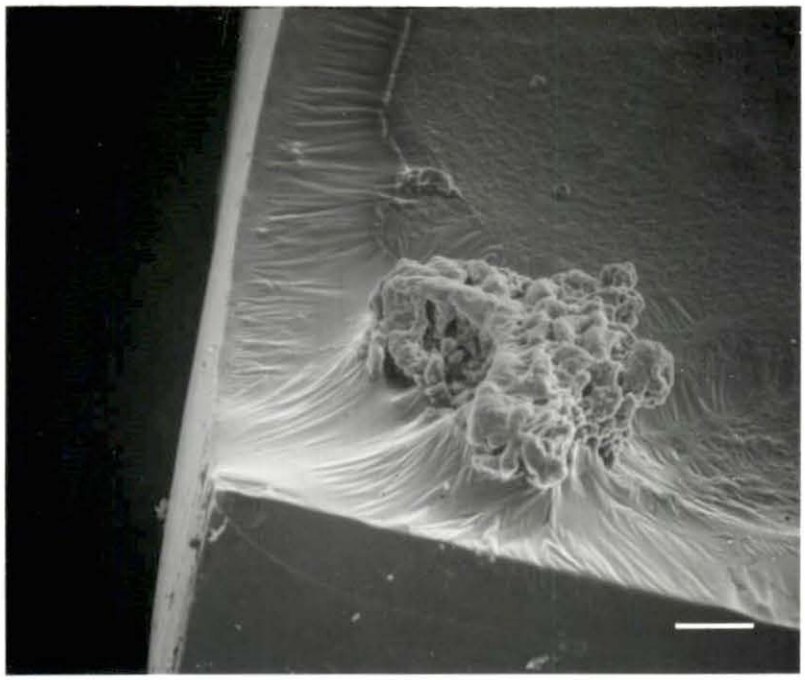

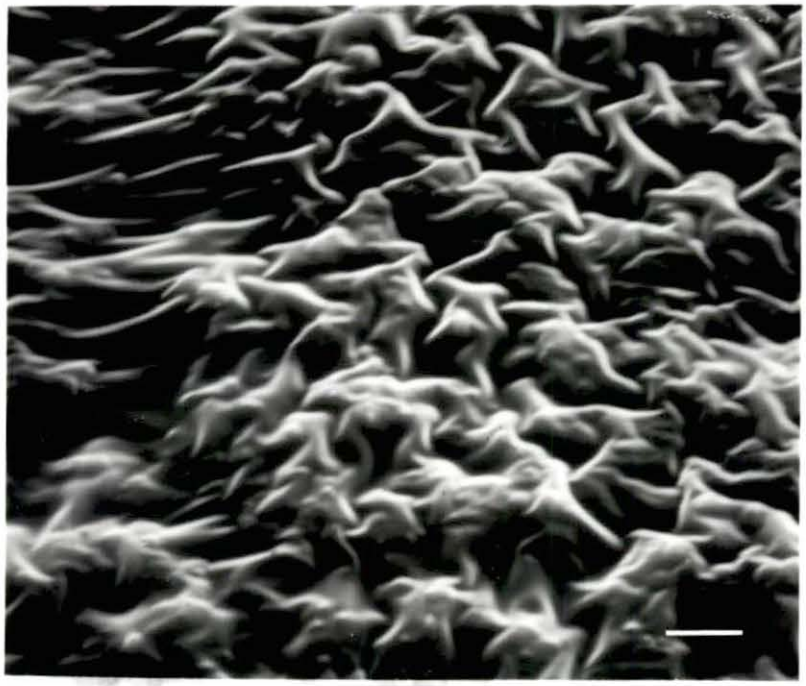

Figure 69. SEM micrograph of 2%SR/15%H/5%N shunt surface after 15 minutes of exposure to blood. (scale bar = 10 μm)

Figure 70. Low magnification micrograph of 2%SR/15%H/5%N shunt surface after 15 minutes of blood exposure showing a thrombus formation. (scale bar = 100 μm)

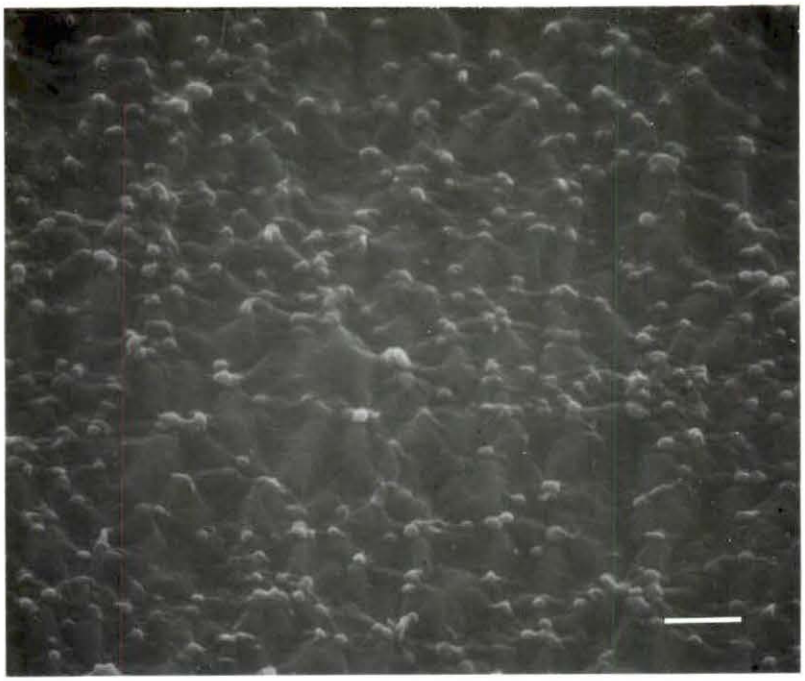

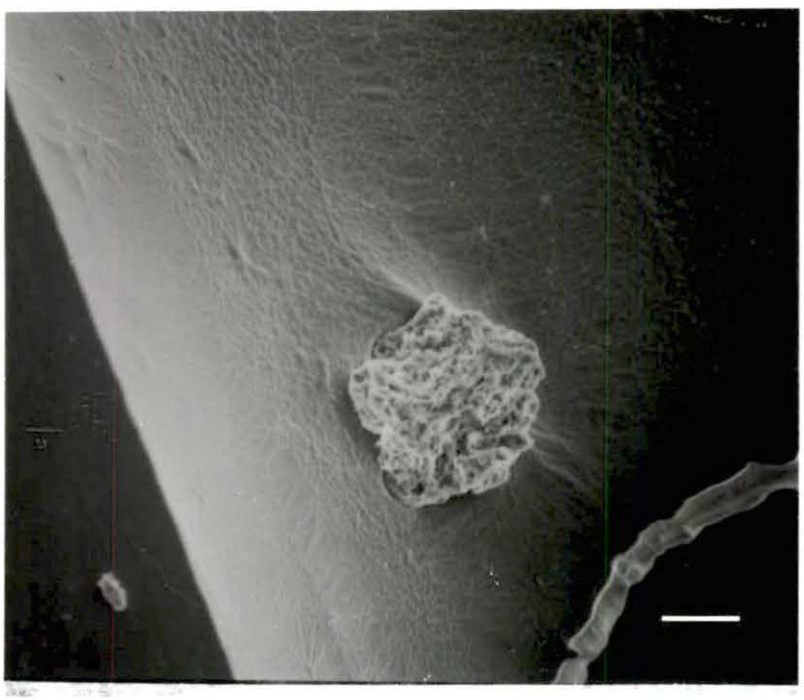

Figure 71. SEM micrograph of 2%SR/10%H/10%N shunt surface after 15 minutes of exposure to blood. (scale bar = 10 μm)

Figure 72. Low magnification micrograph of 2%SR/10%H/10%N shunt surface after 15 minutes of blood exposure showing a thrombus formation. (scale bar = 100 μm)

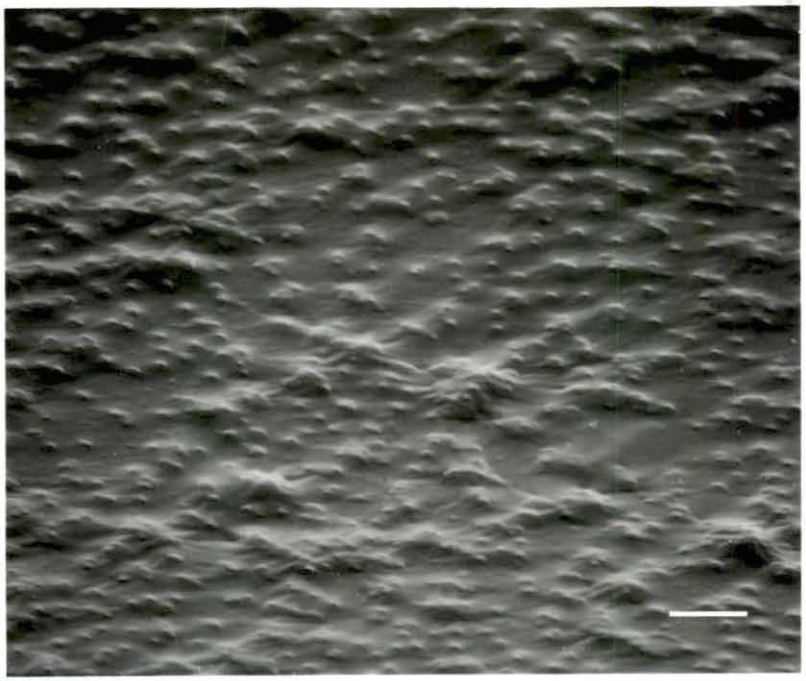

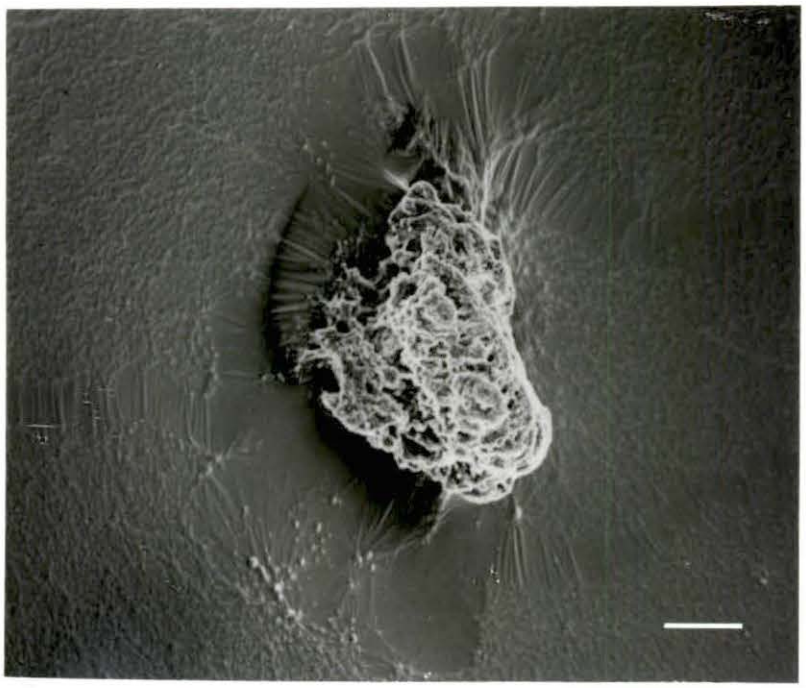

displays the pulling up effect as well as a rough texture. Another thrombus formation on this surface (Figure 73) shows no pulling up effect, and is relatively smooth in texture. Figure 74 shows no, or only a small, increase in the number of platelets adhered to the 2%SR/5%H/15%N surface compared to Figure 51. There are scattered clusters of 3 or more platelets that display some puckering. A thrombus which is seen on the surface (Figure 75) has a rough texture and shows the pulling up effect on some sides of the clot, but not on others. The base of the clot is elliptical, with the long axis oriented in the direction of flow. Concentrically from the clot, there are ridges of platelet aggregates (similiar to that seen in Figure 50) showing the pulling up effect. Figure 76 shows an increase in the number of platelets adhered to the 2%SR/0%H/20%N surface compared to Figure 52. The platelets are in the discocyte form for the most part, with some clusters displaying the puckering effect. A thrombus formation on the surface (Figure 77) shows a matted structure as opposed to a globular structure. The matted thrombus shows the pulling up effect around its borders. There are thrombus formations on top of the matted thrombus where thrombi built up into globular structures. Figure 78 shows at higher magnification that the thrombus is composed of an extensive aggregation of platelets remaining predominately in the discocyte form. However, there are areas where pseudopod extensions have formed bridges. Figure 79 shows the surface of the 12%SR/20%H/0%N shunt. The surface is somewhat rough in texture, with a decreased number of platelets adhering compared to Figure 53. Those platelets that are adhered are in the discocyte form, and the puckering effect is seen. A thrombus on this surface (Figure 80) shows a flattened clot with a smooth texture. An unsymmetrical pulling up effect

Figure 73. High magnification micrograph of a thrombus formation on 2%SR/10%H/10%N shunt surface after 15 minutes of exposure to blood. Note smooth texture of the surface. (scale bar = 10 μm)

Figure 74. SEM micrograph of 2%SR/5%H/15%N shunt surface after 15 minutes of exposure to blood. (scale bar = 10 μm)

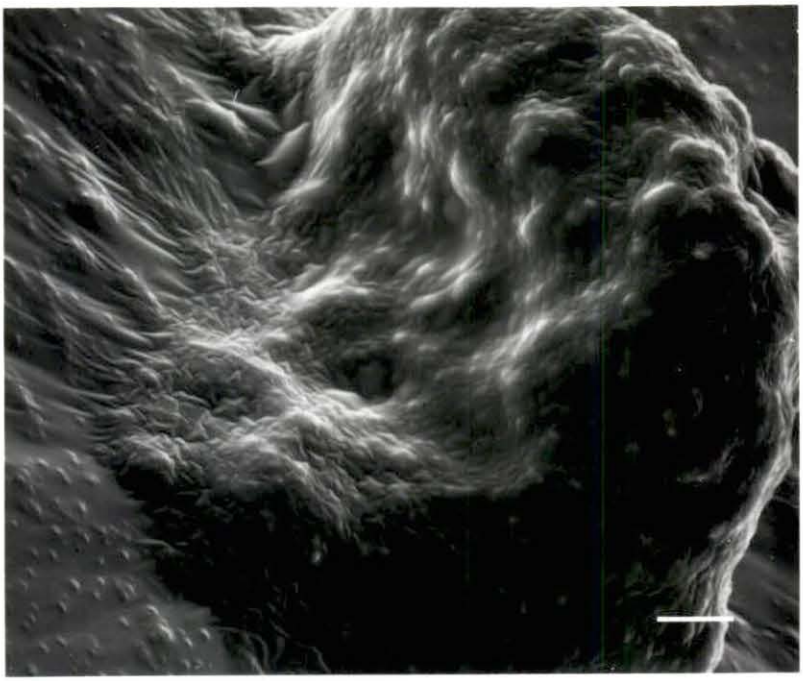

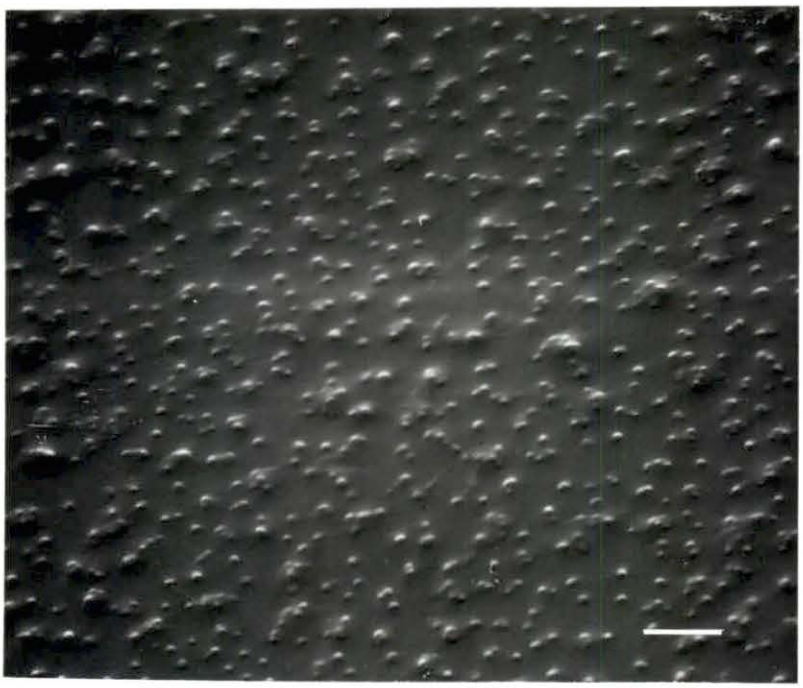

Figure 75. Low magnification micrograph of 2%SR/5%H/15%N shunt surface after 15 minutes of blood exposure showing a thrombus formation. (scale bar = 100 μm)

Figure 76. SEM micrograph of 2%SR/0%H/20%N shunt surface after 15 minutes of exposure to blood. (scale bar = 10 μm)

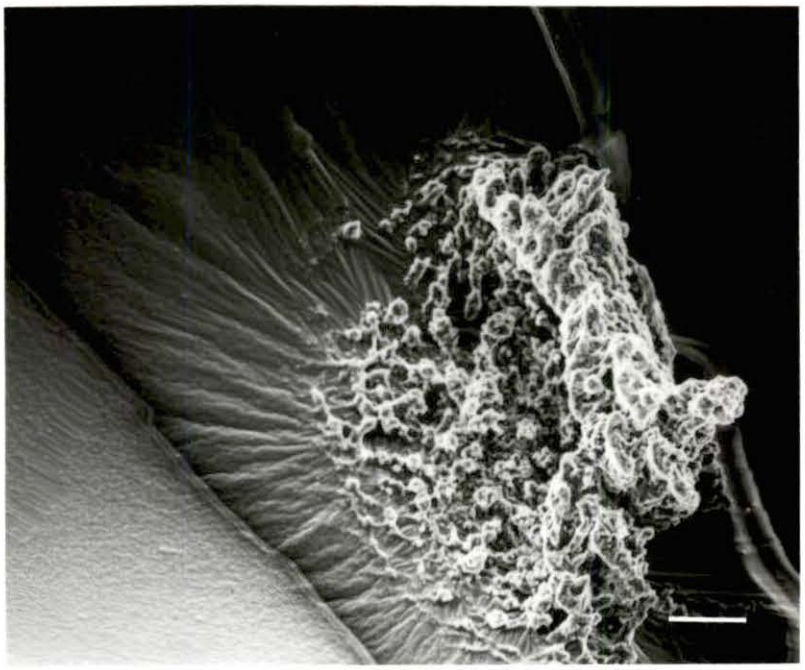

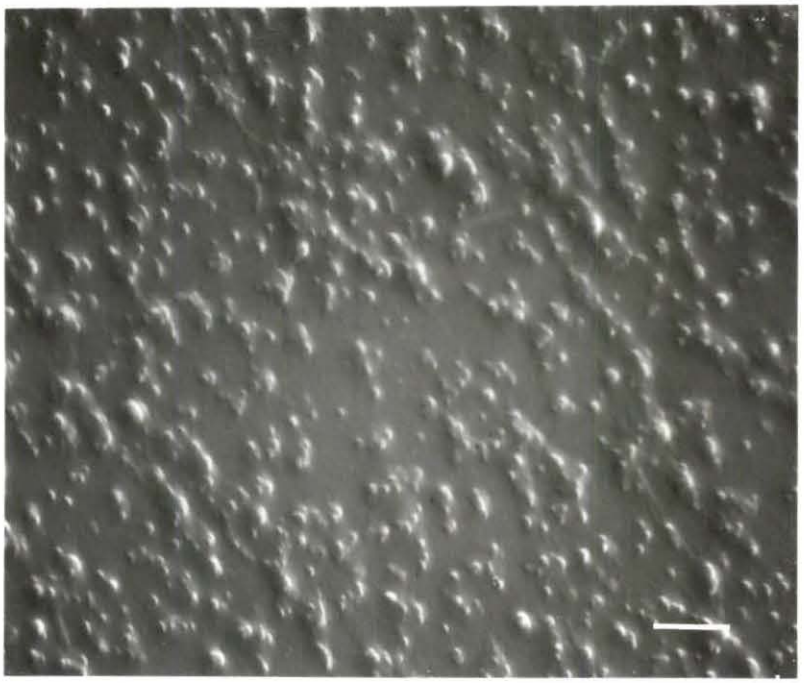

FIUGRE 77. Low magnification micrograph 2%SR/0%H/20%N shunt surface after 15 minutes of blood exposure showing a thrombus formation. Note matted appearance of the thrombus over the surface. (scale bar = 100 μm)

Figure 78. High magnification micrograph of a thrombus formation on 2%SR/0%H/20%N shunt surface after 15 minutes of exposure to blood. Note discocyte morphology of platelets in the aggregate with some bridging of pseudopods. (scale bar = 10 μm)

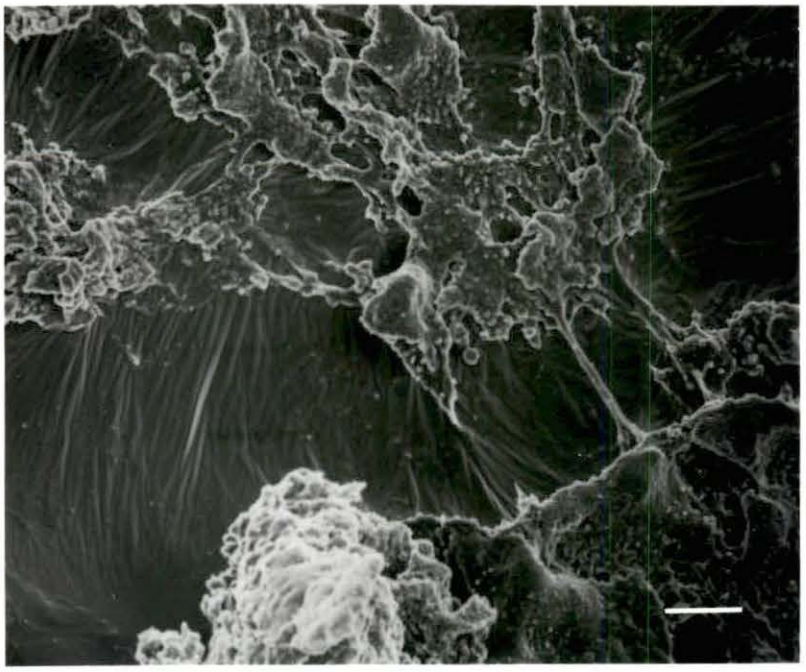

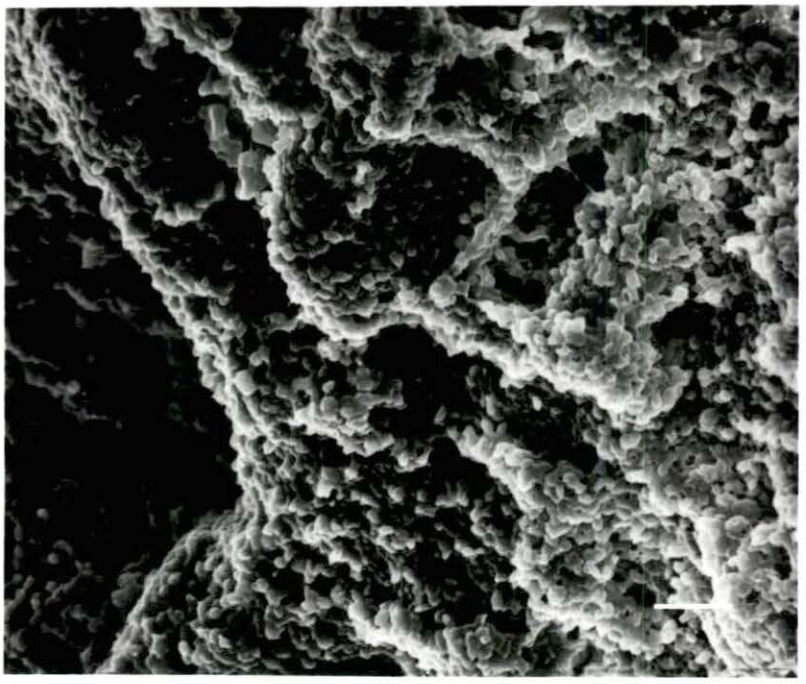

Figure 79. SEM micrograph of 12%SR/20%H/0%N shunt surface after 15 minutes exposure to blood. (scale bar = 10 μm)

Figure 80. Low magnification micrograph of a thrombus formation on 12%SR/20%H/0%N shunt surface after 15 minutes of exposure to blood. (scale bar = 10 μm)

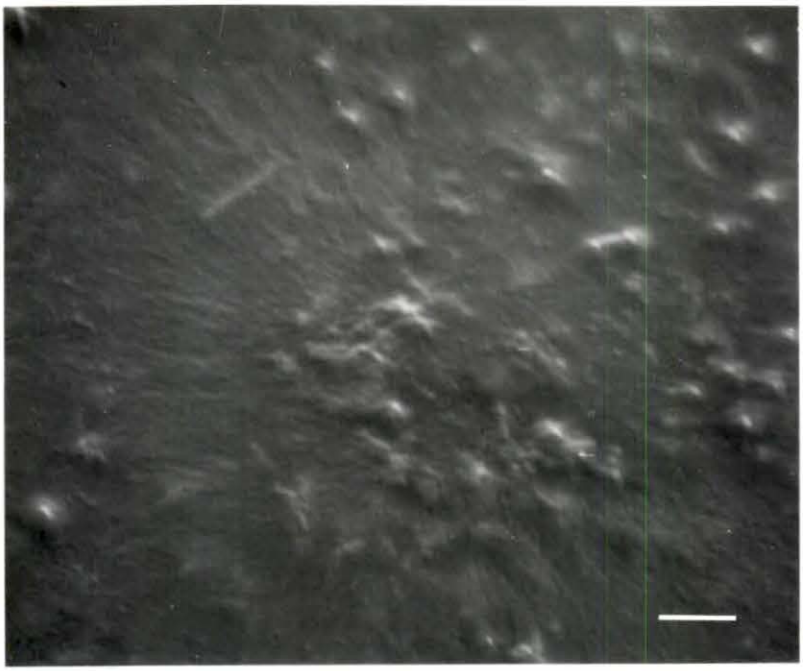

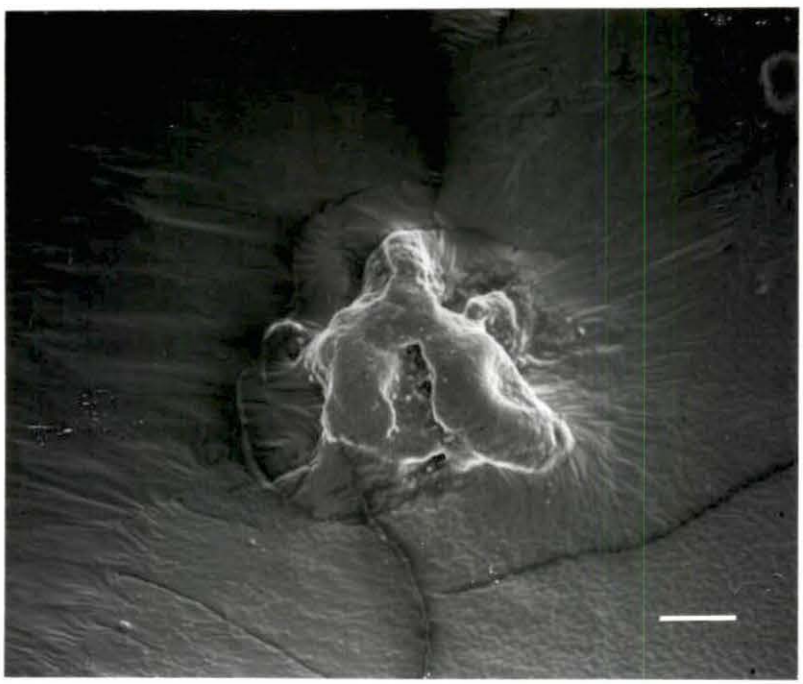

is seen around the clot, also. The clot is somewhat elliptical at the base with the major axis approximately oriented in the direction of flow. The surface of the 12%SR/15%H/5%N shunt (Figure 81) shows that there was little change in the number of platelets adhering compared to Figure 54. The platelets are in the discocyte form for the most part, with some clustering and puckering seen. A thrombus seen on this surface (Figure 82) shows extensive porosity under the clot. The pulling up effect is seen, also. The clot appears to have grown in the direction of flow through the tube; however, it is not apparent what the base of the clot looks like. Figure 83 shows at high magnification that platelets in the aggregated state form small spherical domains about 5-7 μm in diameter. There is a large increase in the number of platelets adhered to the 12%SR/10%H/10%N (Figure 84) surface compared to Figure 55. The platelets are echinocytes, showing extensive puckering between platelets. A higher magnification view (Figure 85) shows that the puckering that forms ridges between platelet adhesions may be caused by the pseudopod extensions that connect the platelets together. Further increase in magnification (Figure 86) shows that the platelets adhering to the surface/protein layer are in a spread state (7 μm in diameter), and platelets adhering on top of these platelets show pseudopod extensions. A clot that formed on this surface is shown in Figure 87. The clot has a smooth texture and displays the pulling up effect. Figure 88 shows a decrease in the number of platelets adhered to the surface of the 12%SR/5%H/15%N surface compared to Figure 56. However, the platelets form into spheres 5-7 μm in diameter (similiar to the clot seen in Figure 83). These spheres appear to aggregate to form larger spheres or thrombi. High magnification of the spheres (Figure 89) shows

Figure 81. SEM micrograph of 12%SR/15%H/5%N shunt surface after 15 minutes of exposure to blood. (scale bar = 10 μm)

Figure 82. Low magnification micrograph of a thrombus formation on 12%SR/15%H/5%N shunt surface after 15 minutes of exposure to blood. (scale bar = 100 μm)

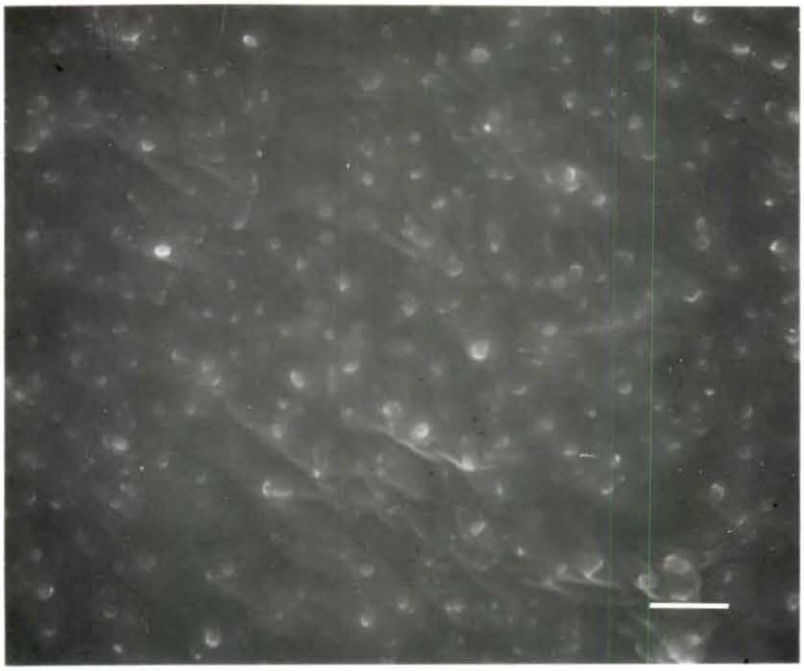

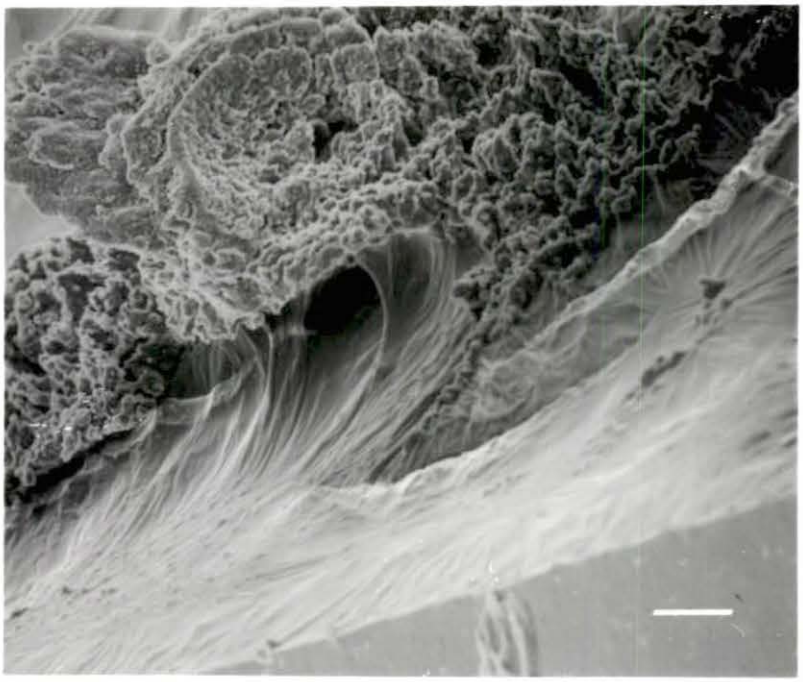

Figure 83. High magnification micrograph of a thrombus formation on 12%SR/15%H/5% shunt surface after 15 minutes of exposure to blood. Note spherical platelet aggregate formations. (scale bar = 10 μm)

Figure 84. SEM micrograph of 12%SR/10%H/10%N shunt surface after 15 minutes of exposure to blood. (scale bar = 10 μm)

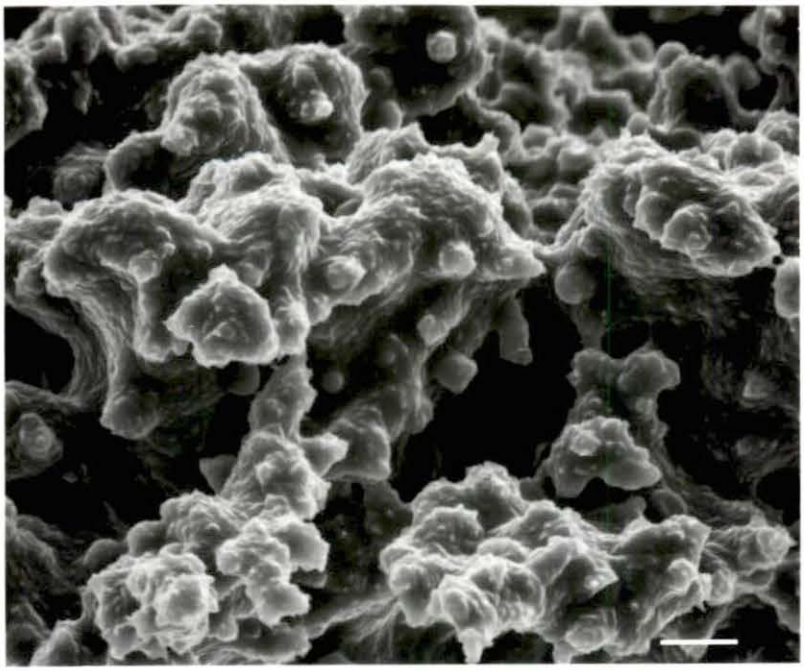

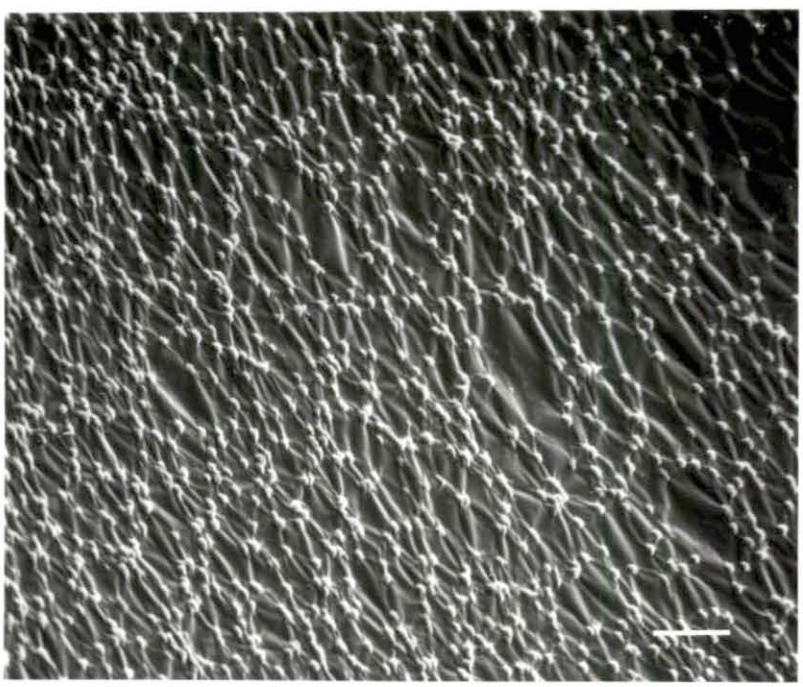

Figure 85. High magnification micrograph of 12%SR/10%H/10%N shunt surface after 15 minutes of blood exposure. Note echinocyte form of platelets. (scale bar = 5 μm)

Figure 86. High magnification micrograph of 12%SR/10%H/10%N shunt surface after 15 minutes of blood exposure. Note echinocytes adherent to spread platelets. (scale bar = 4 μm)

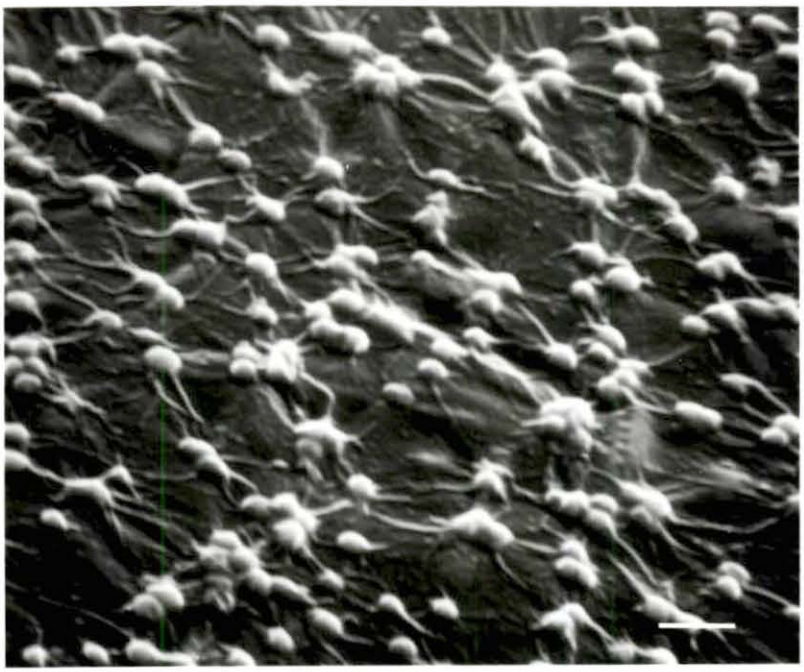

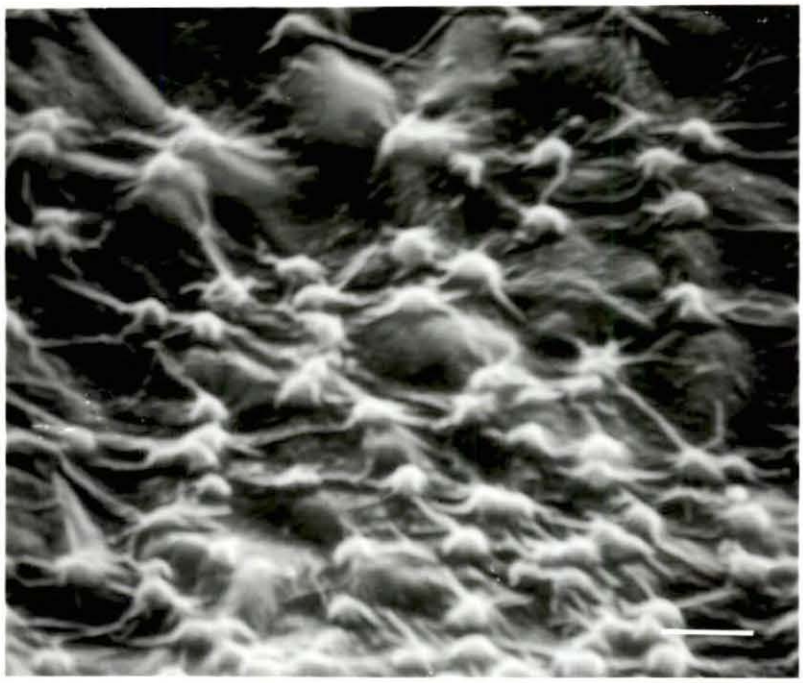

Figure 87. Low magnification micrograph of thrombus formation on 12%SR/10%H/10%N shunt surface after 15 minutes of blood exposure. (scale bar = 100 μm)

Figure 88. SEM micrograph of 12%SR/5%H/15%N shunt surface after 15 minutes of exposure to blood. Note spherical platelet aggregates (compare to Figure 83). (scale bar = 10 μm)

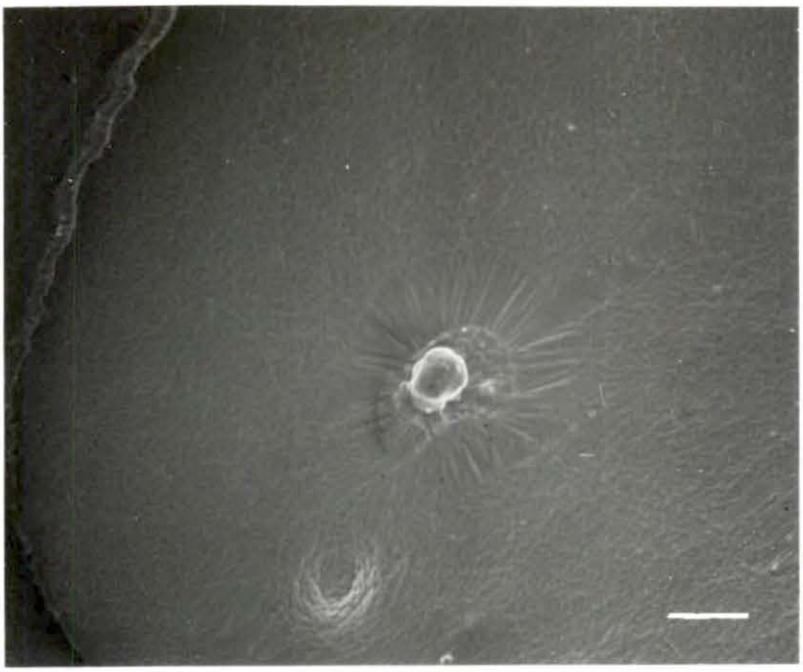

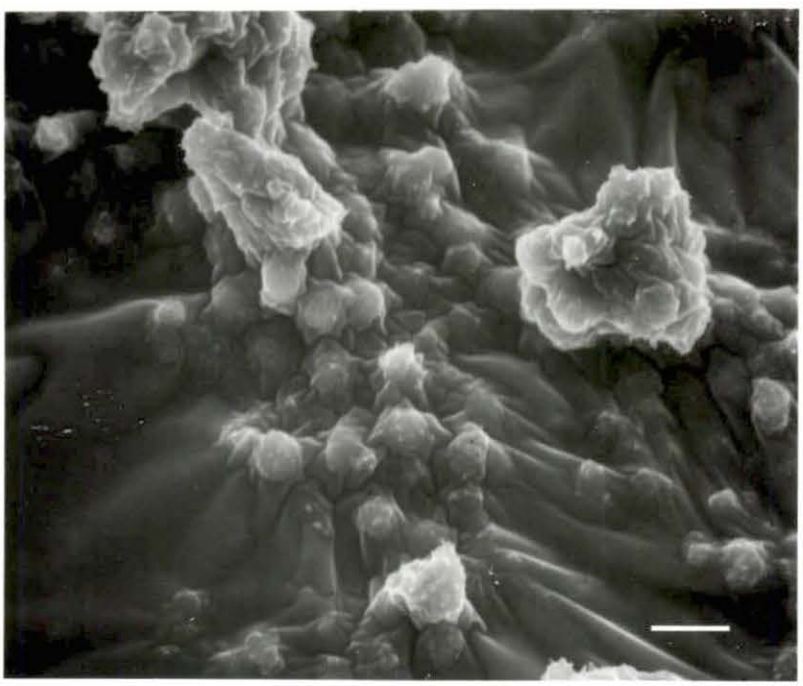

that they are possibly made of spread platelets (7 μm in diameter), with blebs formed on the surface of the platelet by the underlying granules (dense). Figure 90 shows a thrombus on the surface which was rough in texture, and the thrombus displays the pulling up effect. The 12%SR/0%H/20%N surface (Figure 91) shows no increase in the number of platelets adhered with the additional time of exposure to blood. A clot on the surface shows a rough texture and the pulling up effect (Figure 92). A higher magnification shows that there are small cells (leukocytes), 4-6 μm in diameter, on the clot (Figure 93). Figure 94 shows that these cells have very similar features to B- or T-lymphocytes, both in size and surface morphology; however, the specific type of leukocyte is not known. These cells were seen on the following other surfaces with clots: 2%SR, 2%SR/15%H/5%N, 2%SR/10%H/10%N, 12%SR/20%H/0%N, 12%SR/15%H/5%N, and 12%SR/5%H/15%N (all at 15 minutes exposure to blood).

75 minutes exposure Figure 95 shows that there was a decrease in the number of platelets adhered to the SR surface at the end of 75 minutes of exposure to blood. Platelets are seen in the echinocyte form with some in various stages of spreading. The 2%SR surface (Figure 96) shows a few scattered platelets in the discocyte form, and a small amount of puckering is seen. The area between the platelets looks somewhat rough in comparison to the other samples at shorter periods of exposure. The 12%SR surface (Figure 97) looks similar to the 2%SR surface, with a decreased number of platelets adhered compared to Figure 63. Figure 98 shows that the 2%SR/20%H/0%N surface looks like the same surface after 5 minutes of blood exposure (Figure 48). However, the area between platelets is rough in comparison to the shorter time periods of exposure, also. The

Figure 89. High magnification micrograph of spherical platelet aggregate on 12%SR/5%H/15%N shunt surface after 15 minutes of blood exposure. Note surface blebs. (scale bar = 4 μm)

Figure 90. Low magnification micrograph of a thrombus formation on 12%SR/5%H/15%N shunt surface after 15 minutes of blood exposure. (scale bar = 100 μm)

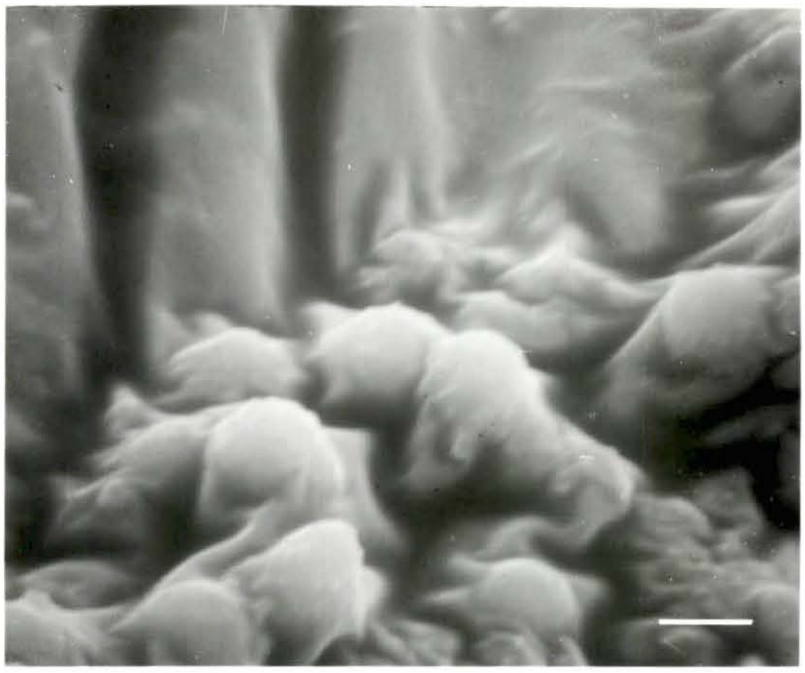

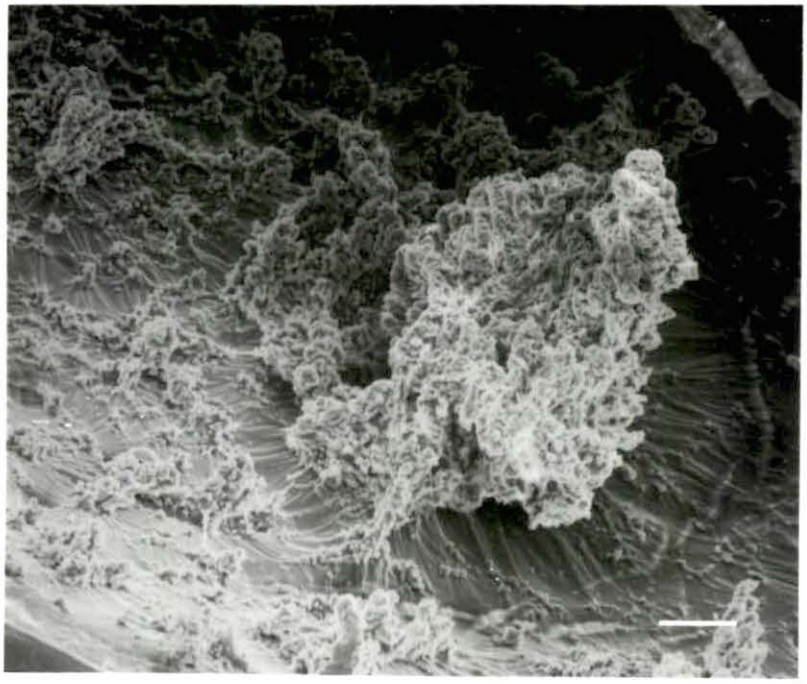

Figure 91. SEM micrograph of 12%SR/0%H/20%N shunt surface after 15 minutes of exposure to blood. (scale bar = 10 μm)

Figure 92. Low magnification micrograph of a thrombus formation on 12%SR/0%H/20%N shunt surface after 15 minutes of exposure to blood. (scale bar = 100 μm)

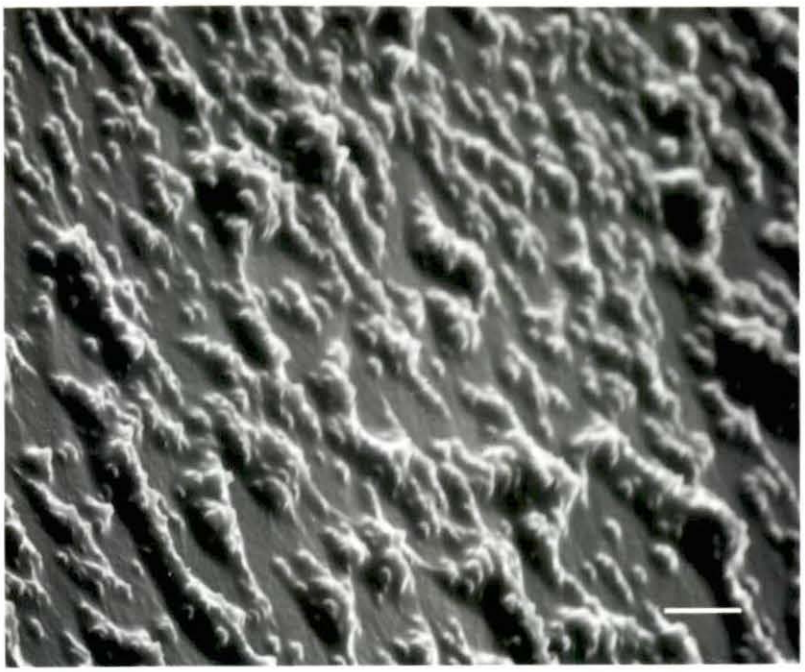

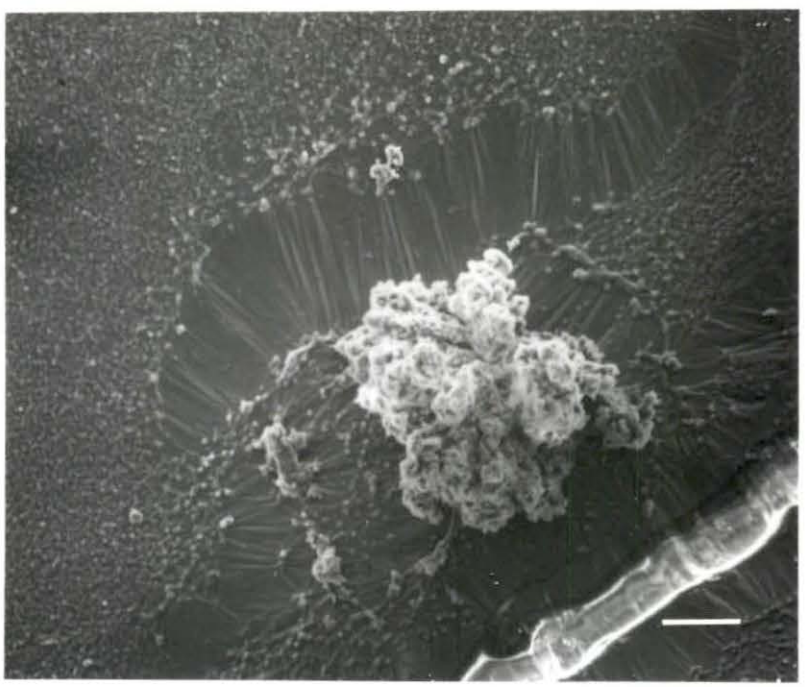

Figure 93. High magnification micrograph of a thrombus formation on 12%SR/0%H/20%N shunt surface after 15 minutes of exposure to blood. Note adherence of cells. (scale bar = 10 μm)

Figure 94. High magnification micrograph of cells on thrombus formation seen in Figure 93. Size and morphology of the cells suggest that these cells are lymphocytes. (scale bar = 3 μm)

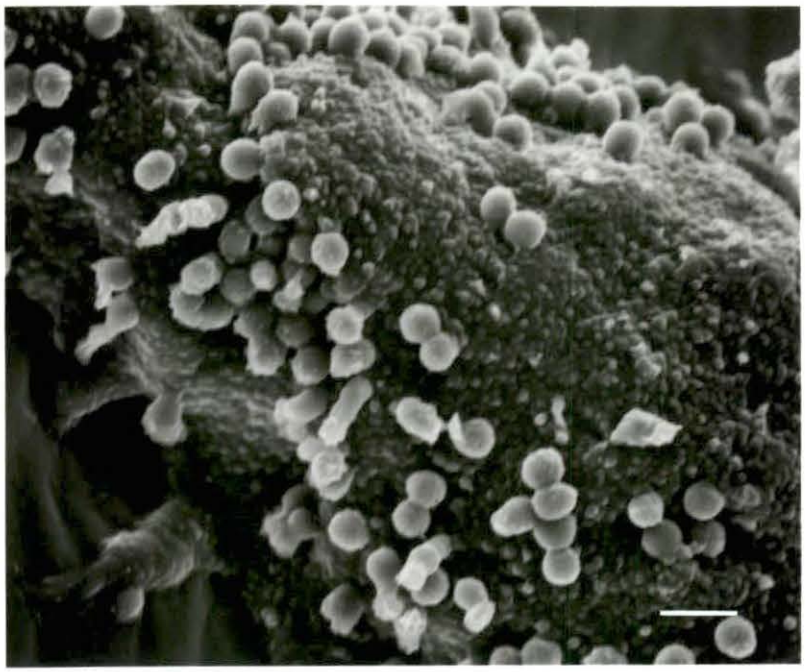

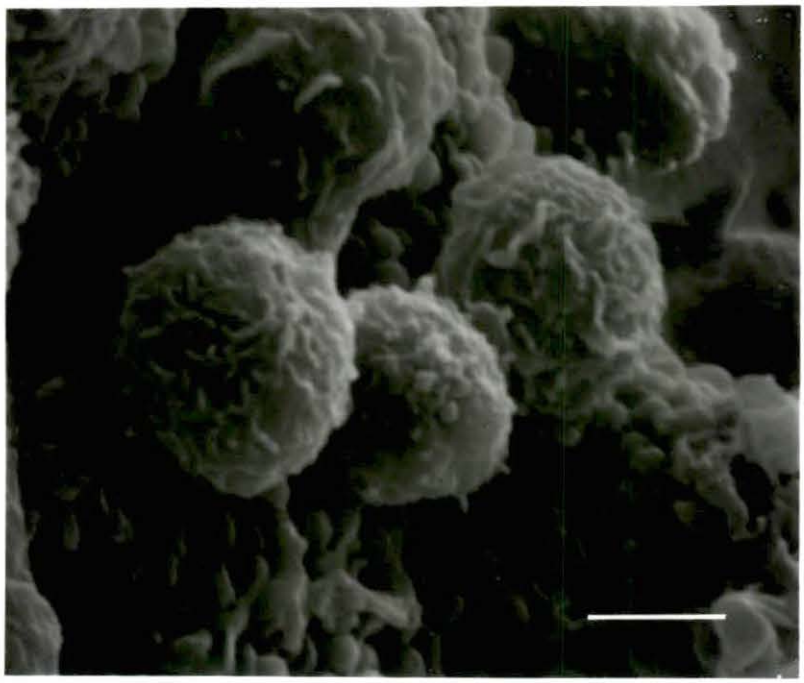

Figure 95. SEM micrograph of SR shunt surface after 75 minutes of exposure to blood. (scale bar = 1Ø μm)

Figure 96. SEM micrograph of 2%SR shunt surface after 75 minutes of exposure to blood. (scale bar = 1Ø μm)

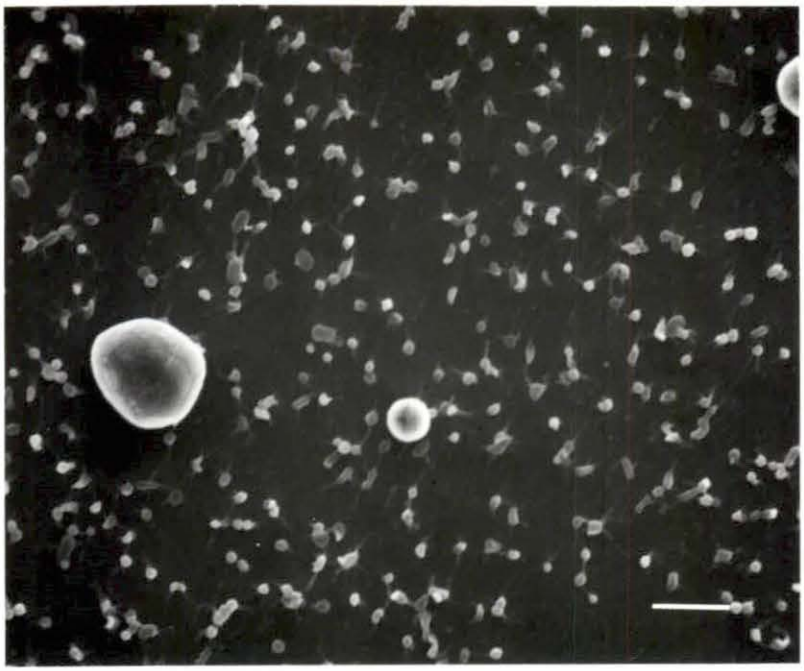

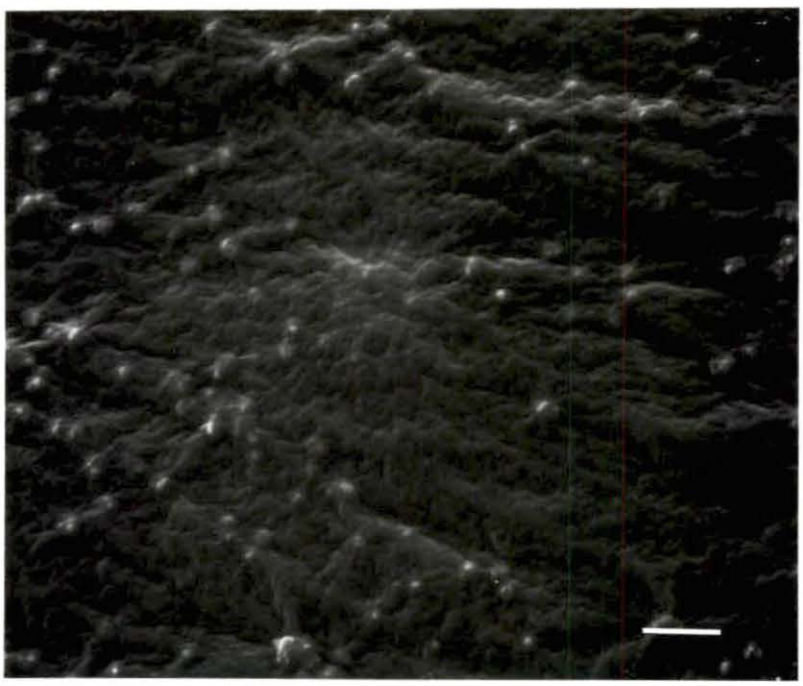

Figure 97. SEM micrograph of 12%SR shunt surface after 75 minutes of exposure to blood. (scale bar = 10 μm)

Figure 98. SEM micrograph of 2%SR/20%H/0%N shunt surface after 75 minutes of exposure to blood. (scale bar = 10 μm)

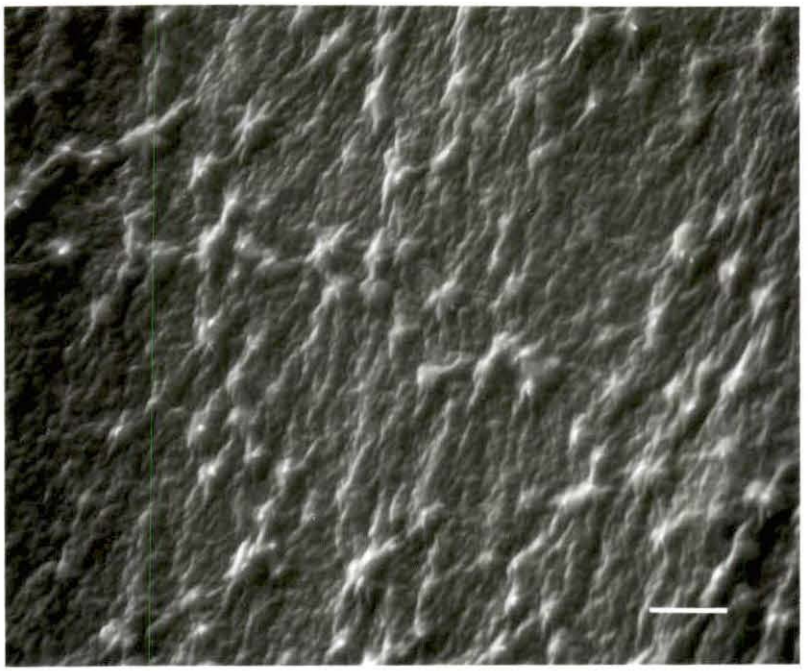

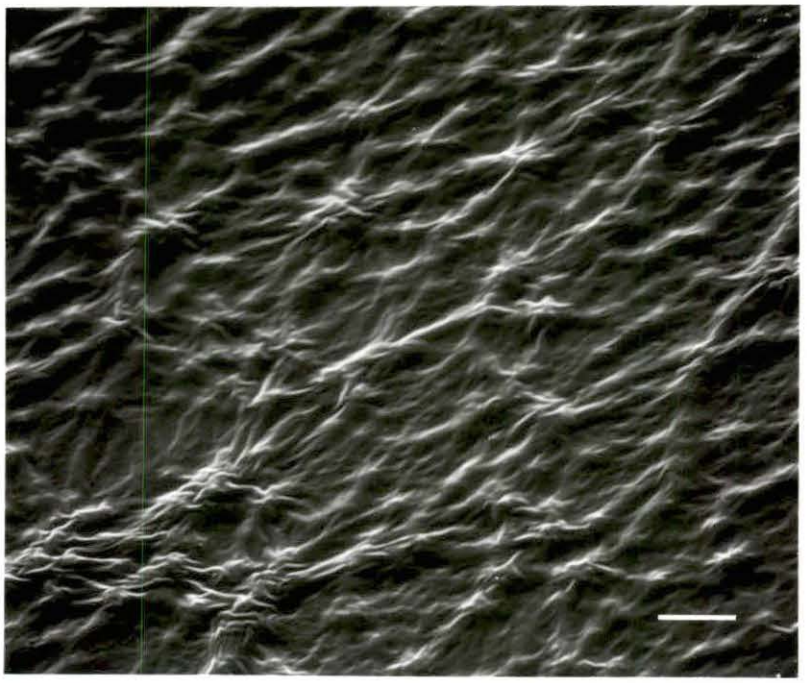

2%SR/15%H/5%N surface (Figure 99) shows the base of a thrombus. Figure 100 shows the surface of the 2%SR/10%H/10%N shunt with a decreased number of adhered platelets compared to Figure 71. The surface looks very similar to the same surface after 15 seconds of exposure (Figure 22), except that a few domains of platelet aggregation are seen. The 2%SR/5%H/15%N surface (Figure 101) morphology looks similar to the same material after 15 minutes of exposure (Figure 74). However, the area between the platelets is rough in comparison to the shorter time periods of exposure. Figure 102 shows the 2%SR/0%H/20%N surface. This surface looks similar to the same surface after 15 minutes of exposure to blood (Figure 76), also. Some clustering and aggregation of platelets is seen, as well as rough texture in areas which were smooth after shorter time periods of exposure. The 12%SR/20%H/0%N surface (Figure 103) shows similarities to the same surface after 5 minutes of exposure (Figure 53). There is some clustering of platelets. The smooth areas between platelets after short periods of exposure now have a rough texture. Figure 104 shows that the 12%SR/15%H/5%N surface looks like the same surface after only 15 seconds of exposure to blood (Figure 26). The areas between platelets remained fairly smooth. The 12%SR/10%H/10%N surface (Figure 105) shows extensive formation of red thrombus. Fibrin strands are seen entrapping red blood cells. Figure 106 shows the 12%SR/5%H/15%N surface which looks much like the same surface after 5 minutes of exposure (Figure 56); however, the thrombus formations in this shunt were flushed out, so it is difficult to analyze blood/material interaction features on this surface. Figure 107 shows the 12%SR/0%H/20%N surface. This surface shows features similar to those of

Figure 99. SEM micrograph of 2%SR/15%H/5%N shunt surface after 75 minutes of exposure to blood. (scale bar = 10 μm)

Figure 100. SEM micrograph of 2%SR/10%H/10%N shunt surface after 75 minutes of exposure to blood. (scale bar = 10 μm)

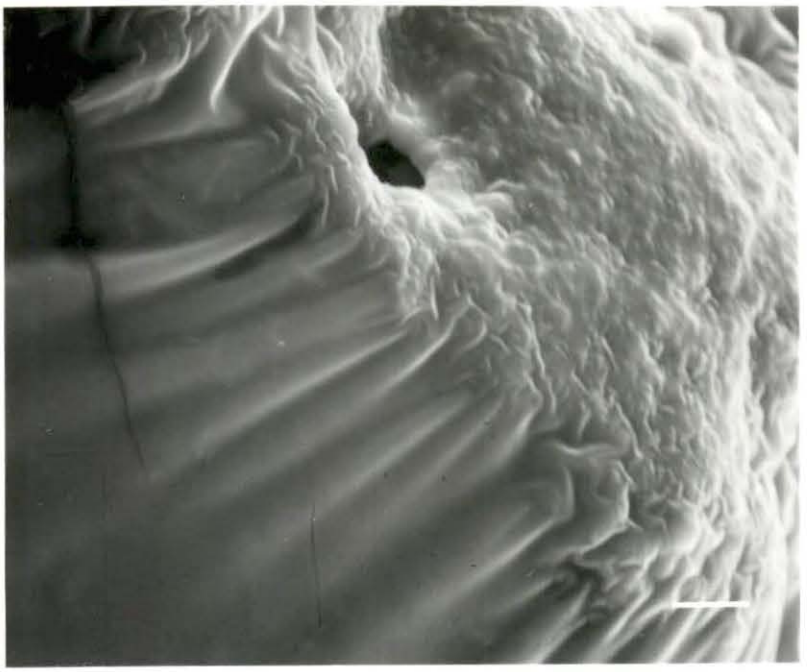

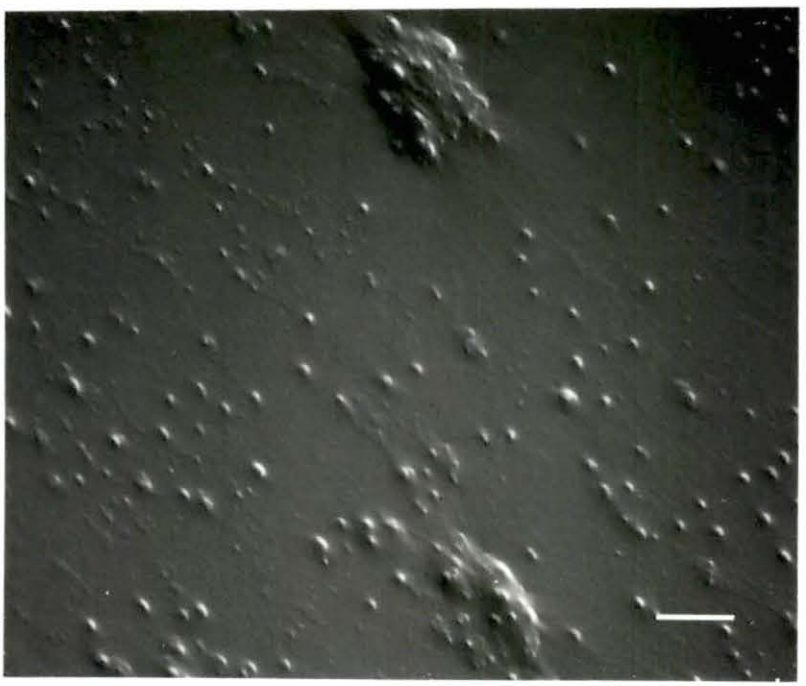

Figure 101. SEM micrograph of 2%SR/5%H/15%N shunt surface after 75 minutes of exposure to blood. (scale bar = 10 μm)

Figure 102. SEM micrograph of 2%SR/0%H/20%N shunt surface after 75 minutes of exposure to blood. (scale bar = 10 μm)

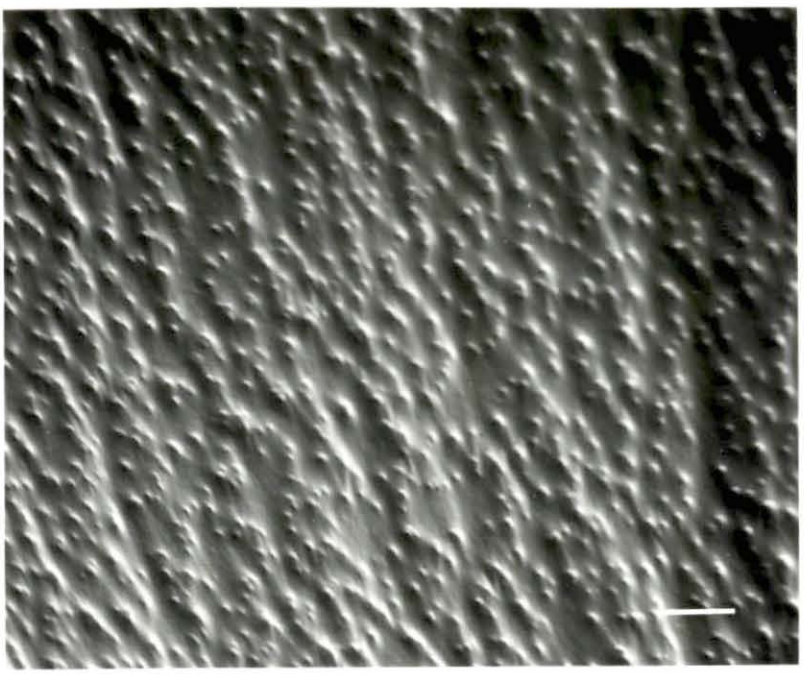

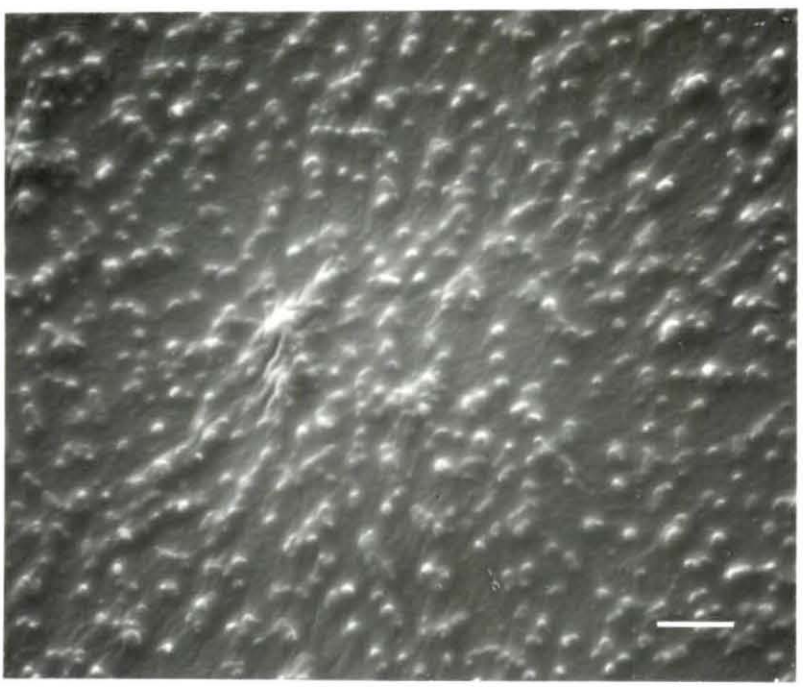

Figure 103. SEM micrograph of 12%SR/20%H/0%N shunt surface after 75 minutes of exposure to blood. (scale bar = 10 μm)

Figure 104. SEM micrograph of 12%SR/15%H/5%N shunt surface after 75 minutes of exposure to blood. (scale bar = 10 μm)

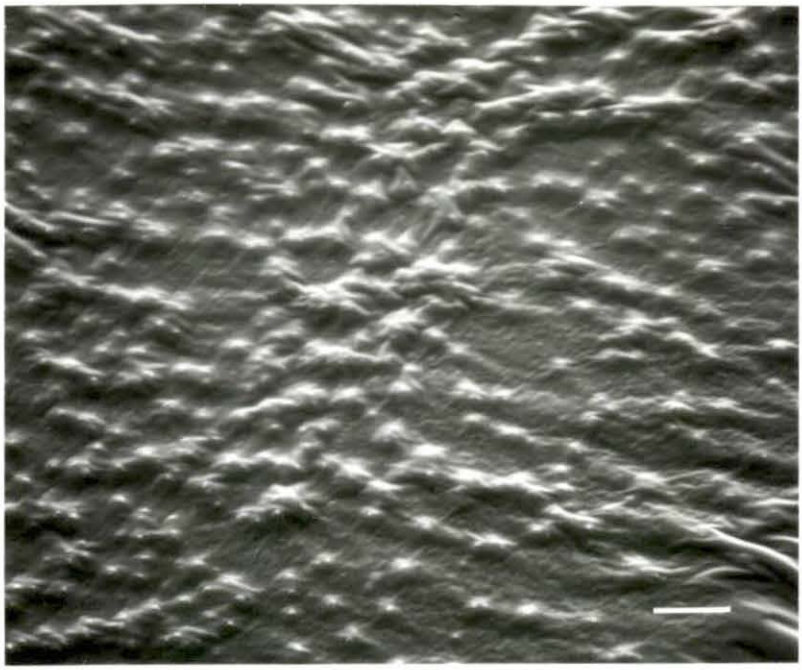

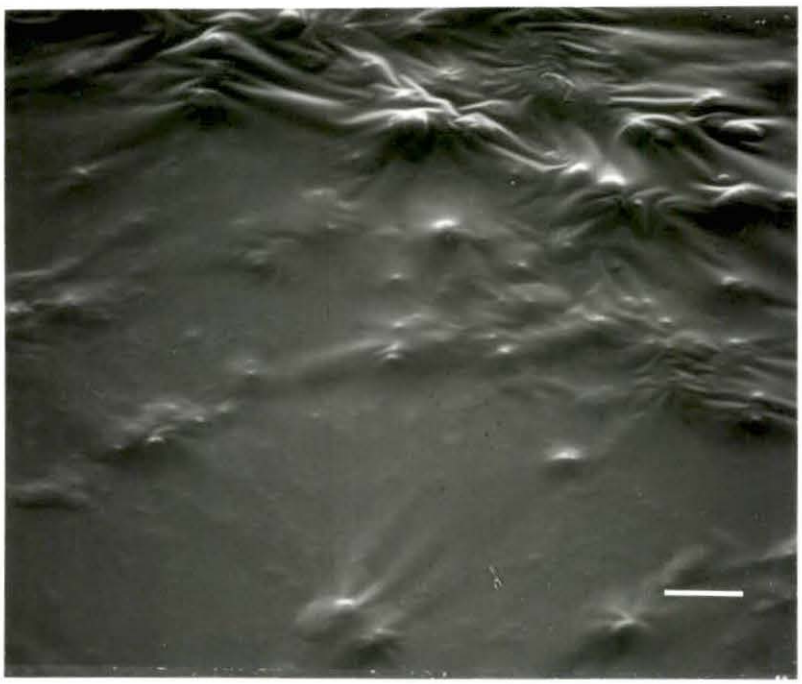

Figure 105. SEM micrograph of 12%SR/10%H/10%N shunt surface after 75 minutes of exposure to blood. Red blood cells are seen entrapped in a fibrin network. (scale bar = 10 μm)

Figure 106. SEM micrograph of 12%SR/5%H/15%N shunt surface after 75 minutes of exposure to blood. Clot was flushed from the tube. (scale bar = 10 μm)

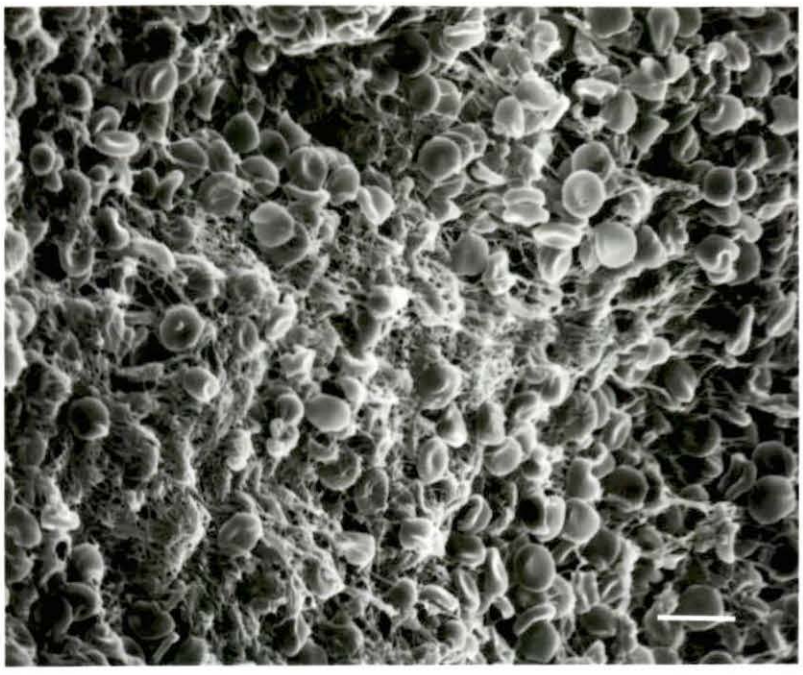

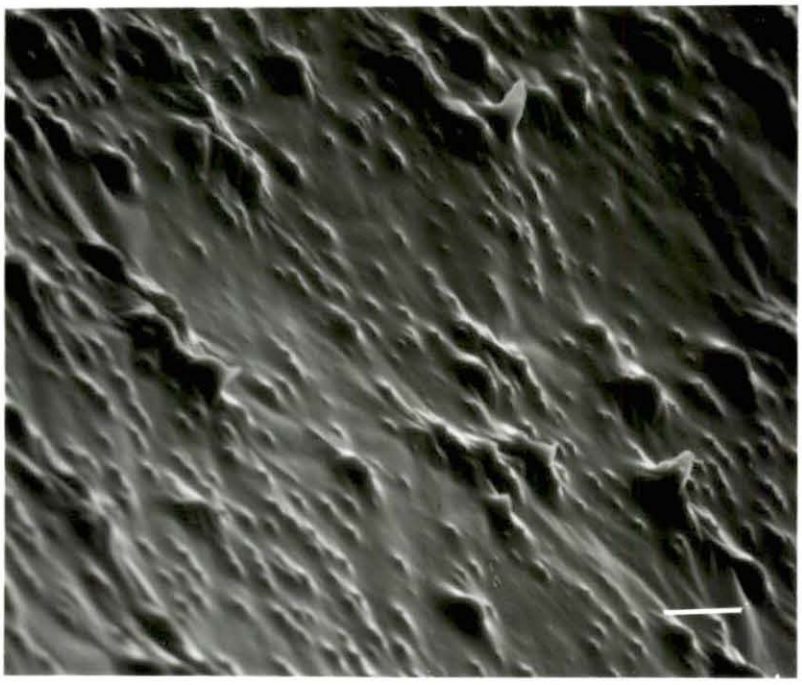

Figure 107. SEM micrograph of 12%SR/0%H/20%N shunt surface after 75 minutes of exposure to blood. Surface has red blood cells and some fibrin strands (compare to Figure 105). Clot was flushed from the tube. (scale bar = 10 μm)

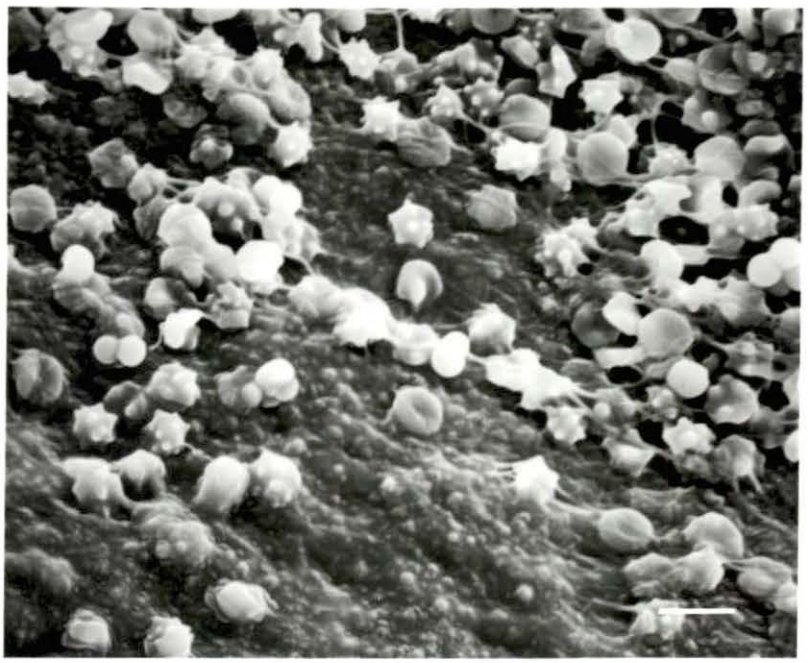

Figure 105, with fibrin strands and red blood cells seen. However, this clot was flushed from the tube, also.

FTIR analysis of shunt surfaces

Appendix A lists the parameters used in collection of each single beam spectrum file. The FTIR spectra of all shunt surfaces after all appropriate spectral subtractions are shown in Appendix B. Absorbance bands occurred at 1730, 1650, 1550, 1450, 1385, 1160, 1100, 1080, and 1040 cm^{-1}. However, the most consistent bands were the 1650 and 1550 cm^{-1} bands. The others were seen occasionally on some of the spectra. Table 3 shows graphically the intensity of the 1550 cm^{-1} band for all formulations at each period of exposure to blood. Table 4 lists the integrated intensities for the 1550 cm^{-1} band of the samples for each time period. Table 5 summarizes integrated areas under weak 1550 cm^{-1} bands seen on NVP containing formulations.

The SR sample showed about average absorbance intensities for the first 2 time periods of exposure to blood (average refers to the average intensity of all 13 samples at one time period; see Table 4). After 5 minutes of exposure, the intensity was almost double the intensity of the average for this period. The intensity then dropped to about half the average intensity seen for 15 and 75 minutes of exposure, respectively. The 2%SR surface had absorbance band intensity that was about average for the first 30 seconds, also. The 5 minute intensity was above the average, as well as the 15 and 75 minute intensities. The 12%SR surface showed no detectable absorbance intensity for the 15 and 30 second exposure periods. After 5 minutes of exposure, the intensity was above the average for this

Table 3. Summary of 1550 cm^{-1} bands at each time period of exposure

Sample	Time Period (minutes) 0.25	0.5	5	15	75
SR					
2%SR					
12%SR					
2%SR/20%H/0%N					
2%SR/15%H/5%N					
2%SR/10%H/10%N [a]					

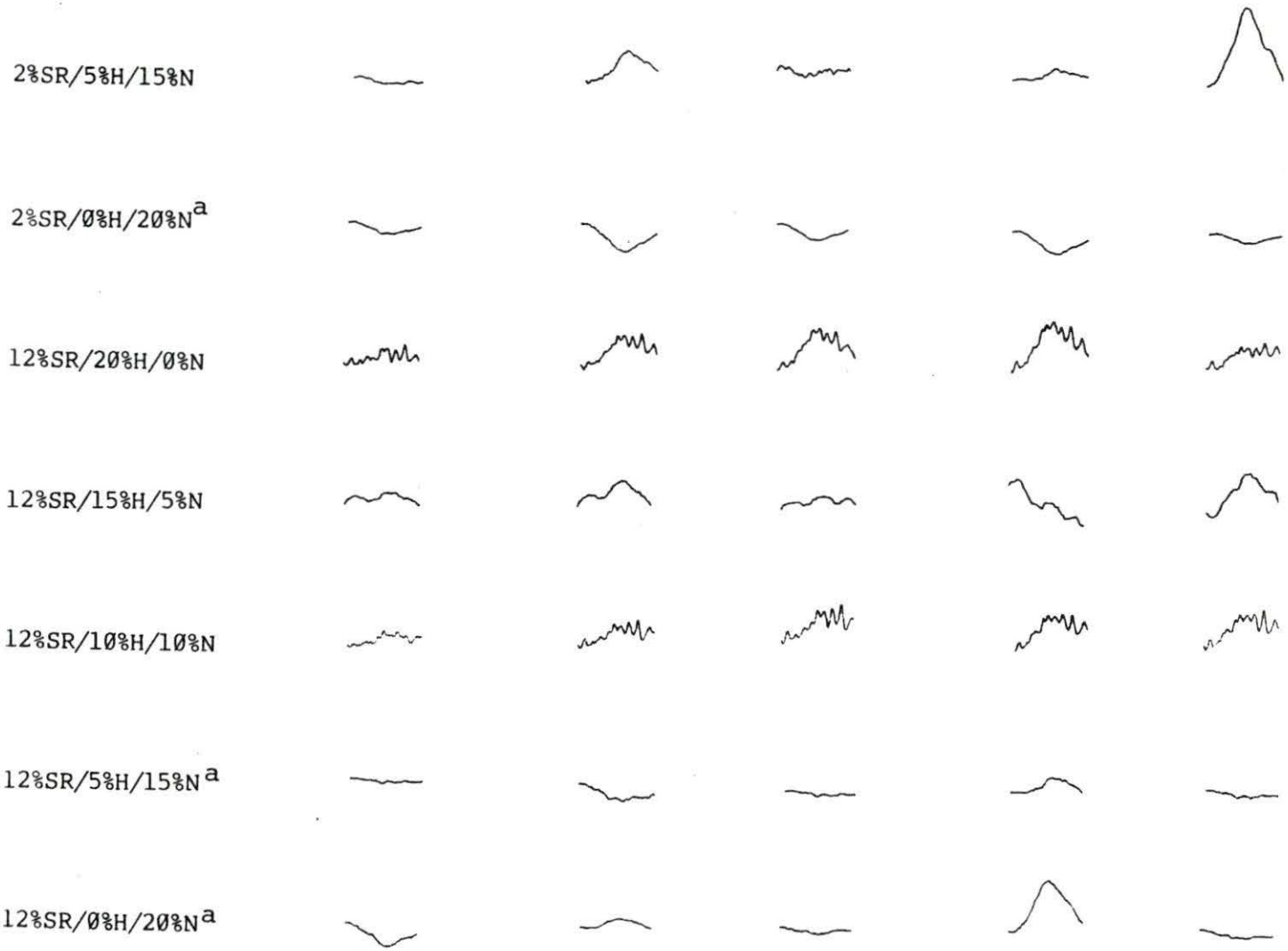

[a]Samples were three times larger than other samples, so the band shown is compressed by a factor of three.

Table 4. Integrated area of 1550 cm^{-1} band at each time period for exposed samples, (absorbance units·cm^{-1})

Sample	Time (minutes) 0.25	0.5	5	15	75
SR	0.067	0.070	0.441	0.168	0.176
2%SR	0.093	0.191	0.335	0.311	0.252
12%SR	0.087	n.d.[a]	0.454	0.274	0.196
2%SR/20%H/0%N	0.273	0.214	0.767	0.367	0.288
2%SR/15%H/5%N	0.162	0.279	0.406	0.503	0.581
2%SR/10%H/10%N[b]	0.190	0.024	0.033	0.168	0.011
2%SR/5%H/15%N	n.d.	0.353	n.d.	0.102	1.017
2%SR/0%H/20%N[b]	n.d.	n.d.	n.d.	n.d.	n.d.
12%SR/20%H/0%N	0.087	n.d.	0.495	0.575	0.235
12%SR/15%H/5%N	0.033	0.074	0.046	0.032	0.547
12%SR/10%H/10%N	0.098	0.169	0.306	0.407	0.401
12%SR/5%H/15%N[b]	0.001	0.001	0.001	0.209	0.001
12%SR/0%H/20%N[b]	n.d.	0.100	n.d.	0.669	n.d.
Mean	0.084 ±0.081	0.113 ±0.113	0.253 ±0.245	0.291 ±0.199	0.285 ±0.284

[a]Indicates samples that were three times larger than the others, therefore the tabulated values represent 1/3 of the 1550 cm^{-1} band measured for a sample.

[b]None determined by the integration measurement.

Table 5. Integrated area of 1550 cm^{-1} band (unexposed reference samples), (absorbance units·cm^{-1})

Sample	Area[a]
SR	n.d.[b]
2%SR	n.d.
12%SR	n.d.
2%SR/20%H/0%N	n.d.
2%SR/15%H/5%N	n.d.
2%SR/10%H/10%	0.049
2%SR/5%H/15%N	0.186
2%SR/0%H/20%N	0.333
12%SR/20%H/0%N	n.d.
12%SR/15%H/5%N	0.362
12%SR/10%H/10%N	n.d.
12%SR/5%H/15%N	0.130
12%SR/0%H/20%N	0.131

[a]These factors may be added to the various exposed formulation band areas in Table 4 for the appropriate formulations in efforts to further adjust spectra for an indication of the amount of protein build-up. These reflect a possible weak 1550 cm^{-1} band on NVP containing formulations. As the source of this band is not understood, these values are listed separately. These are determined from the F series of FTIR spectra in Appendix B.

[b]None determined by the integration measurement.

period. The 15 minute intensity was about average, while the 75 minute intensity was below average. The 2%SR/20%H/0%N surface showed double the average intensity for the first 30 seconds. After 5 minutes of exposure, the intensity was triple the average. The 15 minute intensity dropped to slightly above average, while the 75 minute intensity was about average to slightly below average. The 2%SR/15%H/5%N surface showed about average intensity for the first 30 seconds. The intensity at 5 minutes was above average, as were the intensities for the 15 and 75 minute periods. The 2%SR/10%H/10%N surface showed an intensity of about double for the 15 second sample, while the intensity dropped to below average during the next 15 seconds of exposure. The intensity of the 5 minute sample was well below the average. The 15 minute sample had about half the average intensity, and the 75 minute sample had well-below the average intensity. The 2%SR/5%H/15%N surface had no measurable intensity for the first 15 seconds of exposure. However, the intensity of the 30 second sample was more than double the average before dropping to unmeasurable amounts for the 5 minute sample. The intensity of the 15 minute sample was about half of the intensity of average. After 75 minutes of exposure, the intensity increased to about 3.5 times the average. The 2%SR/0%H/20%N shunt showed no measurable intensity for each of the time periods. The 12%SR/20%H/0%N surface had about average intensity for the first 15 seconds of exposure. The intensity increased during the 30 second exposure to more than double the average, and stayed that way for the next two time periods before dropping to below average intensity for the 75 minute period. The 12%SR/15%H/5%N surface had about an average intensity for the first 15 seconds before increasing to almost double for the 30 second sample. The

intensity then dropped to about half the average intensity for the next two time periods before increasing to almost double the average for the 75 minute sample. The 12%SR/10%H/10%N surface displays about average intensity for the first 5 minutes of exposure. However, the intensity seen for the final two periods is above average. The 12%SR/5%H/15%N surface shows no measurable intensity for the first 5 minutes of exposure. The 15 minute intensity is below average before dropping to a level below the detection limit for the last time period. The 12%SR/0%H/20%N surface shows no measurable intensity for the first 15 seconds, average for the 30 second sample, and unmeasurable for the 5 minute sample. The intensity at 15 minutes is more than double the average before dropping below the detection level for protein deposition when evaluated at the 75 minute exposure period.

Discussion

SEM analysis

The first visible change in the materials after only 15 seconds of exposure to blood is loss of surface texture, probably as a result of protein deposition. This is best seen in the SR shunt samples. It is also apparent that platelets adhere very soon after blood comes in contact with a surface. The SR surface (as well as the others) showed adherent platelets on the surface after 15 seconds of exposure to blood. Some of these platelets had changed to echinocytes (a process that has been reported to take as little as 5 seconds), indicating that some of the platelets may have been adhered as early as 10 seconds after exposure to the surface.

With increased exposure, there is an increase in the number of platelets adhered to the surfaces. Most of the surfaces showed this increase up to the 5 minute period (Figure 1). Surfaces with low critical surface tension (26-28 dynes/cm) appeared to have fewer adherent platelets than surfaces with higher critical surface tensions (Figure 2, and a comparison of Figures 1 and 2). Surfaces with critical surface tensions below 20 dynes/cm had increased numbers of adherent platelets, also (Figure 2, and a comparison of Figures 1 and 2). However, after this time, the number of platelets adhering appeared to reach a plateau in which the platelet lawns did not grow. Instead, during this time, the predominant activity on the surface, during the 5 and 15 minute periods, appeared to be aggregation and thrombus formation. Most of the thrombi that formed had elliptical bases with the major axis oriented in the direction of blood flow through the tube. By 75 minutes of exposure, most of the surfaces had platelet lawns that looked like the samples exposed for shorter periods of time. This suggests that the surfaces are not static, but undergo dynamic cyclic changes which appear to be the following: (1) loss of surface texture of the material through adsorption of protein and adhesion of platelets, (2) increases in the number of platelets adhering up to about the 5 minute mark, (3) clustering, aggregation, and thrombus formation by 15 minutes, (4) embolization, which either re-exposes the surface of the material or reveals the proteins that were sandwiched between the surface of the material and the thrombus, (5) re-initiation of the process, leading to new thrombus formation.

Although the SR surface did not have any thrombus formations by 15 minutes and that all the other surfaces did, this does not mean that this

surface is better in terms of blood compatibility. Since extensive aggregation was seen on the surface by 5 minutes of exposure, it appears that thrombi may have formed, and subsequently embolized before the end of the 15 minute period. Thus, it would be expected that the process of thrombus formation would be re-initiated. Looking at Figure 59 (which shows the SR surface at 15 minutes), one can see a platelet lawn that appears to have reached a plateau. Thus, this may be the case. All of the surfaces when considered in time sequence display the dynamic cycling events on the surface, but the rates appear to be different among these samples.

After the platelets become adhered to the surface, a shape change occurs. Echinocytes are clearly visible on the SR surface, indicating that a shape change has occurred. Higher magnification of the platelets reveals that the release reactions accompany the shape change in most cases. These changes are manifested in surface pits and small blebs seen as part of the surface morphology. In the work of Allen et al. (1979), pits have been reported to represent the site where a granule has fused, and has been released. The blebs are suggested to be sites where a granule is protruding under the plasma membrane. In the SEM of the current study, analogous features are seen, and are interpreted to be the result of the release reactions as suggested in the work of Allen et al. (1979). Some platelets on the SR surface display these features as early as 30 seconds after exposure to blood. Most of the other surfaces showed platelets adhered in discocyte form, with a smooth surface. It appears that surfaces that are more blood compatible may directly or indirectly (through interactions with protein adsorption) delay the shape change. This may

explain why there are different rates seen in the dynamic cycling events on the different surfaces.

Most of the surfaces show a puckering effect under the platelets that are adhered to the surface. In some cases, it appears only when the platelets are in clusters. This may be due to the interactions occurring between the platelet membrane and the adsorbed protein, as well as the interactions between the adsorbed protein and the surface of the material. Since platelets have many sites on the surface of the membrane with which to bind, the puckering effect may be due to the processes involved in the shape change. For example, the platelet may be undergoing shape changes such that, as the shape change occurs, there is an accompanying increase in the number of binding sites becoming bound to the protein layer, and this results in the protein layer being lifted off the surface of the material. This may be an indication of how strongly the protein layer is bound to the surface. In some cases, individual platelets exhibit some puckering, while in others, puckering is seen only when there is clustering. The puckering effect produced by individual platelets is generally on the hydrophilic surfaces, while the hydrophobic surfaces generally display the effect when the platelets are clustered. It may be that when an individual platelet can exhibit the puckering effect, the protein layer/surface adhesion may not be strong. As indicated earlier, a hydrophilic surface would not be expected to hold a protein layer tightly. When puckering is seen only with clustering, it may mean that the protein is tightly bound and that it takes the concerted efforts of the platelets in the cluster to lift the protein off the surface.

By about the 5 minute mark, the platelets begin to aggregate. Some of the higher magnification pictures show the early stages of aggregation. In some cases, the platelets adhere to the surface/protein layer, and show signs of spreading. On top of these platelets, it can be seen that another platelet, usually in discocyte form, is adhered. This can also be seen at the base of thrombus formations, as well.

After 15 minutes of exposure, a thrombus has usually formed. The thrombus has many textures ranging from rough to smooth. The differences in texture may be due to the way the thrombus was formed or due to the hydrophilicity/ hydrophobicity of the surface. The rough thrombus displays an extensive aggregation of platelets when seen at high magnification. These platelets are usually in the discocyte form. Some of the platelets in the aggregate have changed to echinocytes which have pseudopods that have joined to form bridges. This type of clot may possibly be formed by the adherence of a platelet on top of a spread platelet, much like the process outlined by Adams et al. (1983). The process just continues, with adhering platelets remaining in the discocyte form for the most part, since these platelets do not come in contact with the surface, where a shape change would otherwise be initiated and which would then lead to spreading. Other thrombi appear to be comprised of platelets that have initially formed into spheres of about 5-7 μm in diameter, which have then aggregated to form larger aggregates, which finally form the thrombus. Through the process of thrombus formation, the arrangement of the spheres/small aggregates in the thrombus may detemine the texture. Aggregates that are smooth may be the result of a dense fibrin layer forming over the aggregate in response to the action of thrombin. Generally, this would be expected

to occur on hydrophobic surfaces, since the action of thrombin would occur on the thrombus formation for a longer period of time than on a hydrophilic surface which loosely holds the clot.

Around the majority of the clots is an area clean of platelets. This area appears to be under tension, and material deposited on the surface (protein) has been pulled up into the clot. This pulling up feature may be due to highly exaggerated effects that may be producing the puckering effect. The pulling up feature may also be a manifestation of the thrombus undergoing consolidation through the effects of the enzyme, thrombosthenin. In either case, the pulling up feature may be a precursor to the embolization process.

On some of the thrombus formations, it can be seen at high magnification that there are cells (leukocytes) that appear to be B- or T-lymphocytes in both size and surface morphology; however, the types of leukocytes present were not determined in this study. Lymphocytes are nongranular leukocytes that are spherical and usually 7 to 8 μm in diameter. These cells are usually involved in immunological reactions (Bloom and Fawcett, 1975, p. 148). Their function in thrombus formation (if any), or in possible embolization, is not known. It may be possible that some of the released products from the platelet may be chemotactic to these cells. Occasional neutrophils and monocytes have been observed in association with thrombi (Lelah et al., 1983; Barber et al., 1978, 1979). Lelah et al. (1983) found that leukocytes were associated with the presence of large thrombus formations, while no leukocytes are seen on small thrombi. It is suggested that leukocytes seen during the acute inflammation case are probably the result of fibrin degradation products

present during the embolization phase that are chemotactic to the leukocytes. In general, in this study, the large clots (after the 15 minute exposure period) had lymphocytes while smaller clots did not.

After 75 minutes of exposure, most of the surfaces showed signs of the dynamic cycling events. The surfaces usually looked like the same surface exposed for shorter periods of time (15 seconds to 5 minutes). The hydrophilic shunts generally showed surfaces that looked like the same shunt exposed for shorter time periods (15 seconds to 5 minutes) while the hydrophobic shunts had surfaces that appeared to have reached a plateau for platelet adhesion (like the plateau seen generally after 5 to 15 minutes of exposure). This may be a result of the hydrophilic surfaces having a higher 'turn-over rate' of platelets and thrombi since the adsorbed protein would be less tightly held, while hydrophobic surfaces tightly hold the protein that is adsorbed and, thus, the adherent platelets, and this may slow the 'turn-over rate' down. However, the area between platelets, that on shorter periods of exposure looked smooth, is rough. This may be a result of the embolization process. The protein that was once adhered may have been partially detached, leaving areas of more protein build-up than in others. Or it may be that the detachment of the thrombus may have altered the texture of the surface.

In general, the shunts of 2%SR grafted with NVP exhibit the best blood compatibility. This surface generally had adhered platelets in the discocyte form, suggesting that the surface is not as harsh as a surface such as the SR shunt. This surface also appears to be more stable to the course of exposure to blood as indicated by the firm adherence of protein and platelet elements that are adsorbed, and by the matted thrombus (due to

the tightly held protein adsorbate). Although the 12%SR/0%H/20%N surface did clot, it was probably due to the roughness created by the underlying filler or possibly the filler itself. Nyilas et al. (1970) have found that the filler used in the matrix of silicone rubber as a strengthening agent can possibly be covered by only a monolayer (60-80 Å) of poly(dimethyl siloxane) molecules. If the silicone layer is imperfect, the high energy surface of the filler particles could be exposed and act directly on the proteins that adsorb. This high energy surface would exert a denaturing effect on the proteins, similar to that of glass (highly thrombogenic), as they adsorb. The 20% HEMA grafted shunts exhibited characteristics of hydrophilic surfaces as indicated the high 'turn-over rate' and the pulling up effect displayed by individual platelets. The critical surface tension of this surface is just above the 20-30 dynes/cm range of blood compatibility, and shows its effects by platelets adhered predominately in the discocyte form. The intermediate graft formulations show a poor response to the blood, in general. These surfaces (particularly the 10% HEMA/10% NVP grafts) show more platelets in the echinocyte form, suggesting that the surface is harsher to the blood than the other surfaces. It appears that the surfaces which exhibit better blood compatibility had critical surface tensions in the 26-30 dynes/cm range, while those with critical surface tensions outside of this were relatively poor.

FTIR analysis

In general, there was an increase in the intensity of the 1550 cm^{-1} band, related to the amount of protein deposited, up to the 5 minute

period. After this time, some shunts showed a decrease in intensity, while others showed an increase, or remained approximately the same. The best shunts (20% NVP grafted; SEM evaluation) had the lowest intensities, while the relatively poor (10% HEMA/10% NVP) surfaces generally had large intensities.

The other bands were too inconsistent to permit the evaluation of any trends. Some of the bands were expected, such as the 1730 cm^{-1} band (from HEMA). The 1080 cm^{-1} band may be due to glycoproteins.

Comparison of FTIR and SEM data

It is difficult to draw any conclusions from the comparison of FTIR data to SEM data since the FTIR data are very complicated. Not only is the protein layer supplying information in a spectrum, but the platelets are too, both in isolated and clot form. It would be expected that the more platelets adhered, the larger the 1550 cm^{-1} band would be. This is generally true since there is an increase in the number of platelets adhering to the surface up to 5 minutes, and these SEM observations correlate with the FTIR data of the relative area of the 1550 cm^{-1} bands. The surfaces on which large numbers of platelets were seen to adhere generally had large 1550 cm^{-1} intensities, while those surfaces on which small numbers of platelets were seen to adhere had relatively small 1550 cm^{-1} intensites. Thus, it appears that the 1550 cm^{-1} band varies with the platelet density on the surface of the shunt as well as protein from the plasma. This may explain why there is no information obtainable from the spectra that indicates the presence of a particular protein, such as reported by the Battelle research group. They monitor the information as

it builds up, and away from the crystal surface (and thus with less and less overall contribution to the FTIR spectrum as additional material adheres or adsorbs), whereas in the current study, the material to be deposited last on the surface of the shunt contacts the surface of the analyzing crystal directly, and in certain cases only portions of the initial adsorbed protein layer are in contact, thus decreasing the information of this protein layer in the FTIR spectrum. Since the platelet is a complex multifunctional cell, an FTIR spectrum may represent platelet spectral characteristics to a high degree, compared with that of the initial protein layer that is deposited on a material. The large density of platelets that adheres very quickly on the surface probably overshadows the information associated with the proteins that are adsorbed on the surface. This raises a question of how well the Battelle group has characterized the results of FTIR analysis of protein adsorption, also. The formation of aggregates and thrombi on the surface of the 15 minute samples may further complicate the interpretation. The aggregates and clots may be exceeding the effective sampling depth (and path) of the IR beam because of their size and bulk. This would decrease the information obtainable from the initial protein layer, as well as make contributions to the intensity of the 1550 cm^{-1} band from various locations on the surface of the sample erratic.

CONCLUSION

The characterization of acute phase reactions between blood and biomaterials has been made using the techniques of SEM and FTIR/ATR to determine the compatibility of the material. Through these techniques, the surface parameters of texture, wettability (hydrophilicity compared with hydrophobicity), and critical surface tension were found to have a significant effect on blood compatibility.

In general, surfaces having critical surface tensions in the range of 25-30 dynes/cm were found to exhibit the best compatibility, if the surface texture was smooth. Surfaces within this range generally adhered the least number of platelets and induced little shape change. Surfaces prepared with higher filler content had a pronounced rough texture and, thus, a more severe reaction with blood was seen. Surfaces with lower filler content displayed less severe reactions, generally.

Surfaces which were hydrophilic generally displayed characteristics of less permenent adherence of protein and formed elements, while hydrophobic surfaces had a more stable appearance, indicating permanent adherence. Hydrophilic surfaces appear to undergo dynamic changes at a faster rate than hydrophobic surfaces.

The FTIR data generally were very complicated. The presence of platelets, which were seen with SEM to adhere by 15 seconds after blood exposure (and possibly earlier), seems to complicate the information to an extent that determination of the identity of a specific protein adsorbed to the surface is unobtainable. To the point where thrombus formation becomes prominent, the increase in the area under the Amide II band (1550 cm^{-1}), as

seen using FTIR, follows the SEM observations of an increase seen of adherence of platelets. After this time, it appears that a thrombus may be sufficiently thick to disrupt the contact between the sample and the crystal used for collecting the data such that the Amide II band varies in a way not consistent with the amount of build-up seen by direct observation of an exposed surface.

The FTIR results reported by other groups may benefit from additional characterization information, including analysis of the surface of the crystal on a microscopic scale (i.e., using SEM) so as to determine what other plasma material, besides protein, is adhering to the crystal face.

In this study, the sample area in contact with an analyzing crystal was small. Since absorbance is linear with concentration, an improvement would be to use larger samples (studies to determine the optimum size would need to be done consistent with the signal strength of absorbance bands of interest).

The ideal FTIR spectral subtraction method would be to have two spectra that have a common absorbance band (similiar in terms of absorbance intensity). Thus, when subtraction of one band from the other is complete, the common band would be reduced to the background level and other bands present would be revealed. However, even when conditions such as these are obtained, it may not be possible to subtract effectively because of slight band shifts. When this occurs, the best that subtraction can be done is to the 'first derivative' which obscures any hidden bands. If the intensities of the two bands are orders of magnitude different (in terms of absorbance units), it may be possible to generate artifacts. Incomplete subtraction

might leave a band hidden, while over subtraction could generate a band, especially at the shoulders or base of the bands used for subtraction.

Real-time FTIR spectral analysis would be of interest for protein adsorption characteristics. A liquid cell would offer many advantages by providing a constant sized 'window', thus, providing more control over the intensity of the absorbance bands. However, further work is needed to clarify the role that the spectral characteristics of platelet adhesion have on FTIR data where the initial protein layer on a surface is of primary interest. It is apparent that platelets will be present, as well as the initial protein layer.

In view of the limited number of shunt tests performed for each formulation, there are apparent trends that warrant further investigation. The poly-N-vinyl-pyrrolidone/silicone rubber composite was a better substrate than silicone rubber for compatibility in terms of the relative number of platelets adhering and the minimal shape changes seen for the platelets. The 10% HEMA/10% NVP graft samples appeared to be the same as, or worse, than the silicone rubber shunt. The presence of filler tends to induce surface roughness, and this has a negative effect on the outcome of the acute response to blood of these materials. In some of the SEM micrographs, it is very difficult to determine the presence of platelets and to differentiate them from other surface features such as filler projections and other surface imperfections such as wrinkles. Light microscopy and transmission electron microscopy of cross sections are needed to verify the presence and character of platelets and other cellular elements such as lymphocytes.

Future research that could extend from this work might include studying the mechanism of 'fine' control of the acute response of blood-surface interactions, especially on surfaces that are relatively smooth. Also, it would be useful to study the characteristics of a tertiary solution of proteins, such as albumin, fibrinogen, and gamma globulin. If a liquid cell were to be used, complications, such as sample size, could be avoided. If an analyzing crystal is coated with a very thin layer of a material such as silicone rubber, absorbance bands will be present in both the single beam sample spectrum and the single beam reference spectrum and will cancel each other (if the adsorption of protein does not cause shifts in the bands). Small differences of build-up representing successive layers of proteinaceous material can then be monitored.

BIBLIOGRAPHY

Adams, G. A., S. J. Brown, L. V. McIntire, S. G. Eskin, and R. R. Martin. 1983. Kinetics of platelet adhesion and thrombus growth. Blood 62: 69-74.

Adams, R., J. R. Johnson, and C. F. Wilcox, Jr. 1979. Laboratory experiments in organic chemistry. Seventh edition. Macmillan Publishing Co., Inc. New York, NY.

Allen, R. D., L. R. Zucharski, S. T. Widirstky, R. Rosenstein, L. M. ZaiHin, and D. Burgess. 1979. Transformation and motility of human platelets. J. Cell. Biol. 83: 126-142.

Alpert, N. L., W. E. Keiser, and H. Szymanski. 1970. IR: Therory and practice of infrared spectroscopy. Second edition. Plenum, New York, NY.

Bagnall, R. D. 1977. Adsorption of plasma proteins on hydrophobic surfaces. I. Albumin and γ-globulin. J. Biomed. Mater. Res. 11: 947-978.

Baier, R. E. 1972. The role of surface energy in thrombogenesis. N. Y. Academy Medicine 48: 257-272.

Barber, T. A., L. K. Lambrecht, D. L. Moser, and S. L. Cooper. 1979. Influences of serum proteins on thrombosis and leucocyte adherence on polymer surfaces. Scanning Electron Microscopy 3: 881-890.

Barber, T. A., T. Mathis, J. V. Inlenfeld, S. L. Cooper, and D. F. Moser. 1978. Short-term interactions of blood with polymeric vascular graft materials: Protein adsorption, thrombus formation, and leucocyte deposition. Scanning Electron Microscopy 2: 431-440.

Bloom, W. and D. W. Fawcett. 1975. A textbook of histology. Tenth edition. W. B. Saunders Co., Philadelphia, PA.

Braley, S. 1970. The chemistry and properties of the medical-grade silicones. J. Macromol. Sci. Chem. 4: 529-544.

Brash, J. L. and D. J. Lyman. 1969. Adsorption of plasma proteins in solution to uncharged, hydrophobic polymer surfaces. J. Biomed. Mater. Res. 3: 175-189.

Brash, J. L., S. Uniyal, and Q. Samak. 1974. Exchange of albumin adsorbed on polymer surfaces. Trans. Am. Soc. Artif. Internal Organs 20: 69-76.

Bruck, S. D. 1977. Interactions of synthetic and natural surfaces with blood in the physiological enviroment. J. Biomed. Mater. Res. Symp. 11: 1-21.

Caen, J. P., S. Cronberg, P. Kubisz. 1977. Platelets: Physiology and pathology. Stratton Intercontinental Medical Book Corp., New York, NY.

Chawla, A. S. 1978. In vivo interactions between novel filler free silicone rubber and blood. Biomater. Med. Dev. Artif. Organs 6: 89-102.

Cooper, H. A., R. G. Mason, and K. M. Brinkhous. 1976. The platelet: Membrane and surface reactions. Ann. Rev. Physiology 38: 501-535.

Curtis, H. 1975. Biology. Worth Publishers, Inc., New York, NY.

Dutton, R. C., R. E. Baier, R. L. Dedrick, and R. L. Bowman. 1968. Initial thrombus formation on foreign surfaces. Trans. Am. Soc. Artif. Internal Organs 14: 57-62.

Frojmovic, M. M. and J. G. Milton. 1982. Human platelet size, shape, and related functions in health and disease. Physiol. Rev. 62: 185-261.

Gendreau, R. M. and R. L. Jakobsen. 1978. Fourier transform infrared techniques for studying complex biological systems. Applied Spect. 32: 326-328.

Gendreau, R. M., S. Winters, R. I. Leininger, D. Fink, and R. J. Jakobsen. 1981. Fourier transform infrared spectroscopy of protein adsorption from whole blood: Ex vivo dog studies. Applied Spect. 35: 353-357.

Gendreau, R. M. 1982. Breaking the one second barrier: Fast Kinetics of protein adsorption by FT-IR. Applied Spect. 36: 47-49.

Gendreau, R. M., R. I. Leininger, S. Winters, and R. J. Jacobsen. 1982. Fourier transform infrared spectroscopy for protein-surface studies. Adv. Chem. Ser. 199: 371-394.

Goodman, S. L., M. D. Lelah, L. K. Lambrecht, S. L. Cooper, and R. M. Albrecht. 1984. In vitro vs ex vivo platelet deposition on polymer surfaces. Scanning Electron Microscopy 1: 279-290.

Gordon, J. L. and A. J. Milner. 1976. Blood platelets as multifunctional cells. Pages 3-22 in J. L. Gordon, ed. Platelets in biology and pathology. North-Holland Publishing Co., New York.

Grant, W. H., L. E. Smith, and R. R. Stromberg. 1977. Radiotracer techniques for protein adsorption measurements. J. Biomed. Mater. Res. Symp. 8: 33-38.

Hoffman, A. S. 1974. Principles governing biomolecular interactions at foreign interfaces. J. Biomed. Mater. Res. Symp. 8: 77-83.

Horbett, T. A. and A. S. Hoffman. 1975. Bovine plasma protein adsorption onto radiation-grafted hydrogels based on hydroxyethyl methacrylate and N-vinyl-pyrrolidone. Adv. Chem. Ser. 145: 230-254.

Jakobsen, R. J., S. Winters, and R. M. Gendreau. 1981. Biological applications of FT-IR or bloody FT-IR. Page 469 in H. Sakai, ed. Proceedings of the International Conference on Fourier Transform Infrared Spectroscopy. Vol. 289. S. P. I. E. - The Society for Optical Engineering, held at Columbia, SC.

Kendall, D. N. 1966. Applied infrared spectroscopy. Reinhold Publishing Corp., New York.

Kim, S. W., R. G. Lee, H. Oster, D. Coleman, J. D. Andrade, D. J. Lentz, and D. Olsen. 1974. Platelet adhesion to polymer surfaces. Trans. Am. Soc. Artif. Internal Organs 20: 449-455.

Koenig, J. L. and D. L. Tabb. 1980. Infrared spectra of globular proteins in aqueous solutions. Page 247 in J. During, ed. Proceedings of the NATO Advanced Study Institute. D. Reidel Publishing Company, Boston.

Lee, R. G. and S. W. Kim. 1974a. Adsorption of proteins onto hydrophobic polymer surfaces: Adsorption isotherms and kinetics. J. Biomed. Mater. Res. 8: 251-259.

Lee, R. G. and S. W. Kim. 1974b. The role of carbohydrate in platelet adhesion to foreign surfaces. J. Biomed. Mater. Res. 8: 383-398.

Lelah, M. D., C. A. Jordon, M. E. Pariso, L. K. Lambrecht, S. L. Cooper, and R. M. Albrecht. 1983. Morphological changes occurring during thrombogenesis and embolization on biomaterials in a canine ex vivo series shunt. Scanning Electron Microscopy 4: 1983-1994.

Lewis, J. C., T. Prater, R. G. Taylor, and M. S. White. 1980. The use of correlative SEM and TEM to study thrombocyte and platelet adhesion to artifical surfaces. Scanning Electron Microscopy 3: 189-202.

Lindsay, R. M., R. G. Mason, S. W. Kim, J. D. Andrade, and R. M. Hakim. 1980. Blood surface interactions. Trans. Am. Soc. Artif. Internal Organs 26: 603-610.

Low, M. J. D. 1970. LI. Fourier transform spectrometers- Part one. J. Chem. Educ. 47: A163-A172.

Lyman, D. J., J. L. Brash, S. W. Chaikin, K. G. Klein, and M. Carini. 1968. The effect of chemical structure and surface properties of synthetic polymers on the coagulation of blood. II. Protein and platelet interaction with polymer surfaces. Trans. Am. Soc. Artif. Internal Organs 14: 250-255.

Lyman, D. J., L. C. Metcalf, D. Albo, K. F. Richards, and J. Lamb. 1974. The effect of chemical structure and surface properties of synthetic polymers on the coagulation of blood. III. In vivo adsorption of proteins on polymer surfaces. Trans. Am. Soc. Artif. Internal Organs 20: 474-478.

Macintyre, D. E. 1976. The platelet release reaction: Association with adhesion and aggregation, and comparison with secretory responses in other cells. Pages 61-85 in J. L. Gordon, ed. Platelets in biology and pathology. North-Holland Publishing Co., New York.

Mattson, J. S., C. A. Smith, and K. E. Paulson. 1975. Infrared internal reflection spectroscopy of aqueous protein films at the germanium-water interface. Anal. Chem. 47: 736-738.

Medway, W., J. E. Prier, and J. S. Wilkinson. 1969. A textbook of veterinary clinical pathology. Williams and Wilkins Co., Baltimore.

Meloan, C. E. 1963. Elementary infrared spectroscopy. The Macmillan Company, New York.

Merrill, E. W. and E. W. Salzman. 1978. Properties of materials affecting the behavior of blood at their surfaces. Pages 119-129 in P. N. Sawyer and M. J. Kaplitt, eds. Vascular Grafts. Appleton- Century-Crofts, New York.

Morrison, R. T. and R. N. Boyd. 1973. Organic chemistry. Third edition. Allyn and Bacon, Inc., Boston.

National Institutes of Health. 1979. Guidelines for physiochemical characterization of biomaterials. NIH Publication No. 80-2186.

Nyilas, E., E. L. Kupski, P. Burnett, and R. M. Haag. 1970. Surface microstructural factors and blood compatibilty of a silicone rubber. J. Biomed. Mater. Res. 4: 369-432.

Nyilas, E., W. A. Morton, D. M. Lederman, T-H. Chiu, and R. D. Cumming. 1975. Interdependence of hemodynamic and surface parameters in thrombosis. Trans. Am. Soc. Artif. Internal. Organs 21: 55-70.

Puszkin, S., S. Kochwa, E. G. Puszkin, and R. E. Rosenfield. 1975. A solid-liquid biphasic model for characterization of properties of muscle and platelet contractile proteins. J. Biol. Chem. 250: 2085-2094.

Ratner, B. D. and Hoffman. 1976. Synthetic hydrogels for biomedical applications. Pages 1-36 in J. D. Andrade, ed. Hydrogels for medical and related applications. American Chemical Society, Washington, D. C.

Ratner, B. D., A. S. Hoffman, and J. D. Whiffen. 1975. Blood compatibility of radiation-grafted hydrogels. Biomater. Med. Dev. Artif. Organs 3: 115-120.

Robbins, S. L., M. Angell, and V. Kumar. 1981. Basic pathology. W. B. Saunders Co., Philadelphia.

Roseman, S. 1970. The synthesis of the complex CAS by using multiglycosyltransferase systems and their potential function in intercellular adhesions. Chem. Phys. Lipids 5: 270-297.

Shirasawa, K., B. P. Barton, and A. B. Chandler. 1972. Localization of ferritin-congugated anti-fibrin/fibrinogen in platelet aggregates produced in vitro. Am. J. Pathol. 66: 379-406.

Thomson, R. G. 1984. General veterinary pathology. Second edition. W. B. Saunders Co., Philadelphia.

Vroman, L., A. L. Adams, M. Klings, G. Fisher, P. C. Munoz, and R. P. Solensky. 1977. Reaction of formed elements of blood with plasma proteins at interfaces. Annals New York Academy Sciences 283: 65-76.

Watkins, R. W. and C. R. Robertson. 1977. A total internal-reflection technique for the examination of protein adsorption. J. Biomed. Mater. Res. 11: 915-938.

Weathersby, P. K., T. A. Horbett, and A. S. Hoffman. 1977. Fibrinogen adsorption to surfaces of varying hydrophilicity. J. Bioeng. 1:395-410.

Wenning, M. and W. W. Höpker. 1981. Scanning electron microscopic comparison between the thrombogenic properties of heparinized and non-heparinized vena cava catheters. Virchows Arch. [Path. Anat.] 391: 207-215.

White, J. G. 1979. Current concepts of platelet structure. Am. J. Clin. Pathol. 71: 363-378.

APPENDIX A: PARAMETER SETTINGS

The following parameters were used during the collection of each single beam file.

APF=HG	APT=3	BMS=6	CON=1	COR=LO
CSU=IN	DLY=40	DTC=MI	HFQ=5000	HPF=6
LFQ=0	LPF=2	LWN=15800.0	NLV=0.000625	NSR=100
NSS=100	OPF=2	PIP=128	PTS=1024	RES=4
RGN=-1	SGN=-1	SMF=0	SPZ=NO	SSP=-1
SVI=NO	TGD=1	VEL=5	WTM=13800	ZFF=2

FLR was set equal to the filename given to the crystal single beam spectrum (reference), and FLS was set equal to the filename given to the sample single beam spectrum.

The following parameters were used for obtaining a hardcopy plot of the spectrum.

ASE=NO	CSU=IN	LAB=LN	LGO=NO	PLF=AB
POP=DP	XAU=WN	XAX=NO	XEP=1000	XSP=1900
XSL=-6.5	XST=0	YHT=0.5	YSL=4.5	YST=5.5
YTC=3				

APPENDIX B: FTIR SPECTRA

The following spectra are the results of all spectral subtractions. The code names printed at the top of each spectrum is listed. The last letter in the spectrum code indicates how long the shunt was exposed to blood (A=0.25 minute, B=0.50 minute, C=5.0 minutes, D=15.0 minutes, E=75.0 minutes, and F= unexposed). The other letters and numbers indicate the formulation of the shunt surface.

CNN= SR shunt

TWO= 2%SR shunt

TWE= 12%SR shunt

TWO20= 2%SR/20%H/0%N shunt

TWO15= 2%SR/15%H/5%N shunt

TWO10= 2%SR/10%H/10%N shunt

TWO05= 2%SR/5%H/15%N shunt

TWO00= 2%SR/0%H/20%N shunt

TWE20=12%SR/20%H/0%N shunt

TWE15=12%SR/15%H/5%N shunt

TWE10=12%SR/10%H/10%N shunt

TWE05=12%SR/5%H/15%N shunt

TWE00=12%SR/0%H/20%N shunt

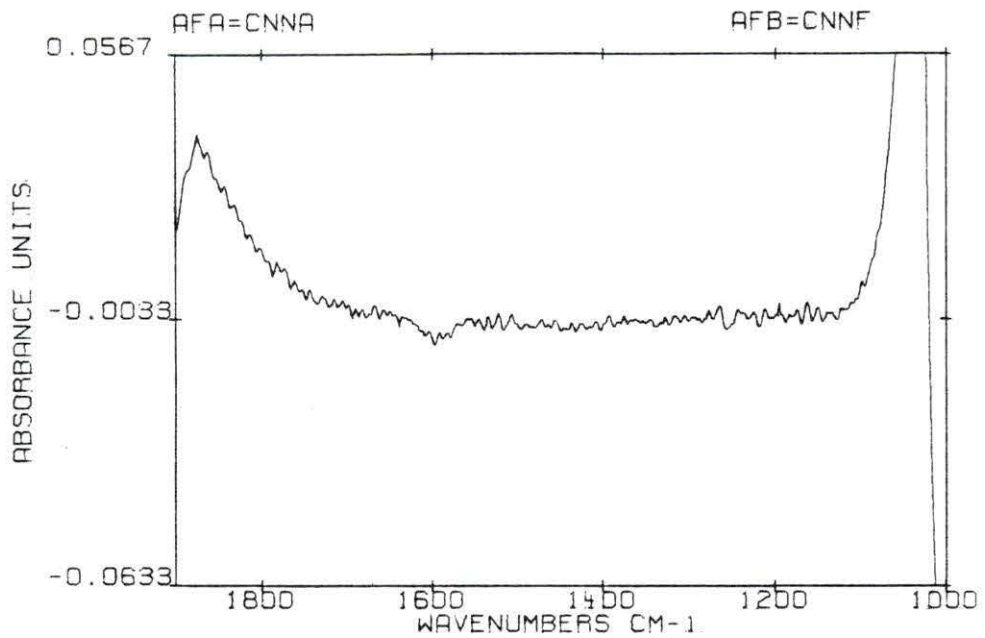

Figure 108. Absorbance spectrum of spectrally subtracted SR shunt after 0.25 minute of exposure to blood

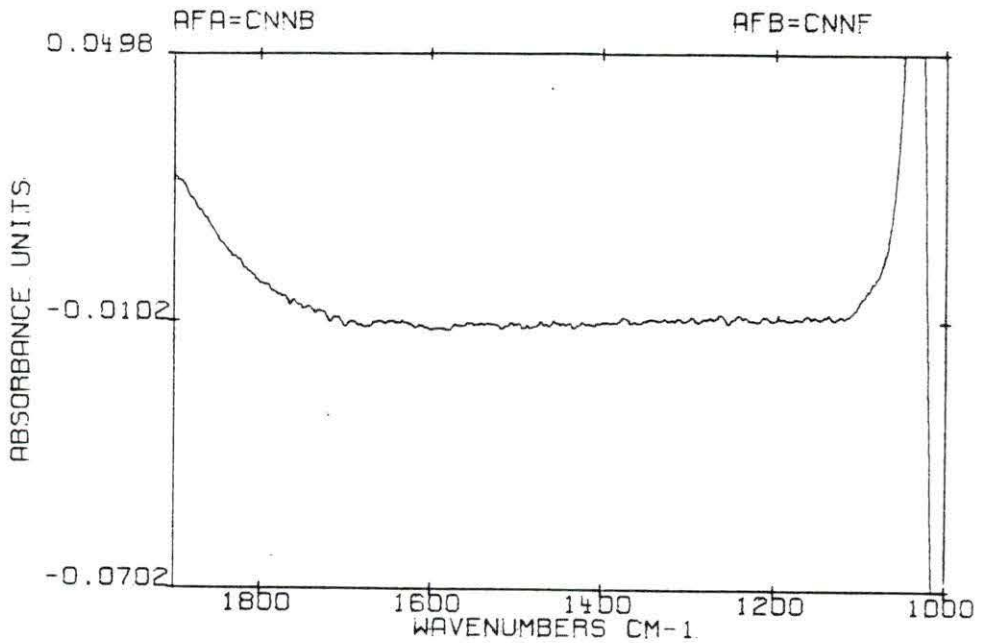

Figure 109. Absorbance spectrum of spectrally subtracted SR shunt after 0.50 minute of exposure to blood

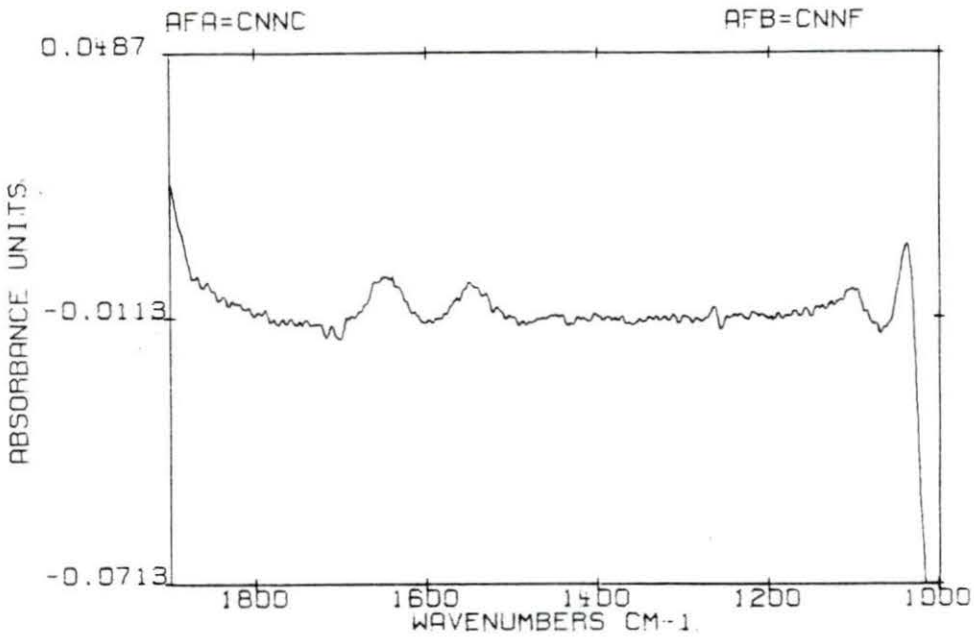

Figure 110. Absorbance spectrum of spectrally subtracted SR shunt after 5 minutes of exposure to blood

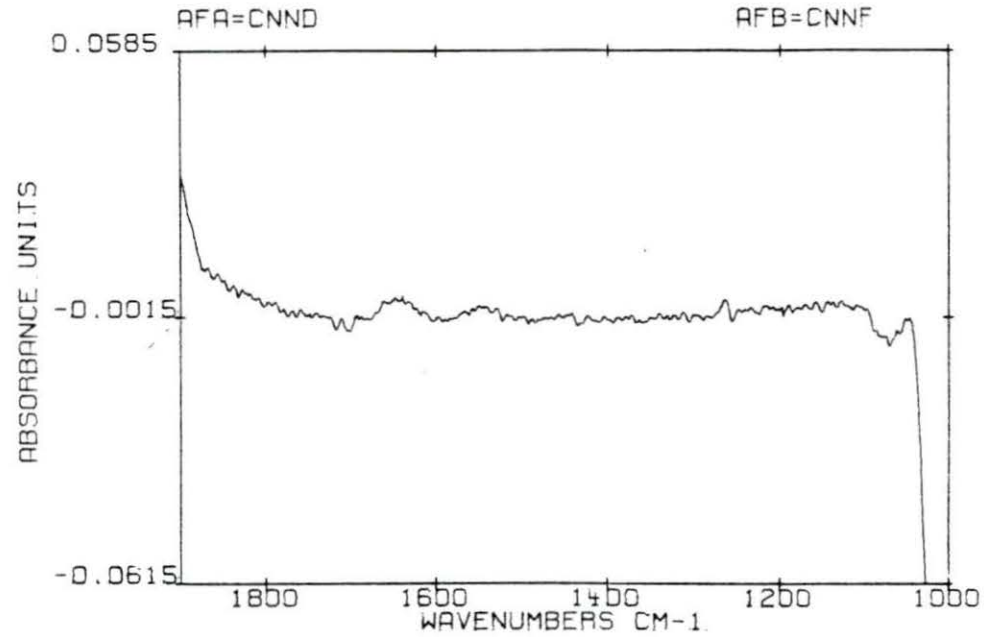

Figure 111. Absorbance spectrum of spectrally subtracted SR shunt after 15 minutes of exposure to blood

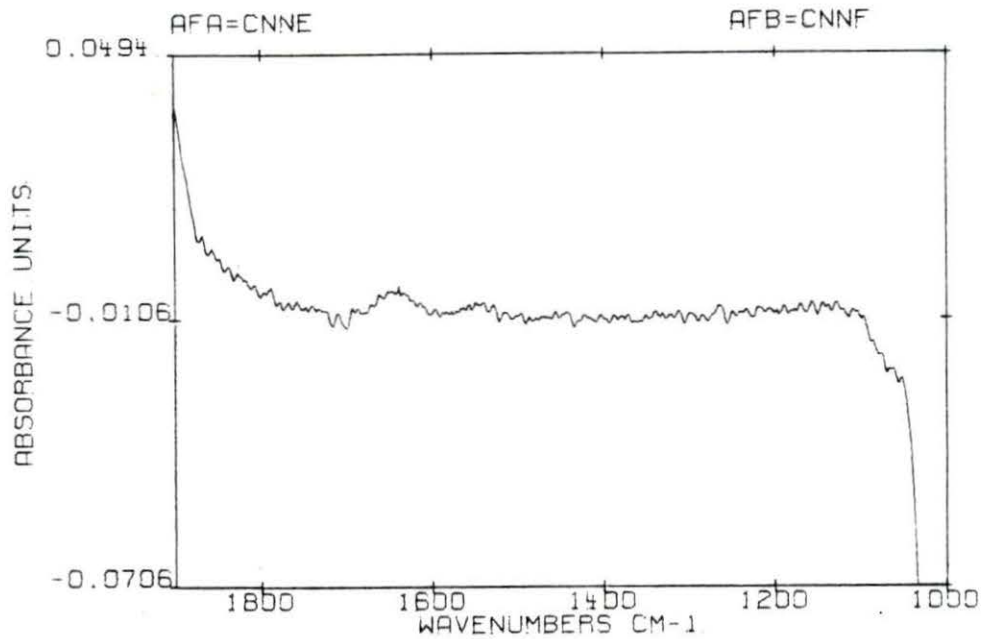

Figure 112. Absorbance spectrum of spectrally subtracted SR shunt after 75 minutes of exposure to blood

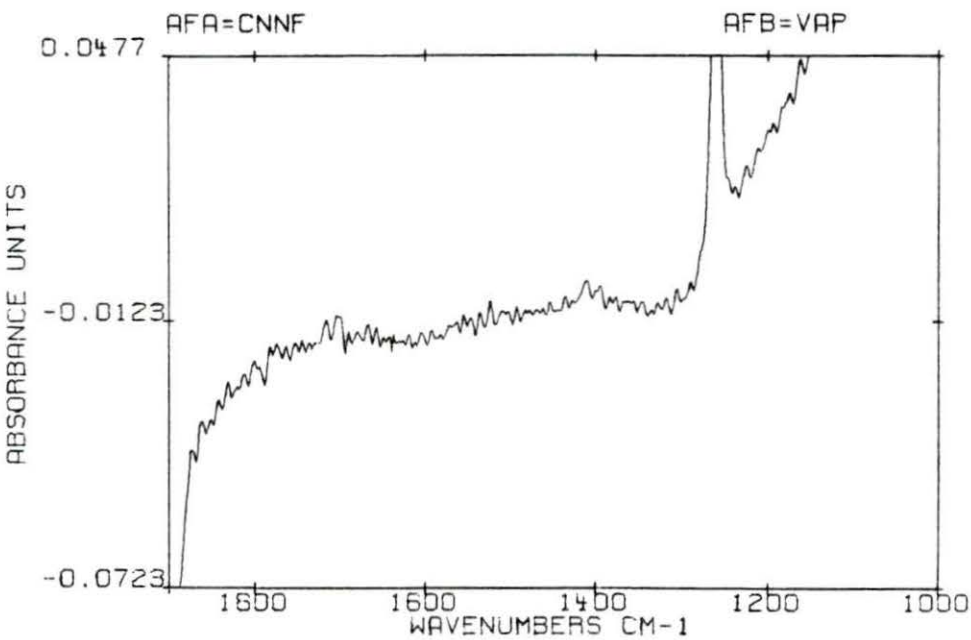

Figure 113. Absorbance spectrum of unexposed SR shunt after subtraction of saline and water vapor

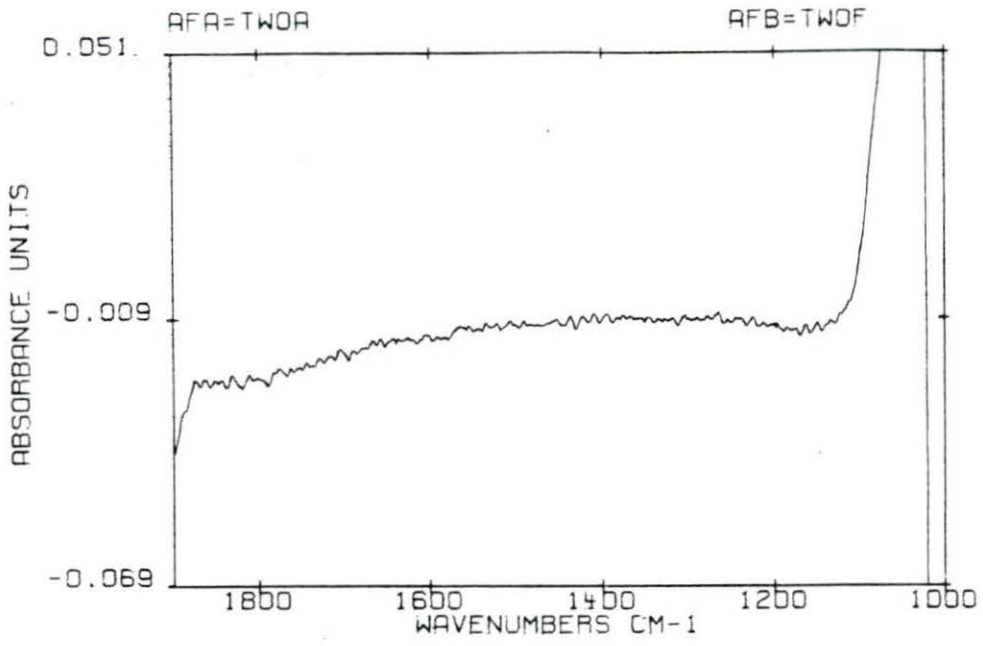

Figure 114. Absorbance spectrum of spectrally subtracted 2%SR shunt after 0.25 minute of exposure to blood

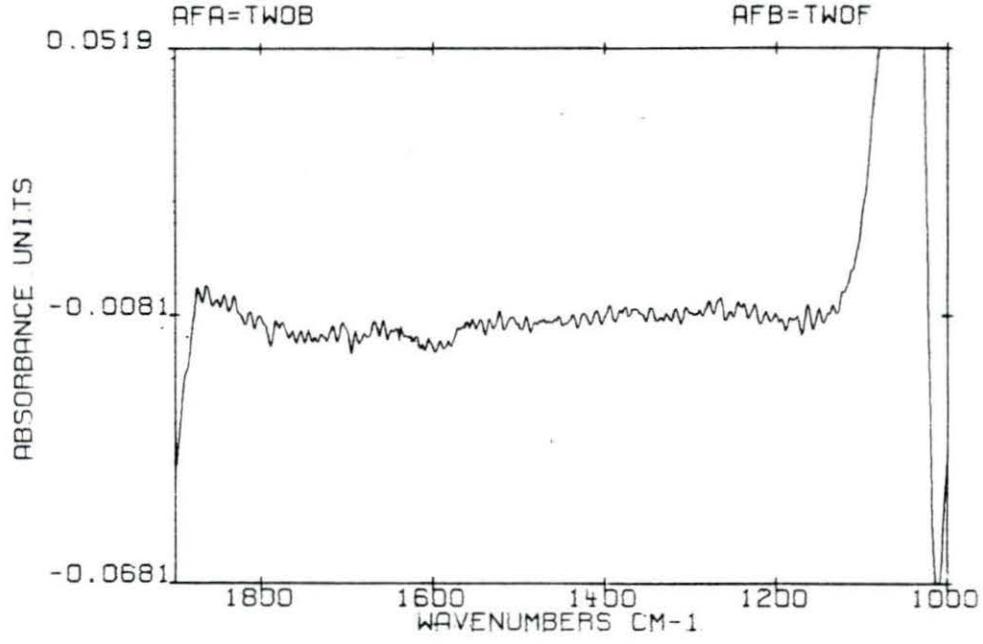

Figure 115. Absorbance spectrum of spectrally subtracted 2%SR shunt after 0.50 minute of exposure to blood

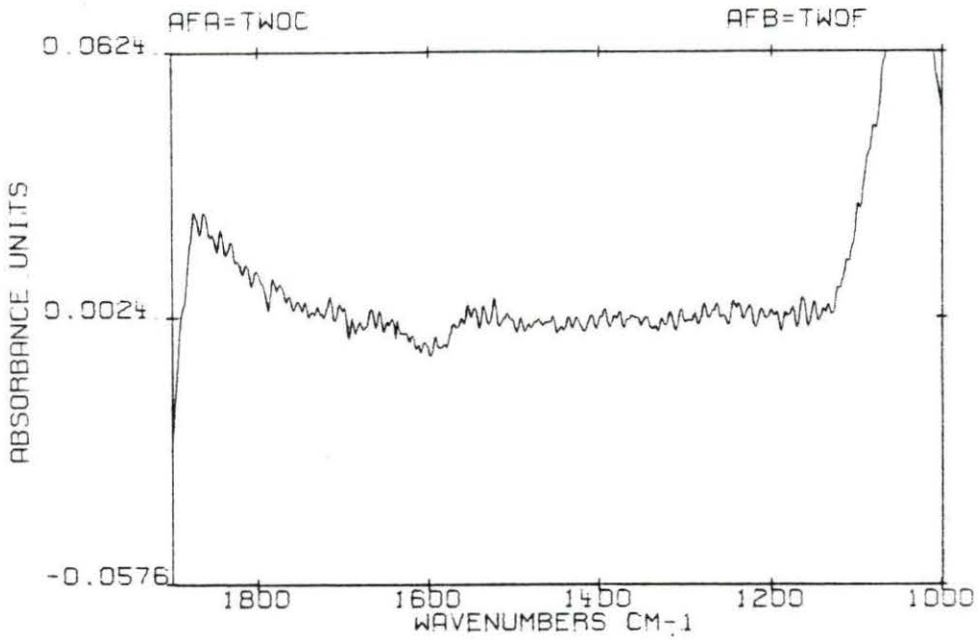

Figure 116. Absorbance spectrum of spectrally subtracted 2%SR shunt after 5 minutes of exposure to blood

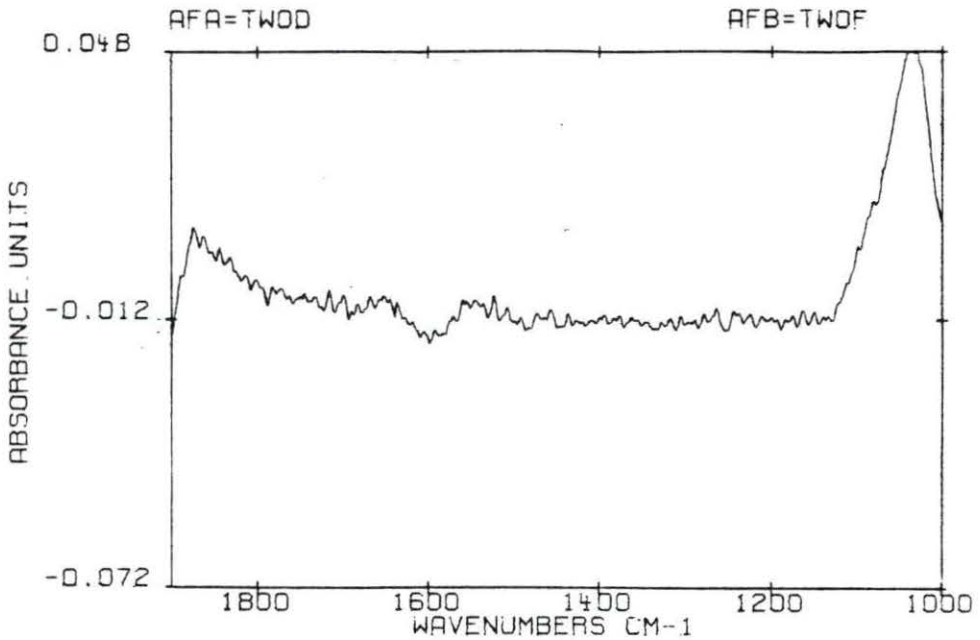

Figure 117. Absorbance spectrum of spectrally subtracted 2%SR shunt after 15 minutes of exposure to blood

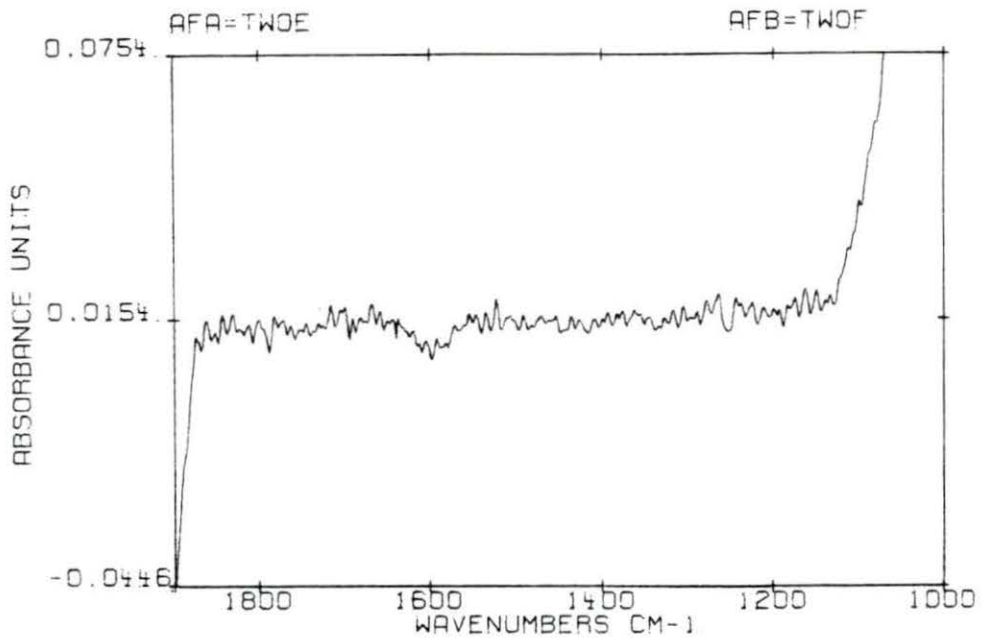

Figure 118. Absorbance spectrum of spectrally subtracted 2%SR shunt after 75 minutes of exposure to blood

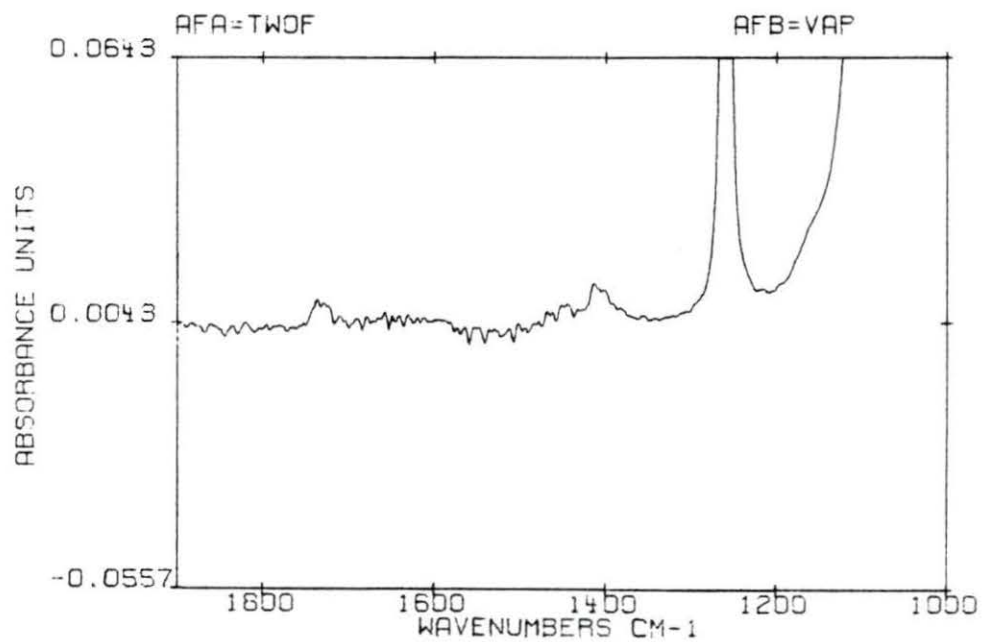

Figure 119. Absorbance spectrum of unexposed 2%SR shunt after subtraction of saline and water vapor

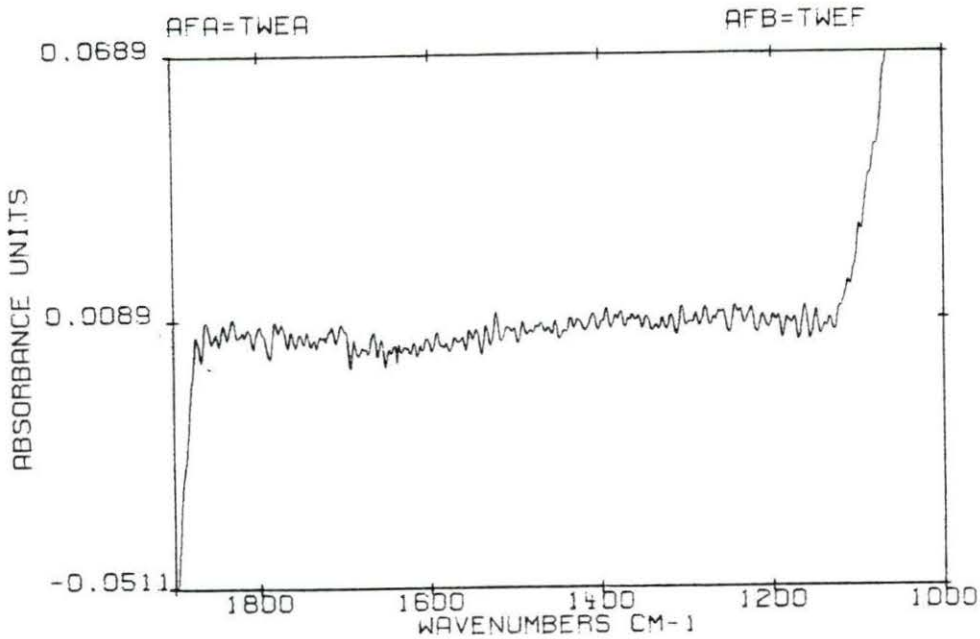

Figure 120. Absorbance spectrum of spectrally subtracted 12%SR shunt after 0.25 minute of exposure to blood

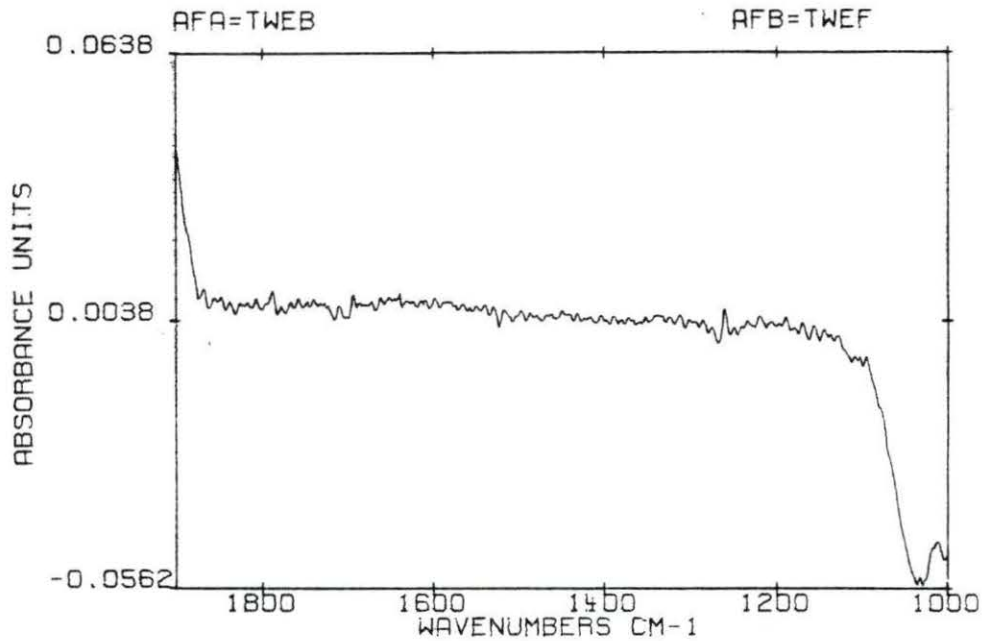

Figure 121. Absorbance spectrum of spectrally subtracted 12%SR shunt after 0.50 minute of exposure to blood

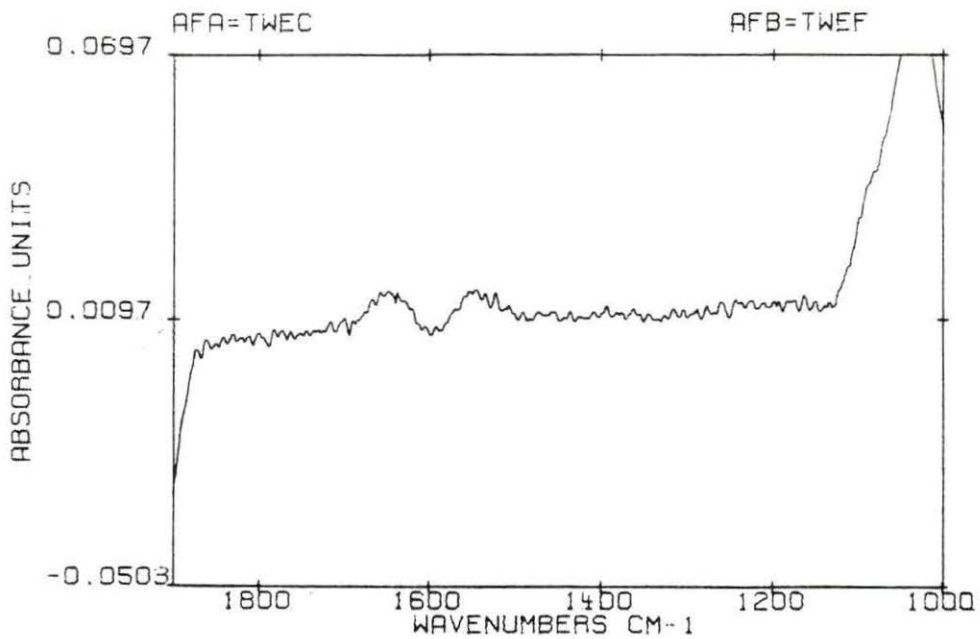

Figure 122. Absorbance spectrum of spectrally subtracted 12%SR shunt after 5 minutes of exposure to blood

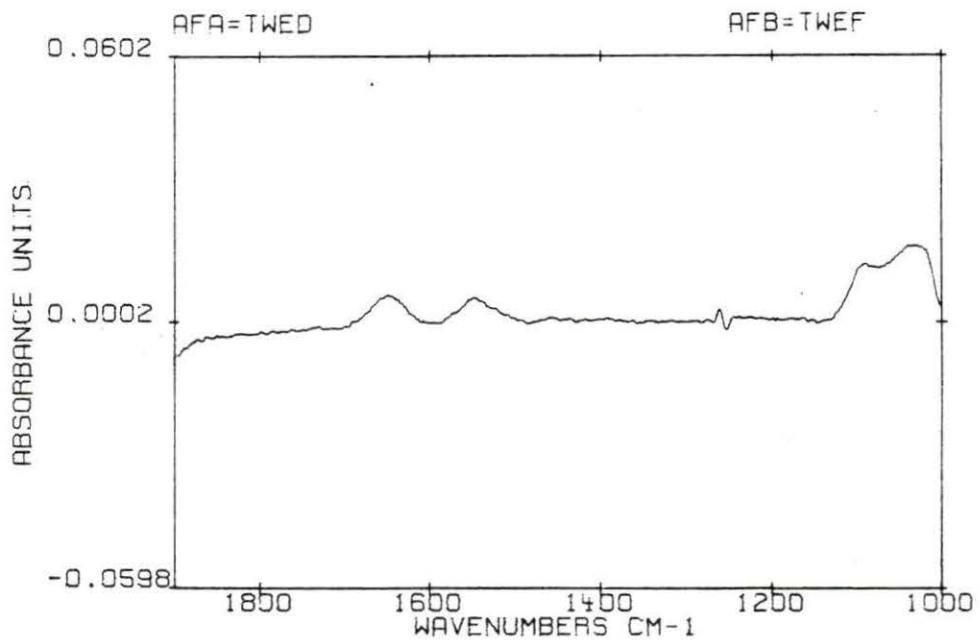

Figure 123. Absorbance spectrum of spectrally subtracted 12%SR shunt after 15 minutes of exposure to blood

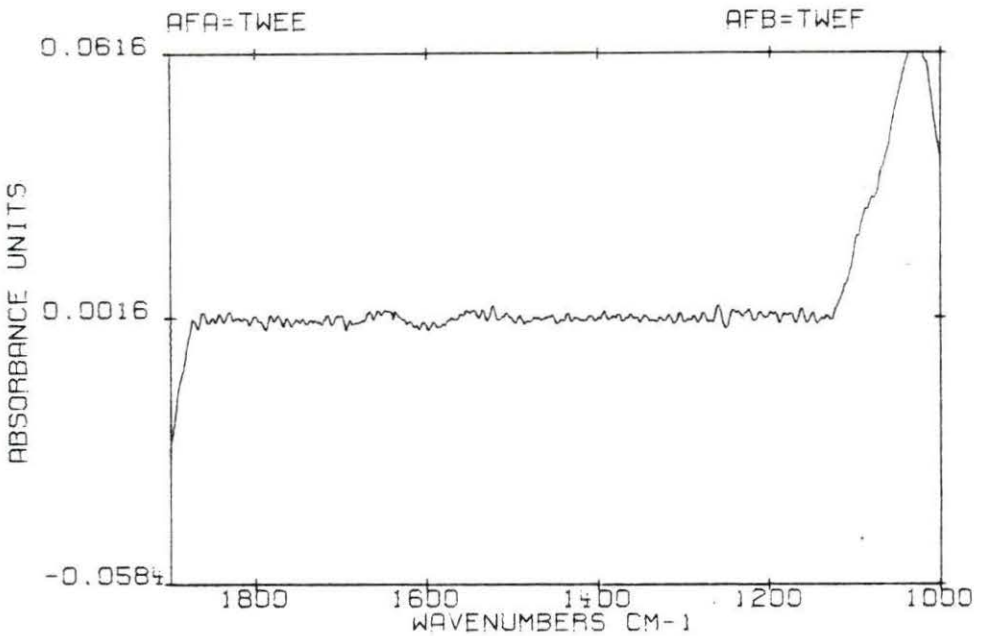

Figure 124. Absorbance spectrum of spectrally subtracted 12%SR shunt after 75 minutes of exposure to blood

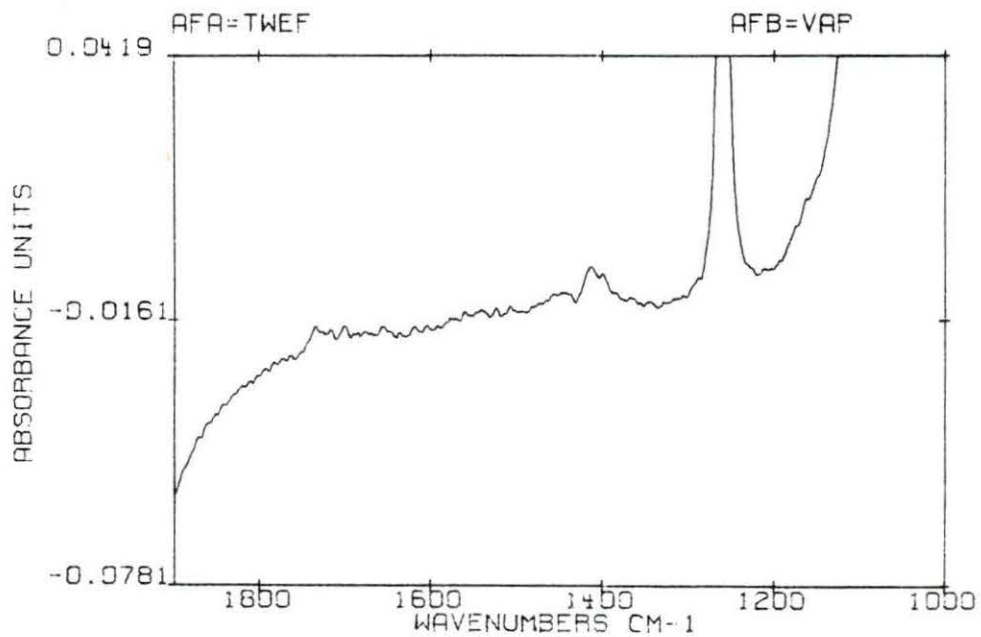

Figure 125. Absorbance spectrum of unexposed 12%SR shunt after subtraction of saline and water vapor

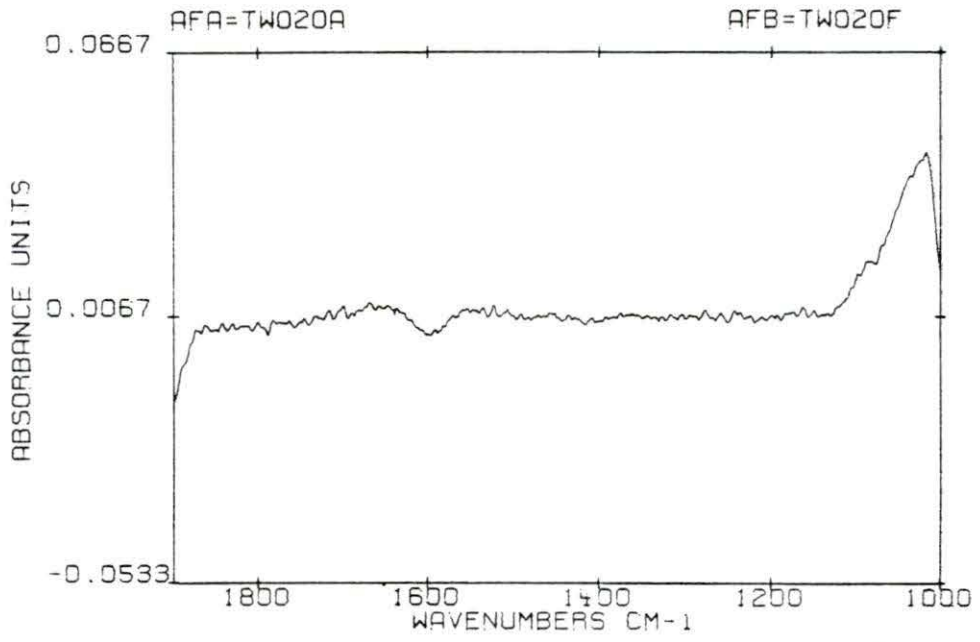

Figure 126. Absorbance spectrum of spectrally subtracted 2%SR/20%H/0%N shunt after 0.25 minute of exposure to blood

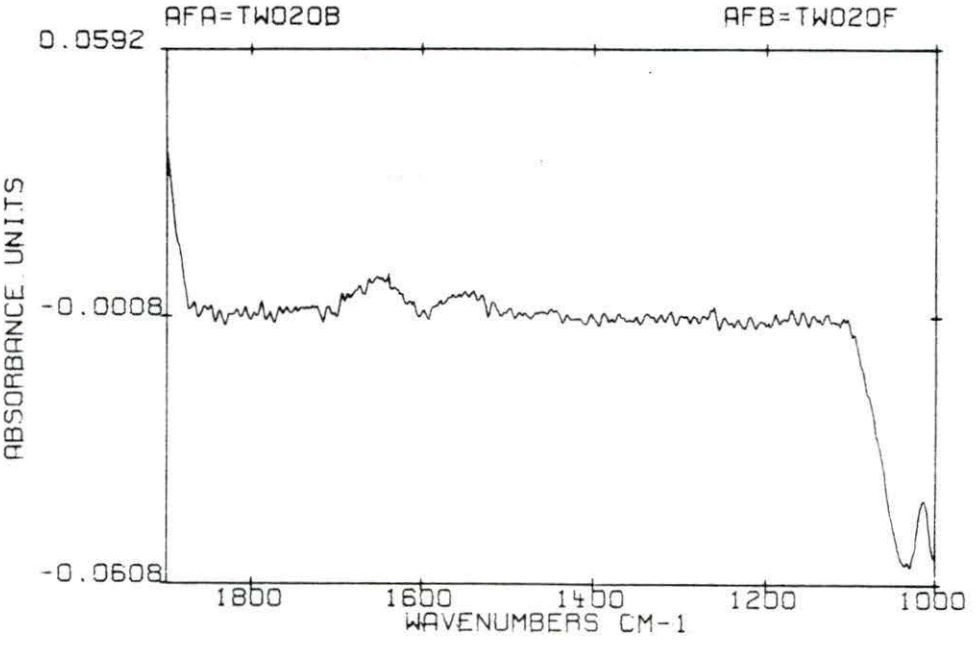

Figure 127. Absorbance spectrum of spectrally subtracted 2%SR/20%H/0%N shunt after 0.50 minute of exposure to blood

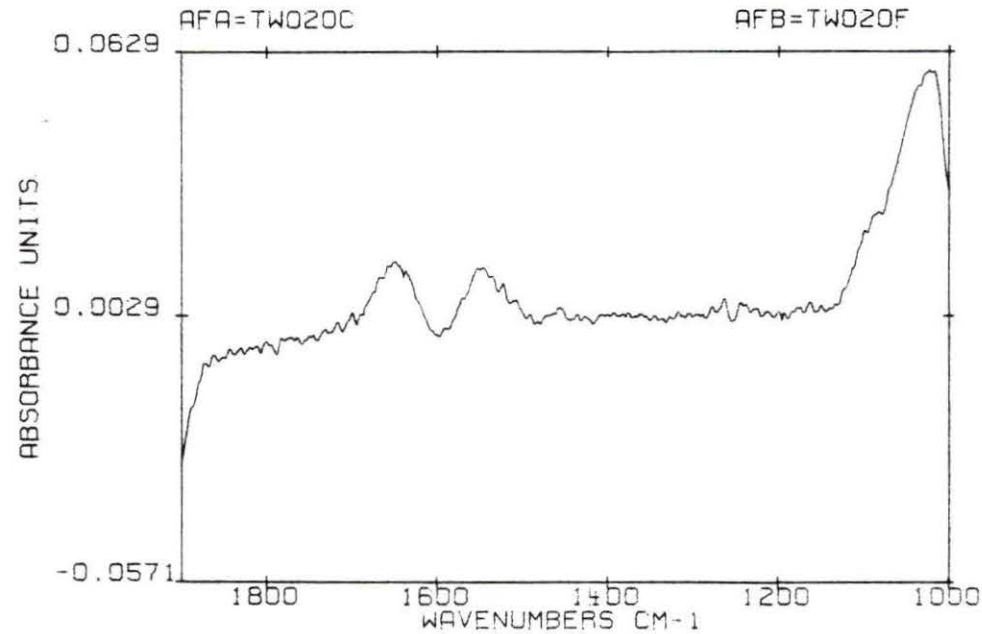

Figure 128. Absorbance spectrum of spectrally subtracted 2%SR/20%H/0%N shunt after 5 minutes of exposure to blood

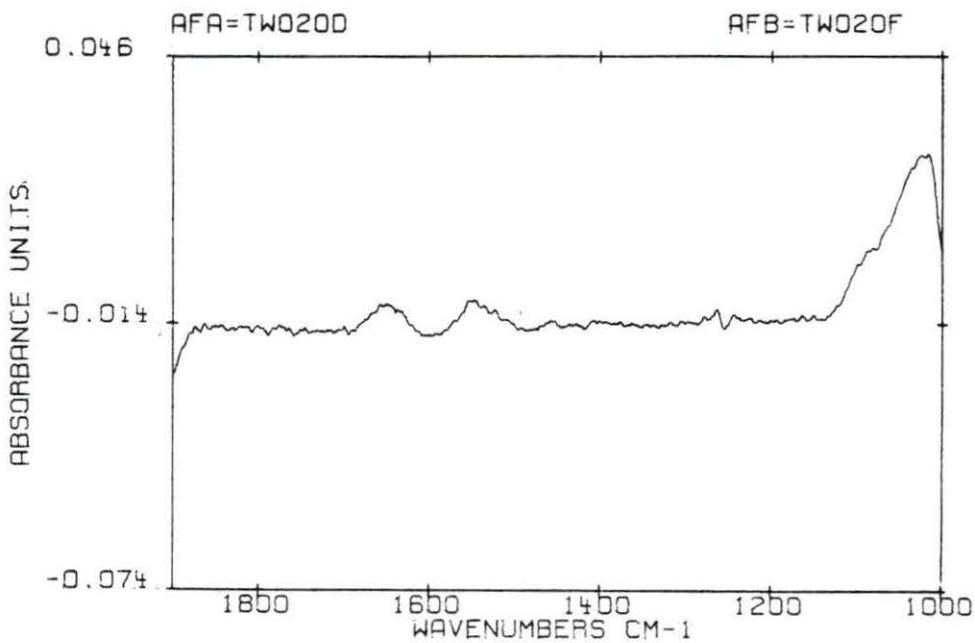

Figure 129. Absorbance spectrum of spectrally subtracted 2%SR/20%H/0%N shunt after 15 minutes of exposure to blood

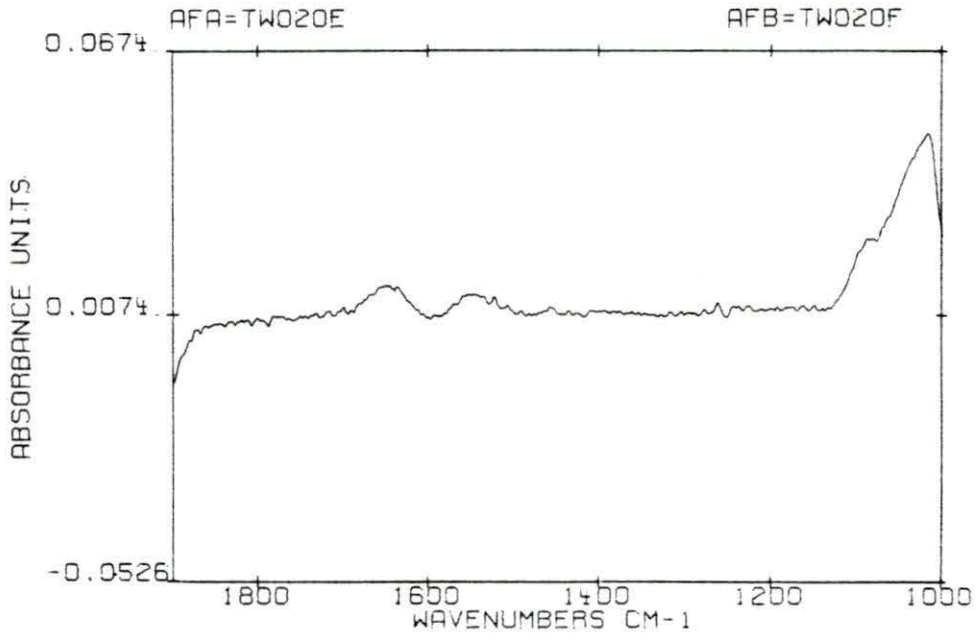

Figure 130. Absorbance spectrum of spectrally subtracted 2%SR/20%H/0%N shunt after 75 minutes of exposure to blood

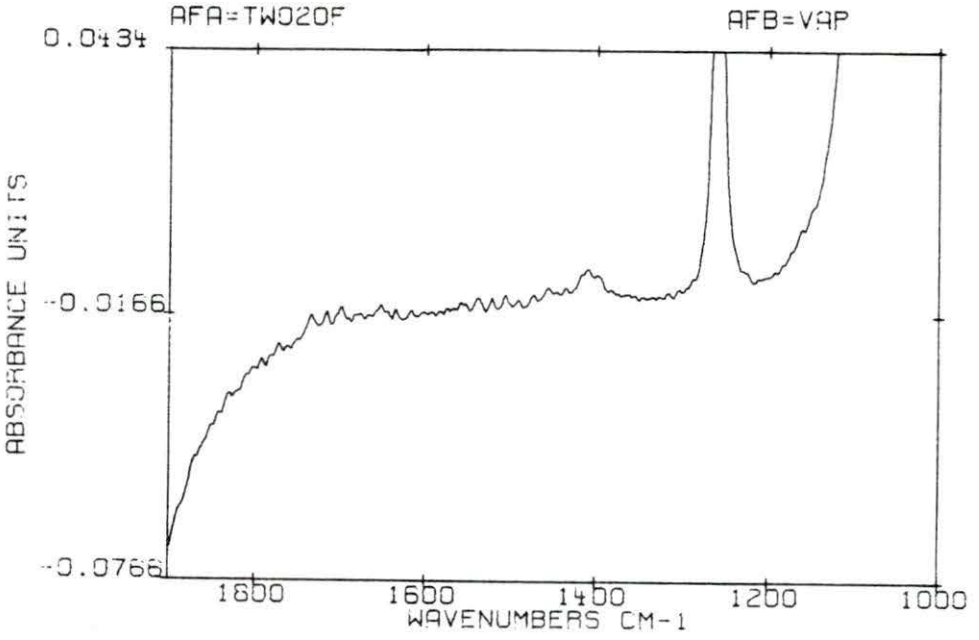

Figure 131. Absorbance spectrum of unexposed 2%SR/20%H/0%N shunt after subtraction of saline and water vapor

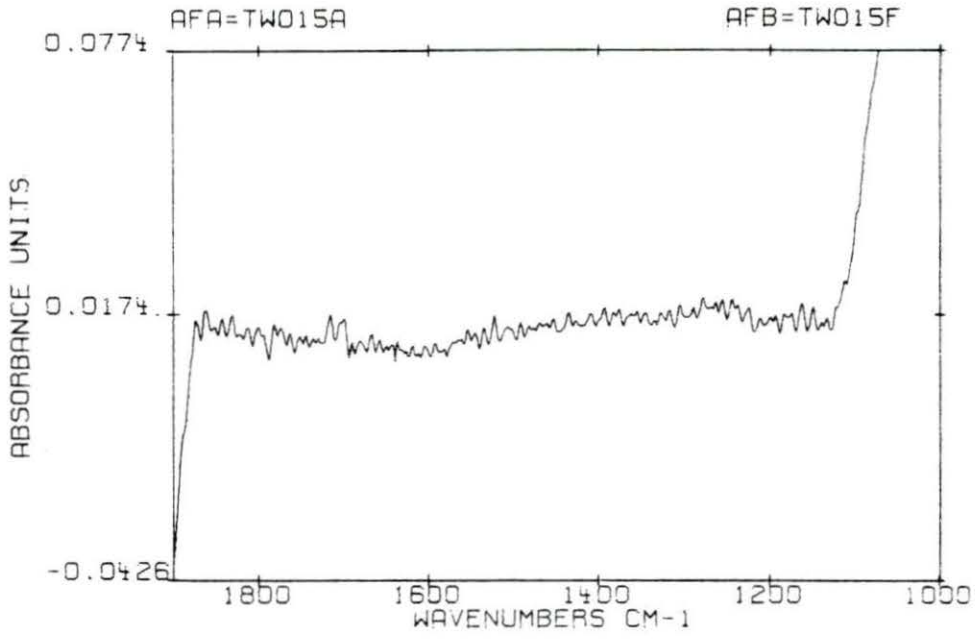

Figure 132. Absorbance spectrum of spectrally subtracted 2%SR/15%H/5%N shunt after 0.25 minute of exposure to blood

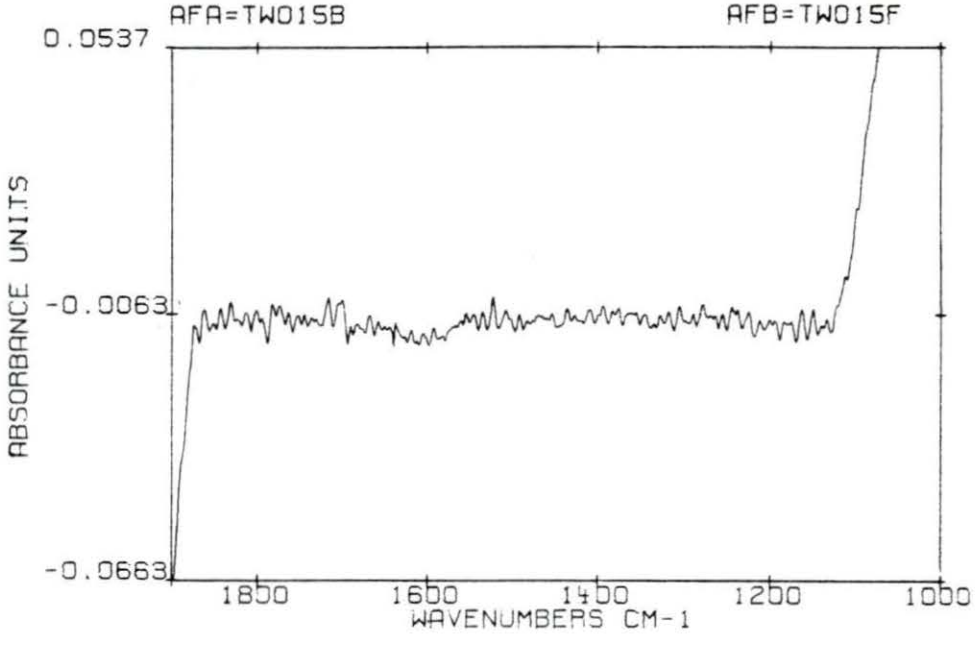

Figure 133. Absorbance spectrum of spectrally subtracted 2%SR/15%H/5%N shunt after 0.50 minute of exposure to blood

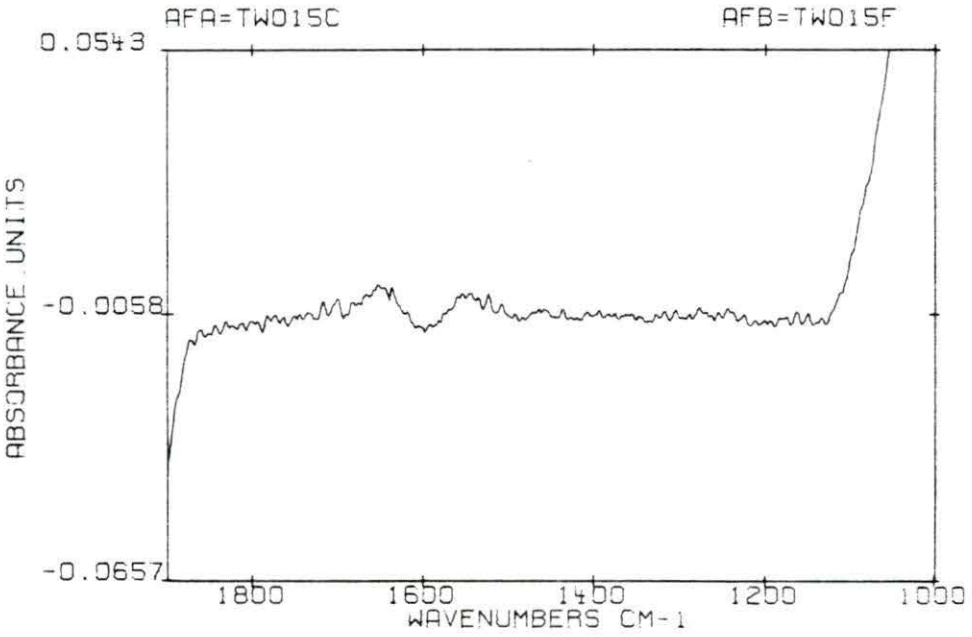

Figure 134. Absorbance spectrum of spectrally subtracted 2%SR/15%H/5%N shunt after 5 minutes of exposure to blood

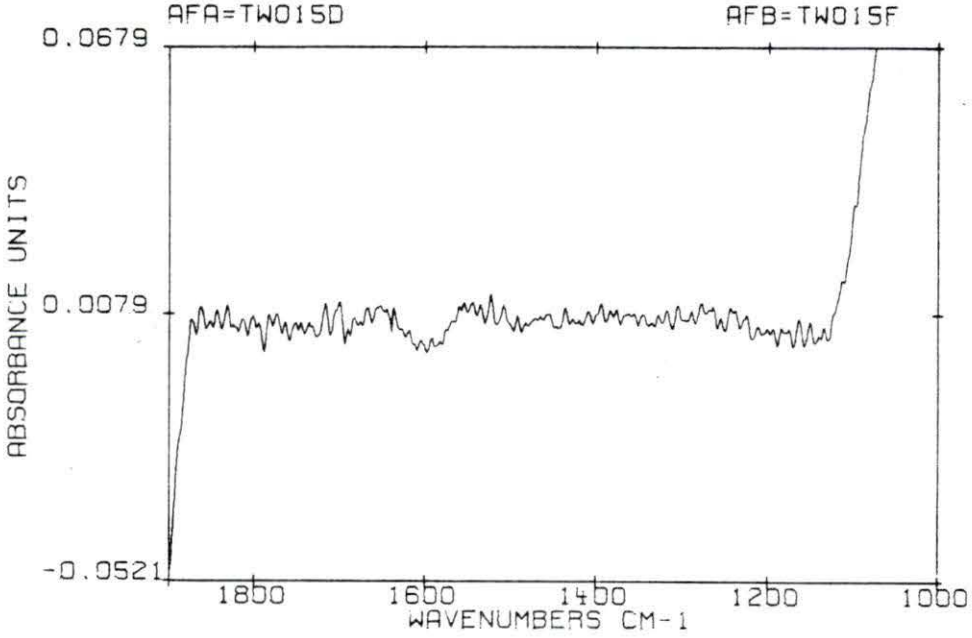

Figure 135. Absorbance spectrum of spectrally subtracted 2%SR/15%H/5%N shunt after 15 minutes of exposure to blood

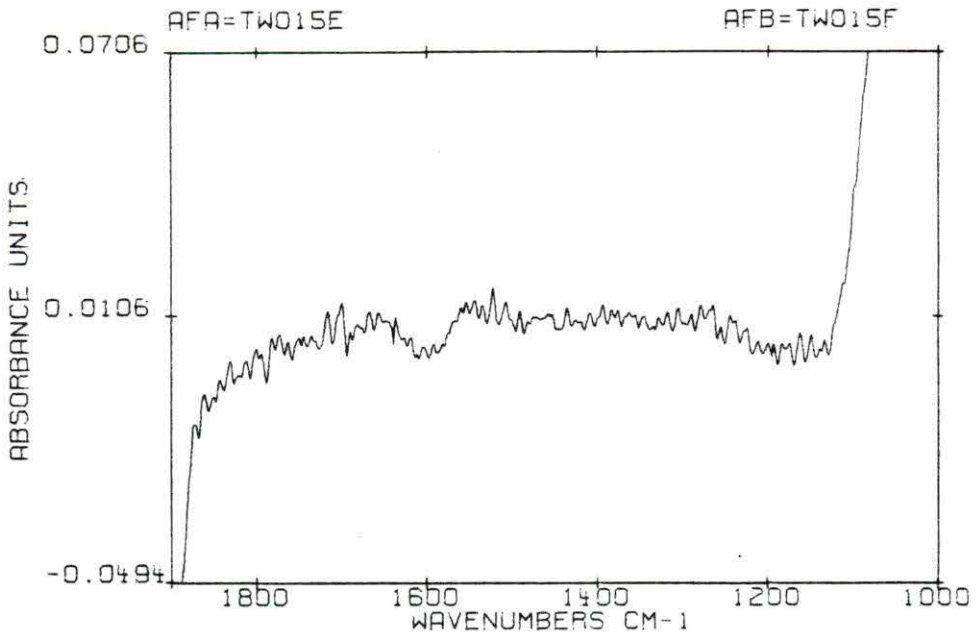

Figure 136. Absorbance spectrum of spectrally subtracted 2%SR/15%H/5%N shunt after 75 minutes of exposure to blood

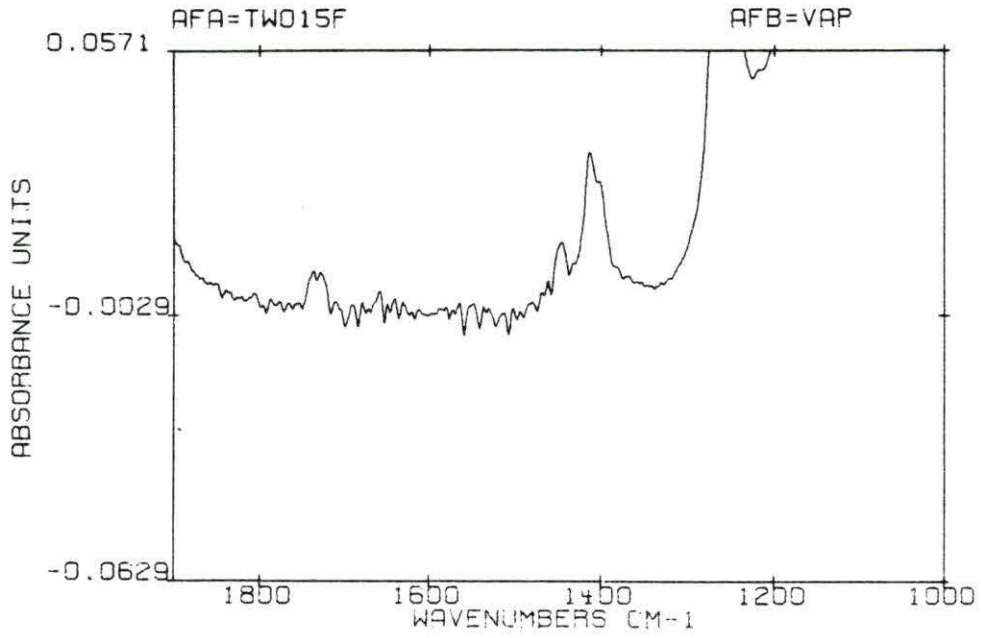

Figure 137. Absorbance spectrum of unexposed 2%SR/15%H/5%N shunt after subtraction of saline and water vapor

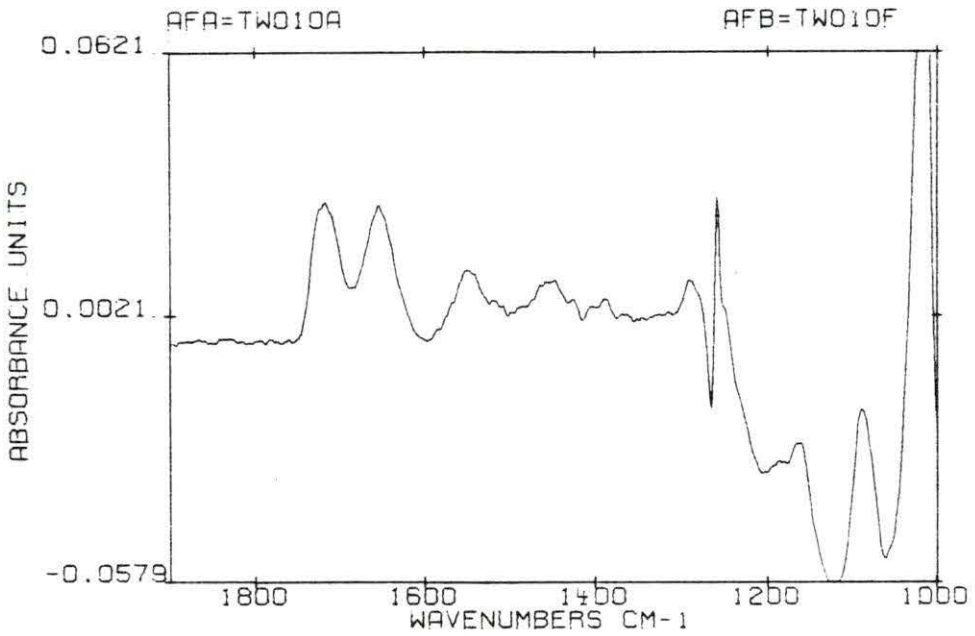

Figure 138. Absorbance spectrum of spectrally subtracted 2%SR/10%H/10%N shunt after 0.25 minute of exposure to blood

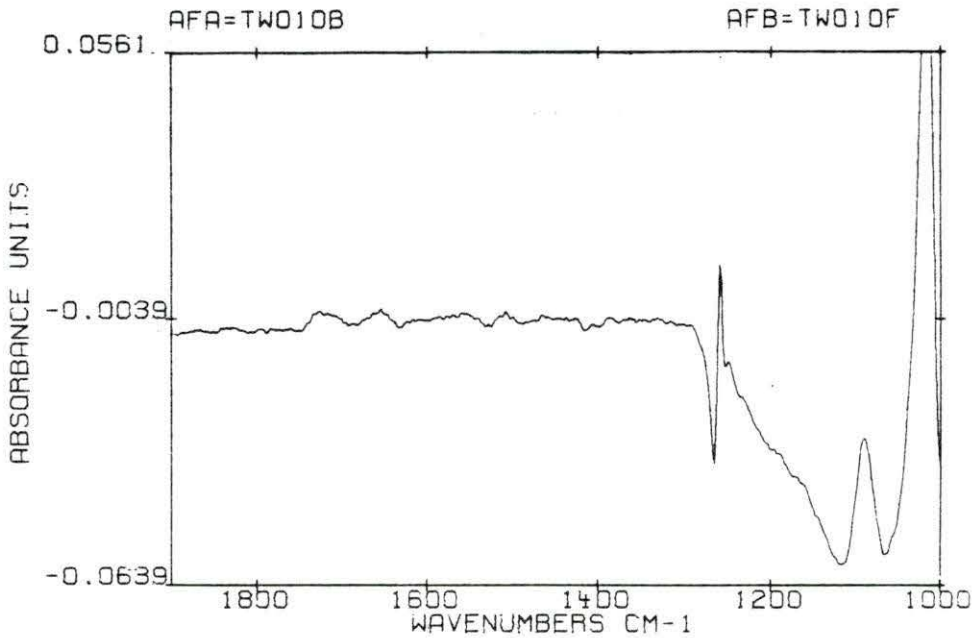

Figure 139. Absorbance spectrum of spectrally subtracted 2%SR/10%H/10%N shunt after 0.50 minute of exposure to blood

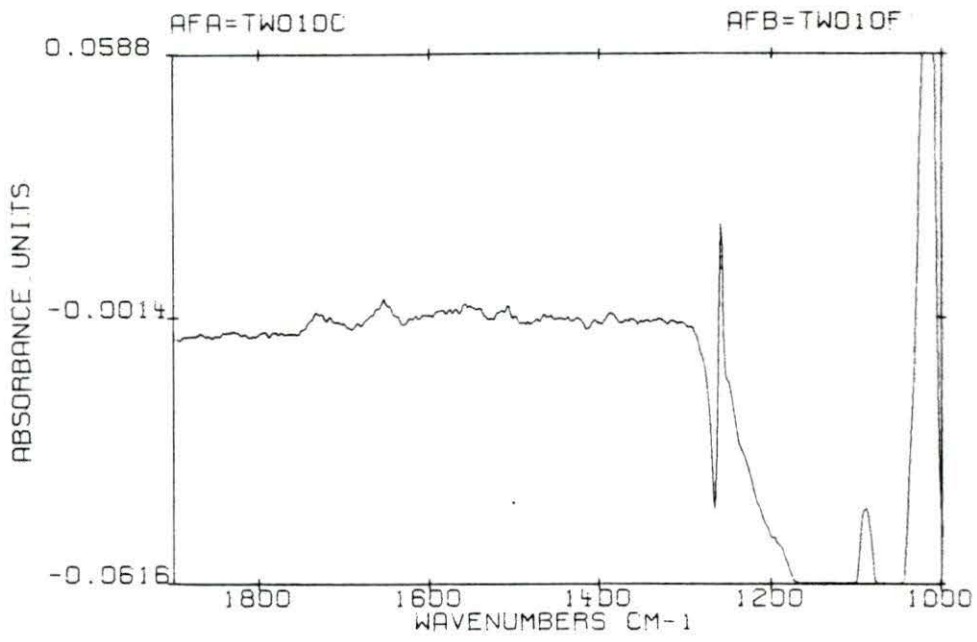

Figure 140. Absorbance spectrum of spectrally subtracted 2%SR/10%H/10%N shunt after 5 minutes of exposure to blood

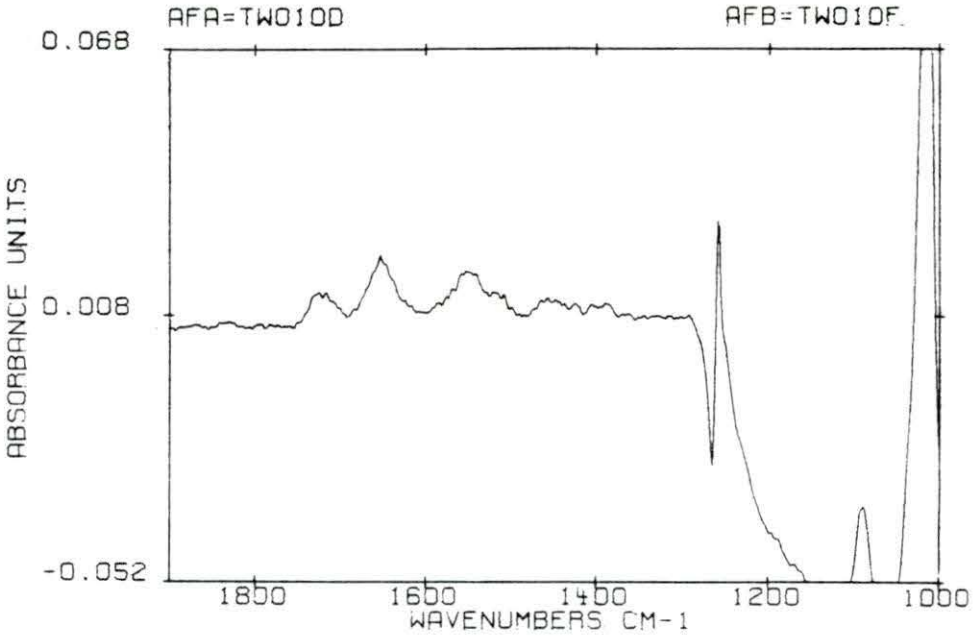

Figure 141. Absorbance spectrum of spectrally subtracted 2%SR/10%H/10%N shunt after 15 minutes of exposure to blood

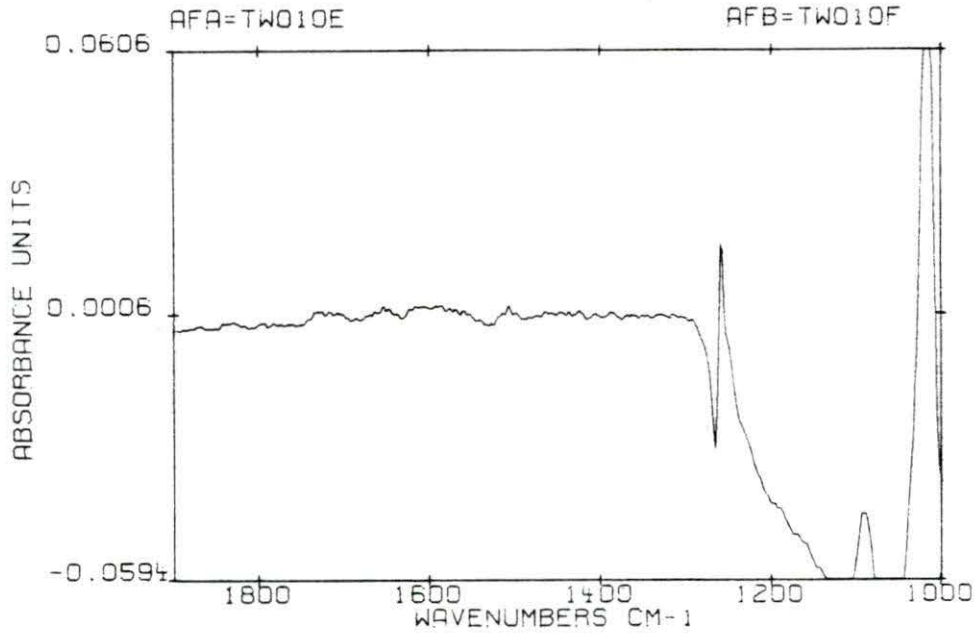

Figure 142. Absorbance spectrum of spectrally subtracted 2%SR/10%H/10%N shunt after 75 minutes of exposure to blood

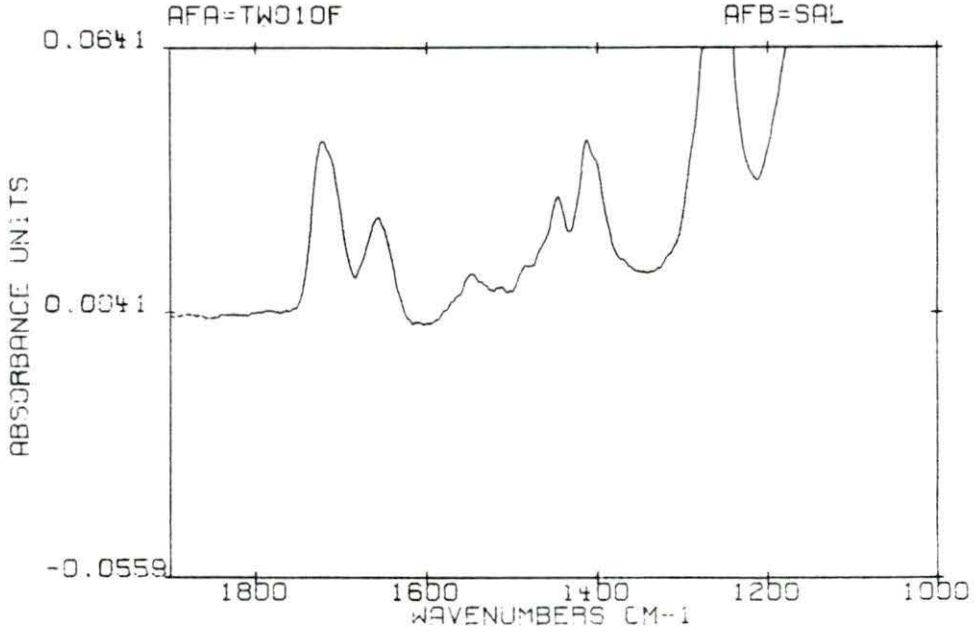

Figure 143. Absorbance spectrum of unexposed 2%SR/10%H/10%N shunt after subtraction of saline

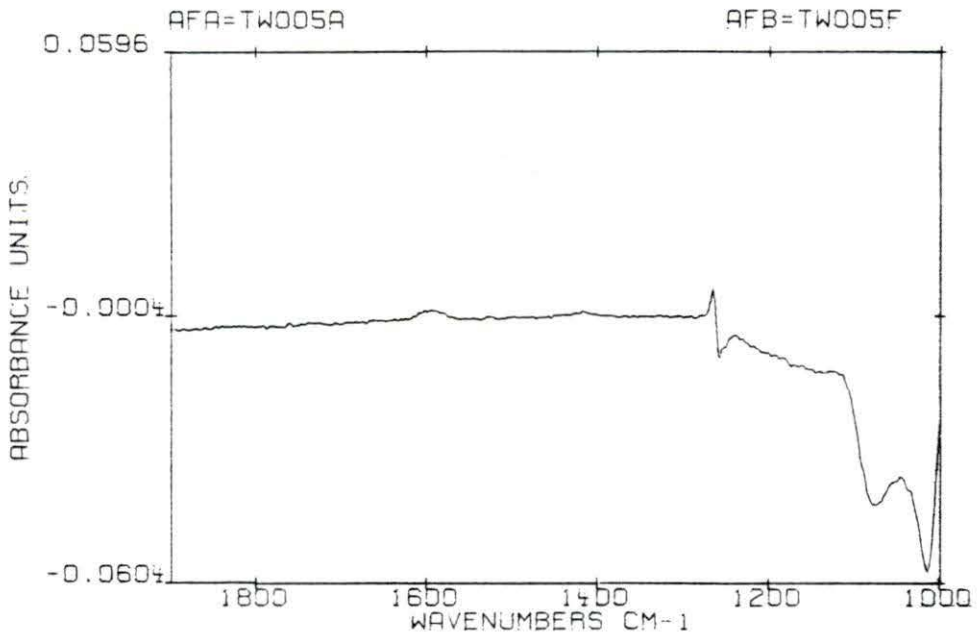

Figure 144. Absorbance spectrum of spectrally subtracted 2%SR/5%H/15%N shunt after 0.25 minute of exposure to blood

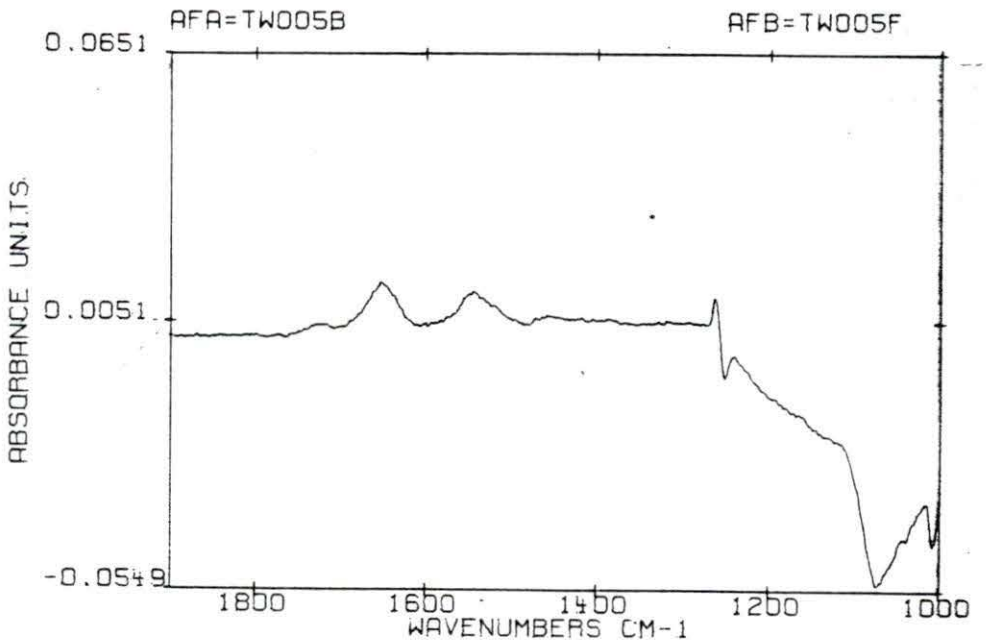

Figure 145. Absorbance spectrum of spectrally subtracted 2%SR/5%H/15%N shunt after 0.50 minute of exposure to blood

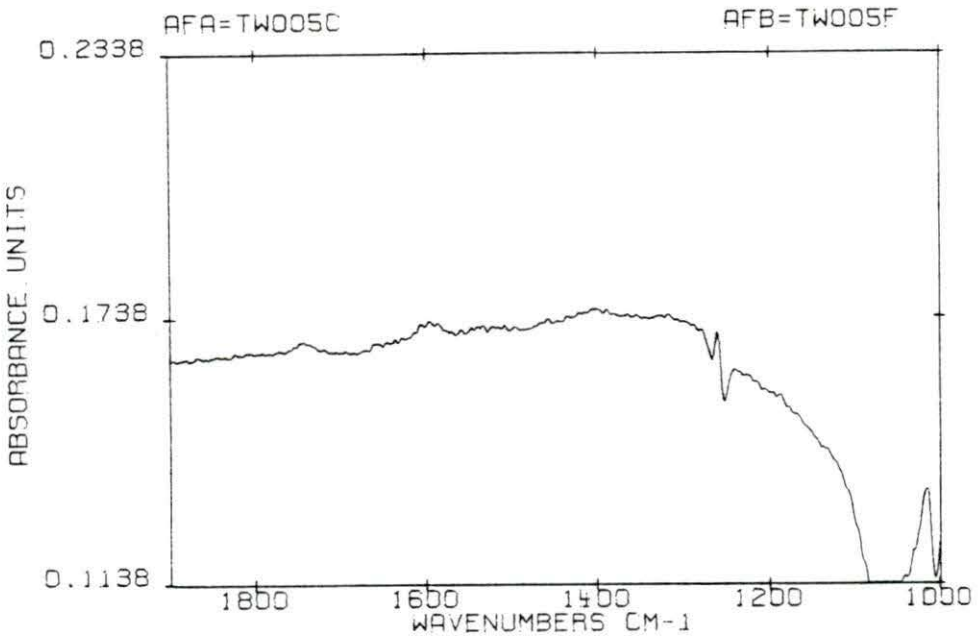

Figure 146. Absorbance spectrum of spectrally subtracted 2%SR/5%H/15%N shunt after 5 minutes of exposure to blood

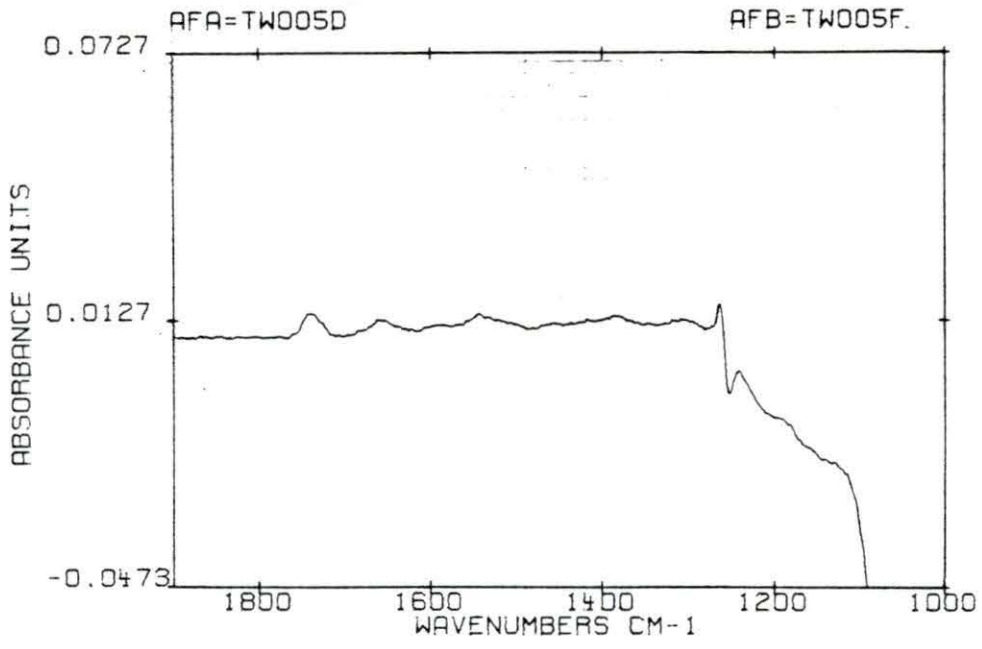

Figure 147. Absorbance spectrum of spectrally subtracted 2%SR/5%H/15%N shunt after 15 minutes of exposure to blood

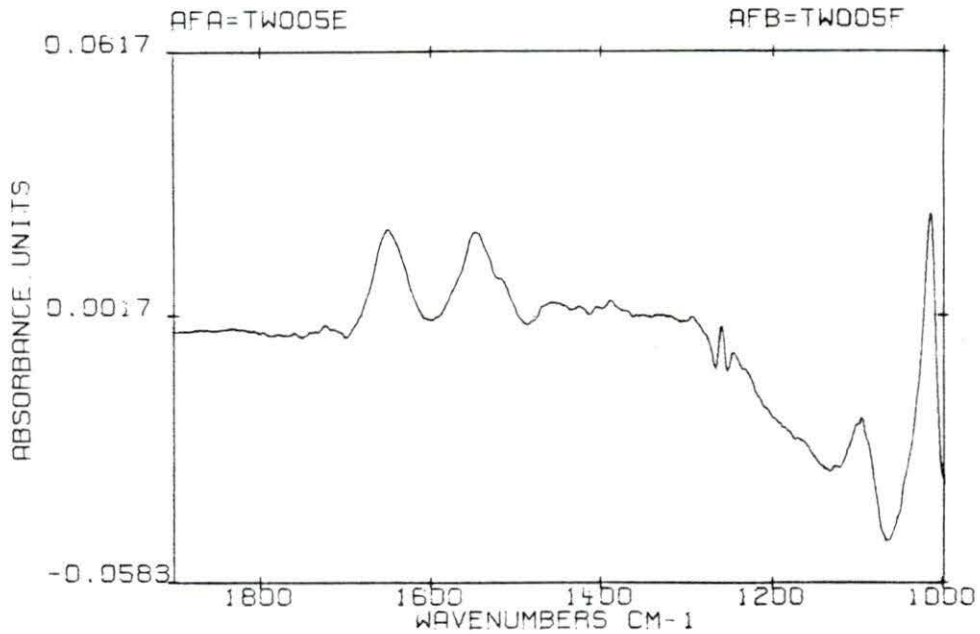

Figure 148. Absorbance spectrum of spectrally subtracted 2%SR/5%H/15%N shunt after 75 minutes of exposure to blood

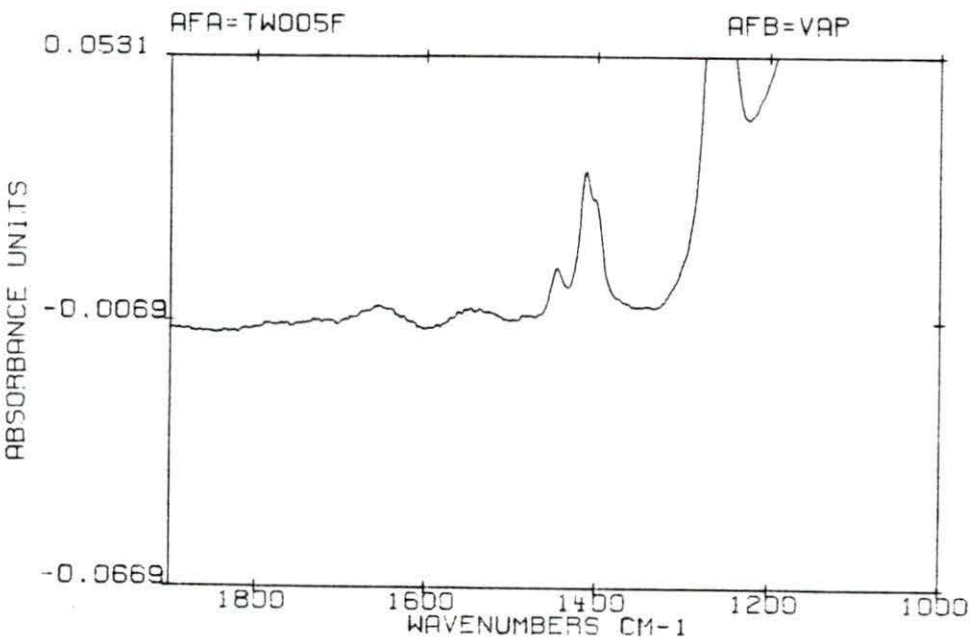

Figure 149. Absorbance spectrum of unexposed 2%SR/5%H/15%N shunt after subtraction of saline and water vapor

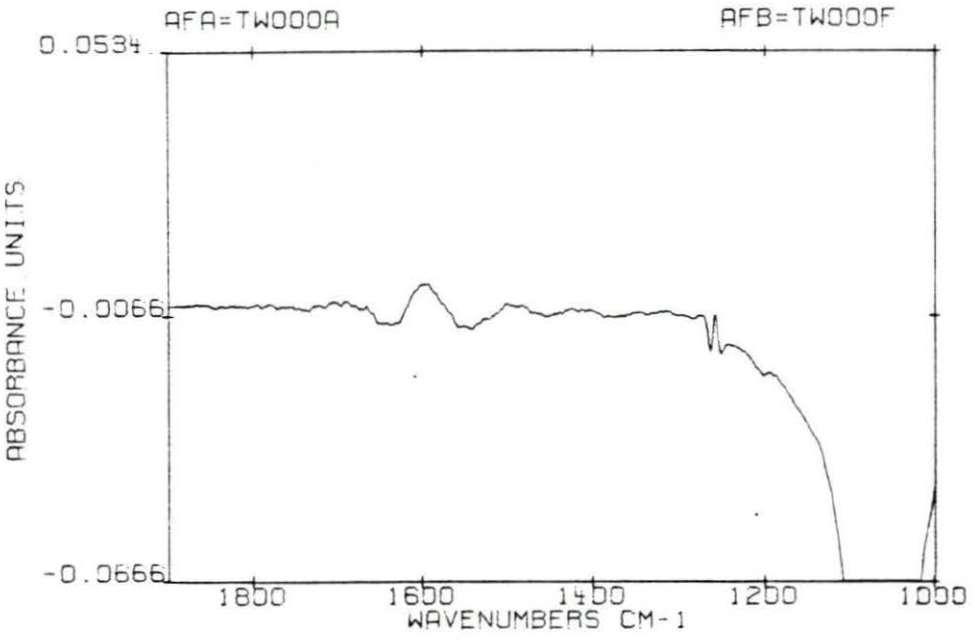

Figure 150. Absorbance spectrum of spectrally subtracted 2%SR/0%H/20%N shunt after 0.25 minute of exposure to blood

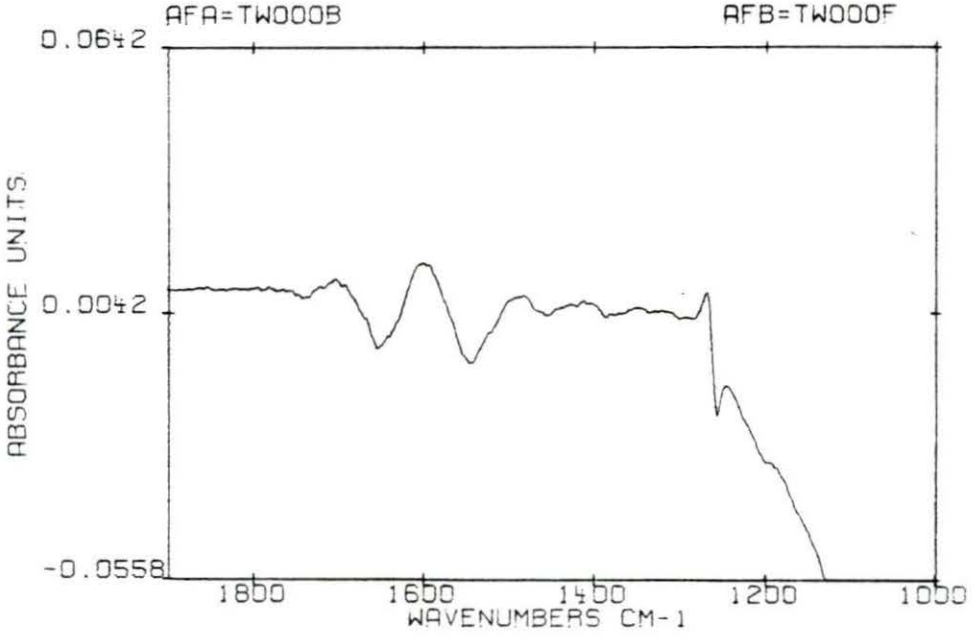

Figure 151. Absorbance spectrum of spectrally subtracted 2%SR/0%H/20%N shunt after 0.50 minute of exposure to blood

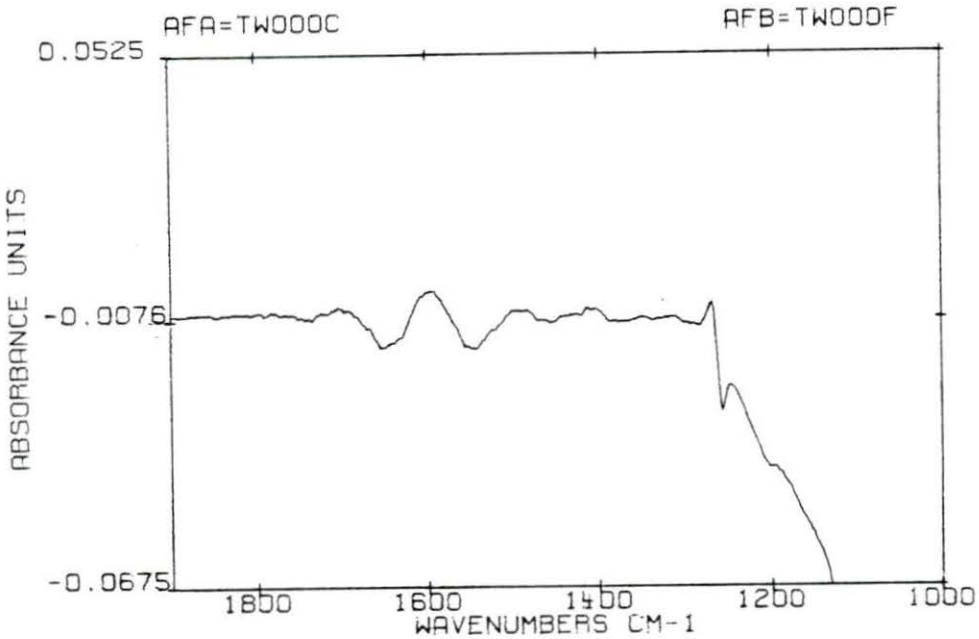

Figure 152. Absorbance spectrum of spectrally subtracted 2%SR/0%H/20%N shunt after 5 minutes of exposure to blood

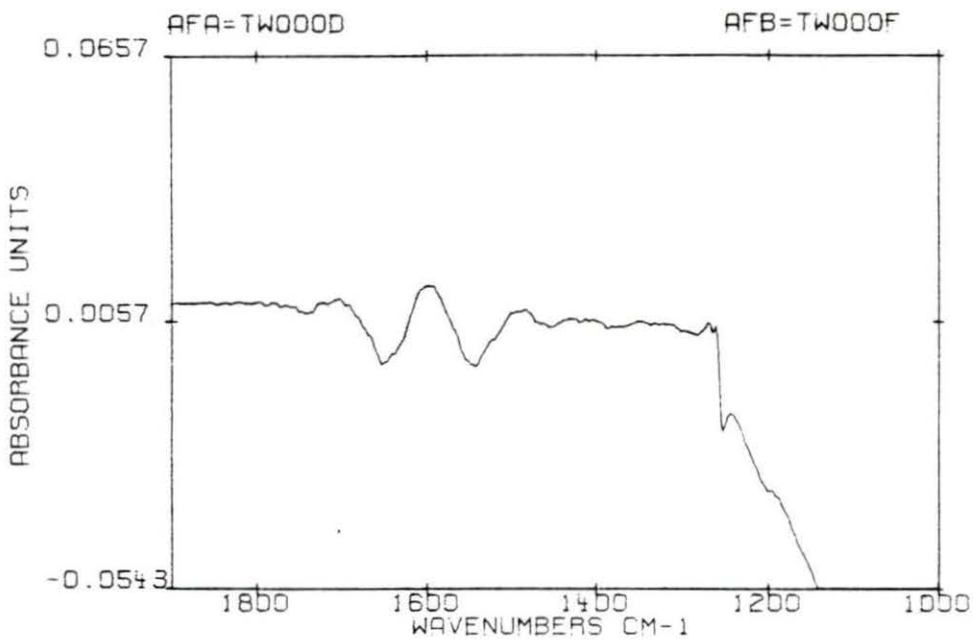

Figure 153. Absorbance spectrum of spectrally subtracted 2%SR/0%H/20%N shunt after 15 minutes of exposure to blood

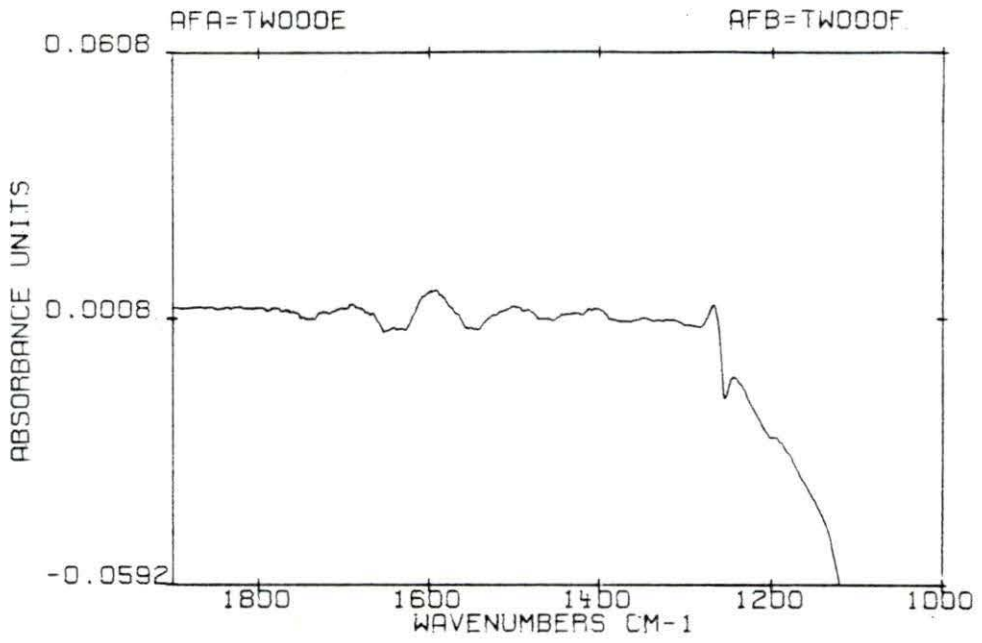

Figure 154. Absorbance spectrum of spectrally subtracted 2%SR/0%H/20%N shunt after 75 minutes of exposure to blood

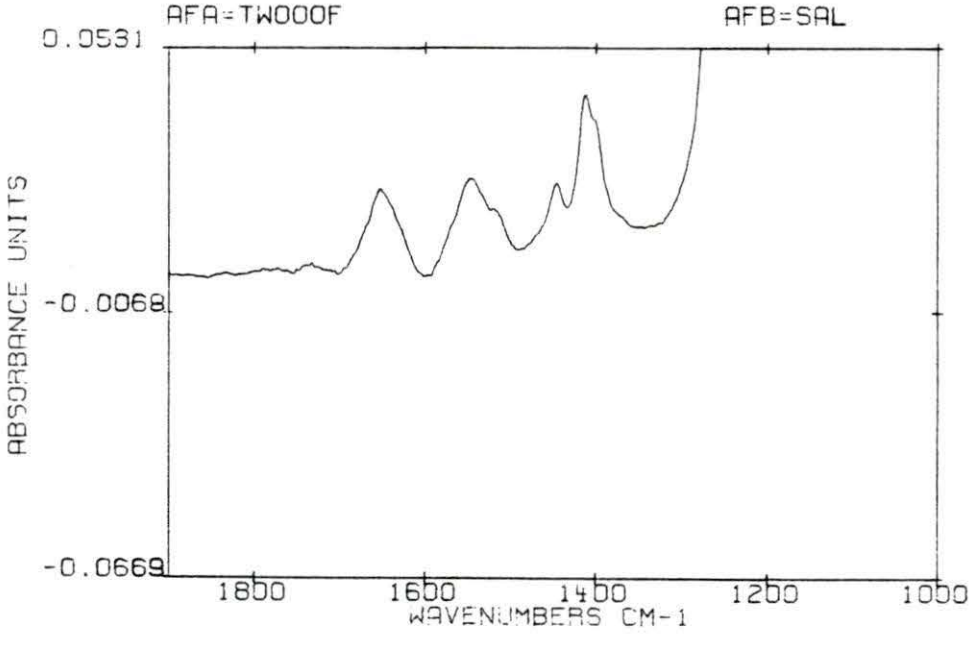

Figure 155. Absorbance spectrum of unexposed 2%SR/0%H/20%N shunt after subtraction of saline

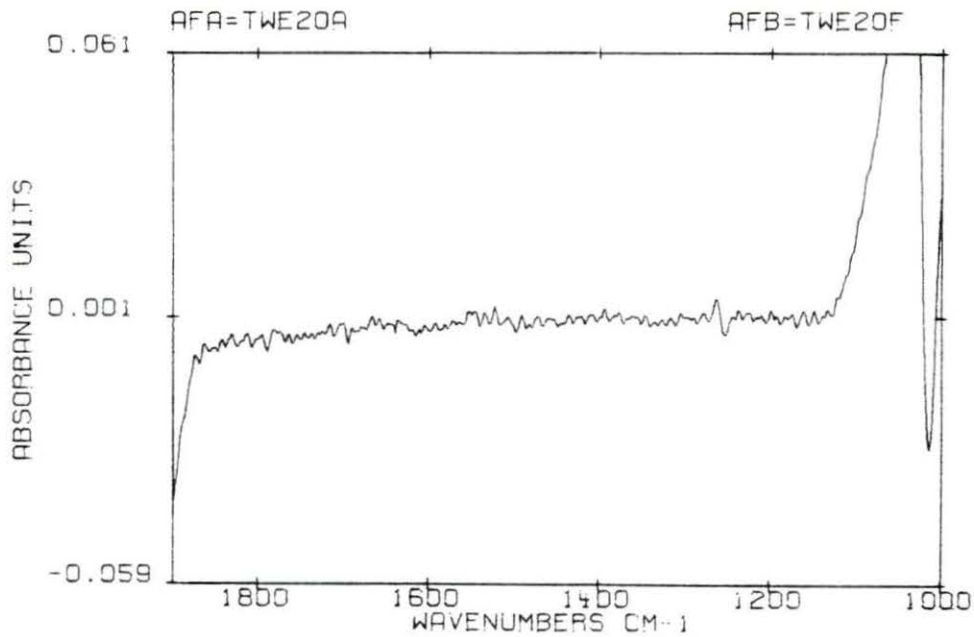

Figure 156. Absorbance spectrum of spectrally subtracted 12%SR/20%H/0%N shunt after 0.25 minute of exposure to blood

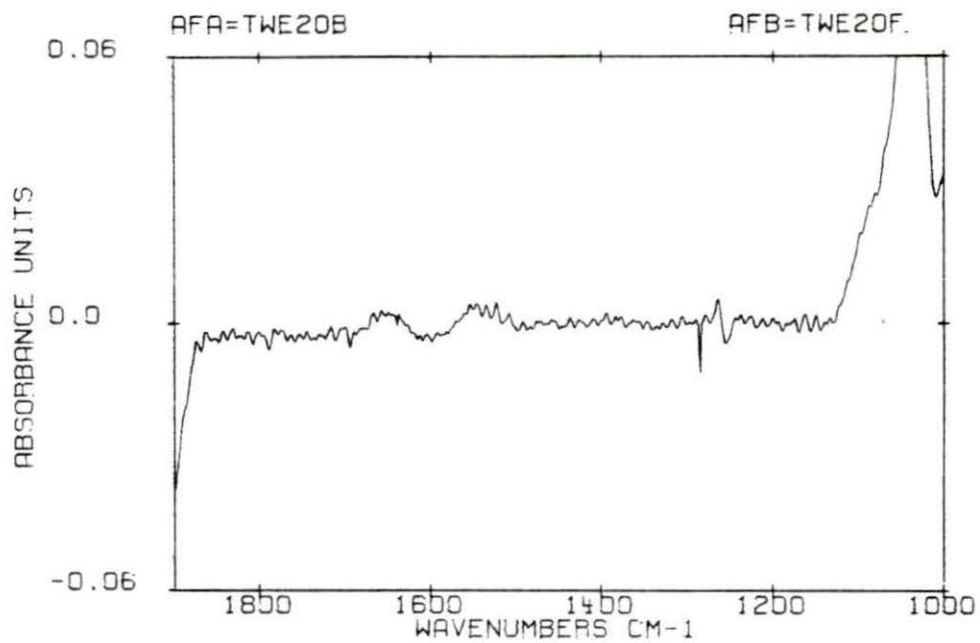

Figure 157. Absorbance spectrum of spectrally subtracted 12%SR/20%H/0%N shunt after 0.50 minute of exposure to blood

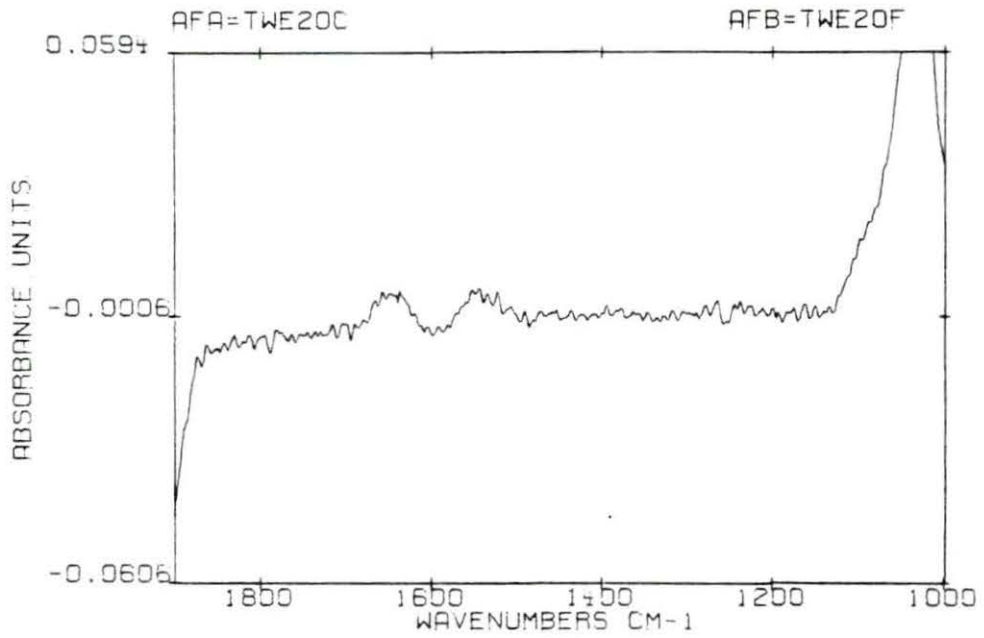

Figure 158. Absorbance spectrum of spectrally subtracted 12%SR/20%H/0%N shunt after 5 minutes of exposure to blood

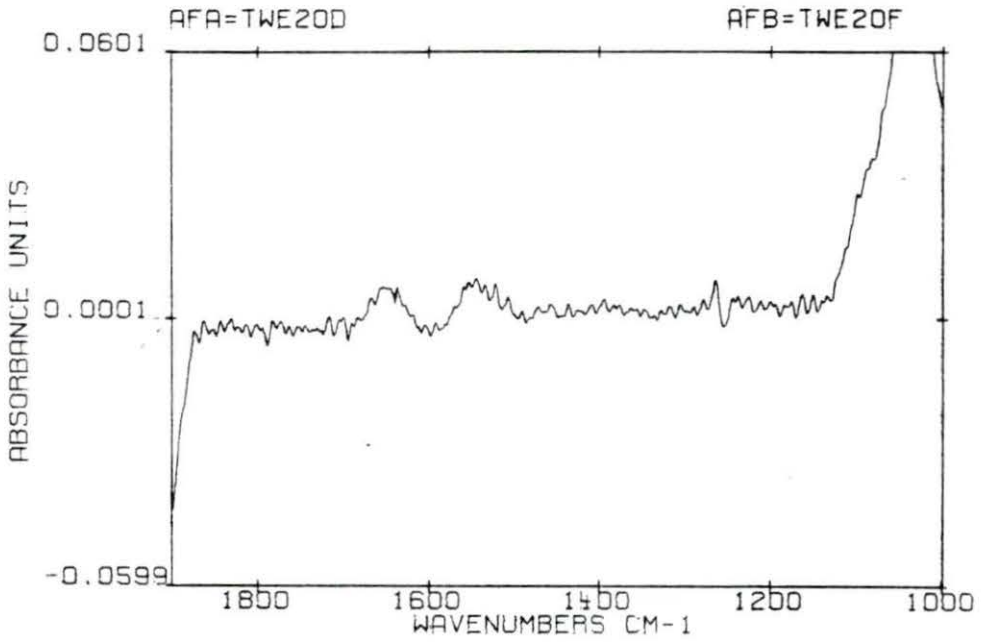

Figure 159. Absorbance spectrum of spectrally subtracted 12%SR/20%H/0%N shunt after 15 minutes of exposure to blood

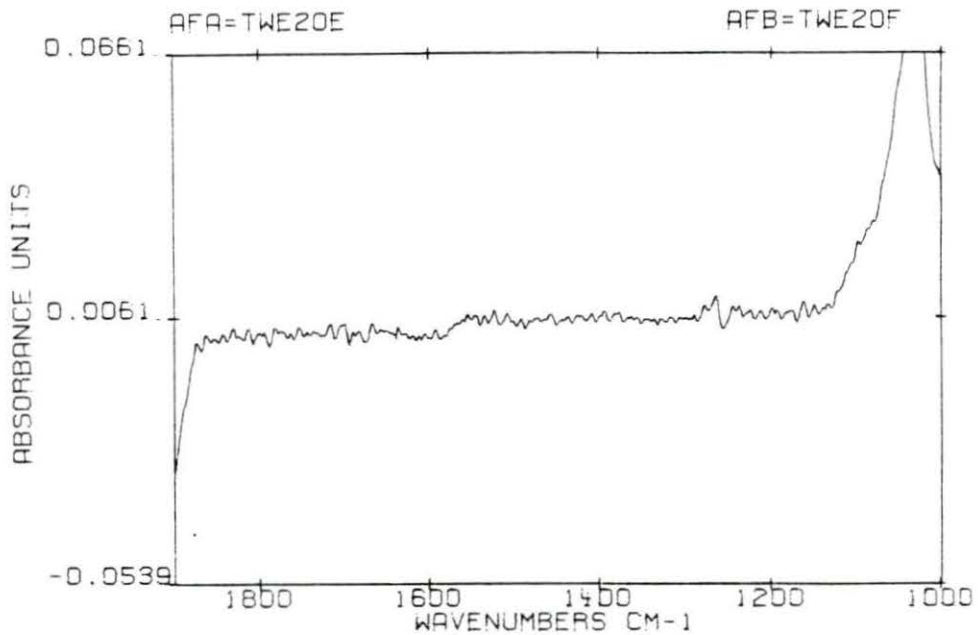

Figure 160. Absorbance spectrum of spectrally subtracted 12%SR/20%H/0%N shunt after 75 minutes of exposure to blood

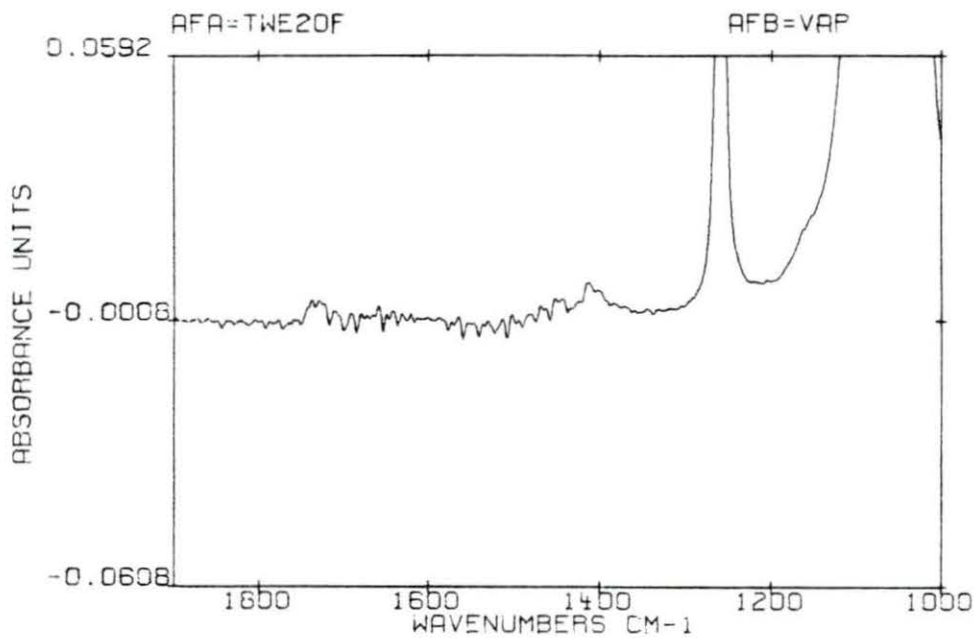

Figure 161. Absorbance spectrum of unexposed 12%SR/20%H/0%N shunt after subtraction of saline and water vapor

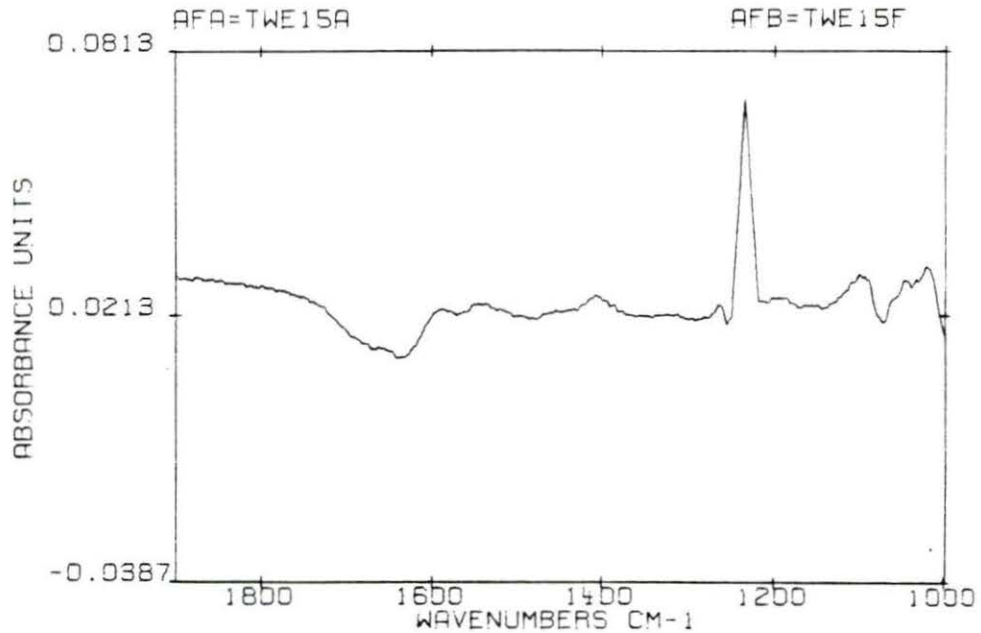

Figure 162. Absorbance spectrum of spectrally subtracted 12%SR/15%H/5%N shunt after 0.25 minute of exposure to blood

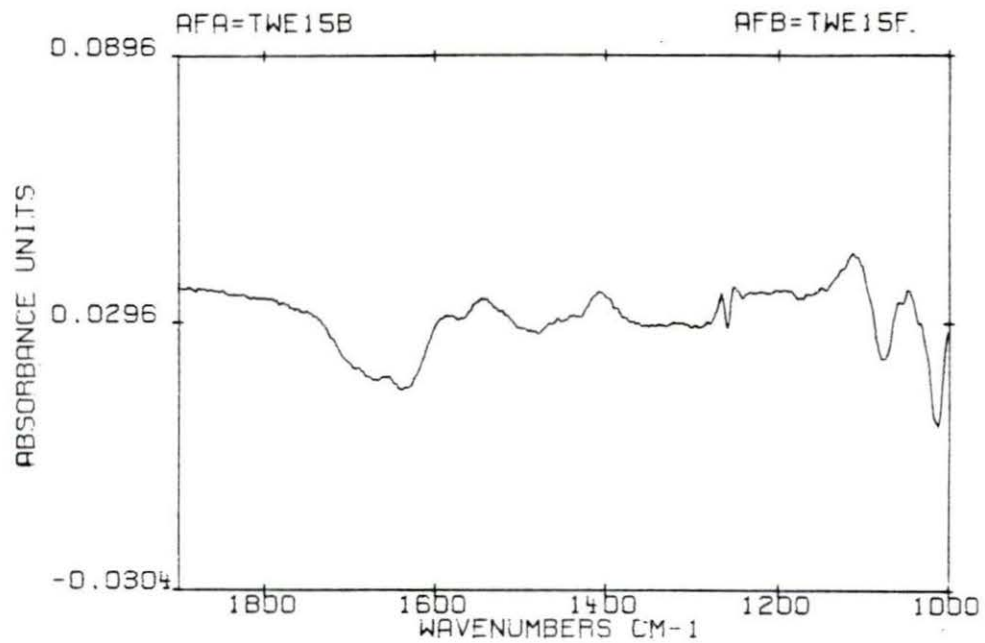

Figure 163. Absorbance spectrum of spectrally subtracted 12%SR/15%H/5%N shunt after 0.50 minute of exposure to blood

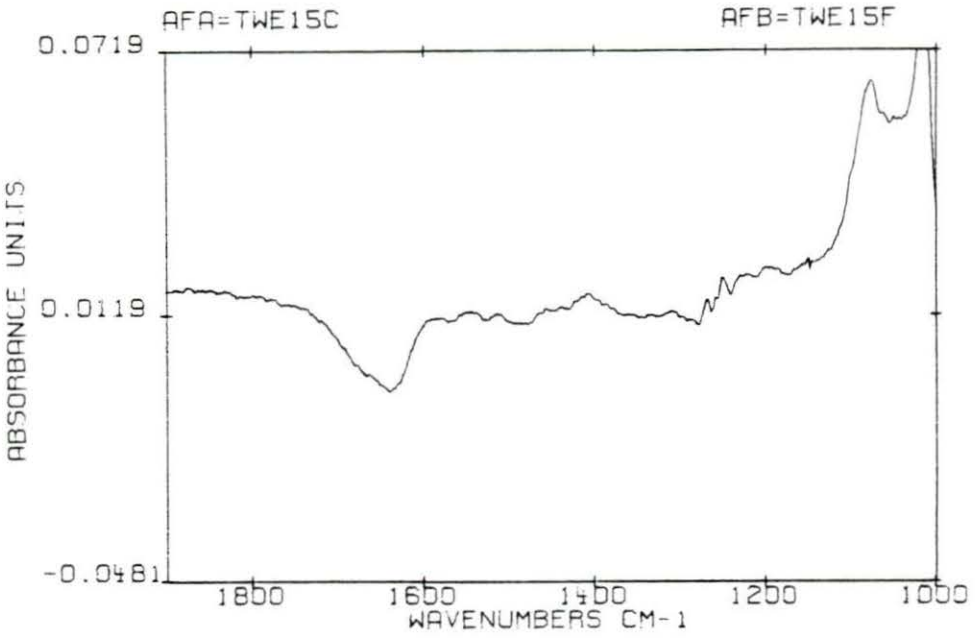

Figure 164. Absorbance spectrum of spectrally subtracted 12%SR/15%H/5%N shunt after 5 minutes of exposure to blood

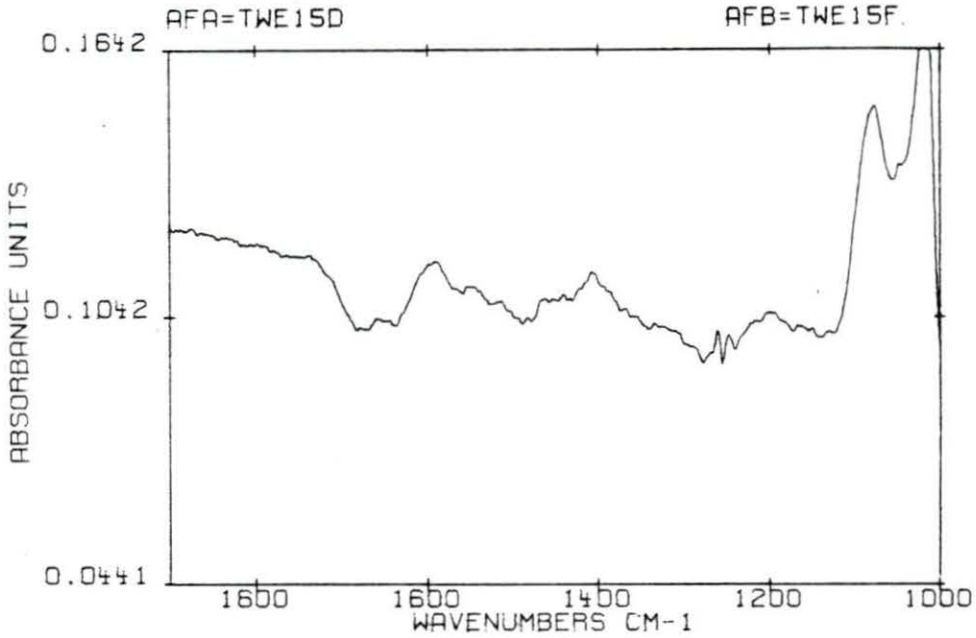

Figure 165. Absorbance spectrum of spectrally subtracted 12%SR/15%H/5%N shunt after 15 minutes of exposure to blood

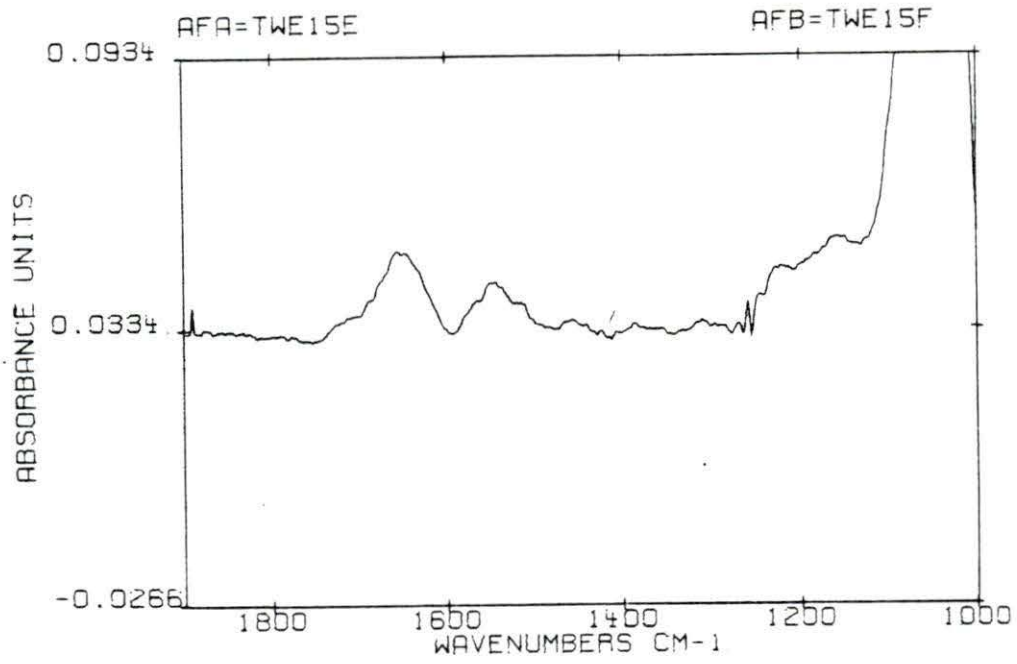

Figure 166. Absorbance spectrum of spectrally subtracted 12%SR/15%H/5%N shunt after 75 minutes of exposure to blood

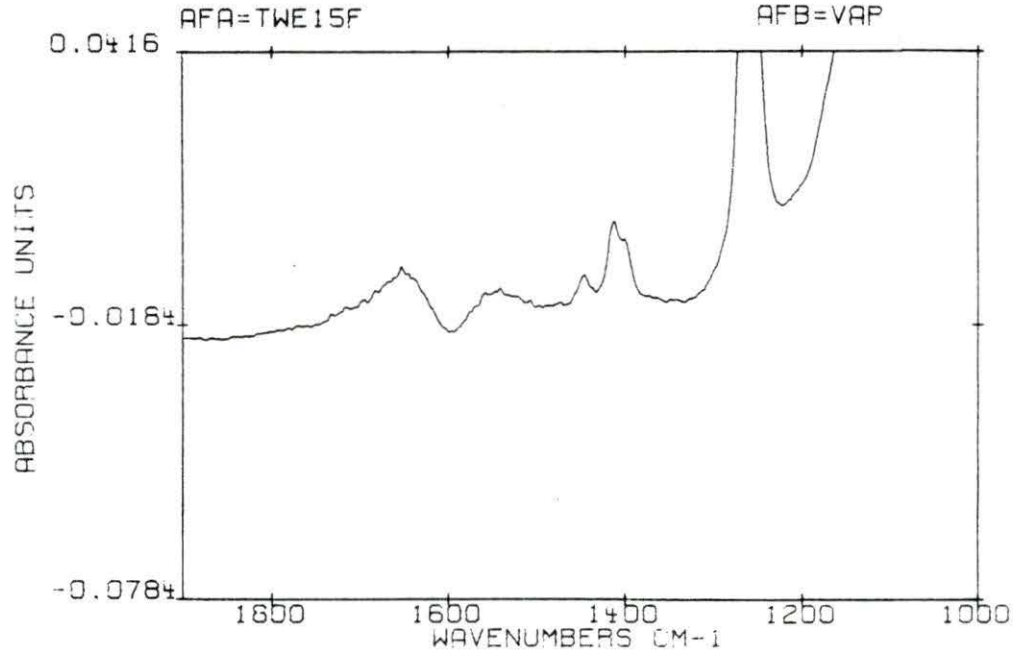

Figure 167. Absorbance spectrum of unexposed 12%SR/15%H/5%N shunt after subtraction of saline and water vapor

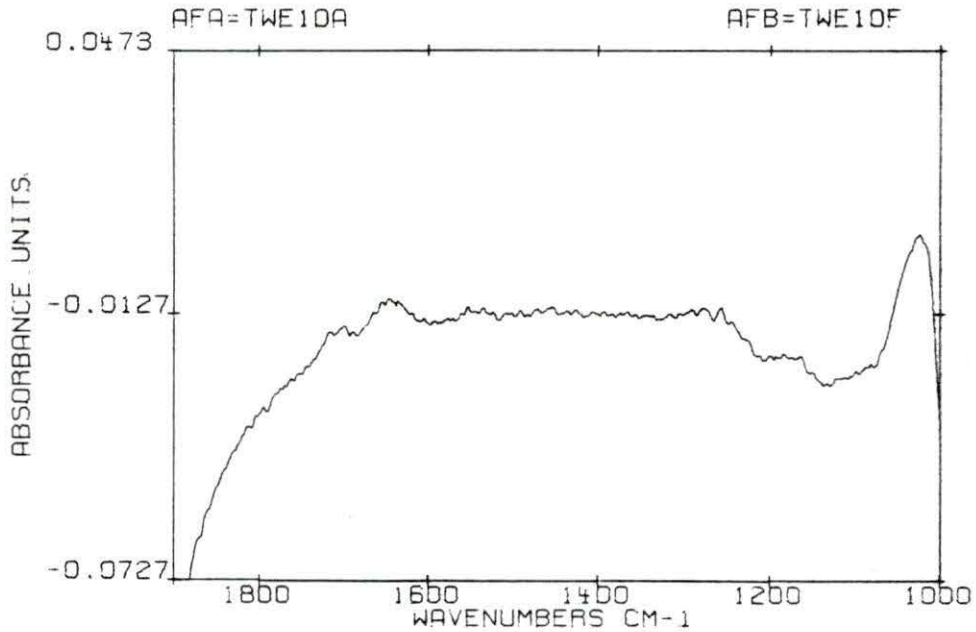

Figure 168. Absorbance spectrum of spectrally subtracted 12%SR/10%H/10%N shunt after 0.25 minute of exposure to blood

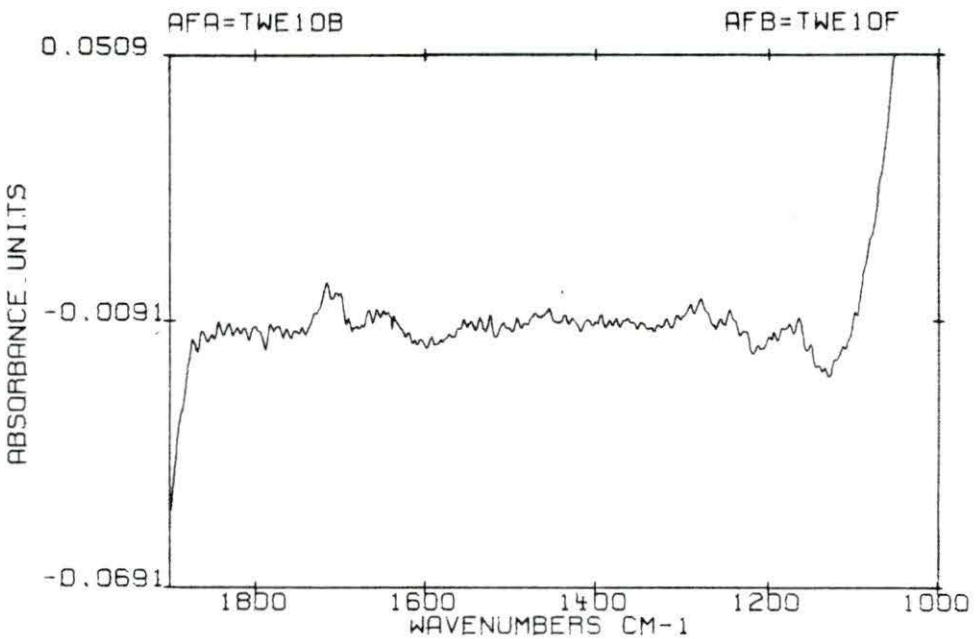

Figure 169. Absorbance spectrum of spectrally subtracted 12%SR/10%H/10%N shunt after 0.50 minute of exposure to blood

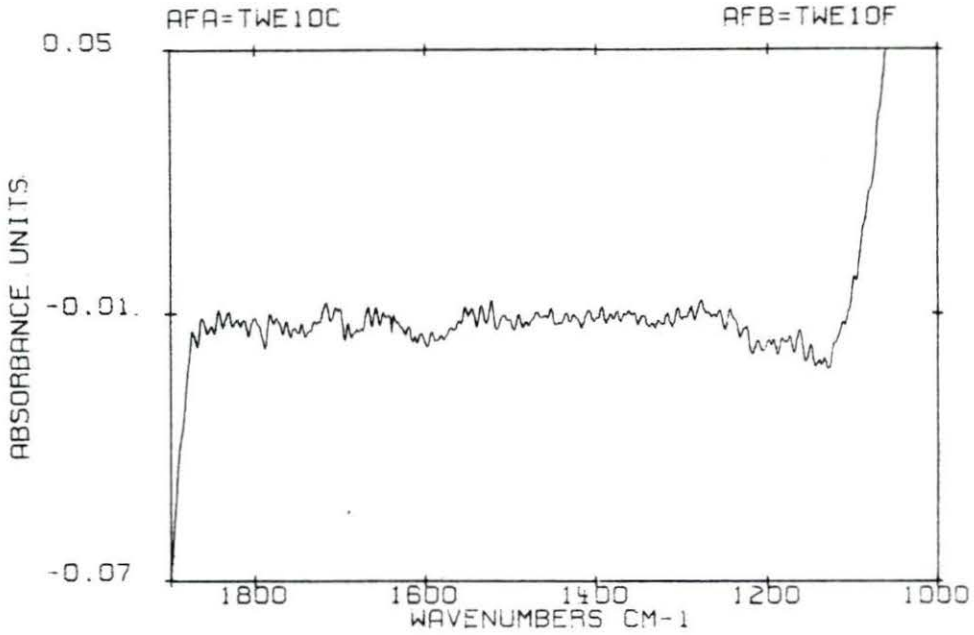

Figure 170. Absorbance spectrum of spectrally subtracted 12%SR/10%H/10%N shunt after 5 minutes of exposure to blood

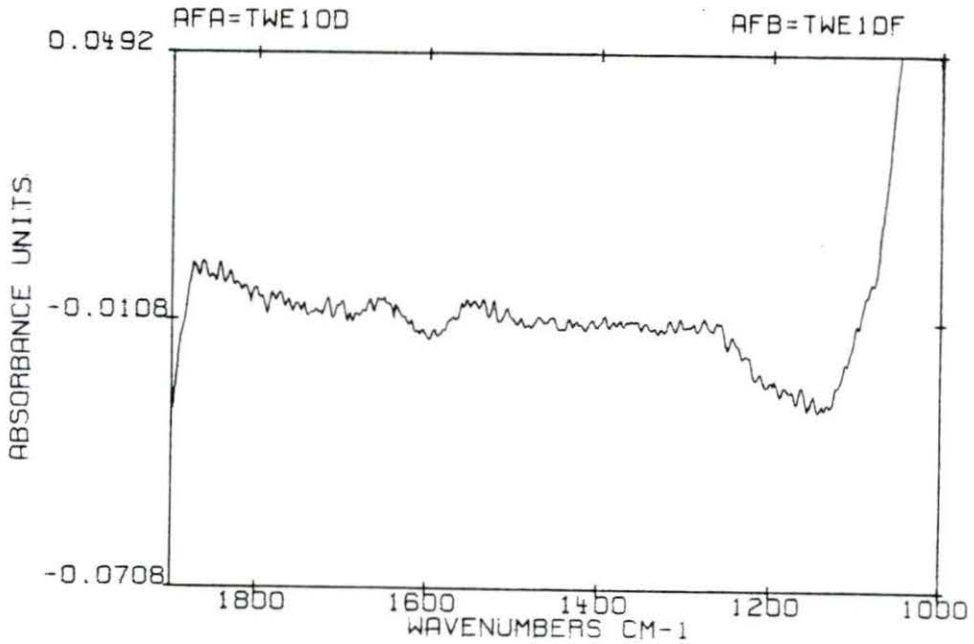

Figure 171. Absorbance spectrum of spectrally subtracted 12%SR/10%H/10%N shunt after 15 minutes of exposure to blood

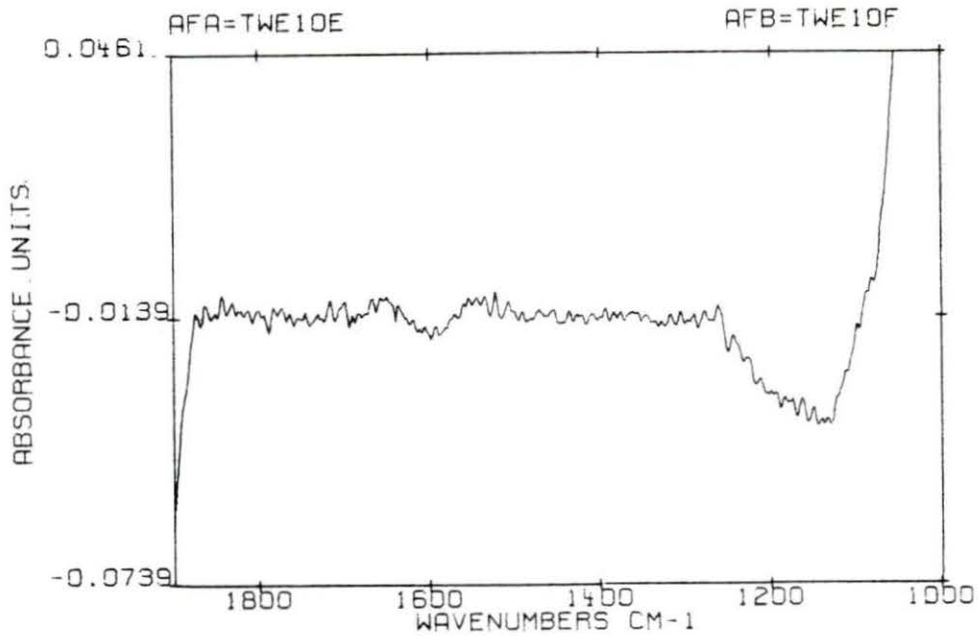

Figure 172. Absorbance spectrum of spectrally subtracted 12%SR/10%H/10%N shunt after 75 minutes of exposure to blood

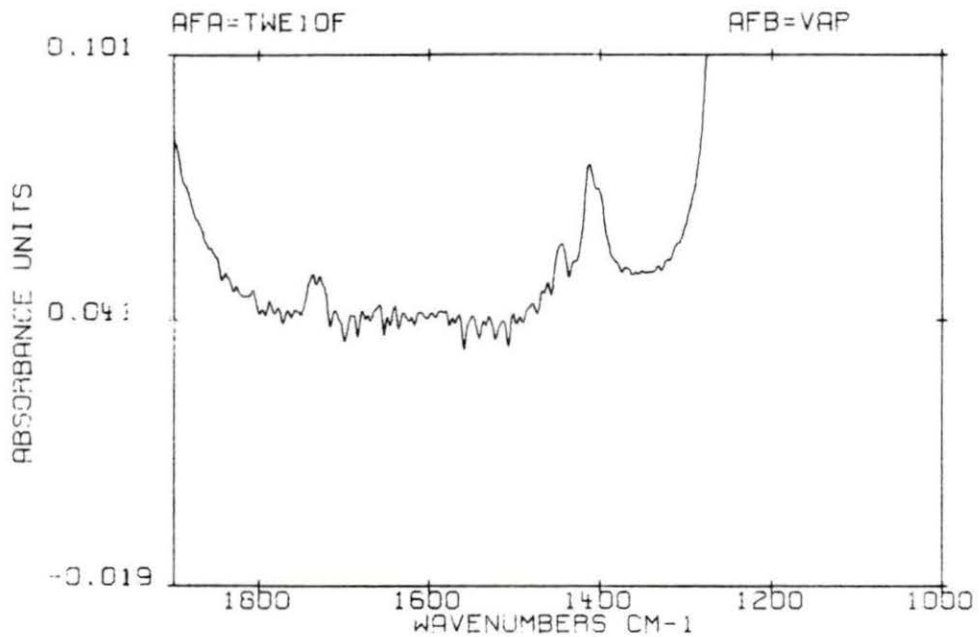

Figure 173. Absorbance spectrum of unexposed 12%SR/10%H/10%N shunt after subtraction of saline and water vapor

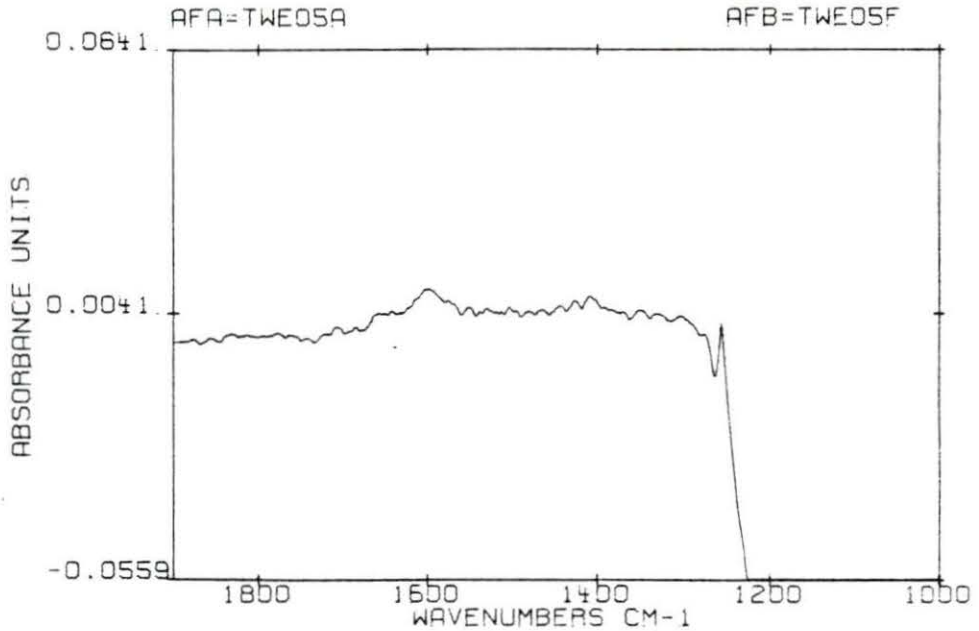

Figure 174. Absorbance spectrum of spectrally subtracted 12%SR/5%H/15%N shunt after 0.25 minute of exposure to blood

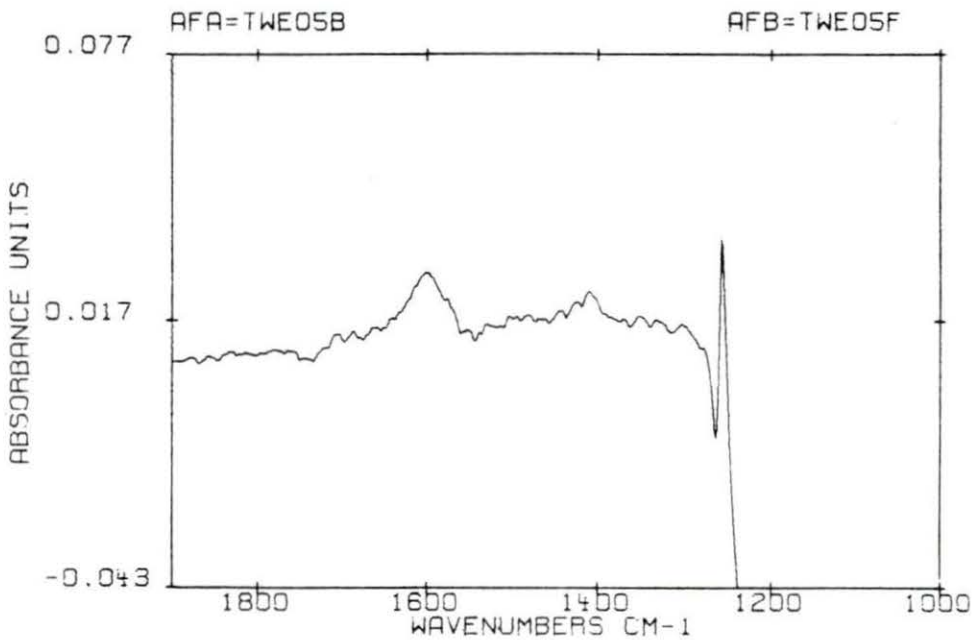

Figure 175. Absorbance spectrum of spectrally subtracted 12%SR/5%H/15%N shunt after 0.50 minute of exposure to blood

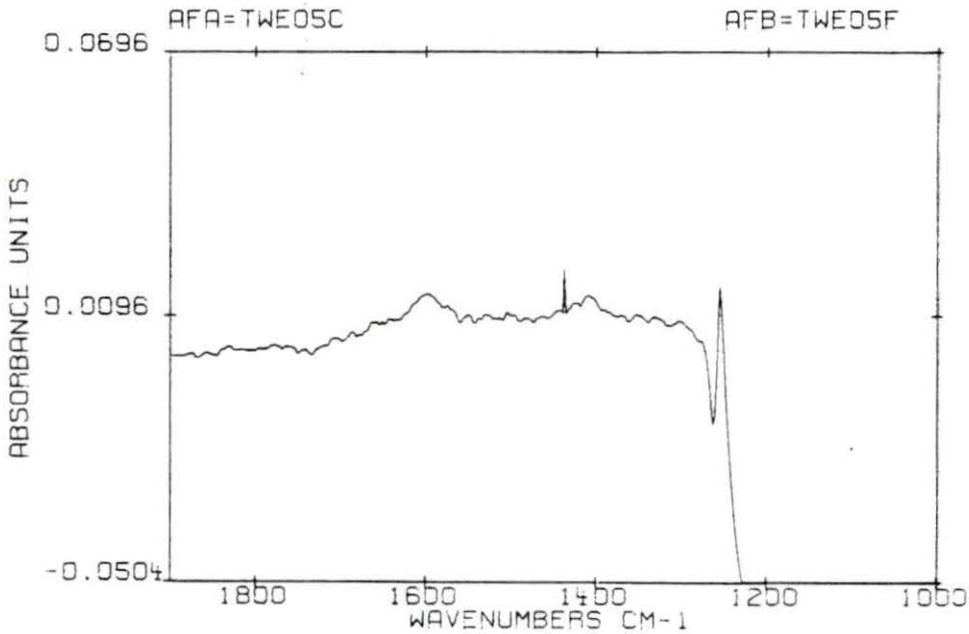

Figure 176. Absorbance spectrum of spectrally subtracted 12%SR/5%H/15%N shunt after 5 minutes of exposure to blood

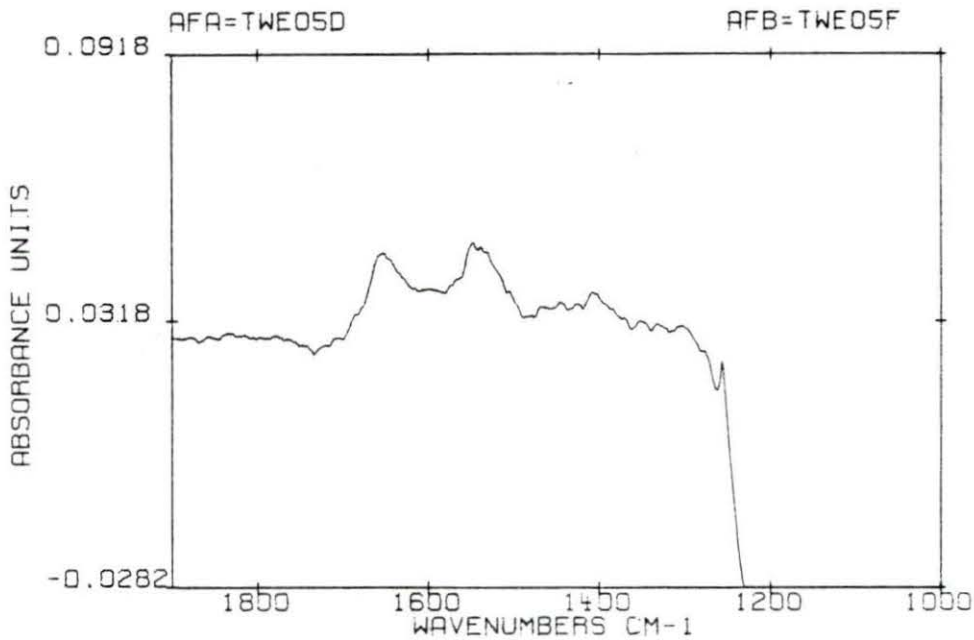

Figure 177. Absorbance spectrum of spectrally subtracted 12%SR/5%H/15%N shunt after 15 minutes of exposure to blood

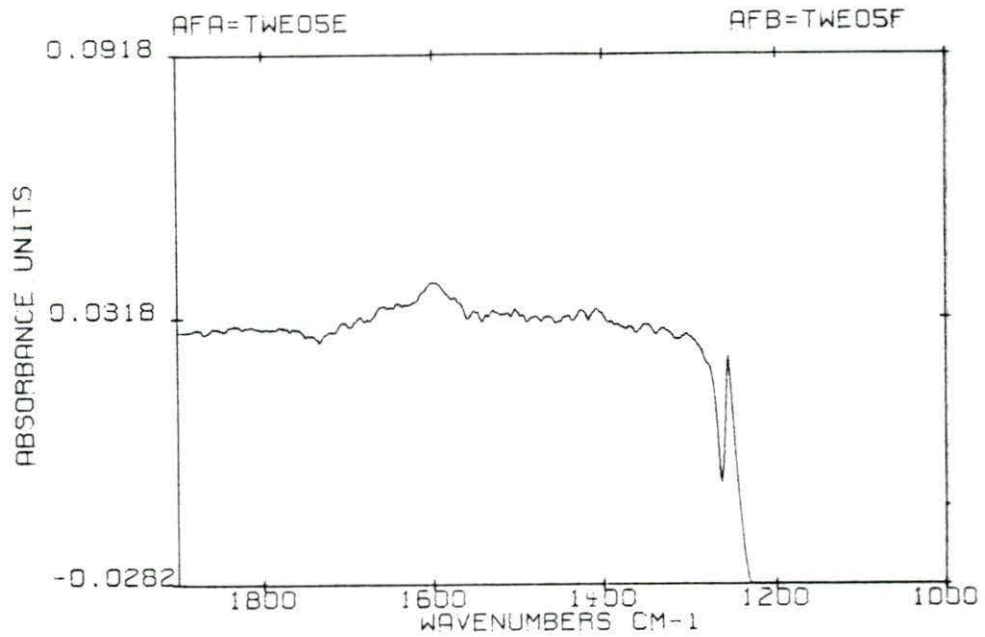

Figure 178. Absorbance spectrum of spectrally subtracted 12%SR/5%H/15%N shunt after 75 minutes of exposure to blood

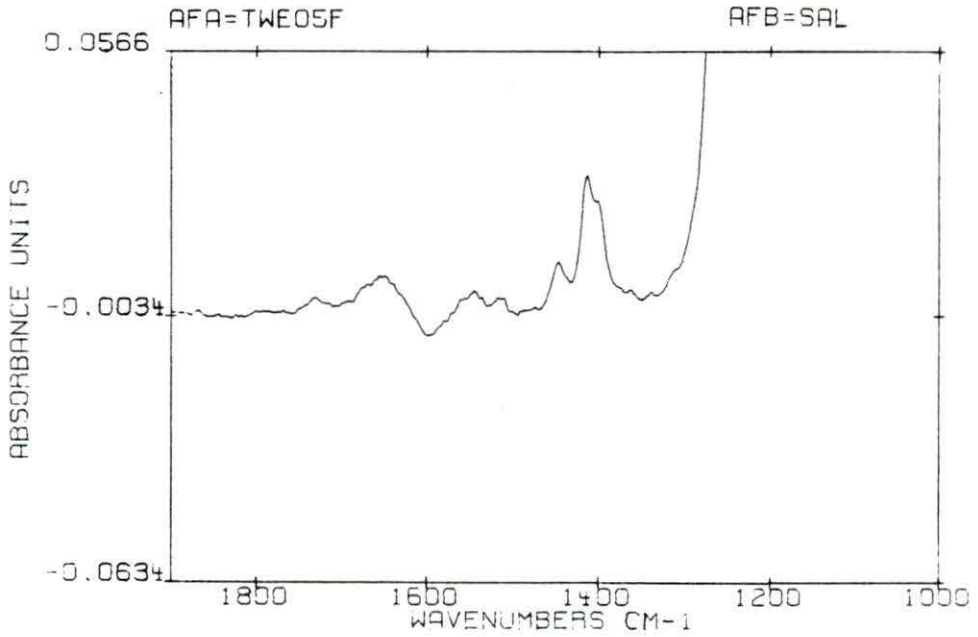

Figure 179. Absorbance spectrum of unexposed 12%SR/5%H/15%N shunt after subtraction of saline

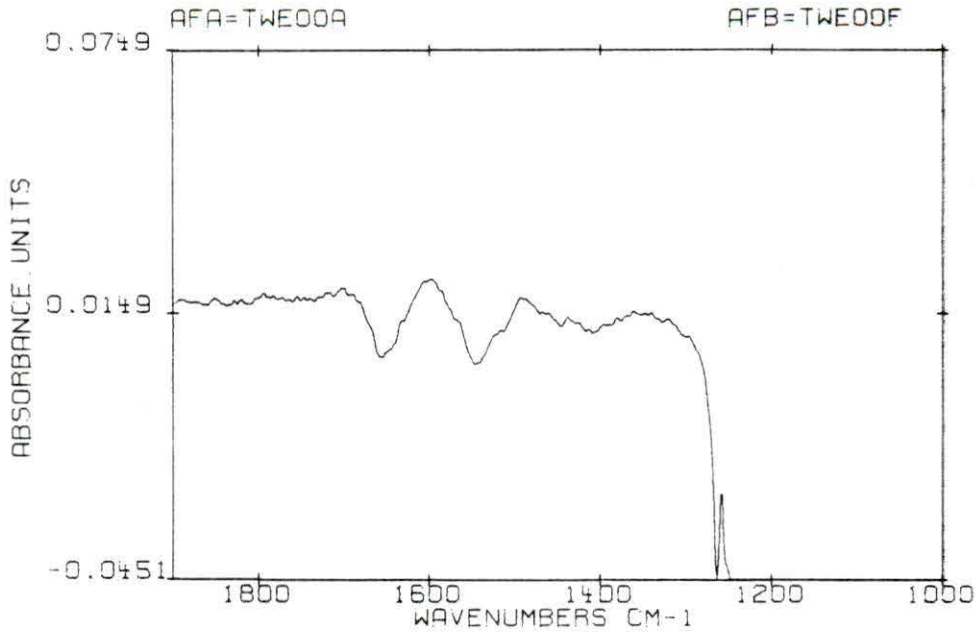

Figure 180. Absorbance spectrum of spectrally subtracted 12%SR/0%H/20%N shunt after 0.25 minute of exposure to blood

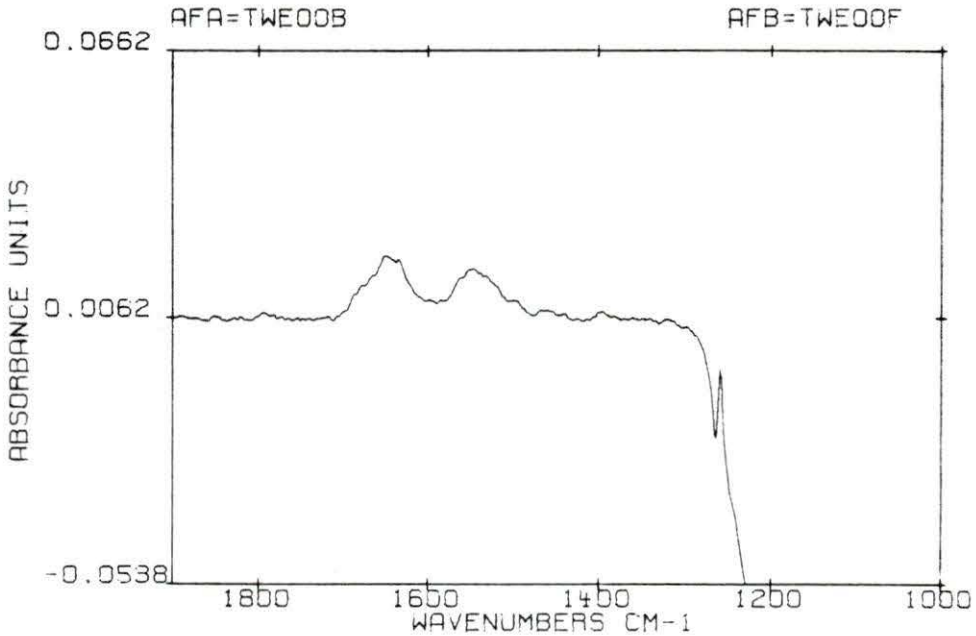

Figure 181. Absorbance spectrum of spectrally subtracted 12%SR/0%H/20%N shunt after 0.50 minute of exposure to blood

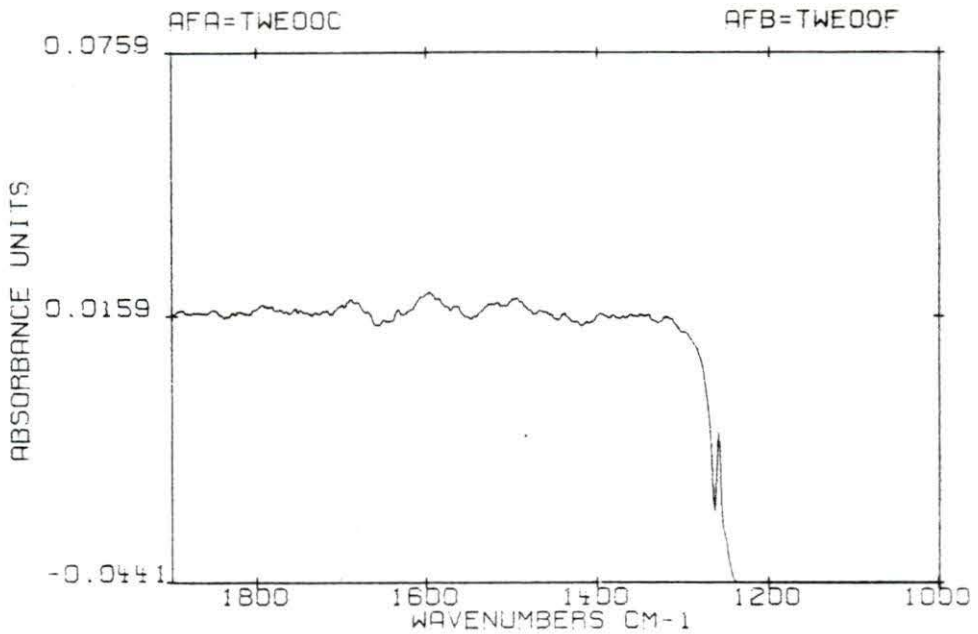

Figure 182. Absorbance spectrum of spectrally subtracted 12%SR/0%H/20%N shunt after 5 minutes of exposure to blood

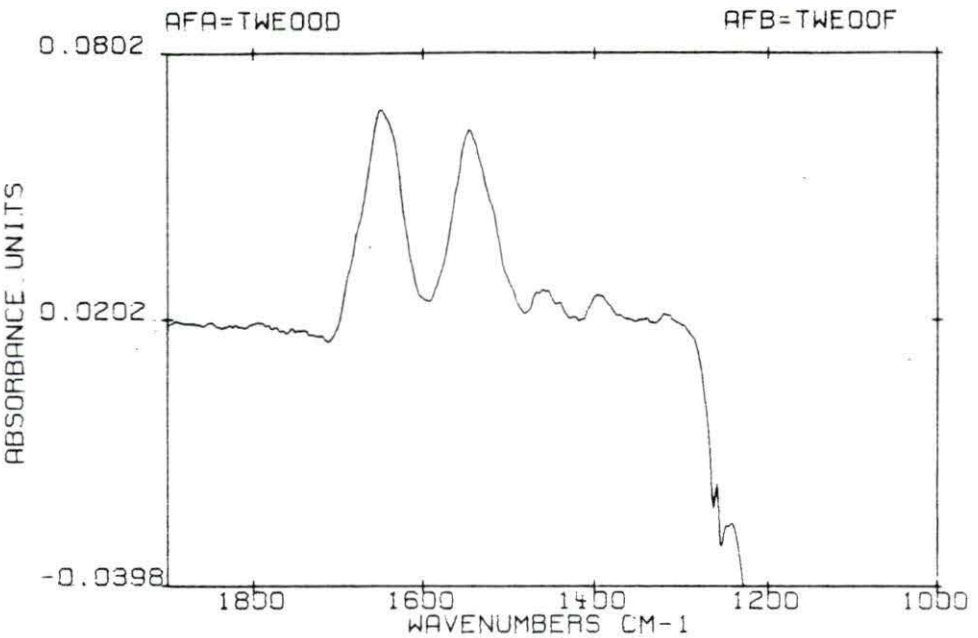

Figure 183. Absorbance spectrum of spectrally subtracted 12%SR/0%H/20%N shunt after 15 minutes of exposure to blood

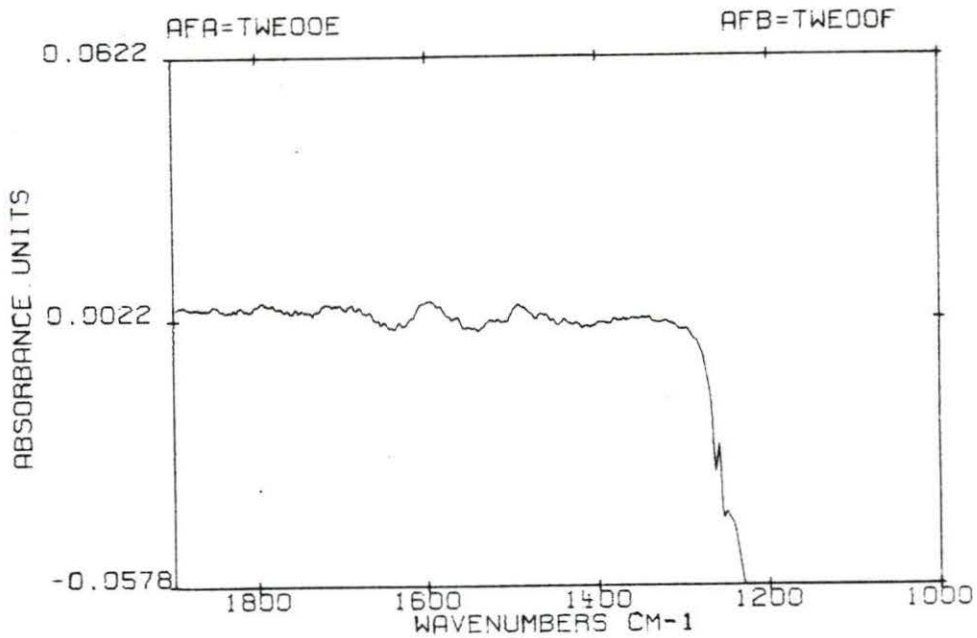

Figure 184. Absorbance spectrum of spectrally subtracted 12%SR/0%H/20%N shunt after 75 minutes of exposure to blood

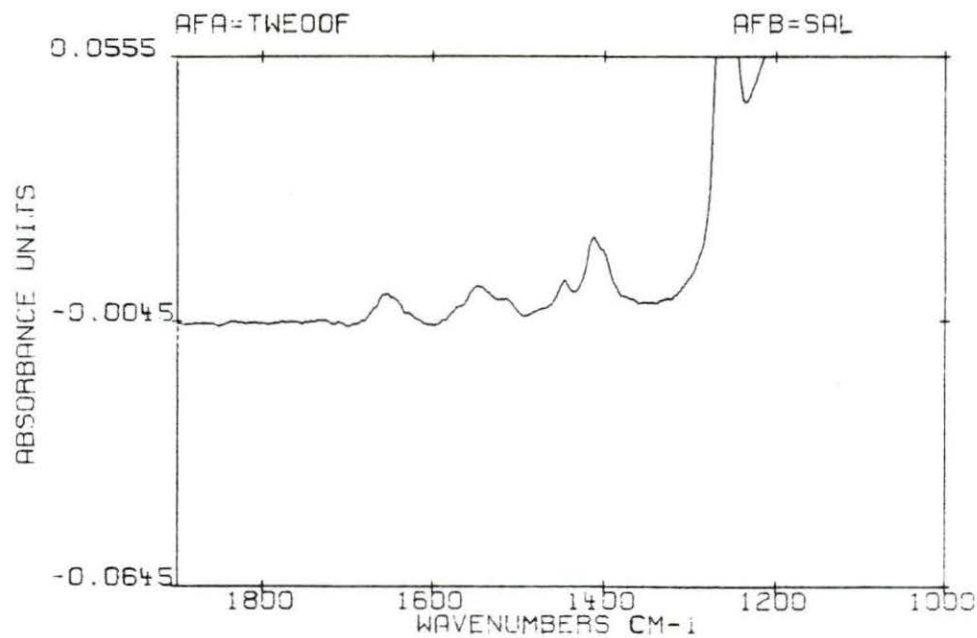

Figure 185. Absorbance spectrum of unexposed 12%SR/0%H/20%N shunt after subtraction of saline

APPENDIX C: CRITICAL SURFACE TENSION AND CONTACT ANGLE VALUES

Contact angle and critical surface tension measurements were done by Mr. D. T. Zhang. These values were provided by Dr. R. T. Greer. Note that a contact angle measurement for water of greater than or equal to 90 degrees indicates a hydrophobic surface while measurements of less than 90 degrees indicates a surface that is hydrophilic.

Formulation	Critical Surface Tension (dynes/cm)	Contact Angle (degrees) (of water in air)
SR	20	124
2%SR	18	108
12%SR	15	108
2%SR/20%H/0%N	31	56
2%SR/15%H/5%N	33	65
2%SR/10%H/10%N	35	76
2%SR/5%H/15%N	33	95
2%SR/0%H/20%N	29	97
12%SR/20%H/0%N	34	59
12%SR/15%H/5%N	35	66
12%SR/10%H/10%N	36	78
12%SR/5%H/15%N	29	97
12%SR/0%H/20%N	26	101

ACKNOWLEDGEMENTS

I would like to express my appreciation to my major professor, Dr. Raymond T. Greer, for his advice and guidance throughout this work. I would also like to thank Dr. Pam McAllister for her help during the surgeries and photographic reproductions.

I would like to express my gratitude to the Veterinary Medical Research Institute for the financial assistance that made it possible for me to attend graduate school. Support from the American Heart Association Iowa Affiliate is also gratefully acknowledged.

Finally, I would like to thank my parents for the encouragement they have given me throughout my studies.